Edge emission and deep centre luminescence in zinc selenide

Gezci, Sami

EDGE EMISSION AND DEEP CENTRE LUMINESCENCE IN ZINC SELENIDE

by

SAMI GEZCI, B.Sc.

A thesis presented to the UNIVERSITY OF DURHAM in support of the author's candidature for the degree of Doctor of Philosophy

November 1973

ACKNOWLEDGEMENTS

I wish to thank the Turkish Ministry of Education for financial support during the course of this research and Professor D.A. Wright for allowing me the use of his laboratory facilities.

I must express my sincere gratitude to Dr. J. Woods for his excellent supervision, inspiration and invaluable advice throughout both the course of the research and the preparation of this thesis.

I would like to thank all my colleagues in the department for their stimulating interest and discussions, and the workshop staff, headed by Mr. F. Spence for their help in the construction and modification of the apparatus. I would also like to thank my wife Inci Gezci for her invaluable encouragement and patient typing of the draft copies of this thesis.

ABSTRACT

The photoluminescent properties of a wide range of single crystals of zinc selenide have been examined at liquid nitrogen and helium temperatures. The crystals were grown either using a continuous flow process or in sealed capsules in controlled partial pressures of zinc and selenium. Crystals doped with a number of acceptor and donor-like impurities have been studied as have nominally pure samples. The object of the work was to determine whether there was any correlation between the observed edge emission spectra and the crystal growth conditions. Transmission and absorption spectra have also been investigated.

At temperatures below 10 K the luminescence emission of ZnSe in the vicinity of the band gap consists of a series of sharp lines and broad bands. The sharp lines are identified as I_1 and I_2 lines which are associated with the recombination of excitons bound to neutral acceptors and donors respectively. At least two different I_1 lines and one I_2 line have been observed. Their origin is discussed.

The broad band emission close to the band gap consists of pairs of series of bands. One component of the pair is the high energy series (HES) while the other is the low energy series (LES). The HES is associated with the recombination of a free electron and a bound hole. This leads to the zero phonon band of the series, the remaining members of the series are longitudinal optical phonon replicas. The LES is associated with distant pair

recombination between electrons bound at shallow donors and holes bound at the same acceptors which are responsible for the HES. The LES also consists of a zero order member and phonon replicas. Three different pairs of high and low energy series have been observed. The appearance of particular pairs is determined by the way in which the crystal was grown rather than by the nature of the impurities added.

From the spectral locations of the HES components three possible acceptor levels with ionisation energies of 0.095, 0.112 and 0.122 eV have been found. In undoped crystals the donor ionisation energy is 32 meV. Chlorine and aluminium impurities lead to donors with ionisation energies of 27 meV while the indium donor has an ionisation energy of 29 meV. The mean separation of the donors and acceptors contributing to the distant pair band is estimated to be of the order of 100 Å.

A number of luminescence bands associated with deep centres have also been studied, in particular in crystals doped with copper or manganese. The origin of these bands is discussed.

CONTENTS

CHAPTER 1

PROPERTIES OF ZINC SELENIDE

1.1 Introduction

Zinc selenide is a member of the group of compounds, which are formed from the elements of group IIB and VIB of the periodic table. Most of these compounds are semiconductors or insulators which crystallise in an arrangement where each atom is at the centre of a regular tetrahedron. In ZnSe each atom is spaced 2.45Å distant from the nearest neighbouring atoms of the opposite kind which lie at the corners of the tetrahedron. The tetrahedra can either be arranged into a cubic zinc blende form, with the Td^2-F $\bar{4}$3m space group, or into a hexagonal, wurtzite form with space group C^4_{6v} - $P6_3mc$. The most stable phase of ZnSe is the cubic blende type structure in which the Zn and Se atoms each lie on a face-centred cubic sub-lattice, the two sub-lattices being displaced relative to one another by one quarter of the body diagonal of the cube. The lattice parameter in the cubic modification is a=5.6687Å (1). ZnSe can also exist in the hexagonal modification, depending on the methods of synthesis used, the growth temperature, and subsequent heat treatment (2,3,4).

The electrical and optical properties of zinc selenide can be explained in terms of the electronic band structure, which unfortunately has not yet been firmly established. However the physical properties of interest in this thesis, depend only on the form of the maximum of the valence band or the minimum of the conduction band which in ZnSe are at k=0 at the centre of the Brillouin zone. The normally accepted values for the direct energy gap at

temperatures of 300 K (room), 79 K (near liquid nitrogen), 60 K (near pumped liquid nitrogen), and 4.2 K (liquid helium) are 2.67, 2.809, 2.813 and 2.818 eV respectively (5,6).

Pure stoichiometric zinc selenide is normally n-type with a resistivity of the order of 10^{+12} ohm-cm, so that it is an insulator at room temperature. However, lattice defects and deliberately introduced impurities lead to deviations from stoichiometry in the ZnSe crystal so that impurities greatly affect the electrical and optical properties. The effects of such imperfections and some information concerning the band structure are described in this chapter. The principal properties and applications of zinc selenide crystals are also reviewed.

1.2 Effects of crystal imperfections in ZnSe

In general the II-VI compounds are less pure than the group IV elemental semiconductors such as Si or Ge, or the III-V compounds, because the well established purification methods used with these semiconductors cannot be utilized. This is because most II-VI compounds can only be melted under high pressure, therefore crystal growth from the melt involves high temperatures with the attendant possibilities of container contamination, and decomposition leading to non-stoichiometry. In consequence crystals are grown by sublimation or by high temperature vapour reaction of the elements. Although the resultant crystals are of high purity, trace contamination of the order of 1 ppm is still present. Comparatively little is known about the properties of substitutional impurities in ZnSe.

Various investigators have attempted to study the mechanism of crystal growth by examining the crystal morphology, crystal surfaces, and structural imperfections. Crystalline imperfections such as dislocations, twinning, stacking faults and low angle boundaries have been discussed by Gezci and Woods (7).

The most important point defects are probably lattice vacancies and interstitials. Anion vacancies and cation interstitials would be expected to introduce donor states in the energy gap, while cation vacancies and anion interstitials would introduce acceptor states. Foreign elements such as the halogens are important impurity defects. Shallow donor levels some 0.19 eV below the conduction band are formed when chlorine is substituted for selenium (8). The Group III, metals such as Al, Ga and In substituted for zinc produce similar shallow donor levels. An important defect centre is also formed from an association of a donor impurity ion and a zinc lattice vacancy in nearest neighbour configuration (8,9). This is the so-called A-centre and is thought to be responsible for self-activated luminescence.

Substitutional impurity ions from group IB (Cu, Ag, Au) form acceptors because they readily accept an electron from the covalent band structure (10). Copper and manganese impurities are well known as luminescent activators while Fe, Ni and Co act as killers both of luminescence and photoconductivity (11,12). Divalent copper ions form double acceptors while zinc vacancies form acceptors with very similar properties.

1.3 Band structure of ZnSe

The band structure of ZnSe crystals has been calculated by a variety of methods and some extremely useful review articles have been written by numerous workers (13-38) in this field. Calculations are normally concerned with the energy separation between the s-like conduction band states and the p-like valence band states. The conduction band of zinc selenide may be considered to originate from the 4s atomic levels of the zinc ions while the valence band originates from the 4p atomic levels of the selenium ions. The zinc blende structure is identical to the diamond structure as far as the Brillouin zone is concerned. The main difference between the energy bands of diamond and zinc blende (see Figure 1.1) is at the point X=(1,0,0) $2\pi/a$ of the Brillouin zone (Figure 1.2) where the extra degeneracies associated with diamond are lifted. Herman (14 a,b,c) developed a semi-empirical method of deducing the electronic energy band structure of zinc blende materials from those of the diamond type materials, germanium and silicon.

The Brillouin zone of the zinc blende structure is a truncated octahedron which is shown in Figure 1.2. The constant energy surfaces consist of a number of ellipsoids, which lie at the symmetry points corresponding to the minimum values of electron energy. The high symmetry points and lines of the Brillouin zone are the zone centre (Γ), and the intersections with the zone faces (L, X, K) on the [111], [100] and [110] symmetry axes respectively. The deepest minima may also occur inside the zone along the symmetry axes and it is thought that for the conduction band of ZnSe there are two minima, Γ_1 and Γ_{15} at k=0, which correspond

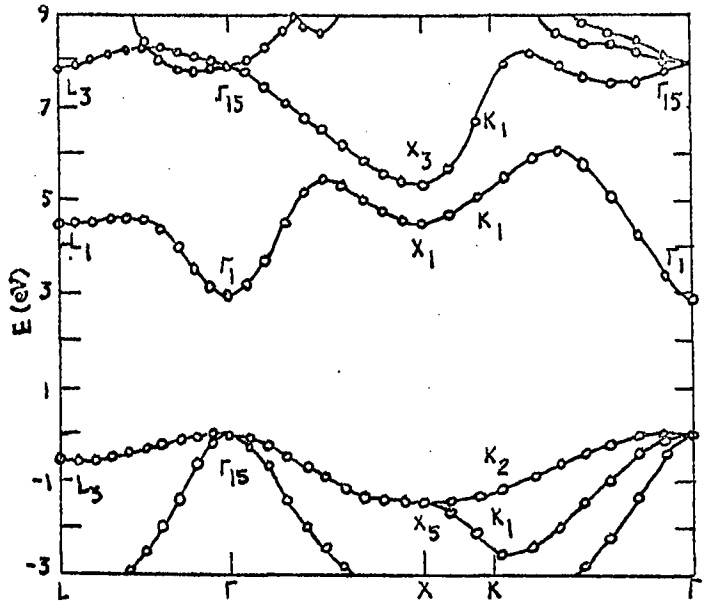

Figure 1.1 Energy band structure of ZnSe along the [111], the [100], and the [110] symmetry axes calculated by the pseudo-potential method (39)

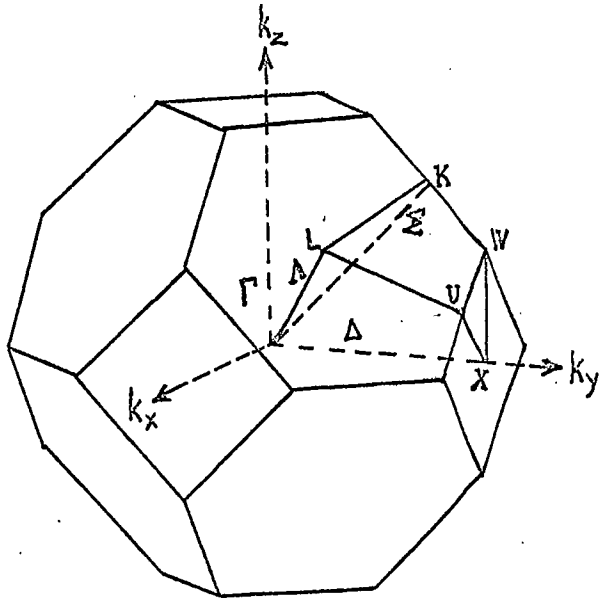

Figure 1.2 The Brillouin zone for the lattices with the translational symmetry of a face centred cubic lattice.

to two- and sixfold spin degeneracy. The Γ_1 level is associated with the s-electrons and Γ_{15} with the p-electrons. The other positions in k-space where the lowest minima can be observed on the [111] symmetry axis are at L_1 or L_3 and also on the [100] symmetry axis at X_1 and X_3 in the conduction bands, but the energy gap is rather wide along the [100] symmetry axis.

The best estimate of the configuration of the conduction and spin-orbit split valence bands of a zinc blende crystal near k=0 is shown schematically in Figure 1.3. The irreducible representations for the single groups are given within the parentheses. The dashed curves in the upper valence bands represent the effects of the small linear terms (15). The valence bands of zinc selenide have two nearly parabolic bands with different curvatures touching at centre of the zone. The Γ_8 term splits into two bands resulting in a heavy hole band, V_1, and a light hole band, V_2, which are four fold spin degenerate. The lowest valence band state (Γ_{15}) which forms the V_3-band is twofold spin degenerate.

In ZnSe the concept of the Fermi surface is relatively unimportant, although it plays a role in highly doped ZnSe crystals. Optical methods provide the major tools for investigating the electronic band structure of ZnSe. Absorption and reflection measurements yield the frequency dependent dielectric constant which depends on the joint density of states of the valence and conduction bands (16). Two-photon absorption gives additional information since the selection rules are different from those in a simple absorption measurement (17). Photoemission

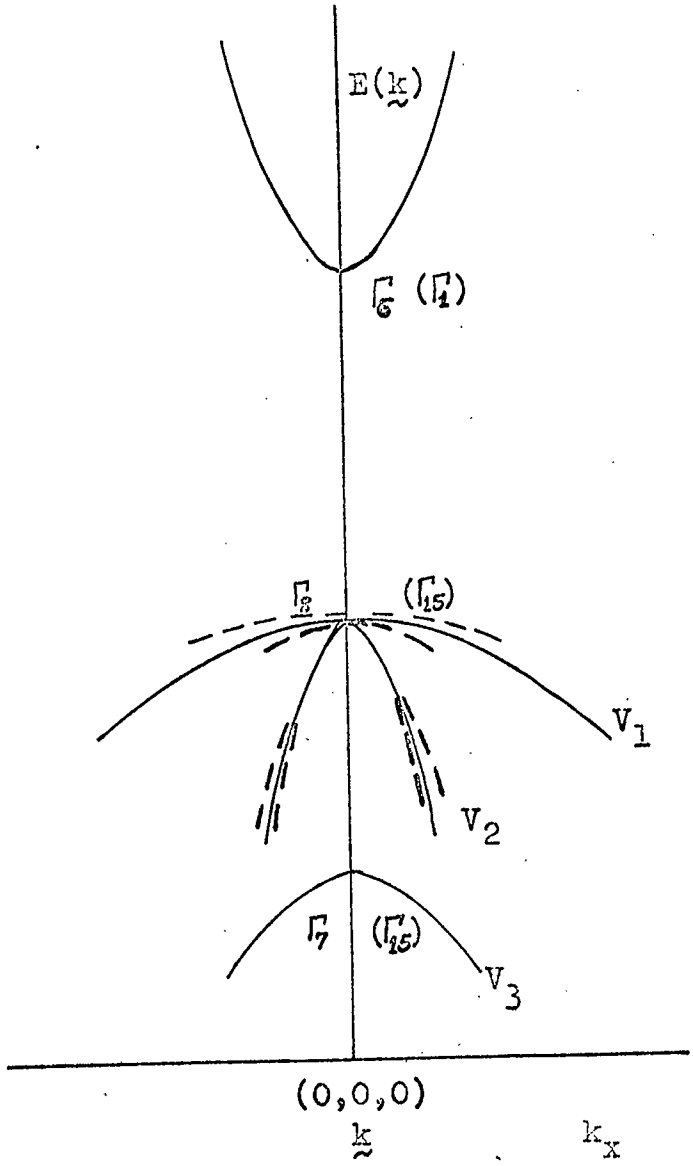

Figure 1.3 The conduction and spin-orbit split valence bands of a zinc blende crystal around k=0.

experiments yield information about the density of states in a rather involved form (18). Edge emission measurements help to identify energy levels associated with defects which perturb the lattice (19). All these methods may be extended by using an externally applied field so that the selection rules are changed, or energy levels split.

In the one-electron approximation the energy spectrum and wave functions in the Brillouin zone are sufficient to explain excitons (20), the line width and shape of absorption peaks (21), and the behaviour of acceptor or donor states (19). The energy band scheme can be used successfully as a starting point if the electron-hole, electron-electron and electron-phonon interactions are not too strong. The effective mass approximation is extremely valuable in the description of transport properties of semiconductors (22). Electronic charge densities in ZnSe may be calculated using wavefunctions resulting from band calculations (23) and these have been compared with X-ray measurements (24,25).

The methods which have been employed to calculate the band structure of zinc selenide may be summarised as follows:-

1. The OPW method: (26,27,28). This uses Herring's idea that the crystal wavefunction is plane-wave-like in the interspace between the atoms constituting the crystal, and a mixture of the plane-wave and core states within the electron shells of the ions.

2. The APW method: (29,30). In this approximation the crystalline wave functions are plane-wave-like in the space between ions and similar to atomic functions in the close neighbourhood of the nuclei.

3. KKR method: (31,32,33). The method named after Korriga, Kohn and Rostoker (31), has long been considered mathematically fascinating but in practice is inferior to other methods such as OPW and APW.

4. The pseudopotential scheme (34,35,36). This method was the most revolutionary scheme in the history of band structure theory. The idea is based on the OPW formalism. Historically two developments were made in the construction of pseudopotentials. The first, which one might call the semi-empirical method, falls back on experimental data provided by atomic spectroscopy to define a model potential. The second, often called the fully-empirical method, fits pseudopotentials directly to solid state data and is based on the free-electron exchange approximation.

5. The LCAO method and mixed schemes: (37,38). The tight-binding or LCAO (linear combination of atomic orbitals) method is frequently employed today. Successful application of this method is restricted to flat bands, such as the valence bands of molecularly bonded semiconductors or ionic crystals.

The first electronic band structure calculation for ZnSe was done using the empirical pseudopotential method (39). The authors calculated the band structure of zinc selenide and thirteen other semiconductors with the zinc blende structure, essentially by fitting to experimental data on the reflectivity and photoemission (40,41).

The application of the empirical pseudopotential method and the calculation of the electronic structure of some II-VI semiconductors have been reviewed by Cohen (35). Results were presented for CdTe, ZnS, ZnSe with the zinc blende structure. Herman et al (27) calculated the

electronic band structure for nine cubic II-VI compounds using the perturbed energy band model. They evaluated band structures for cubic zinc selenide which made use of the experimental work on photoemission by Aven et al (41) and of the reflectivity data collected by Pollak (42). Walter et al (43) reported details of the reflectivity data for cubic ZnTe and ZnSe at 15 K and 300 K. Their relativistic energy band structures for ZnTe and ZnSe were calculated using the empirical pseudopotential method, modified by spin-orbit coupling. They also calculated the imaginary part of the frequency dependent dielectric function, the reflectivity and the logarithmic derivative of the reflectivity R'(W)/R(W).

Shortly afterwards the energy band structure of ZnSe was calculated by means of a Green's function method (KKR) by Treusch et al (44) using the muffin-tin potential. Their results explained the most important optical transition from the d-bands to the conduction band.

Collins et al (45) calculated the band structure of hexagonal ZnSe using the spin-orbit matrix elements and the crystal field splittings of the valence bands. Stukel et al (13) reported the highly self-consistent OPW band calculation for cubic ZnSe and compared their results with experimental and other theoretical results. Table 1.1 lists the various values of the theoretical energy levels which have been calculated for cubic ZnSe using the schemes described above (13).

Measurements of the effective mass can be used to provide information about the curvature of the bands in which the carriers move and hence electron (m_e^*) and hole (m_h^*)

Table 1.1 Comparison of various theoretical energy-level schemes for cubic ZnSe.

Level	SC-OPW	NSC-OPW	ER-OPW	ER-KKK	Pseudo Calc. (est)
$\Gamma 15c$	6.7	7.6	7.7	8.0	7.9
$\Gamma 1c$	2.9	3.2	2.8	2.9	2.9 (2.9)
$\Gamma 15v$	0.0	0.0	0.0	0.0	0.0
Zn 3d	-12.6	-5.3	-6.3	-7.1	
X_{3c}	4.5	5.1	5.4	5.1	5.4
X_{1c}	4.2	5.0	4.2	4.9	4.5
X_{5v}	-1.7	-1.3	-1.4	-1.6	-1.5
X_{3v}	-4.3	-3.7	-3.4	-4.0	
$X_{3c}-X_{5v}$	6.2	6.4	6.8	6.7	6.9 (7.2)
$X_{1c}-X_{5v}$	5.9	6.3	5.6	6.5	6.0 (6.4)
$X_{3c}-X_{1c}$	0.3	0.1	1.2	0.2	0.9 (0.8)
L_{3c}	7.4	8.1	8.1	8.5	7.9
L_{1c}	3.8	4.3	4.5	4.3	4.5
L_{3v}	-0.6	-0.5	-0.4	-0.7	-0.5
L_{1v}	-4.4	-3.8	-3.7	-4.2	
$L_{3c}-L_{3v}$	8.0	8.6	8.5	9.2	8.4 (8.4)
$L_{1c}-L_{3v}$	4.4	4.8	4.9	5.0	5.0 (5.0)

effective masses clarify the details of the band structure at certain symmetry points. The conduction band at k=0 is well described by the electron effective mass (m^*_e) and the maximum energy in the valence band may be represented as two sets of spherical surfaces each corresponding to a scalar effective mass. One of these effective masses m^*_{h1} is much larger than the other and the corresponding holes are generally referred to as the heavy holes. A similar effective mass m^*_{h2} corresponds to the light holes. The first rough estimates of electron and hole effective masses were obtained by Aven et al (41) using the electron and hole mobilities of ZnSe, combined with the reduced mass of the exciton. They found an exciton reduced mass μ = (0.10±0.03) m and calculated effective masses of m^*_e = 0.1 m, and m^*_h = 0.6 m. Aven and Segall (8) obtained better estimates of the electron effective mass by fitting the observed temperature variation of the mobility to the variation predicted by optical mode scattering. The effective mass was approximately 0.15 m. Subsequently Marple (46) determined an electron effective mass of (0.17±0.02) m from measurements of infra-red Faraday rotation. Quite recently Merz et al (9) have measured the effective electron mass from the Zeeman splitting of the 2p states of the donors and they found its value to be (0.16±0.01) m for ZnSe.

1.4 Electrical Properties of ZnSe

1.4.1 Introduction

Measurements of the electrical properties of ZnSe provide valuable information concerning the band structure,

the density of carriers and the electron scattering processes. These in their turn provide information about electron-phonon interactions and specific impurity states. Although considerable interest has been shown in the photoluminescence and electroluminescence of ZnSe, little work has been carried out on its transport properties. The resistivity of ZnSe is a function of its state of purification. The resistivity of as grown crystals is very high ($\sim 10^{14}$ ohm-cm) but this can be reduced to 10-100 ohm-cm by heating in molten zinc at 900-1000^{o}C for one or two days. The electrical conductivity is given by $\sigma = ne\mu$. Both the carrier concentration (n) and mobility (μ) vary with temperature. The temperature dependence of the mobility, gives an indication of the operative carrier scattering mechanisms. The principal scattering mechanisms which are likely to affect the mobility are briefly summarized below. This is followed by an account of the effects of the absorption of radiation on the conductivity.

1.4.2 Mobility

The mobility of electrons in ZnSe is limited fundamentally by the scattering of conduction electrons by lattice vibrations. Table 1.2 summarizes the temperature dependences of mobility to be expected for the various lattice and impurity scattering mechanisms:-

1. Lattice scattering: Lattice scattering processes are those which result from the interaction of electrons (or holes) with lattice vibrations. Charge carriers travelling through a crystal have their mobility limited by their interaction with the thermal vibrations of the ~~initial~~ lattice.

Table 1.2 The temperature dependence of mobility for the principal carriers scattering mechanisms in II-VI compounds.

Scattering Mechanism	Dependence of mobility		References
	Absolute Temp. (T)	Effective mass m*	
Lattice: polar optical mode	(exp T)	$m^{*-3/2}$	47
: deformation potential (or acoustic mode)	$T^{-3/2}$	$m^{*-5/2}$	48,49
: Piezoelectric mode	$T^{-\frac{1}{2}}$	$m^{*-3/2}$	50,51
: Inter-Valley	$T^{-3/2}$ uncertain see reference		52
Impurity: Unionized	Sometimes determines the mobility at low temperature	m*	47
: Ionized	$T^{3/2}$	$m^{*-\frac{1}{2}}$	53
Ionized dislocation	Linear temp. dependence	m*	54

The lattice can vibrate in both acoustical and optical modes. More thermal energy is required to excite optical mode vibrations which are important in scattering electrons in ionic crystals. At moderate temperatures acoustic vibrations become increasingly important. Since cubic ZnSe has no centre of inversion symmetry a piezo electric polarisation is developed by the strain associated with acoustic vibrations, this process leads to a mobility which varies as $T^{-\frac{1}{2}}$, and is known as piezoelectric scattering. Deformation potential scattering by acoustic phonons is relatively unimportant in limiting the majority carrier mobility in cubic II-VI compounds.

2. Impurity scattering: Impurity scattering processes naturally depend upon the nature of the impurity atoms and structural imperfections in the crystal lattice. The presence of an impurity in a crystal will usually alter the electrostatic potential in its neighbourhood and create an aperiodicity in the potential field. Ionized impurity scattering is usually the dominant scattering process at low temperatures, the mobility is dependent on the concentration of impurities and varies as $T^{3/2}$. Neutral impurity centres may give rise to appreciable scattering effects. However, this process is independent of temperature and hence may be of importance at low temperatures when lattice scattering is negligible and most of the impurities are unionized.

Other mobility limiting processes such as carrier-carrier scattering, ionized dislocation scattering and inter-valley scattering have been discussed in relation to ZnSe but are relatively unimportant.

The first optical and electrical measurements on ZnSe crystals were reported by Aven et al (41). They measured the electron and hole mobilities, and obtained values of μ_e = 260 $cm^2\ V^{-1}\ sec^{-1}$ at 300 K, and μ_h = 15 $cm^2\ V^{-1}\ sec^{-1}$ at 473 K. They also obtained a rough estimate of the effective masses of electrons and holes, viz. m_e^* = 0.1 m, m_h^* = 0.6 m. Aven and Segall (8) measured the temperature dependence of the Hall mobility of electrons and found $\mu_e \sim 720$ $cm^2\ V^{-1}\ sec^{-1}$ at 100 K. They thought that optical mode scattering was dominant and that the piezoelectric and deformation potential scattering processes were negligible. Fukuda and Fukai (55) measured the Hall mobility of electrons in ZnSe and at low temperatures observed values of about 3000 $cm^2\ V^{-1}\ sec^{-1}$ at 75 K, which were higher than values predicted by ionized impurity scattering. They assumed that neutral impurity scattering was important in the low temperature range, while polar optical processes were dominant at room temperature.

The resistivity and Hall coefficient of cubic zinc selenide crystals were measured by Smith (56) at temperatures between 500-1000°C in zinc vapour. The values of Hall mobility obtained did not depend on carrier concentration, or vary appreciably from sample to sample. However, he found good agreement between his experimental results and the theoretically calculated mobility. He suggested that if the observed values of mobility were extrapolated to room temperature, the mobility should be about 500 $cm^2\ V^{-1}\ sec^{-1}$. Such a value has in fact been observed (57).

Woodbury and Aven (58) obtained a maximum mobility of 2700 $cm^2\ V^{-1}\ sec^{-1}$ at 55.6 K with their samples, while

Aven and Kennicott (59) found higher values of about 7000 $cm^2\ V^{-1}\ sec^{-1}$ at 200 K. A higher value still of about 12000 $cm^2\ V^{-1}\ sec^{-1}$ at 50 K was reported by Aven (60). This improvement in the magnitude of the electron mobility is due partly to improved purity of the crystals and partly to the discovery of a technique of annealing out native doubly charged defect centres which are responsible for a large fraction of the total ionized impurity scattering. Aven used a standard 6 probe measuring technique and annealed his crystals in liquid zinc at 650°C for 152 hours. In Figure 1.4 the temperature dependence of Hall mobility in n-type ZnSe, as measured by Aven (60), is illustrated. The experimental results (solid line with points) are compared with a theoretical curve which takes ionized impurity and polar optical mode scattering into account. The agreement is not too unreasonable but it would appear that some additional process must be operative.

1.4.3 Photoconductivity

Free electrons and holes can be created in semiconductors by illuminating the crystal with light of appropriate wavelength such that the photon energy equals or exceeds the forbidden gap energy. Under these conditions free electrons and holes are produced and lead to an increased conductivity of the crystal. In ZnSe the holes are generally very much less mobile than the electrons, and are captured more readily by defect centres, so that in the steady state the concentration of free electrons exceeds that of the free holes. Defect centres can behave either as recombination centres or electron traps and determine the

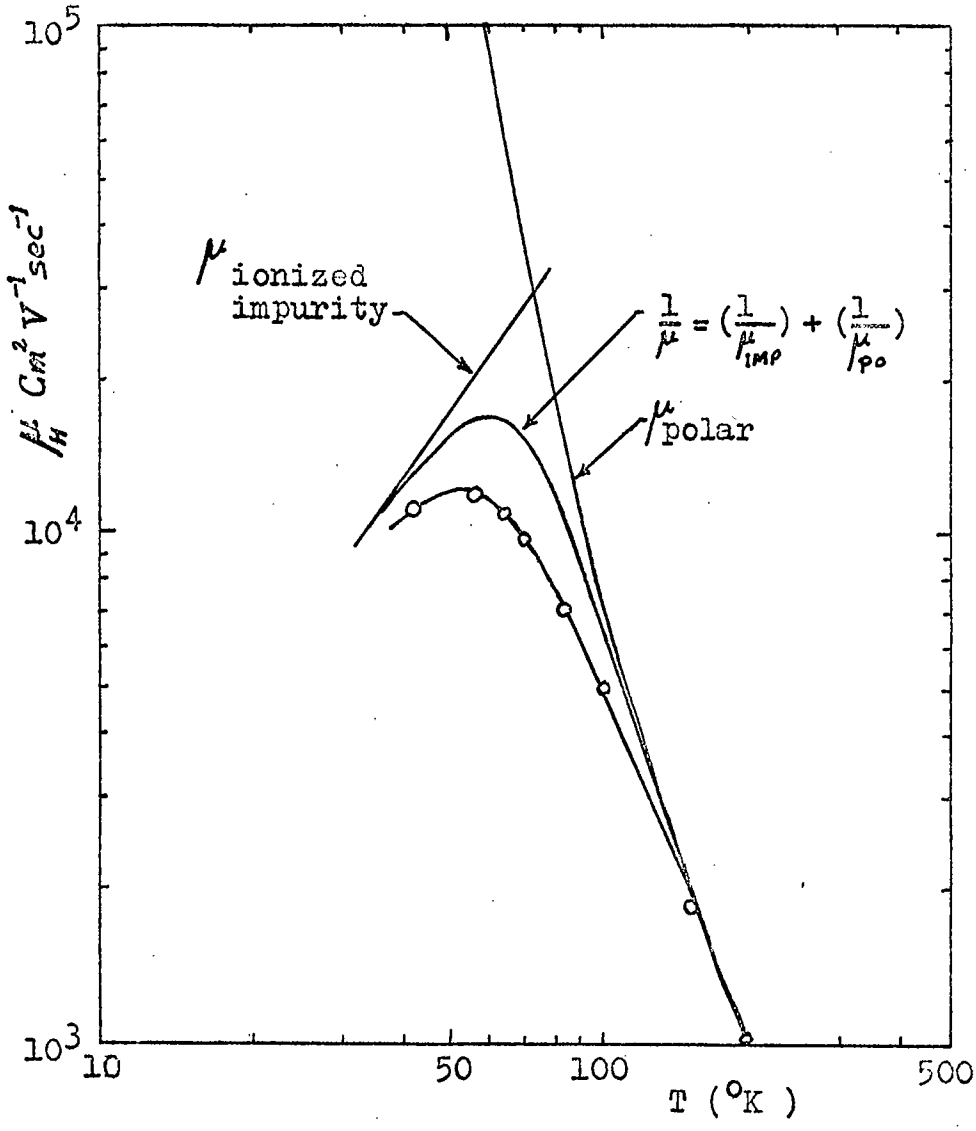

Figure 1.4 The temperature dependence of Hall mobility in ZnSe.

lifetime of the majority carriers. Majority carrier lifetimes in ZnSe vary from fractions of microseconds in insensitive "pure" crystals to fractions of milliseconds in suitably doped material.

An energy model has been proposed by Rose (61) to explain the sensitisation of photoconductivity on the basis of two competing centres A and B as shown in Figure 1.5. In a pure unsensitized material, recombination centres known as "A centres" are present. These lead to a small free lifetime for photo-excited carriers, since they have an approximately equal capture cross-section for both electrons and holes. With the incorporation of suitable impurities recombination centres known as "B centres" are produced. These centres have a small cross-section for electron capture but their cross-section for hole capture is similar to that of the "A centres." At high temperatures and with low light intensities, the demarcation level for "B centres" will lie above these levels and the imperfections will therefore function as hole traps only, with no consequent effect on the photo-sensitivity. However at high light levels and at low temperatures, the hole demarcation level will lie below the levels of the "B centres" which then function as recombination centres. The concept of the "demarcation level" was introduced by Rose (61). When the demarcation level coincides with the energy level of a centre, there is an equal probability of the centre acting as a trap or as a recombination centre. The hole demarcation level always lies in the lower half of the band gap and below the "A centres." Figure 1.5(a) shows a material containing recombination centres with a large capture cross-section only. This

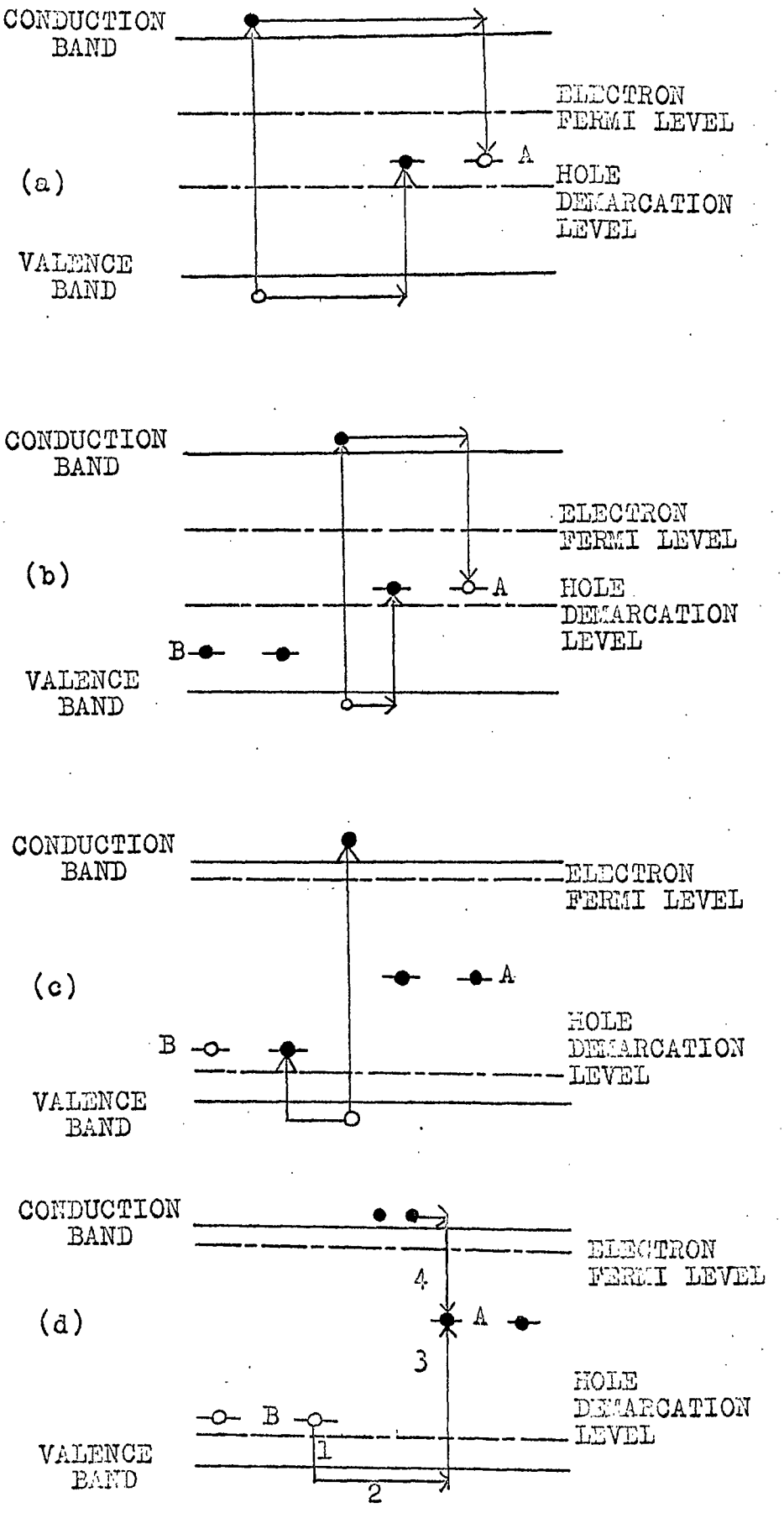

Figure 1.5 Imperfection sensetization of photoconductivity by " A centre " and " B centre".

results in low free carrier lifetimes. In Figure 1.5(b) sensitizing centres have been incorporated but the conditions are such that they act as hole traps. Figure 1.5(c) shows what happens when the sensitizing centres act as recombination centres when they become largely occupied with holes and the "A centres" become occupied with electrons. In consequence the electron lifetime is high. Figure 1.5(d) illustrates the process of infra-red quenching of photoconductivity by the freeing of holes from sensitizing centres by optical means. Thermal quenching occurs when the demarcation level rises above the level B. Thermal and infra-red quenching can be used to obtain information about the energy levels and capture cross-sections of sensitizing centres in ZnSe. At low temperatures the infra-red quenching of photoconductivity in ZnSe consists of one broad "band", with its maximum at about 1.03 μm. The threshold of this band suggests that the hole ionization energy of a sensitizing centre lies between 0.66 and 0.78 eV above the valence band (62).

The photoconductive properties of cubic ZnSe crystals have been reported by Bube (63) and Stringfellow and Bube (64). The spectral sensitivity of undoped ZnSe crystals reached a maximum at 0.462 μm corresponding to excitation across the forbidden gap. With the introduction of different acceptor and donor impurities, such as Br, Cu, Ag, Sb and As, the maximum sensitivity was shifted to longer wavelengths. Bube and Lind (2) measured the spectral sensitivity of photoconductivity and infra-red quenching. They found a donor ionization energy of 0.21 eV in Br doped ZnSe and an acceptor ionization energy of 0.7 eV in Sb doped ZnSe. Ag and As doped ZnSe crystals have been studied by Bube (63). They

give rise to acceptor centres with hole ionization energies of 0.6 and 0.7 eV respectively. Photoconductivity spectra have been extensively studied in Cu doped crystals. Stringfellow and Bube (64) have observed the excitation of p-type photoconductivity in Cu doped crystals and noted that the energy required is similar to that for the optical quenching of n-type photoconductivity. They associated this behaviour with copper centres located 0.72 eV above the valence band. Stringfellow and Bube (65) subsequently discussed a multivalent-copper-impurity model in which Cu^{+} and Cu^{++} ions were substituted on the Zn sublattice. They suggested that Cu^{+} ions were responsible for the two red bands with maxima at 1.95 and 1.97 eV and that Cu^{++} ions were responsible for the green emission at 2.34 eV. They also concluded that copper leads to three charged states within the forbidden gap of ZnSe. The first copper state is the dominant acceptor centre for p-type conductivity, with an associated energy level 0.72 eV above the valence band. This centre is the major sensitizing centre for n-type photoconductivity and has an electron capture cross section of about 4.10^{-19} cm^{2}. The second copper state fixes the lowest obtainable position of the Fermi level at 0.53 eV above the valence band. Green emission associated with copper impurity results from the recombination of an electron in the conduction band with a hole captured at a third copper state, located 0.35 eV above the valence band.

Park and Chan (66) observed the spectral response of the photoconductivity of hexagonal ZnSe at room temperature using polarized light. They found two different high energy peaks near the energy band gap, at about 0.437 μm and 0.443 μm.

This corresponds to the separation between the two highest valence bands in ZnSe.

1.4.4 Electroluminescence

Electroluminescence is the name given to the emission of light from a solid under the action of an electric field. The preparation of electroluminescent ZnSe owes much to the techniques developed to produce phosphors suitable for cathodoluminescence and photoluminescence. In general the zinc selenide is doped with small quantities of activators (usually aluminium, manganese, copper or chlorine), and has been used as a powder in large area a.c. electroluminescent panels or as a single crystal in small d.c. light emitting diodes.

Light-emitting semiconductor diodes based on GaAs-P usually consist of p-n junctions, in which minority carriers are injected across the junction and recombine at luminescent centres. ZnSe cannot be made sufficiently p-type, for a p-n homojunction to be formed in ZnSe. However Aven and Cusano (67) have prepared p-n junctions by depositing an epitaxial layer of p-type Cu_2Se on to n-type ZnSe. The electroluminescent emission spectrum of junctions formed on chlorine doped ZnSe consisted at 77 K of three bands at 1.96 eV in the red, at 2.35 eV in the green and at 2.68 eV near the band edge. Al doped ZnSe produced a single yellow band at 2.07 eV at room temperature. Similar heterojunctions with Cu-chalcogenides have also been reported with ZnS. Unfortunately the electroluminescence efficiency is not particularly good. Fischer (68) observed emission in a band at 1.97 eV with n-type undoped ZnSe crystals, and showed

that the metal semiconductor contacts produced light by impact ionization in reverse bias, and by hole injection in forward bias, if the work function of the contacting metal exceeded 4.8 eV (e.g. Pt or Ir). More recently Allen et al (69) have prepared Schottky diodes which are electroluminescent when biassed in the reverse direction. They used Au and In contacts on Mn or Cu doped n-type ZnSe. Their electroluminescent spectrum consisted of a red band at 1.91 eV in Cu doped ZnSe and a yellow band at 2.10 eV in Mn doped ZnSe crystals. According to Allen et al, electrons tunnel from the gold into the ZnSe where they are accelerated in the high field of the Schottky barrier. The manganese activation centres are then excited by impact and electroluminescence results. Work on such devices is proceeding in these laboratories and the need to understand the basic luminescent properties of ZnSe which is suitable for this application was one of the incentives for studying edge and deep centre emission.

1.4.5 Electron Spin Resonance

Under certain circumstances electron spin resonance can be a powerful method of investigating the chemical nature, the crystalline symmetry and the electronic structure of paramagnetic defects in solids. The spin resonance effects which have been observed in ZnSe can be divided into three classes:-

1. Mobile electrons: The mobile conduction electrons represent the most elementary source of paramagnetism in a solid. The mobile electrons move either in the conduction band or in a shallow donor band. Such donor states are

formed by substitutional halogen or group III metal ions such as Cl, Br, I, Zn, Al and Ga. Free electron resonance has been observed in cubic ZnS (70,71) and in cubic ZnS/ZnSe mixed crystals (72). Donor resonance in ZnSe due to a centre which is an association of a Se vacancy and a P, As or Sb acceptor centre has also been observed (73).

2. "Deep" impurity centres which are normally diamagnetic can exist in the crystal. Such a centre can often be converted into a paramagnetic state by trapping a photo-excited electron or hole. Subsequently, a conduction electron may recombine with the trapped hole, leading to a characteristic luminescence band in the visible region. "Deep" impurity defect centres commonly known as "A centres" have been found in ZnS (70,74), ZnSe (75) and mixed ZnS/ZnSe (72) crystals. They are formed by the association of a negatively charged zinc vacancy with Cl^-, Br^- or I^- impurity ions on nearest neighbour sulphur or selenium sites, or with Al^{+3} or Ga^{+3} impurity ions on nearest zinc sites. The A-centres are thought to be responsible for the self-activated emission of ZnS and ZnSe.

3. Transition metal ions: Extensive electron spin resonance investigations have been performed on transition metal impurities in ZnSe. The resonance of the iron group impurities such as Cr^+, Mn^{++} and Fe^{+++} is strongly influenced by the covalency in the bonding and by lattice distortions caused by the size mismatch between the impurity and the ion normally occupying the substitutional lattice site. The electron spin resonance spectrum of Fe^{+++} in cubic ZnSe can be identified by the appearance of a characteristic five-line fine structure pattern, and the spectrum of Mn^{++}

in ZnSe can be identified by the appearance of a six line hyperfine structure. A considerable number of defect centres can be formed by paramagnetic 3d ions, which are often active as electron or hole traps. They can occur either in the monovalent or in the trivalent charge states. Electron spin resonance investigations of 3d ions have been performed mainly on ZnS and CdS. The results may be summarized as follows:

$3d^2$ configuration: Vanadium V^{+++} and Titanium Ti^{++} have been observed in cubic ZnS (75,76). The resonance due to the $3d^2$ configuration is characterized by an effective spin value of s=1.

$3d^4$ configuration: Chromium has been reported in two charge states in ZnSe (77) and has been observed as Cr^{++} with a $3d^4$ electron configuration.

$3d^5$ configuration: An analysis of the hyperfine structure of the $3d^5$ ions Cr^{+}, Mn^{++}, Fe^{+++} in II-VI compounds has been given by Estle and Holton (78). The resonance of Fe^{+++} has been reported (79) in ZnSe. More measurements exist for Mn^{++} in ZnS, than for any other impurity, but Mn^{++} in ZnSe crystal has not yet been reported. Some paramagnetic defect involving Mn^{++} has however been observed by electron spin resonance (73,80). In no case could these centres be positively correlated with any of the Mn^{++} emission bands.

$3d^9$ configuration: Electron spin resonance has failed to establish reliable models for the luminescence centres responsible for the characteristic emission bands of copper activated ZnSe and other II-VI compounds.

1.5 Optical properties of ZnSe

The optical absorption, reflection, transmission and luminescence emission spectra of zinc selenide may be divided into "edge" and "infra-red" components. Since the nature of the edge emission and deep centre luminescence forms the major topic for discussion in this thesis, the optical properties associated with processes which occur near the fundamental absorption edge are considered in detail in the next chapter. Processes which occur at rather longer wavelength are described below:

1.5.1 Infra-red emission and absorption

Halsted et al (8) have reported fluorescent emission bands at 25 K, in undoped ZnSe crystals with maxima at 0.78, 0.63 and 0.56 eV. The structure is attributed to the emission associated with the recombination of an electron from an energy level 0.56 eV above the highest valence band with holes in the three valence bands of ZnSe. An emission band at 1.25 eV in copper doped ZnSe was also reported.

Iida (82) observed green (0.530 μm), yellow (0.570 μm) and red (0.640 μm) bands in the visible and two emission bands at 1.05 and 1.40 micron in the infra-red region, in as grown ZnSe crystals containing Cu impurity. The visible emission bands required excitation across the band gap, whereas the two longest wavelength bands required longer wavelength excitation. It is suggested that infra-red irradiation could excite a hole to the valence band and the released hole could then subsequently recombine with a free electron via a non-radiative centre. This would lead to infra-red quenching

when the sample was irradiated with both band gap and infra-red radiation. The proposed energy level scheme and corresponding transitions are shown in Figure 1.6 (82). "I" corresponds to the red emission due to the recombination of the free electrons with holes bound at "I". "II and III" are responsible for yellow emission which occurs when electrons bound at the levels "II" recombine with holes at levels "III". Infra-red absorption excites an electron from the valence band to levels "IV". The level "V" represents the non-radiative centres through which most free electrons recombine with holes.

The infra-red absorption spectra of ZnSe containing impurities such as Al, Al-Li, Mn and Be have been studied by Ibuki et al and Mitsuishi et al (83,84). They observed six absorption peaks (at 0.0487, 0.0481, 0.0445, 0.0429, 0.0424 and 0.0420 eV) the intensities of which depended upon the Al concentration. A study of the effects of heat-treatment on ZnSe and Al-Li doped ZnSe shows that different bands occur when the Li concentration becomes comparable to the Al concentration. Mitsuishi et al (84) suggested that Al occupies the Zn site in ZnSe and acts as a donor, but when Al and Li are used together Al acts as a donor and Li acts as an acceptor, both replacing Zn.

A ZnSe crystal containing phosphorus or arsenic exhibits broad luminescence bands in the red at 1.9 eV and infra-red 1.15 eV (85). The results suggest that the active centre consists of an unassociated phosphorus atom with the excited electronic state lying close to the conduction band edge.

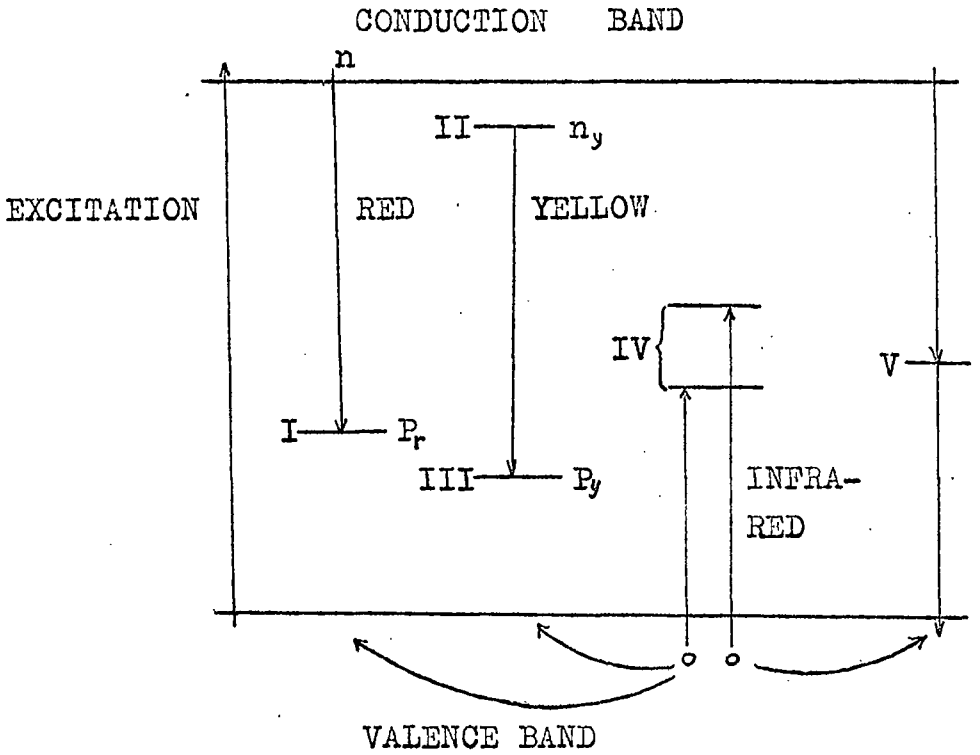

Figure 1.6 Energy level diagram illustrating the processes of recombination, quenching and stimulation.

Miyamoto et al (86) examined the infra-red absorption of undoped ZnSe and ZnSe:Al crystals at liquid nitrogen temperature. They observed weak infra-red absorption in undoped ZnSe which disappeared after the crystal had been fired in a selenium atmosphere. Therefore they suggested that in undoped ZnSe, selenium vacancies are responsible for the photo-induced infra-red absorption which is ascribed to the electronic transition from the neutral donor state of the selenium vacancy to the conduction band.

Most studies of the infra-red properties of ZnSe have been carried out near liquid nitrogen temperature at 77 K. As the temperature is decreased the intensity of the infra-red emission is generally reduced and the edge emission becomes intensive. There is a host of evidence indicating that substantial zinc vacancies are responsible for the infra-red properties of ZnSe.

CHAPTER 1

REFERENCES

1. A.G. Fischer and R.J. Paff, in 'Phys. & Chem. of II-VI Compounds" ed. M. Aven and J.S. Prener (N.Holland) 1967, Ch. 3.
2. R.H. Bube and E.L. Lind, Phys. Rev. 110 (1958) 1040.
3. E.F. Gross, L.G. Suslina and P.A. Kon'kov, Fiz. Tver. Tela 4 (1962) 396, (English transl: Soviet Phys-Solid St. 4 (1962) 287).
4. H. Hartmann, Kristal und Technick 5,4 (1970) 527.
5. M. Cardona, in 'Phys. & Chem. of II-VI Compounds' ed. M. Aven and J.S. Prener (N.Holland) 1967, Ch. 7.
6. G.E. Hite, D.T.F. Marple, M. Aven and B. Segall, Phys. Rev. 156 (1967) 850.
7. S. Gezci and J. Woods, J. Mat. Sci. 7 (1972) 603.
8. M. Aven and B. Segall, Phys. Rev. 130 (1963) 81.
9. J.L. Merz, H. Kukimoto, K. Nassau and J.W. Shiever, Phys. Rev. B, 6 (1972) 545.
10. M.R. Brown, A.F.J. Cox, W.A. Shand and J.M. Williams, J. Phys. C: Sol. St. Phys. 4 (1971) 2550.
11. J.H. Haanstra, in 'II-VI Semiconducting Compounds' ed. D.G. Thomas (New York: Benjamin) 1967 p.207.
12. D. Curie and J.S. Prener, in 'Phys. & Chem. of II-VI Compounds' ed. M. Aven and J.S. Prener (N.Holland) 1967, Ch. 9.
13. D.J. Stukel, R.N. Euwena and T.C. Collins, Phys. Rev. 179 (1969) 740.

14a. F. Herman, Phys. Rev. 95 (1954) 847.

14b. F. Herman, J. Electron 1 (1955) 103.

14c. F. Herman, R.L. Kortum, C.D. Kugling and J.L. Shay in 'II-VI Semiconducting Compounds' ed. D.C.Thomas (New York: Benjamin) 1967 p.503.

15. B. Segall in 'Phys. & Chem. of II-VI Compounds' ed. M. Aven and J.S. Prener (N.Holland) 1967, Ch.1.

16. J.C. Philips, in 'Sol. St. Physics' ed. F. Seitz and D. Turnbull (New York: Academic Press) 18 (1966) 56.

17. D. Fröhlich, 'Festkorperprobleme' Advancas in Sol. St. Phys. ed. O. Madelung (Braunschweig: Pergamon) 10 (1970) 227.

18. U. Gerhardt, ibid 10 (1970) 175.

19. H.J. Queisser, ibid 11 (1971) 45.

20. R.S. Knox, Sol. St. Phys. ed by F. Seita and D. Turnbull (New York: Academic Press) Suppl. 5 (1963) 1.

21. Y. Toyozava, Prog. Theor. Phys. Suppl. 12 (1959) 111.

22. J.M. Luttinger and W. Kohn, Phys. Rev. 97 (1955) 869.

23a. J.P. Walter and M.L. Cohen, Phys. Rev. B. 2 (1970) 1821.

23b. J.P. Walter and M.L. Cohen, Phys. Rev. B. 4 (1971) 1877.

24. S. Göttlicher and E. Wölfel, Z. Elektrochem 63 (1959) 891.

25. J.R. Weiss and W.C. Phillips, Phys. Rev. 176 (1968) 900.

26. C. Herring, Phys. Rev. 57 (1940) 1169.

27. F. Herman, R.L. Kortum, C.D. Kuglin and J.L. Shay, 'II-VI Semiconducting Compounds' ed. D.G. Thomas (New York: Benjamin) 1967, p.503.

28. F. Herman, R.L. Kortum, C.D. Kuglin and J.P. Van Dyke, 'Methods in Computational Physics' (New York: Academic Press) 8 (1968) 193.

29. J.C. Slater, Phys. Rev. 51 (1937) 846.

30. J.O. Dimmock, Sol. St. Phys. ed. H. Ehrenreich, F. Seitz and D.Turnbull (New York: Academic Press) 26 (1971) 104.

31. J. Korringa, Physica 13 (1947) 392.

32. W. Kohn and N. Rostoker, Phys. Rev. 94 (1954) 1111.

33. A.R. Williams, Phys. Rev. B.1 (1970) 3417.

34. J.C. Phillips, Phys. Rev. 112 (1958) 685.

35. M.L. Cohen, in 'II-VI Semiconducting Compounds' ed. D.G. Thomas (New York: Benjamin) 1967, p.462

36. J.P. Walter and M.L. Cohen, Phys. Rev. 183 (1969) 763.

37. J.C. Slater and G.F. Koster, Phys. Rev. 94 (1954) 1498.

38. F.M. Mueller, Phys. Rev. 153 (1967) 659.

39. M.L. Cohen and T.K. Bergstresser, Phys. Rev. 141 (1966) 789.

40. M. Cardona, J. Appl. Phys. Suppl. 32 (1961) 2151.

41. M. Aven, D.T.F. Marple and B. Segall, J. Appl. Phys. Suppl. 32 (1961) 2261.

42. F.H. Pollak, in 'II-VI Semiconducting Compounds' ed. D.G. Thomas (New York: Benjamin) 1967, p.552.

43. J.P. Walter, M.L. Cohen, Y. Petroff and M. Balkanski, Phys. Rev. B.1 (1970) 2261.

44. J. Treusch, P. Eckelt and O. Madelung, in 'II-VI Semiconducting Compounds' ed. D.G. Thomas (New York: Benjamin) 1967, p.588.

45. T.C. Collins, R.N. Euvema and J.S. DeWitt, ibid 1967, p.598.

46. D.T.F. Marple, J. Appl. Phys. 35 (1964) 1879.

47. S.S. Devlin, in 'Phys. & Chem. of II-VI Compounds' ed. M. Aven and J.S. Prener (N.Holland) 1967, Ch.11.

48. W.W. Piper and R.E. Halsted, Proc. Intern. Conf. on Semiconduc. Physics held in Prague (Czechoslovak Academy of Sciences: Prague) 1960, p.1046.

49. H. Ehrenreich and A.W. Overhauser, Phys. Rev. 104 (1956) 331 and 649.

50. W.A. Harrison, Phys. Rev. 101 (1956) 903.

51. A.R. Hutson, J. Appl. Phys. 32 (1961) 2287.

52. C. Herring, Bell Stst. Tech. Journal 34 (1955) 237.

53. H. Brooks, 'Advances in Elec. and Electron Phys.' ed. L. Marton (New York: Academic Press) 7 (1955) 87.

54. W.T. Read, Phil. Mag. 46 (1955) 111.

55. Y. Fukuda and M. Fukai, J. Phys. Soc. Japan 23 (1967) 902.

56. T.F.J. Smith, Solid St. Comm. 7 (1969) 1759.

57. R.C. Whelan and D. Shaw, Phys. Status Solidi, 29 (1968) 145.

58. H.H. Woodbury and M. Aven, '7th Int. Conf. Phys. Semiconduc.', Paris 1964, p.179.

59. M. Aven and P. Kennicott (unpublished data).

60. M. Aven, J. Appl. Phys. 42 (1971) 1204.

61. A. Rose, 'Concept in Photoconductivity and Allied Problems,' (Inter Science Publishers) 19 (1963) 26.

62. R.H. Bube, 'Phys. and Chem. of II-VI Compounds,' ed. M. Aven and J.S. Prener (N.Holland) 1967, p.655.

63. R.H. Bube, Sol. St. Phys. (Academic Press) 11 (1960) 223.

64. G.B. Stringfellow and R.H. Bube, 'II-VI Semiconducting Compounds,' ed. D.G. Thomas (New York: Benjamin) 1967, p.1315.

65. G.B. Stringfellow and R.H. Bube, Phys. Rev. 171 (1968)903.

66. Y.S. Park and F.L. Chan, J. Appl. Phys. 36 (1965) 800.

67. M. Aven and D.A. Cusano, J. Appl. Phys. 35 (1964) 606.

68. A.G. Fischer, 'Phys. and Chem. of II-VI Compounds,' ed. M. Aven and J.S. Prener (N.Holland) 1967, Ch.12.

69. J.W. Allen, A.W. Livingstone and K. Turvey, Sol. St. Electronics 15 (1972) 1363.

70. P.H. Kasai and Y. Otomo, 'Phys. and Chem. of II-VI Compounds,' ed. M. Aven and J.S. Prener (N.Holland) 1967, Ch. 6.

71. K.A. Müller and J. Schneider, Phys. Lett. 4 (1963) 288.

72. J. Schneider, B. Dischler and A. Räuber, J. Phys. Chem. Sol. 33 (1970) 337.

73. R.S. Title, 'Phys. and Chem. of II-VI Compounds' ed. M. Aven and J.S. Prener (N.Holland) 1967, Ch.6.

74. A. Räuber and J. Schneider, ibid, 1967, Chap. 6.

75. W.C. Holton, M. DeWit and T.L. Estle, 'Int. Symp. on Luminescence,' ed. N. Riehl and H. Kallmann (Verlag Karl Thiemig KG, Munchen) 1966, p.454.

76. J. Schneider and A. Räuber, Phys. Lett. 21 (1966) 380.

77. M. DeWit, A.R. Reinberg, W.C. Holton and T.L. Estle, Bull. Am. Phys. Soc. 10 (1965) 329.

78. T.L. Estle and W.C. Holton, Phys. Rev. 150 (1966) 159.

79. J. Dielman in 'Phys. and Chem. of II-VI Compounds,' ed. M. Aven and J.S. Prener (N.Holland) 1967, Ch. 6.

80. J. Schneider, S.R. Sincar and A. Räuber, 'II-VI Semiconducting Compounds,' ed. by D.G. Thomas (New York: Benjamin) 1967 p.40.

81. R.E. Halsted, M. Aven and H.D. Coghill, J. Electrochemical Soc. 112 (1965) 177.

82. S. Iida, J. Phys. Soc. of Japan 26 (1969) 1140.

83. S. Ibuki, H. Komiya, A. Mitsuishi, A. Manabe and H. Yoshinaga, 'II-VI Semiconducting Compounds,' ed. D.G. Thomas (New York: Benjamin) 1967 p.1140.

84. A. Mitsuishi, A. Manabe, H. Yoshinaga, S. Ibuki and H. Komiya, Progress of Theoretical Phys. Suppl. 45 (1970) 21.

85. A.R. Reinberg, W.C. Holton, M. DeWit and R.K. Watts, Phys. Rev. B, 3 (1971) 410.

86. S. Miyamoto, S. Kawashima and S. Shionoya, J. Phys. Soc. of Japan 24 (1968) 1182 and Bulletin of the NHK Broadcasting Sci. Res. Labs. Report 3 (1969) 156.

CHAPTER 2

EDGE EMISSION IN ZnSe

2.1 Introduction

In general the luminescent emission which occurs near the band gap of II-VI compounds at low temperatures is composed of three different groups of bands. The first group is associated with the radiative annihilation of free excitons and their corresponding phonon replicas. The second group is attributed to emission from bound exciton complexes and their phonon replicas. Finally the third group is composed of a comparatively broad band emission and its replicas which occurs at somewhat lower energies.

The term edge emission is loosely employed to describe radiative recombination processes which occur within several tenths of an electron volt of the energy gap. These processes become increasingly more efficient as the temperature is reduced and depend on the crystal and the intensity of the excitation. The near-band gap emission at 4.2 K consists of several series of sharp lines and broad bands. The sharp lines which are at the higher energy limit of the spectrum have been identified in CdS by Thomas and Hopfield (1) as being associated with the recombination of free and bound excitons.

The spectrum on the low energy side of the exciton lines consists of a series of equally spaced bands separated by the energy of the longitudinal optical (LO) phonon of the host lattice. Usually at least two series and sometimes more appear. Often, two associated series are observed, then the high energy series (HES) is dominant

at high temperature, and is usually attributed to the recombination of free electrons with holes bound to acceptors (2) ("free to bound" recombination). The low-energy series (LES) increases in intensity with decreasing temperature and is interpreted as being due to donor acceptor pair-recombination (the so-called "bound to bound" emission). The major part of this chapter is concerned with a discussion of the origin of the exciton lines and of the components of the HES and LES emission in the edge emission spectrum of ZnSe.

The luminescence of ZnSe is also strongly affected by doping with impurities which produces deep acceptors. This deep centre luminescence is also described at the end of the chapter.

2.2 Exciton emission

A bound electron-hole pair can be produced in the crystal under excitation with energy slightly less than the energy gap. Such bound electron-hole pairs are known as excitons. They are uncharged and can move through the crystal and transport excitation energy. Thus an exciton can travel through the crystal and give up its energy of formation on recombination.

Radiative recombination associated with the recombination or annihilation of "free" and "bound" excitons is responsible for the sharp lines close to the band gap. These free and bound excitons in ZnSe are described below.

2.2.1 Free excitons

The free exciton may be though of as an excited state

of the crystal consisting of an electron and hole in orbit about each other at distances large compared with the atomic dimensions. The recombination of the electron and hole may result in the emission of a photon with an energy equal to the band gap energy less the binding energy of the exciton E_{ex}. Similarly, a photon with an energy $E_G - E_{ex}$ may be absorbed to create a free exciton. The free exciton can be treated in the same way as a free hydrogen atom, when it becomes clear that it can exist in a number of excited states with energies given by

$$E_{ex} = 13.6 \frac{\mu}{m \varepsilon_s^2 n^2} \qquad (1)$$

where ε_s is the low frequency dielectric constant of the material and n takes the values 1, 2, 3 for the ground and various excited states. When the electron and hole execute large orbits about their centre of mass their motions are determined by the properties of the conduction and valence band edges, so that they can be described by their effective masses m_e^* and m_h^*. The reduced mass μ of equation (1) is then given by $\mu^{-1} = m_e^{*-1} + m_h^{*-1}$. Free exciton luminescence can occur from the various excited states which may be very similar, or close in energy to, the states responsible for optical absorption and edge emission.

Satisfactory measurements of free exciton absorption spectra have been made in most wurtzite type II-VI compounds, and in ZnO (3) and CdS(1,4) in particular. The exciton absorption spectra of the cubic compounds have also been studied by several authors. Aven et al (5) have measured the absorption and reflectivity spectra of cubic ZnSe

crystals at 300 and 23 K. Their results are shown in Figure 2.1. The curve at 23 K (black points) was obtained by combining the absorption and reflectivity measurements. The curve up to about 2.795 eV was calculated from absorption data while the curve from about 2.785 eV towards higher energies was calculated from reflectivity measurements using a Kramers-Kronig inversion analysis. The peaks labelled n = 1 and n = 2 were interpreted as the ground and first excited states, respectively. The excitons are formed from holes in the Γ_8 valence band and electrons in the Γ_6 conduction band at k = 0. The energy of the n = 1 state relative to the valence band was found to be 2.81 eV. From the differences in energy between the n = 1 and n = 2 states the binding energy of the exciton was calculated to be E_{ex} = (0.020 ± 0.004) eV and the reduced mass μ = 0.10 ± 0.03 m. In consequence the band gap is E_G = 2.83 (4380^{o}A) at 23 K.

Hite et al (6) have examined the thresholds of absorption spectra of cubic ZnSe single crystals at temperatures between 2.1 K and 200 K. They used zinc purified crystals and found the ground state exciton absorption peak at 2.80 eV from the normal-incidence reflectance spectra at 2.1 K by using a Kramers-Kronig inversion. They also measured the absorption coefficient in the weakly absorbing region as a function of photon energy and temperature and suggested that the energies for maximum absorption were associated with the creation of "direct" excitons assisted by the annihilation of one or more longitudinal phonons. The "direct" phonon assisted process is illustrated diagrammatically in Figure 2.2. Absorption

is a two step process. The first step is the absorption of a photon and the creation of the exciton in an intermediate state with K = 0 on any one of the discrete exciton bands which are shown a series of parabolas. In the second step the exciton is "scattered by the absorption of a longitudinal phonon of wave vector q to a final state with $K \approx q$ and energy $h\nu + \hbar\omega_\ell$. This scattering is represented by the small arrow. They assumed that the ground state energy was dependent upon the temperature and they identified the threshold for absorption as the creation of an exciton by absorption of a photon assisted by one longitudinal phonon. At temperatures of 99, 79 and 60 K energies $(E_{x1} - \hbar\omega_\ell)$ for maximum ground state, direct-transition exciton absorption were found at 2.752, 2.758 and 2.762 eV. The longitudinal-optical phonon energy, $\hbar\omega_\ell$, was found to be 31.4×10^{-3} eV. No evidence was found for any indirect transition processes and they concluded that ZnSe has a "direct" minimum band gap with the conduction and valence band extrema at the centre of the Brillouin zone.

Park and Schneider (7) have studied edge emission spectra of structurally pure, cubic ZnSe single crystals. At 4.2 K they observed an oscillatory structure in the excitation spectra of the sharp emission lines and a number of emission peaks at 2.792, 2.790, 2.786, 2.779 and 2.776 eV (that are formed by exciton plus phonons). These emission peaks appeared in the energy region approximately 0.030 eV below the ground state exciton energy.

Liang and Yoffe (8) have investigated optical transitions in hexagonal ZnSe at 15 K. They found ground state energies at about 2.8520, 2.9039 and 3.3199 eV for

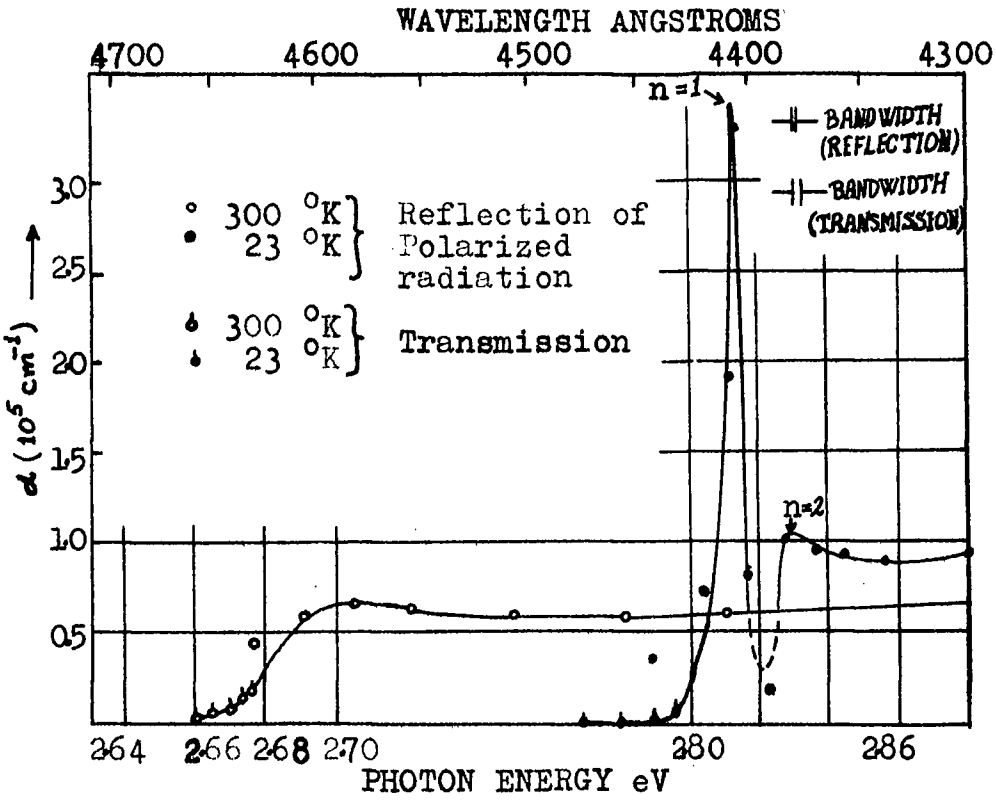

Figure 2.1 **Absorption coefficient α for ZnSe in the absorption edge region as a function of photon energy.**

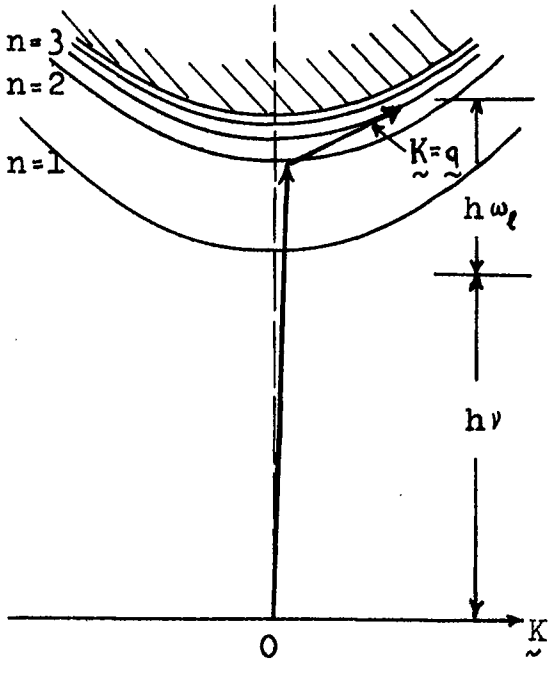

Figure 2.2 **Perturbation-theoretic representation of the creation of a " direct " exciton by optical absorption assisted by one photon.**

the three exciton series associated with the three valence bands of the hexagonal modification. The binding energies of these excitons were 0.022, 0.035 and 0.019 eV, respectively. These transitions have been interpreted as direct, allowed transitions over the minimum band gap associated with the split valence bands at the centre of the Brillouin zone (k = 0). They found the minimum band gap in hexagonal zinc selenide to be 2.87 eV. The splittings of the three valence bandswere found to be $E_C - E_A = 0.465$ eV and $E_B - E_A = 0.065$ eV at 15 K. They estimated the longitudinal optical phonon energy at 0.030 eV from the shape of the absorption curve at 78 K.

2.2.2 Bound Excitons

The excited states involved in one of the edge emission processes in ZnSe can be described in terms of electron hole pairs localized near ionized or neutral crystal defects. For this reason the term "bound exciton complex" has come into general use. Bound exciton complexes can be created by optical excitation. The emission lines which result from the recombination of these bound exciton complexes occur on the long wavelength side of the free exciton emission. The theory of the "bound exciton complex" was developed with reference to CdS and is based on the symmetry properties of the energy bands associated with the wurtzite structure. CdS has been extensively studied by many authors (1,9,10).

In developing the theory, Thomas and Hopfield (1) developed first a special form of direct exciton wave function and then applied group theory to the weakly bound

excitons. Four bound exciton complexes were postulated. These are (1) an exciton bound to be neutral donor, (2) an exciton bound to an ionized donor, (3) an exciton bound to a neutral acceptor, and (4) an exciton bound to an ionized acceptor. In their theory only the lowest states of the complexes were considered and the model was one of the complex being bound together by forces similar to that in the hydrogen molecule ion. The models were verified by observing line splittings in the Zeeman effect.

Reynolds et al (11) made the first detailed study of the low temperature luminescence of zinc-blende ZnSe. They observed many emission lines one of which was located at 2.825 eV at 77 K. They did not give any assignment of this emission line and merely suggested that it was some sort of exciton emission. Comparison with more recent studies suggests that their measurements were probably made on crystals containing an appreciable contamination of sulphur. Their other results will be discussed in Section 2.3.

Halsted and Aven (12) examined the edge emission spectra of various II-VI compounds at 4 K, and established a correlation between the bound exciton line spectra and the broader, lower energy edge emission. They used information gained in a magneto-optical investigation of CdS to identify spectra in other II-VI compounds including ZnSe. Their results are shown in Figure 2.3 which illustrates the procedure employed for acceptor defects. By purification and subsequent introduction of acceptor defects, crystals have been obtained which exhibit an exciton emission process with a near-band-gap energy at 4 K which can be correlated with the presence of a broader band emission

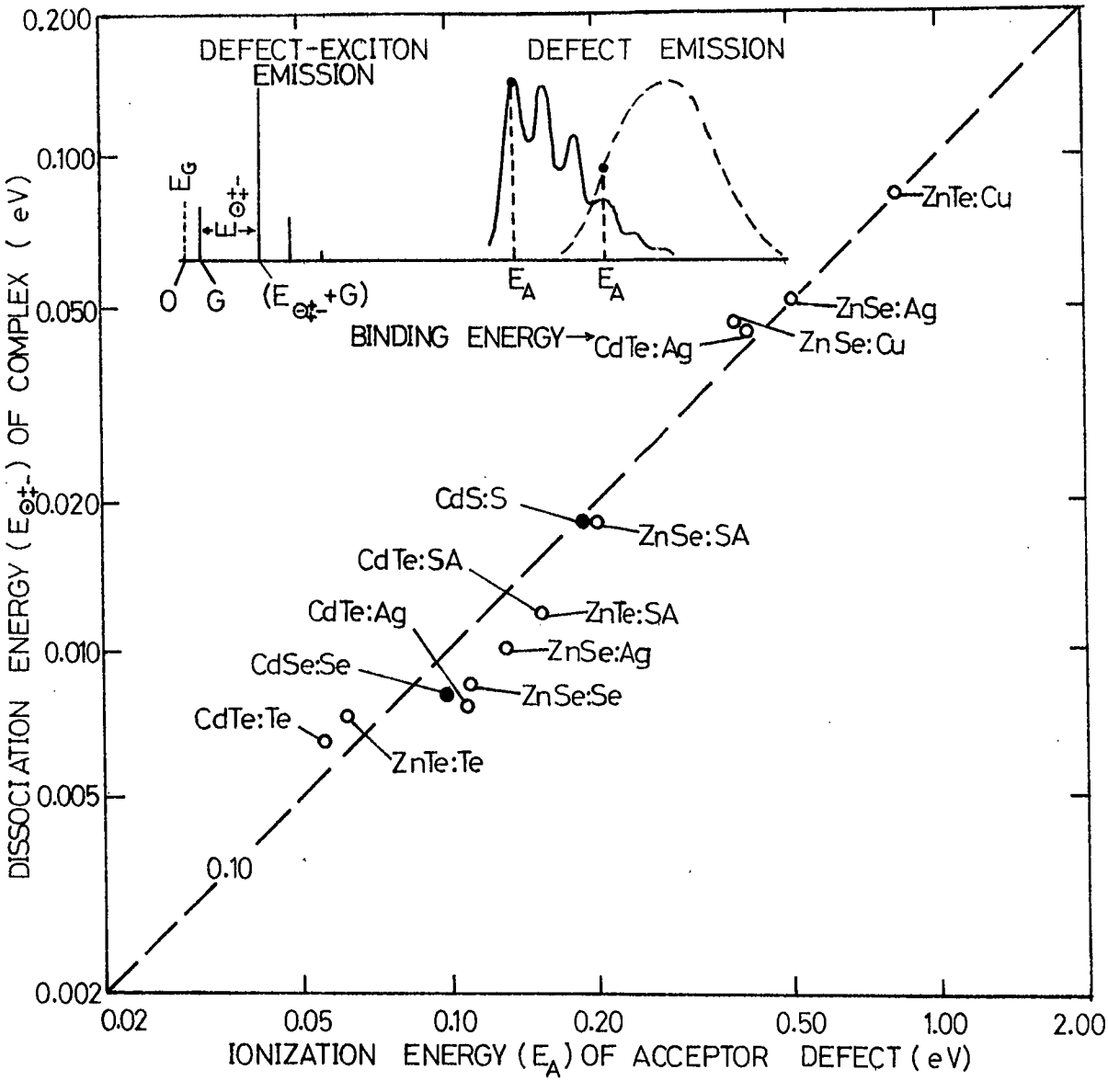

Figure 2.3 $E_{\Theta\ddagger^{-}}$ versus E_A for correlated pairs of fluorescent spectra at 4°K in acceptor-doped II-VI compounds. From Halsted and Aven (12).

process of substantially less than band gap energy. They defined the exciton dissociation energy, $E_{\theta^{+}_{+}-}$ as the energy difference between the zero phonon line and the reflectivity minimum due to exciton absorption. It was assumed that the lower energy emission results from a transition to the same acceptor level from the conduction band or shallow donor state close to the conduction band. The acceptor ionization energy E_A was obtained from the position of the zero phonon band of the lower energy emission. A plot of $E_{\theta^{+}_{+}-}$ versus E_A for all II-VI compounds gave a straight line which leads to a ratio of the dissociation energy of the bound exciton complex to the ionization energy of the neutral acceptor of 0.10. In a similar way the corresponding ratio for a neutral donor was 0.20. The dissociation energy of an exciton bound to a neutral acceptor was found to be 0.018 eV in self-activated ZnSe and about 0.05 and 0.047 eV for Ag and Cu doped (acceptor type) ZnSe crystals, respectively. A transition due to an exciton bound to a neutral donor was identified by examining the edge emission in donor doped II-VI compounds. The dissociation energy of that complex was found to be 0.0042 eV for ZnSe neutral donors at 4 K.

Dean and Merz (13) have observed a large number of sharp lines in the photoluminescence spectra of ZnSe at 4.2 K, under intense excitation with an argon ion laser. The energy and intensity of the sharp lines was explained in terms of recombination between donor-acceptor pairs at various separations. At large separation the individual lines are so closely spaced that they merge to form the first broad band of the lower energy edge emission.

Additional sharp lines were also observed on the high energy side of the paired emission at about 2.802, 2.797, 2.795 and 2.783 eV which were identified as the free exciton, the I_2 doublet and the I_1 lines respectively. The component at about 2.802 eV was very close to the position of the observed reflectivity peak which is due to the ground state of the free exciton formed in the $\Gamma_8 - \Gamma_6$ transition. I_2 lines are due to the decay of excitons bound to neutral donors. The lower energy I_1 line shows strong phonon co-operation, unlike the I_2 lines. The I_1 line seemed to be doublet, (with a weak satellite at about 2.778 eV). Dean and Merz suggested that this was due to a lifting of the electronic degeneracy of the I_1 transition, rather than to the presence of two different acceptor centres.

Dean and Merz (13) also showed that annealing in zinc vapour induced drastic changes in the luminescence of ZnSe. After annealing in Zn vapour for 5 hours at 700°C, they found a new strong I_x sharp line located at about 2.793 eV just below the I_2 lines. Unfortunately, the identity of centre responsible for I_x line is as yet unknown. In addition they also found very distinct pair line structure on the high energy side of the zero-phonon band of the lower energy emission. This will be discussed in the next section.

Following this work Merz et al (14) investigated substitutional donors in cubic ZnSe using argon ion laser excitation. They found the I_2 lines at about 2.797 eV and I_3 lines between 2.794 and 2.797 eV. These I_2 lines result from the recombination of excitons bound to neutral

donors which were inadvertently present in low concentrations. Below the I_2 lines a strong and a weak I_3 line were observed. These doublets result from the recombination of excitons bound to ionized donors. Below the I_3 lines they found two strong lines which were labelled I_1^x and I_1^{Deep}, these were located at approximately 2.792 and 2.782 eV respectively. Both of these lines exhibited a strong series of LO phonon replicas and were explained as excitons bound to neutral acceptors; the so-called I_1 lines. The I_1^{Deep} line exhibited typical behaviour when the crystals were heated in Zn vapour at 700^{o}C being reduced in intensity. In the low-energy region (between 2.775 and 2.780 eV) the weak two-electron transitions were superimposed on the broad background tail below the I_1^{Deep} line.

The measured emission spectra from undoped ZnSe were very complicated and it was difficult to identify the various spectral lines. For this reason two nominally undoped photoluminescence spectra were compared with that from a Cl_2 doped sample. Small shifts were observed for the excited states and I_2 lines but large energy shifts occurred for the doublets. Consequently, the energy level diagram for exciton effects shown in Figure 2.4 was proposed. At the bottom of the diagram, the idealized spectrum containing the two-electron transitions and the I_2 line is shown. The energy-level diagram shows how these transitions arise. The energy-level diagram shows the ground and excited states of the three-particle complex composed of an exciton bound to a neutral donor. The ground state (1s) and the excited state (2s, 2p) of the isolated donor are also shown. The principal transition is the I_2 line (which is labelled

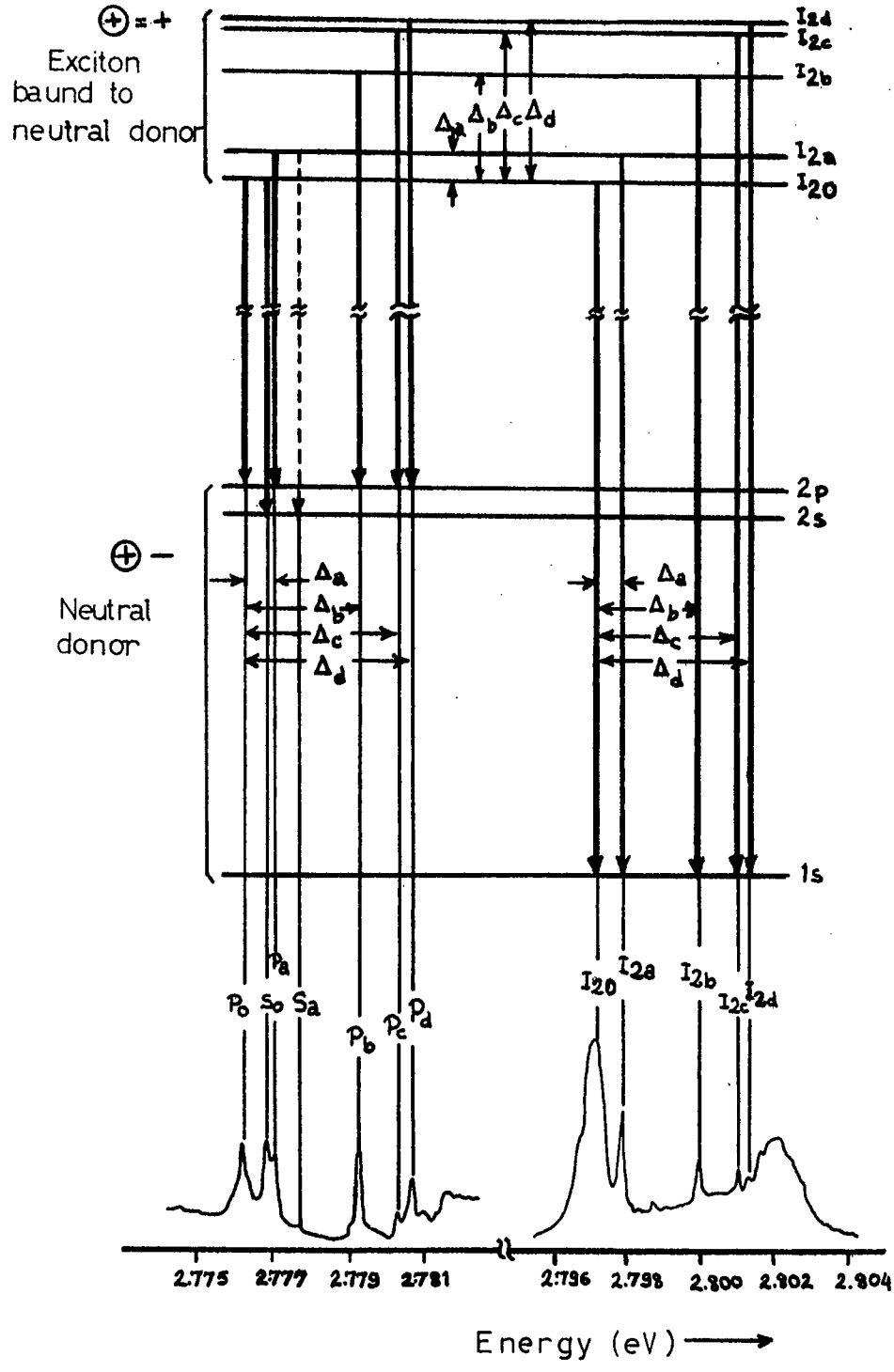

Figure 2.4 Idealized specturum of the two electron and I_2 lines, and energy level diagram showing how these transition arise.

I_{2O}) which originates from the ground state of the bound exciton (I_{2O} state) and terminates with the donor in its ground state. The weaker lines at higher energy originate from excited states of the bound exciton complex which are indicated by the levels $I_{2\alpha}$ (α = a,b,c and d) and also terminate on the donor ground state. Two-electron transitions originate from the ground and excited exciton states, but leave the donor in an excited 2s or 2p state. The model was checked by measuring the energy differences Δ_α (α = a,b,c and d) in two ways as shown in Figure 2.4, (1) from the separations of the bound exciton lines $I_{2\alpha}$ and (2) from the separation in the two-electron transitions. They also identified the chemical species involved in the two-electron transitions. This was done for the donors Al, Ga, In and Cl. A fifth donor (F) was identified from the observation of the I_3 lines. Donor binding energies calculated from these observations were found to be 26.3 ± 0.6, 26.9±0.6, 27.9±0.6, 28.9±0.6 and 29.3±0.6 meV for Al, Cl, Ga, In and F respectively.

From the energies of the I_{2O} lines the exciton binding energies for each of four donors were deduced and plotted as a function of the central cell parameters. These results were remarkably linear and constituted an empirical statement of Haynes rule. Baldereschi has given a simple derivation of this rule in the following way. The donor binding energy E_D can be written as:

$$E_D = E_o + PV$$

where E_o is the effective mass binding energy, V is the square-well potential in the central cell of the donor and

P is the probability that the donor electron is in the central cell. A similar expression holds for the binding energy of the bound exciton, E_{BX}:

$$E_{BX} = E_o' + P'V$$

where E_o' is the exciton reduced mass and P' is the probability of the bound exciton electrons being in the central cell. Combining these two equations gives

$$E_{BX} = E_o' + (P'/P)(E_D - E_o) \simeq A + (P'/P)(E_{2p} - E_{1s})$$

Considering the limiting cases of light and heavy holes, P'/P was estimated for light and heavy holes to have values of 0.033 and 0.4 respectively. The results of Merz et al were a good fit to the above calculation and showed that the variation of the exciton binding energies for different donors is a central cell effect. Similar arguments were also made for excitons bound to ionized donors.

Liang and Yoffe (15) have investigated radiative recombination in hexagonal ZnSe at 4.2 and 77 K. They found the intensity of the bound exciton luminescence to be strongly dependent on temperature. The dissociation energies from the bound state were relatively small, ranging from about 0.3 meV to 10 meV. They studied absorption and luminescence on the same ZnSe crystal in the $E \perp c$ direction, and observed two I_o and I_o' exciton peaks at 2.851 and 2.849 eV, with I_1, I_2 and I_3 lines at about 2.845, 2.842 and 2.838 eV respectively. Several other lines were also observed, for example, I_4 (2.831 eV), I_5 (2.828 eV), I_{1a} (2.816 eV), I_{1b}, I_{3a} (2.812 eV), I_{2b} (2.809 eV) and I_{3b} (2.806 eV). They tentatively assigned the I_1 and I_2

lines to excitons bound to neutral acceptors and neutral donors respectively, and the I_3 line to an exciton bound to an ionized acceptor. They assumed that the I_4 and I_5 lines might be due to the emission of acoustic phonons associated with I_3. The (I_{1a}, I_{2a}, I_{3a}) and (I_{1b}, I_{2b}, I_{3b}) lines were probably due to the emission of transverse and longitudinal phonons associated with (I_1, I_2, I_3), respectively. However, the origin of the I_o and I_o' exciton lines was not well understood.

Liang and Yoffe have also studied the luminescence spectrum of hexagonal ZnSe after it had been bombarded by manganese ions with energies of 75-100 keV. The bound exciton emission was compared before and after bombardment. The ion damage was found to alter the environment of the donor and acceptor impurities, by changing the crystal structure locally from the hexagonal to the cubic modification. In the spectrum of the bombarded crystal, they found an I_3 line (which had appeared in hexagonal ZnSe), new L_1, and L_3 peaks at about 2.797 and 2.783 eV and also L_{3a} and L_{3b} peaks in the region between 2.773 and 2.690 eV. They concluded that L_1 and L_3 were due to excitons bound to neutral donors and to neutral acceptors respectively while L_{3a} and L_{3b} corresponded to one and two LO phonon replicas of L_3.

2.3 Phonon-Assisted Edge Emission

Many of the II-VI compounds exhibit a series of emission peaks on the long wavelength side of the absorption edge. These peaks have an equal energy spacing which is equal to the LO phonon energy of the host lattice. The LO phonon energy is related to the transverse optical (TO)

phonon energy by the Lyddane, Sachs, Teller relation

$$E_{LO} = E_{TO} \ (\varepsilon_s/\varepsilon_\infty)^{\frac{1}{2}} \qquad (2)$$

where ε_s is the static dielectric constant and ε_∞ is the high frequency or optical dielectric constant. The phonon assisted bands in the series have a width of about 12 meV which is quite broad in comparison with the bound exciton emission. The bands occur at lower energies at 4.2 K than they do at 77 K.

Fluorescence emission of near-band-gap energy in II-VI compounds at low temperatures occurs by the simultaneous emission of photons and 0, 1, 2, 3 .... LO phonons. The relative intensities of the bands within a set have been described by a relation of the form (16,17)

$$I_n = I_o \ \bar{N}^n/n! \qquad (3)$$

where I_o is the intensity of the zero phonon line, I_n is the relative intensity of the (n+1) th line involving the emission of a photon plus n phonons. $\bar{N}$ is the average number of emitted LO phonons.

Kröger (18) first recognized the above emission bands in CdS and ZnS crystals. Following this initial observation, a model of fluorescence in II-VI compounds was proposed (19,20) which was based on the recombination between free electrons and trapped holes at an impurity centre. Lambe and Klick (21,22) proposed a different model in which they suggested that the luminescence resulted from the recombination between trapped electrons and free holes.

Reynolds et al (11) have studied the edge emission of ZnSe crystals over a range of temperatures from 4.2 to

77 K. The crystals showed a number of lines and bands near the absorption edge. The onset of intrinsic absorption in ZnSe at 4.2 K occurs at a photon energy of 2.83 eV. Two different characteristic types of spectra were observed in their investigations. With type I crystals, the emission spectrum at 4.2 K contained 10 lines located between 4400 and 4900Å; at 77 K the spectrum contained only two lines. In addition to the 10 line spectra, Reynolds et al (11) observed three broader emission bands at 4950, 5350 and 6110Å. The energy separation of five of the ten lines was equal to the LO phonon energy, 0.03 eV calculated from the measured value of the TO phonon energy, 0.026 eV, indicating that the lines $L_{3a} \rightarrow L_{3e}$ result from the L_{3a}, 4448Å no-phonon line, and LO phonon interactions. At 77 K, the two observed peaks did not appear to belong to the phonon-assisted emission series, but were derived from the shorter wavelength L_1 and L_2 lines.

With type II crystals, the emission spectrum at 4.2 K contained 14 lines and bands located between 4400 and 4900 Å; at 77 K the spectrum contained only three lines one of which was located at the fundamental absorption edge (4388 Å). In the 14 line spectrum a phonon assisted-series was also observed with the no-phonon line L_{10} at 4598Å. At 77 K a different emission series was observed which was shifted to higher phonon energy by about 0.015 eV. This shift in the position of the phonon-assisted emission bands with temperature is similar to that observed in the green emission of CdS.

The changes in the ZnSe phonon-assisted edge emission with temperature are illustrated in Figure 2.5a (11). The

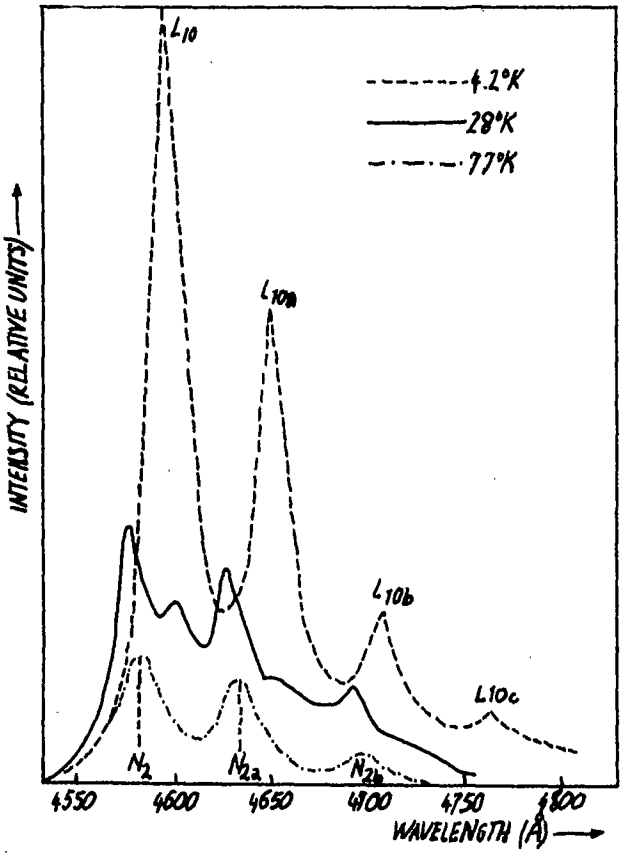

Figure 2.5(a) Relative intensity of edge emission lines vs. wavelength for type II ZnSe single crystals at several crystal temperatures.

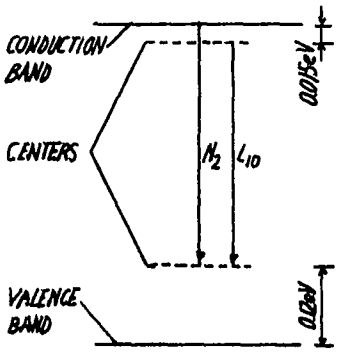

Figure 2.5(b) Suggested energy scheme accounting for edge emission line L_{10} at 4.2°K and line N_2 at 77°K in type II crystals of ZnSe.

line L_{10} and the replicas lines L_{10a} to L_{10c} which are prominent at 4.2 K vanish as the temperature is increased to 77 K, while two different lines N_2 and N_{2a} appear in the process. Since N_{2a} is related to N_2 via a phonon interaction, one need only account for the origin and behaviour of N_2; similar remarks apply to L_{10}. To account for the changes in the edge emission, Reynolds et al suggested the energy scheme depicted in Figure 2.5b, with an acceptor level located 0.12 eV from the valence band, and a shallow trapping level 0.015 eV from the conduction band edge. According to this scheme, L_{10} results from a centre-to-centre transition which is dominant at 4.2 K. When the temperature is increased, the 0.015 eV level becomes depopulated, and the dominant transition N_2 occurs between free electrons in the conduction band and holes trapped at the acceptors.

Reynolds et al (11) have suggested that the different emissions from the two types of ZnSe crystals might be attributable to different host lattice defects. While this is certainly possible it may be that some of the differences are connected with stacking faults and the possibility of obtaining crystals with mixed cubic-hexagonal structures. Park and Chan (23) have pointed out, there is a shift in absorption edge between cubic and hexagonal ZnSe at room temperature of the order of 180 Å.

Halsted et al (24) studied the edge emission spectra of several II-VI compounds. They determinated the LO phonon energy to be 0.0314 eV for cubic ZnSe which is clearly equivalent to the longitudinal phonon energy calculated from equation (2) and restrahlen data. Halsted et al (25) have identified fluorescence emission bands which

result from the addition of specific dopants (Cl, Ag, Cu, Au), and they have used equation (3) as a basis for characterizing spectra with resolved LO phonon structure.

Liang and Yoffe (15) studied hexagonal ZnSe and observed a series of phonon assisted bands near the absorption edge, which were separated by equal energy intervals of 0.0318 ± 0.0004 eV. Their emission spectrum at 77 K contained 5 peaks between 2.7461 and 2.620 eV while at 4.2 K the spectrum also contained 5 peaks between 2.7384 and 2.612 eV. These two series were explained in terms of a transition between an electron in the conduction band and a trapped hole at 77 K, and a transition between a trapped electron and a trapped hole at 4.2 K.

The shift in the phonon-assisted emission peaks with temperature can therefore be explained in terms of various localized defects and an important class of band edge emission processes in II-VI compounds therefore involves two defects. The theory of transitions between pairs of defects, i.e. the "donor-acceptor pair" emission has been confirmed in studies of ZnSe.

2.3.1 Donor-acceptor pair emission

Historically, the donor-acceptor pair recombination process, in which an electron on a donor recombines with a hole on an acceptor, was first suggested by Prener and Williams (26) to explain the broad green and red luminescence bands in ZnS. However, detailed evidence for the existence of this process was not obtained until the characteristic sharp line structure (due to no-phonon recombinations)

resulting from many different discrete pairs was observed by Hopfield et al (27) and Thomas et al (28) in gallium phosphide. As described in the preceding sections Pedrotti and Reynolds (2) have obtained support for the model originally proposed for the edge emission in CdS, in which the high energy series (HES) is attributed to the recombination of free electrons with holes bound to acceptors ("free-to-bound" recombinations) and the low energy series (LES) is associated with the recombination of electrons bound to shallow donors with holes bound at the same acceptors ("pair" recombinations). Colbow (29) extended the measurements on CdS and used the technique of "time-resolved spectroscopy" at different temperatures. His results indicated that the LES spectrum displayed a substantial shift with time at 4.2 K. In addition it was shown that the LES bands also broadened and shifted to higher energies as the excitation intensity increased. However, the HES spectrum was found to show neither the "time-shift" nor the "intensity shift" (29,30). These shifts have been explained in the following way.

The ground state of a donor-acceptor pair is characterized by both particles being in their respective ionized states. A donor-acceptor pair is in an excited state when an electron and hole are captured by the ionized donor and acceptor respectively. Pair emission occurs when the bound electron recombines with the bound hole. The emission energy of a bound-to-bound transition from a donor-acceptor pair, separated by r, where r is large compared to the radii of the wave functions of the donors and acceptors

is given by;

$$E(r) = E_G - (E_D + E_A) + \frac{e^2}{\varepsilon r} \qquad (4)$$

where E_G is the band gap energy, E_D and E_A are the ionization energies of the isolated donors and acceptors respectively, e is the electronic charge and ε is the low frequency dielectric constant. The final term is due to the Coulombic interaction of the donors and acceptors. For an isolated pair, values of r are limited by the crystal structure and range up to a maximum value, r_o, equal to (donor or acceptor concentration)$^{-1/3}$. The possible values of r are discretely distributed and a spectrum of discrete lines will result. Assuming the concentration of the ionized donors and acceptors to be equal for neutrality reasons, and the neutral donor-acceptor pair separation to be r, the recombination transition probability (W(r)) is approximately given by

$$W(r) = W_o \exp(-2r/r_B) \qquad (5)$$

where W_o is the reaction constant and r_B is the Bohr radius of the less tightly bound carrier, which for $E_A > E_D$ is the electron.

Equation (4) shows that recombination of close pairs leads to different values of E(r) for different values of r. For this reason, numerous sharp lines arise for the many possible separations between the donors and acceptors, and a particular line can be assigned to a particular pair separation. It has been shown (27) that by doping the Ga or P sub-lattices of GaP, different values for r are obtained and hence different line spectra result. Using equation (4) the values of (E_D+E_A) for a particular pair of impurities can

be derived. For large r, the discrete, closely spaced lines merge into a broad continuous band which is the zero order member of the LES edge emission. The emission intensity from isolated pairs at separation r will be proportional to the number of pairs. For separations less than r_o the relative number of isolated pairs of separation r is proportional to the number of lattice positions, the thermal history of the sample and the diffusivities of the donors and acceptors. In GaP the broad emission has been clearly associated with the pair lines and shifts with these lines when (E_D+E_A) is varied.

Since the lifetime of the pairs is expected to vary with r, it was anticipated that a study of the spectral distribution during the decay of the broad band emission would be instructive. Thomas et al (30,31) have investigated both theoretically and experimentally the consequences of the varying transition rate with pair separation. For large r, equation (5) predicts that the intensity, I(t), of the emitted light at time t after excitation will involve a sum over all pairs of the product of W(r) for a particular pair with the number of such pairs present after time t. The result is that the decay of the total light intensity is non-exponential, and such a decay does not imply the existence of a distribution of trap depths and thermal detrapping. The spectral distribution of a decaying pair band after flash excitation will shift to lower energies and the band will decrease in width during the decay. This is a direct consequence of the more rapid decay of the pairs with smaller separations which contribute the higher energy photons and the reduced Coulombic broadening with the longer lived pairs of large separations.

One might predict from equation (5) that pairs with large r with the longer decay times, would be saturated with increasing excitation intensity. This would result in a shift of the pair emission band to higher energies, such a shift has been observed in CdS by Orr et al (32).

Sharp line spectra merging into the zero phonon pair band were first observed in GaP. Originally with the II-VI compounds the pair line structure was not observed. Most of the II-VI compounds are direct-gap semiconductors, whereas the III-V compounds, such as GaP in which pair line structure has been observed are indirect-gap semiconductors. In order to observe discrete pair line emission in direct-gap materials very high intensities of excitation are needed since the intensities of pair lines arising from pairs with small separations must be saturated. Such excitation intensities are expected to be much higher in direct semiconductors than in indirect ones. In addition the emission of bound excitons is much stronger in direct II-VI compounds than in indirect III-V compounds, and this luminescence appears in the same region as that in which pair line structure is expected.

Iida (33) studied the edge and self-activated emission of pure ZnSe crystals. At the highest excitation intensity no discrete pair lines were observed. However, the edge emission contained two series of bands attributed to the HES at about 2.703 and 2.675 eV at 77 K and the LES at about 2.700 and 2.671 eV at 4.2 K. Values of the donor and acceptor binding energies were calculated from time-resolved measurements, using equation (4), to be 26 ± 3 meV and 100 ± 1 meV respectively. The observed LES depended on the intensity of excitation and shifted by about 0.005 eV to

lower energy under weak excitation. The LES emission bands also shifted by about 0.003 eV to lower energies some 50μsec after excitation. This is shown in Figure 2.6. As explained above this behaviour is expected from the slow decay of pairs with larger separations.

Very recently discrete donor-acceptor lines have been observed in the emission spectra of cubic ZnSe by Dean and Merz (13). A typical spectrum is shown in Figure 2.7. The assignment of each line was made using the intensity patterns calculated for the zinc blende lattice assuming a type I configuration, i.e. that configuration in which the donors and acceptors occupy the same type of lattice site. The calculated intensity distribution was found to be in satisfactory agreement with the experimental results except for the lines associated with very close pairs. With the type II configuration, i.e. where the donors and acceptors are on opposite lattice sites, no agreement at all was found. In Figure 2.7, the sharp lines are due to electron-hole recombination at distant donor-acceptor pairs with different mutual separations. The integers in parentheses denote the shell numbers m, i.e. the separation of the pairs. m is defined by $r = (\frac{1}{2}\ m)^{\frac{1}{2}}\ a_o$ where $a_o = 5.67$ Å is the lattice constant. The numbers not in parentheses indicate the total number of pairs within a given shell m. For m = 14 or 30 no pairs are possible. The positions corresponding to such shell numbers are denoted by "G" in the spectrum and clearly no sharp lines are observed at these positions which lends strong support to the interpretation. The energy positions of the various lines are also in good agreement with those predicted by equation (4). However, the agreement becomes

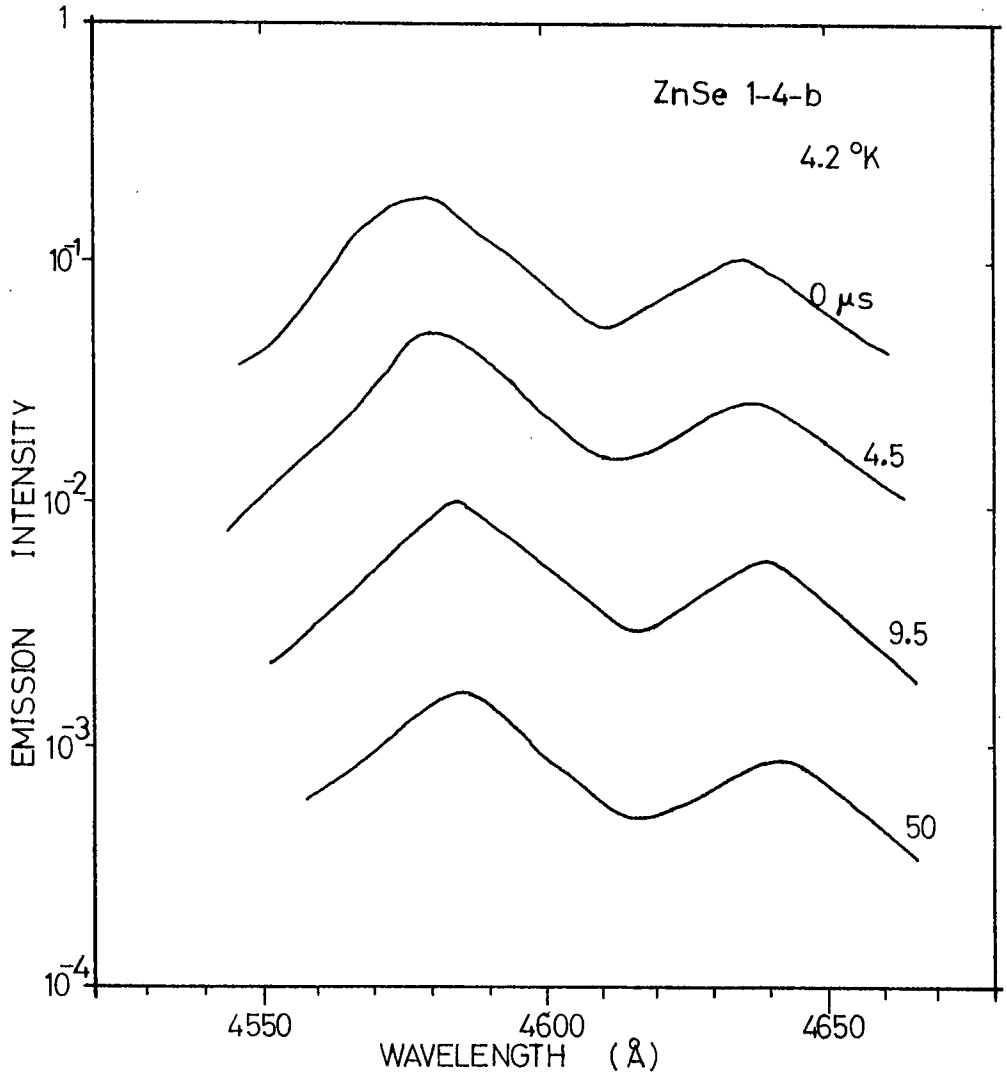

Figure 2.6 Edge emission spectra of the ZnSe crystal at 4.2 °K at various times after excitation. From Iida(33).

worse for close pairs corresponding to $r \lesssim 30$ Å ($m \lesssim 55$). The experimental energies of such lines change with r at a slower rate than predicted. As to the chemical identities of the donor and acceptor responsible for these pair lines, no information can be offered at present.

Dean and Merz found two series of the broader edge emission bands after annealing in Zn vapour at 700°C. The higher energy series had its zero phonon member, R_o at about 2.710 eV with three LO phonon replicas at 2.677, 2.664 and 2.612 eV. In fact this R_o band is associated with the pair emission discussed above and is composed of a large number of unresolved distant pair lines. The second series of bands labelled Q, had its zero order member Q_o at about 2.692 eV with three LO phonon replicas at about 2.659, 2.629 and 2.597 eV. No fine structure associated with Q_o was found. The R bands exhibited several of the characteristic properties of "pair" recombination. In particular they had long non-exponential decays. The high energy tails of the bands decayed first, causing a reduction in bandwidth and displacement of the band maxima to lower energies with time. The R_o band also broadened and shifted to higher energies as the excitation intensity was increased.

Donor-acceptor pairs associated with the three donors (Al, Ga and In) have been observed by Merz et al (34), in the photoluminescence of ZnSe excited by an argon ion laser at 1.6 K. The donors were identified from the radiative recombination of the excitons bound to neutral donors (I_2 lines), the excitons bound to the ionized donors (I_3 lines) and the two electron transitions, which have already been described

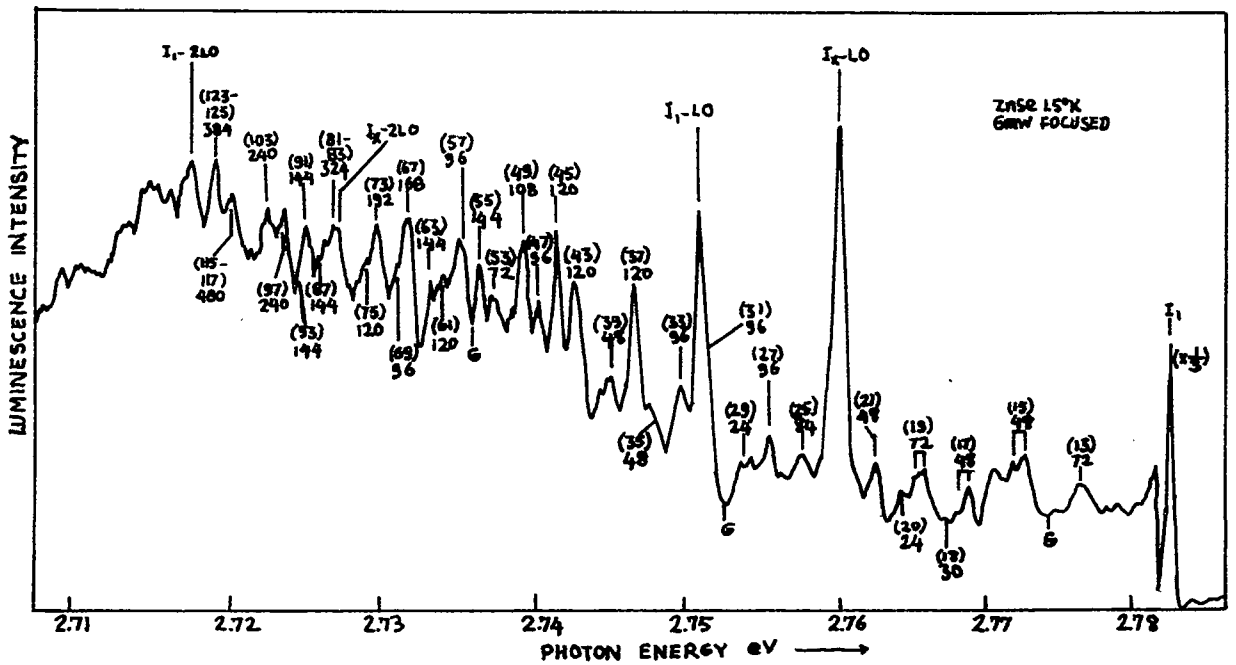

Figure 2.7 Pair line structure in the edge emission of ZnSe at 1.5 °K (13).

in Section 2.2.2 (14). Merz et al observed bound exciton emissions which they called I_1^{Deep} and I_1^x, together with I_2 lines in the region of 2.78 to 2.80 eV. At lower energies below the I_1^{Deep} line, donor-acceptor pair lines were observed at about 2.76 and 2.75 eV together with phonon replicas of the I_1^x and I_1^{Deep} lines. A large number of the sharp, closely-spaced pair lines were observed, which merged into a broad band at about 2.694 eV, which had two LO phonon replicas at 2.662 and 2.632 eV. These donor-acceptor pair lines were explained with the help of equation (4) and the polarization interaction was considered for close pairs by adding a Van der Waals term. For close pairs, the observed photon energy from a donor-acceptor recombination process is significantly increased by the Coulomb interaction. For distant pairs, the differences Δr between successive shells are small, and the lines merge into a broad band. For a low power density of the exciting light, this broad pair band dominates, since the distant pairs have longer lifetimes than close pairs. As the excitation power increases, the distant pairs become saturated and the peak of the pair band begins to move to higher energies. The identification of the individual discrete lines in the spectrum was made on the basis of type I pairing where the pairs occupy the same type of sublattice. Three different pair systems were obtained when the crystals were doped with Al, Ga or In. The intensity of the pair lines depended on the doping level. Li and possibly Na were found to be the only soluble shallow acceptors in ZnSe The pair spectrum reported by Dean and Merz (13), was also observed and re-examined but the chemical identities of the donor and acceptor responsible could not be determined.

2.4 Deep Centre Luminescence

Broad emission bands with photon energies well below the band gap are readily observed in most II-VI compounds. Such bands are associated with deliberately added impurities or defects in the host lattice. Two types of impurities can be introduced into II-VI compounds to modify their luminescent behaviour. They are called (1) activators (acceptors) (2) coactivators (donors). The activator elements are copper, silver, gold, for example, which occupy group II cation sites and behave as deep acceptor levels (luminescent centres). The activator impurity has been thought of as the site at which the recombination of an electron and hole occurs with the radiative emission of of energy. The coactivator elements are Cl, Br, I, Al, Ga, In etc., where the halides occupy group VI anion sites and the aluminium, gallium or indium occupy cation sites. All of these form donor levels. In addition to the defects associated with deliberately added impurities, all crystals contain a certain concentration of native defects. These native defects usually provide self activation or coactivation for the luminescence of II-VI compounds and can behave as double acceptors or donors.

For the most part the numerous emission bands in II-VI compounds have been studied with particular reference to ZnS and CdS. Three basic models to describe the deep centre luminescence have been proposed and these are illustrated schematically in Figure 2.8. (a) The Schön-Klasens (19,20) model regards the luminescence as the result of radiative recombination of an electron from the conduction band with a hole trapped at an acceptor level several tenths

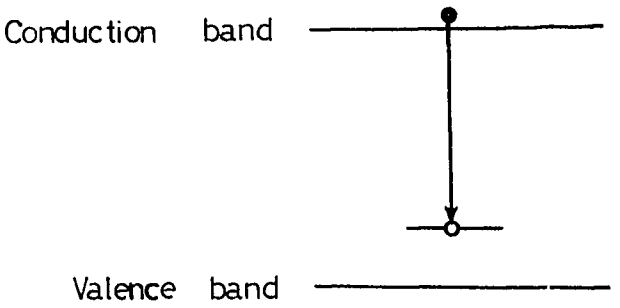

(a) Schön-Klasens model

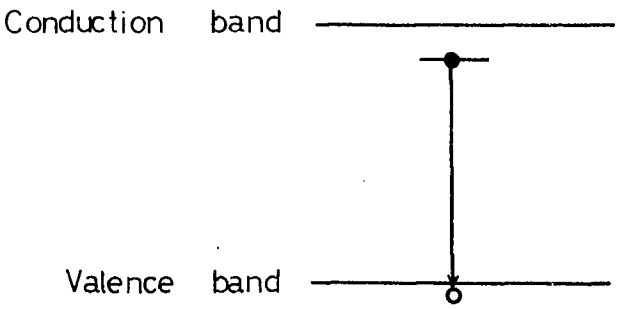

(b) Lambe-Klick model

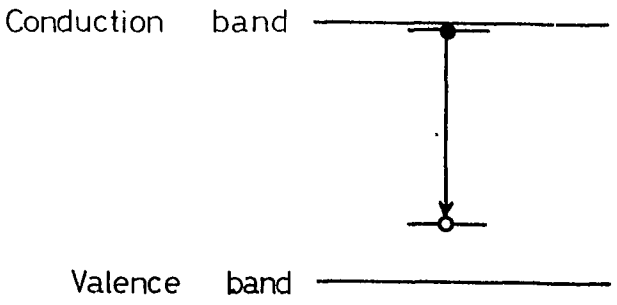

(c) Prener-Apple-Williams model

Figure 2.8 Schematic representation of three models for the radiative recombination processes in II-VI compounds.

of an eV above the valence band, (b) the Lambe and Klick (21) model attributes the luminescence to the recombination of a hole in the valence band with an electron trapped at a level slightly below the conduction band, (c) the Prener-Williams (26) model involves the recombination of an electron captured at a donor with a hole captured at a nearby acceptor; the luminescence is due to a localized electron transition within a centre composed of these associated pairs.

2.4.1 Self-activated emission

The mechanism of the self-activated emission in II-VI compounds generally is uncertain, but in ZnS a consistent interpretation has been achieved on the basis of the Prener-Williams model. A defect consisting of a close association of a doubly ionized zinc vacancy acceptor and an ionized impurity donor has been identified as the luminescent centre. The emission peak shifts to longer wavelengths when the coactivator is changed from anion (Cl) to cation (Al) substitution. This lends further support to the proposed model. A similar conclusion has been suggested for ZnSe by Holton et al (35) who observed self-activated emission bands at about 1.987 in ZnSe : Cl, and 1.934 eV in ZnSe : Al at 80 K.

Lehmann (36) has examined the self-activated emission of cubic zinc selenide at 77 K which according to him consists essentially of a single band with the peak at about 2.0 eV.

Larach (37) observed cathodoluminescence emission bands at about 1.946 and 2.032 eV bands in undoped and

Al doped ZnSe crystals at 300 K. Aven and Woodbury (38) observed a single Gaussian shaped band at about 2.066 eV in zinc selenide following Zn extraction and Halsted et al (25) also found the same band in the emission of undoped ZnSe at 25 K. Stringfellow and Bube (39) examined the luminescence emission spectrum at 85 K and found a broad band with a maximum at 2.03 eV. Liang and Yoffe (15) observed an emission band at 2.02 eV in hexagonal ZnSe and suggested that this was due to the chlorine and bromine impurities in the ZnSe powder.

Iida (33) had made a detailed study of the characteristic self-activated emission in ZnSe at different temperatures. A single band with a peak at about 2.026 eV was observed at 4.2 K. This peak shifted by about 0.04 eV to higher energies between 4.2 to 201 K. The time-resolved spectra of the self-activated emission was examined and a shift of about 0.07 eV to lower energies was apparent at various times after excitation. An "Intensity shift" was also observed. Iida considered the applicability of two models to the self-activated emission. First, the donor acceptor pair recombination model, which involves the shallow electronic levels where the interaction energies of the levels with the lattice are smaller than the Coulomb energy between the donor and the acceptor. Second, the configurational coordinate model, which is used to describe deep and quite localized energy levels where the energy of interaction with the surrounding lattice is an important part of the total energy. In the present case the displacement of atoms surrounding the acceptor was considered.

Consequently, the self-activated emission was attributed to the recombination of electrons bound at shallow donors with holes bound at deep acceptors. The value of the acceptor binding energy was found to be 0.35 eV from the thermal quenching of the luminescence.

2.4.2 Copper activated emission

Copper impurity has long played a central role in the photo-electronic properties of many II-VI compounds and several broad bands are found in ZnS, ZnTe, CdS, CdTe, containing copper. In ZnSe, generally, two broad luminescence bands are found which are known as the copper green and the copper red emissions. Usually the bands shift slightly in wavelength with varying copper concentration. Studies of the luminescence of zinc selenide have been relatively few compared with those of ZnS, and the luminescence in ZnSe is usually interpreted in analogy with ZnS. However, the mechanism of the copper blue and green emissions in ZnS has not been resolved with any great certainty. Curie (40) has suggested that the green emission results from an electron transition (of the Prener-Williams type) between a coactivator level, and an associated copper activator level. The copper blue emission seems to be generally ascribed to a transition between an electron at the bottom of the conduction band and the copper level, i.e. a Schön-Klasens type of transition. Dielman (41) has concluded that with the copper red emission ZnS:Cu the copper behaves as a singly ionized donor defect so that the luminescence transition involves the recombination of a free hole with

a trapped electron and is therefore of the Lambe-Klick type.

A single red band at about 1.907 eV in Cu doped ZnSe was first observed by Larach (37) and three broad bands at about 2.34 eV in the green, 1.95 eV in the red and 1.25 eV in the near infra-red were observed by Halsted et al (25) at 25 K. No detailed conclusions were drawn.

Lehmann (42) has made extensive studies of the copper green and red emissions in ZnSe and several alloy systems formed between ZnS, CdS, ZnSe, CdSe, and ZnTe. The emission from ZnSe:Cu, Cl, consists of two diffuse but fairly well separated bands in the red at 1.95 eV and the green at 2.35 eV at 77 K. In ZnSe replacement of the zinc by cadmium caused a steady shift of both emission bands to lower energies, whereas replacement of the selenium by tellurium caused very little change. Lehmann has proposed a qualitative explanation of his results which assumes a predominantly ionic type of binding. He associated the cation with the conduction band and the anion with the valence band. The luminescence is ascribed to electron transitions from the conduction band into previously emptied levels of centres which consist of the activator ions and the four surrounding chalcogenide anions. Replacement of zinc by cadmium causes a variation of the conduction band only, while the activator electron levels and the valence band remain unchanged. Hence the energy separation of the activator level and the valence band is independent of the Zn/Cd ratio while replacement of selenium by tellurium only affects the energy separation between the activator level and the valence band.

Iida (43) has studied the luminescence of as-grown zinc selenide crystals contraining Cu impurity. He found three luminescence bands in the green at 2.339 eV, yellow at 2.175 eV and red at 1.937 eV. The green and yellow bands could only be observed below 77 K. The yellow emission shifted with excitation intensity. An examination of the time-resolved spectra showed that the green emission decayed faster than the red emission and no spectral shift was observed with either emission bands. As the delay time was increased from zero to 300 μ sec a large shift to lower energies by 0.15 eV was observed in the yellow emission. The green emission was considered to correspond to the blue-copper emission in zinc sulphide, because no shift was observed in the time-resolved spectra. On the other hand the green emission was discussed in terms of a multivalent copper impurity model. No correlation was found between the green emission and photoconductivity. For this reason no decisive statement as to the nature of the centre could be made. The yellow emission was attributed to donor-acceptor pair recombination. The absence of a "time-shift", and the non-exponential decay of the red emission led Iida to suggest that the transition involved a free electron and a hole bound at a deep acceptor.

Stringfellow and Bube (39) proposed a recombination mechanism for ZnSe:Cu in terms of a multivalent-copper-impurity model. This model required Cu^{+} and Cu^{++} ions substituting on the Zn sublattice to be responsible for the red and green luminescence bands, respectively. The emission spectrum at 77 K reveals a red band with a maximum at 1.97 eV and a more intense green band with a maximum at 2.34 eV. At

16 K another red band was found with a maximum at 1.95 eV. The photoelectronic properties of ZnSe:Cu were described in terms of a defect which is optically active in three charge states, Cu'_{Zn}, Cu^{x}_{Zn} and Cu_{Zn}. The Cu'_{Zn} which is the dominant acceptor centre, with an energy level 0.72 eV above the valence band is responsible for the red emission at 1.97 eV. The red emission at 1.95 eV is associated with the recombination of an electron, either in a shallow level 0.012 eV below the conduction band or in the conduction band itself, with a hole captured at the Cu'_{Zn} centre. Cu^{x}_{Zn} is responsible for the green emission, which results from the recombination of an electron in the conduction band with a hole captured at a Cu^{x}_{Zn} centre, which has a level 0.35 eV above the valence band. The neutrality condition that $Cu'_{Zn} = Cu_{Zn}$ fixes the lowest position of the Fermi level obtainable at 0.53 eV above the valence band.

2.4.3 Manganese emission

Manganese as a luminescence activator in zinc sulphide has been studied most thoroughly and various investigators agree that the Mn^{++} ion occupies a substitutional anion site. In ZnS the emission consists of an orange band at 2.116 eV. The optical absorption spectrum of Mn^{++} in ZnS consists of five peaks in the visible region which have been identified by McClure (44) and by Langer and Ibuki (45) in terms of electronic transitions between the levels of the Mn^{++} ion split by the crystal field.

In ZnSe, fine structure in the optical absorption spectra of ZnSe containing 0.1 mole% Mn has been reported by Langer and Richter (46). They observed three bands at

about 2.617, 2.429 and 2.234 eV at 4.2 K, which correspond to the following transitions in the tetrahedrally coordinated Mn^{++} ion: $^6A_1 \rightarrow {}^4A_1, {}^4E$; $^6A_1 \rightarrow {}^4T_2$ and $^6A_1 \rightarrow {}^4T_1$ respectively. The $^6A_1 \rightarrow {}^4A_1, {}^4E$ transition was associated with the third absorption band, which lay in the region of high intrinsic absorption. Seven strong and weak lines were observed between 2.626 eV to 2.647 eV. These lines were attributed to interactions with lattice phonons. The $^6A_1 \rightarrow {}^4T_2$ transition was associated with the second absorption band which was also superimposed on the tail of the intrinsic absorption edge. Weak structure lines were observed at higher energies. The $^6A_1 \rightarrow {}^4T_1$ transition was associated both with the emission and the absorption band of lowest energy. No structure was found in absorption, but three emission lines were found at about 2.275, 2.232 and 2.132 eV at 4.2 K. The 2.132 eV emission line corresponds to the zero phonon $^4T_1 \rightarrow {}^6A_1$ transition.

The properties of the manganese luminescence centre in ZnSe have not yet been firmly established because the self-activated and the copper red emissions lie in the same spectral region. However, Larach (35) observed an emission band at 2.087 eV in the cathodoluminescence of Mn doped ZnSe. Apperson et al (47) observed three luminescence emission bands at about 1.95, 1.24 and 0.5-0.7 eV at 90 K in manganese activated ZnSe. They suggested that the 1.97 eV band was characteristic of 3d shell transitions in the Mn^{++} ions while the other two were independent of the manganese concentration. Asano et al (48) found a broad emission at 1.925 eV in ZnSe:Mn at 80 K while Allen et al (49) reported a rather broad band at 2.10 eV at 118 K. Recently Jones and Woods (50) have measured the excitation

and emission spectra of a single crystal of ZnSe doped with $MnCl_2$. They observed three excitation bands with maxima at about 2.308, 2.467 and 2.667 eV, and they identified the characteristic, relatively narrow Mn^{++} emission band as having a maximum at 2.115 eV when excited by 2.308 eV radiation. The emission was thermally quenched with activation energies of 0.03 and 0.3 eV.

CHAPTER 2

REFERENCES

1. D.G. Thomas and J.J. Hopfield, Phys. Rev. 128 (1962) 2135.
2. L.S. Pedrotti and D.C. Reynolds, Phys. Rev. 120 (1960) 1664.
3. D.G. Thomas, J. Phys. Chem. Sclids 15 (1960) 86.
4. D.G. Thomas and J.J. Hopfield, Phys. Rev. 124 (1961) 657.
5. M. Aven, D.T.F. Marple and B. Segall, J. Appl. Phys. Suppl. 32 (1961) 2261.
6. G.H. Hite, D.T.F. Marple, M. Aven and B. Segall, Phys. Rev. 156 (1967) 850.
7. Y.S. Park and J.R. Schneider, Phys. Rev. Letters 21 (1968) 789.
8. W.Y. Liang and A.D. Yoffe, Proc. of Royal Soc. A. 300 (1967) 326.
9. M.A. Lambert, Phys. Rev. Letters 1 (1958) 450.
10. D.C. Reynolds and C.W. Litton, Phys. Rev. 132 (1963) 1023.
11. D.C. Reynolds, L.S. Pedrotti and O.W. Larson, J. Appl. Phys. Suppl. 32 (1961) 2250.
12. R.E. Halsted and M. Aven, Phys. Rev. Letters 14 (1965) 64.
13. P.J. Dean and J.L. Merz, Phys. Rev. 178 (1969) 1310.
14. J.L. Merz, H. Kukimoto, K. Nassau and J.W. Shiever, Phys. Rev. B, 6 (1972) 545.
15. W.Y. Liang and A.D. Yoffe, Phil. Mag. 16 (1967) 1153.
16. K. Huang and A. Rhys, Proc. Roy. Soc. A, 204 (1950) 406.
17. J.J. Hopfield, J. Phys. Chem. Sol. 10 (1959) 110.
18. F.A. Kröger, Physica 7 (1940) 1.
19. M. Schön, Z. Phys. 119 (1941) 463.
20. H.A. Klasens, Nature 158 (1946) 306.
21. J.J. Lambe and C.C. Klick, Phys. Rev. 98 (1955) 909.

22. J.J. Lambe, C.C. Klick and D.L. Dexter, Phys. Rev. 103 (1956) 1715.

23. Y.S. Park and F.L. Chan, J. Appl. Phys. 36 (1965) 800.

24. R.E. Halsted, M.R. Lorenz and B. Segall, J. Phys. Chem. Sol. 22 (1961) 109.

25. R.E. Halsted, M. Aven and H.D. Coghill, J. Electrochem. Soc. 112 (1965) 177.

26. J.S. Prener and F.E. Williams, J. Electrochem. Soc. 103 (1956) 342.

27. J.J. Hopfield, D.G. Thomas and M. Gershenzon, Phys. Rev. Letters 10 (1963) 162.

28. D.G. Thomas, M. Gershenzon and F.A. Trumbore, Phys. Rev. 133 (1964) A269.

29. K. Colbow, Phys. Rev. 141 (1966) 742.

30. D.G. Thomas, J.J. Hopfield and W.M. Augstyniak, Phys. Rev. 140 (1965) A202.

31. D.G. Thomas, J.J. Hopfield and K. Colbow, in "7th Int. Conf. Phys. Semiconduc." held in Paris (Dunold, Paris) Vol. 4 (1964) p.67.

32. D.S. Orr, L. Clark and J. Woods, Brit. J. Appl. Phys. D, 2 (1968) 1609.

33. S. Iida, J. Phys. Soc. of Japan 25 (1968) 177.

34. J.L. Merz, K. Nassau and J.W. Shiever, to be published.

35. W.C. Holton, M. DeWit and T.L. Estle, in "Phys. and Chem. of II-VI Compounds" ed. M. Aven and J.S. Prener (N. Holland) 1967, Ch.9.

36. J. Lehmann, J. Electrochem. Soc. 114 (1967) 83.

37. S. Larach, J. Chem. Phys. 21 (1953) 756.

38. M. Aven and H.H. Woodbury, Appl. Phys. Letters 1 (1963) 53.

39. G.B. Stringfellow and R.H. Bube, Phys. Rev. 177 (1968) 903.

40. D. Curie, "Phys. and Chem. of II-VI Compounds" ed. M. Aven and J.S. Prener (N. Holland) 1967, Ch.9.

41. J. Dielman, S.H. De Bruin, C.Z. Van Doorn and J.H. Haanstra, ibid 1967, Ch.9.

42. J. Lehmann, J. Electrochem. Soc. 113 (1966) 449.

43. S. Iida, J. Phys. Soc. Japan 26 (1969) 1140.

44. D.S. McClure, J. Chem. Phys. 39 (1963) 2850.

45. D.W. Langer and S. Ibuki, Phys. Rev. 138 (1965) A809.

46. D.W. Langer and H.J. Richter, Phys. Rev. 146 (1966) 554.

47. J. Apperson, Y. Vorobiov and G.F.J. Garlick, Brit. J. Appl. Phys. 18 (1968) 398.

48. S. Asano, N. Yamashita, M. Oishi and K. Omori, J. Phys. Soc. Japan 24 (1968) 1302.

49. J.W. Allen, A.W. Livingstone and K. Turvey, Sol. State Elec. 15 (1972) 1363.

50. G. Jones and J. Woods, to be published.

CHAPTER 3

EXPERIMENTAL APPARATUS AND PROCEDURE

3.1 Introduction

A good general picture of the optical properties of the ZnSe crystals can be obtained by measuring their luminescence emission and absorption spectra near the band edge. A number of interesting characteristics of edge emission spectra may be observed at low temperatures, under continuous band gap excitation. The edge emission spectra are strongly dependent upon the stoichiometry and impurity content of the ZnSe crystals, and on the intensity of the excitation. The purpose of this work has been to examine the photo-excited edge emission, deep centre luminescence and optical absorption edge of the ZnSe crystals, at liquid nitrogen and liquid helium temperatures in an attempt to establish a correlation between the growth conditions and the spectral distribution of the various luminescence emissions. The present chapter describes the major experimental details of the material preparation, the cryostat, and the optical apparatus. The experiments have been performed in an attempt to analyse more accurately and to develop a more useful understanding of the edge emission in ZnSe single crystals.

3.2 Crystal growth

The zinc selenide crystals studied during the course of this research were grown in this laboratory in a furnace arrangement used earlier to grow crystals of cadmium sulphide. The original technique was first described by Clark and Woods (1,2), and developed by Burr and Woods (3) for the

growth of ZnSe. A brief description of the method of growing single crystals of ZnSe is given in this section.

The starting material used was either British Drug Houses "Optran" grade or Derby Luminescents "Electronic" grade ZnSe. It was necessary to purify these materials. For this purpose they were subjected to a vacuum sublimation process to remove volatile materials and zinc oxide impurity. During sublimation the zinc oxide remained with the charge. Some 80 gm. of the sublimate was then crushed, placed in a silica boat, and loaded into a long silica growth tube, as illustrated in Figure 3.1. A stream of high purity argon (350 ml/min) was then passed over the ZnSe which was held at a temperature of 1150^{o}C. Zinc selenide vapour was transported in the stream of argon to a cooler part of the growth tube where it condensed and crystals grew on a silica liner at about 1050^{o}C. The flow was maintained for five or six days during which time some 50 gm. of the charge sublimed. The crystals produced were pale yellow in colour and grew in the form of rods and irregularly shaped plates containing various low index faces. In this thesis such crystals will be called flow-run crystals. The platelet crystals were found to have a cubic structure as identified by X-ray back reflection and powder photographs together with examination under the polarising microscope. In general the growth surfaces of the plate-shaped crystals are (111) planes and contain triangular growth patterns, which seem to be characteristic of such crystals grown by the flow technique. Similar growth patterns have also been observed by Park and Chan (4). The rod shaped crystals were found to have a mixed cubic-hexagonal structure under the polarising

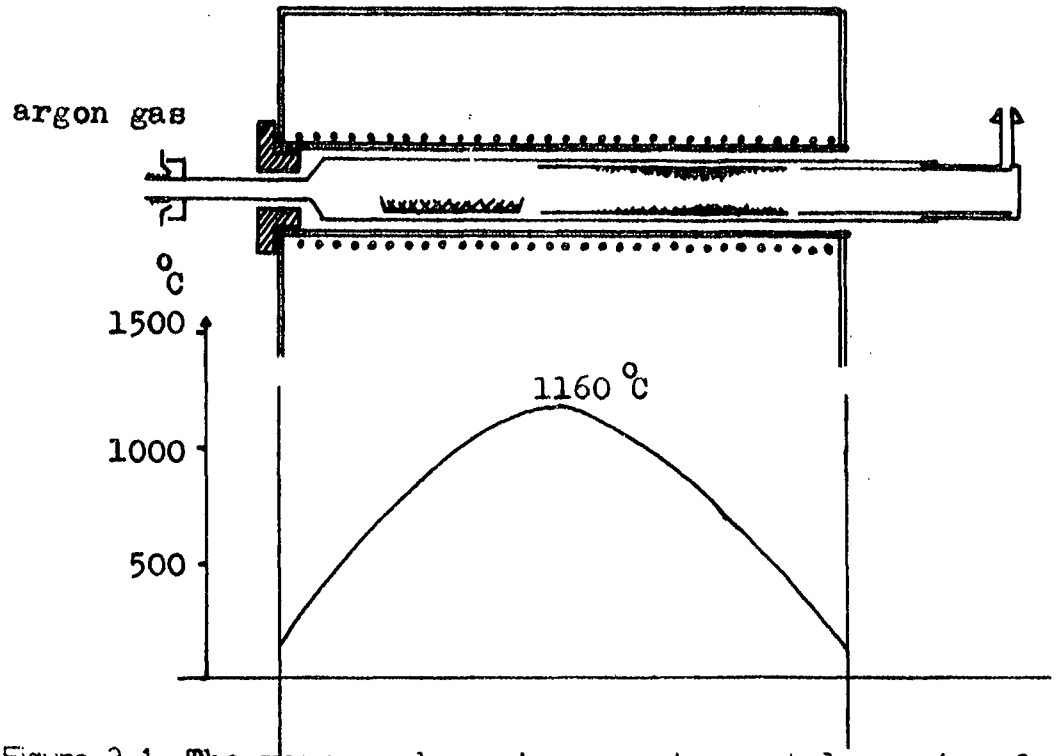

Figure 3.1 The vapour-phase-transport crystal growing furnace arrangement with temperature profile.

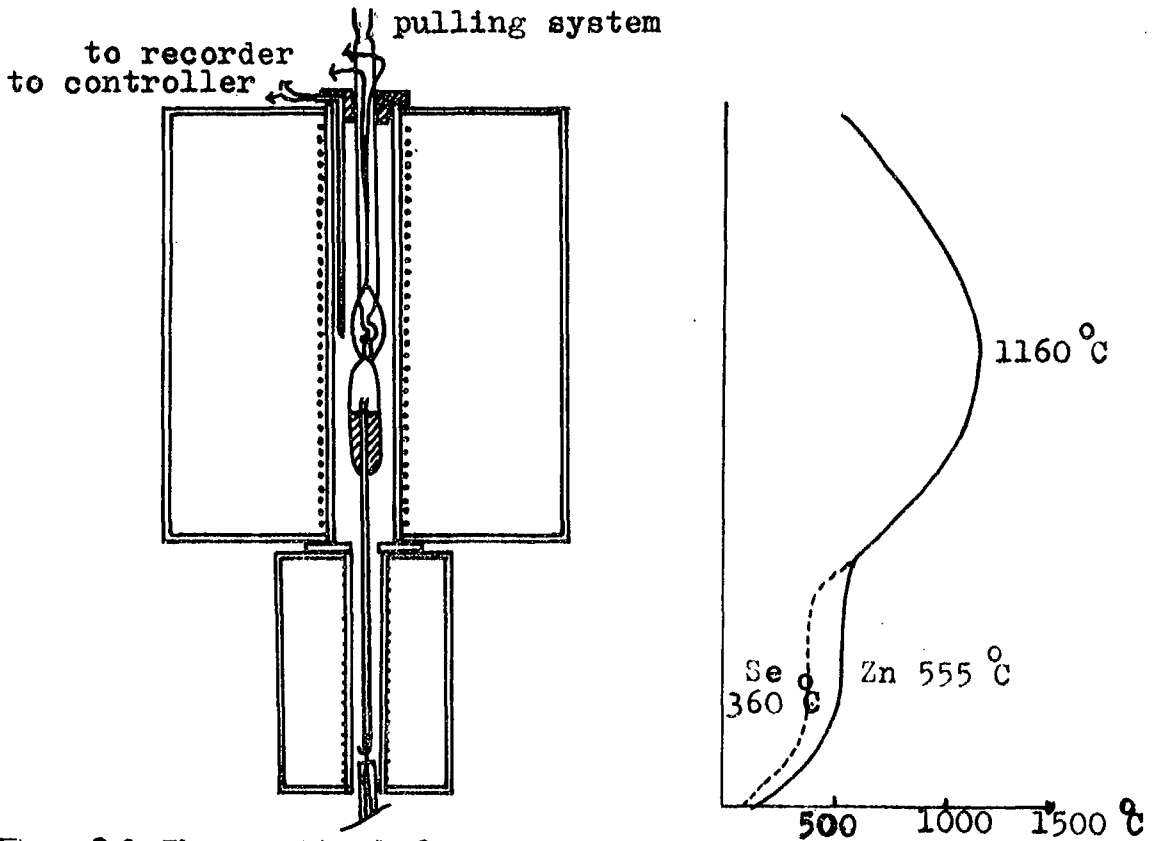

Figure 3.2 The vertical furnace arrangement shown with growth tube in initial position and temperature profile.

microscope and the optical c-axis was found to be parallel to their length. Both platelet and rod-shaped flow-run crystals were used as the starting material for the production of a large boule by sublimation in a sealed silica capsule.

The vertical furnace arrangement and a typical quartz glass capsule used to grow large boules are shown in Figure 3.2. A schedule of evacuation, baking and flushing with argon was used to remove volatile impurities from the quartz glass tube. The procedure was repeated after an excess of either selenium or zinc had been placed at the bottom of the long silica reservoir shown in Figure 3.2. Finally the purified flow-run ZnSe crystals were loaded into the capsule together with any dopant which might be required. After flushing three times with argon and several hours evacuation to 10^{-6} torr, the tube was sealed off from the vacuum system and inserted in the furnace arrangement in the position indicated in Figure 3.2. The upper furnace was then brought to the ZnSe sublimation temperature near 1160°C. Growth occurs at the top of the quartz tube at a temperature of about 1100°C. The ambient vapour pressure during growth was stabilised by an excess of zinc in the reservoir which was held at a temperature of 555°C, this leads to the so-called p_{min} condition. An identical situation arises with an excess of selenium in the reservoir at 360°C. The tube was then steadily pulled through the furnace system when the temperatures were stable. As a result the temperature gradient was effectively moved across the growth chamber and led to the vapour transport of the ZnSe from the charge to the upper part of the growth capsule, where the boule crystal formed. The reservoir was maintained at a steady

temperature to ensure a constant elemental partial pressure during growth. The pull was usually stopped when about half the charge had sublimed, but the quality of the resultant boules did not appear to be dependent on the pulling rate. Using this method it was possible to grow a crystal 30-40 mm long, weighing 20 gm. in approximately 240 hours. The crystals were either cooled rapidly by removing the tube from the furnace system or more usually, were cooled slowly over a period of some 48 hours. The latter procedure resulted in a considerable reduction in the built-in strain in a crystal. The boules grown in this manner have a body colour which varies from pale yellow to green and are circular in section with a 1 cm. diameter. X-ray back reflection and powder photographs show that these crystals possessed the cubic zinc blende structure.

The changes in the physical properties of the "doped" crystals containing added impurities such as Mn, Cu, Al, Ga, In, Cl, $MnCl_2$, ZnS and Li compared with those of "pure" crystals grown under the same conditions, confirmed that transport of the dopant from the charge to the boule had taken place.

3.3 Sample preparation

Plane parallel slices had to be cut from the boules and polished to produce samples for the transmission and absorption measurements. These were then etched to remove surface damage. In contrast the luminescence measurements were made on cleaved faces which according to reflection electron-diffraction were free from damage. The cleaved samples were selected from the central volume of a boule,

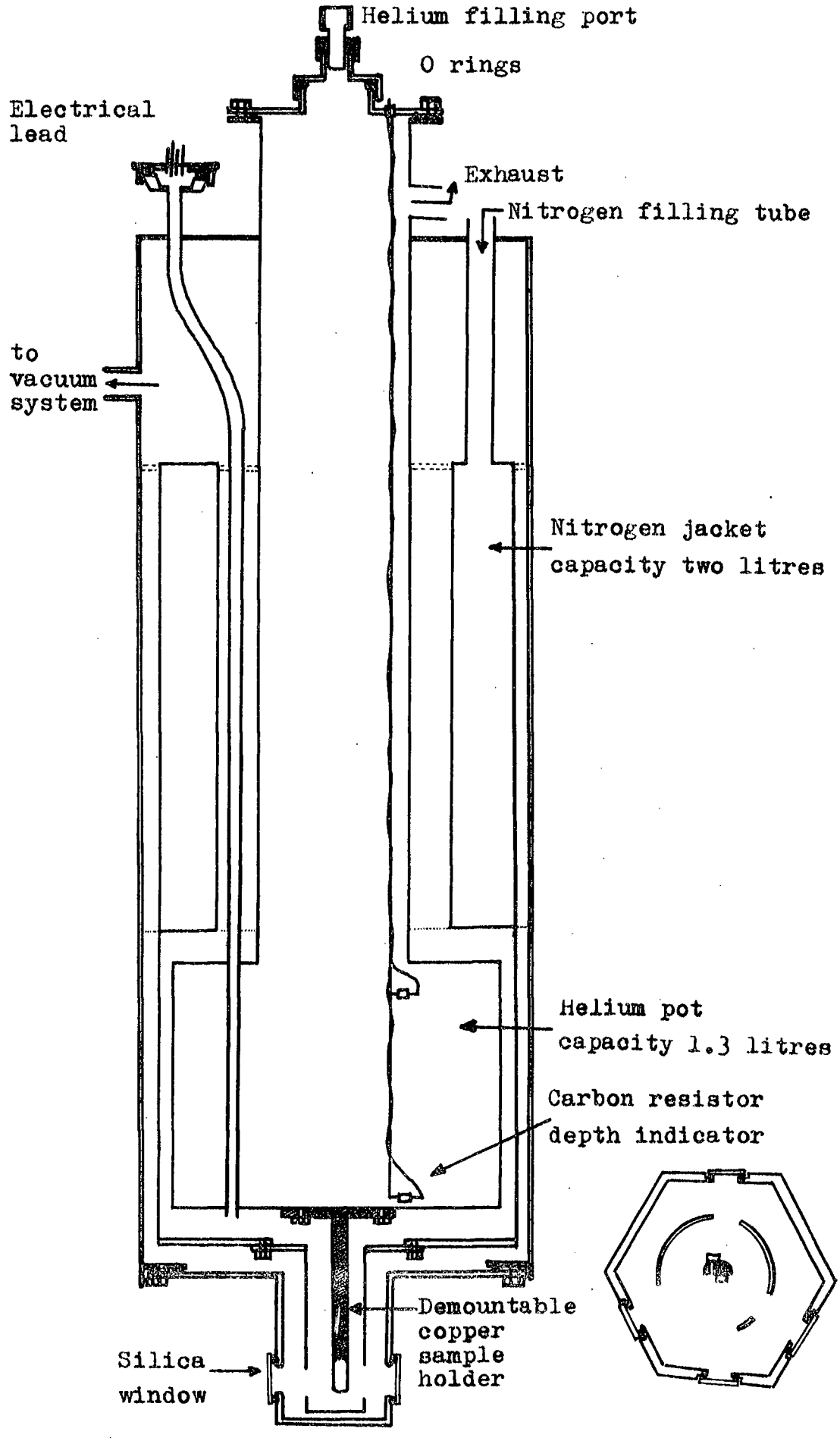

Fig. 3.3. Diagram of the metal helium cryostat.

thus avoiding the strain and damage produced by cutting and polishing, and also avoiding regions possibly contaminated by the wall of the growth tube. Cleaving meant that the sample geometry was irregular, so that cleaved samples were oriented by X-ray back reflection technique when necessary.

For the absorption and transmission measurements it was necessary to orient the ZnSe crystals before taking any measurements. The first step was to hold the rough uncut boule crystal on an X-ray goniometer and take an X-ray back reflection photograph. Examination of the photograph provided information about the crystal orientation. The goniometer was then readjusted until the (111) zone axis was found. Having been locked, the entire goniometer with its mounted crystal was transferred to a diamond saw where slices of various thickness (0.5 mm to 5 mm) were cut from the boule. A slice was then mounted with "Durafix" glue on to the mounting plate of a "Logitech" polishing machine and carefully polished using 0.25 micron diamond paste. The polished surfaces were examined under the microscope. The flatness of the polished surface could be measured to high accuracy, by observation of the interference fringe pattern formed between the specimen surface and an adjacent flat glass reference surface. Finally the specimen was remounted to polish the second surface. The second face of the specimen was reasonably parallel to the first, further high parallelism could be achieved if required by using an autocollimator system calibration on the mounting plate. The ZnSe slice was then etched in a dilute solution of

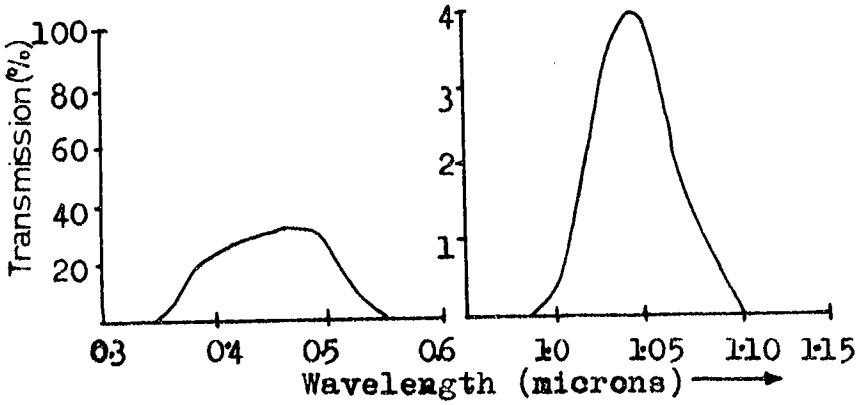

Figure 3.4 (a) Transmission characteristic of a three inch cell containing a saturated solution of copper sulphate.

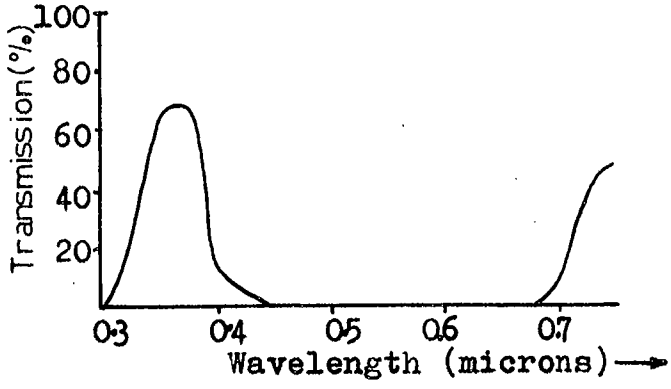

Figure 3.4(b) Transmission characteristic of OX 1A filter.

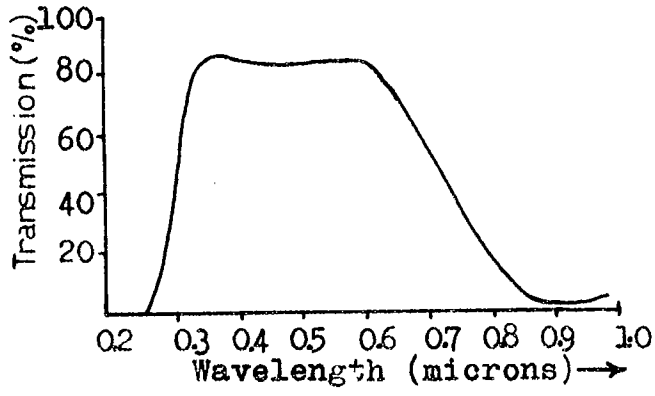

Figure 3.4(c) Transmission characteristic of HA 1 filter.

bromine in methanol. The details of the etching technique have already been fully described by Gezci and Woods (5).

3.4 The Cryostat

The all brass, helium cryostat was manufactured by the Oxford Instrument Co. Ltd. and has been slightly modified. The construction of the cryostat is illustrated schematically in Figure 3.3. The essential features are:

(1) A two litre capacity liquid nitrogen jacket.

(2) A 1.3 litre capacity liquid helium pot.

(3) Two carbon resistors, mounted on a thin stainless steel tube, for use as a depth gauge in liquid helium pot.

(4) A demountable copper sample holder situated below the liquid helium pot. The copper radiation shield is also demountable and is usually attached to the liquid nitrogen jacket. The outer vacuum wall contains four silica windows in different positions surrounding the tail.

(5) A facility for electrical and thermocouple leads which allows connection to be made to the sample from outside the cryostat.

(6) The sample is maintained under a vacuum of at least 10^{-3} torr.

A conventional vacuum system, incorporating an Edwards High Vacuum Ltd. ES 150 rotary pump and water cooled EO 1 oil diffusion pump,was used to evacuate the cryostat. Provision was made for the helium exhaust gas to be collected and the liquid nitrogen to be pumped for quick cooling of the cryostat.

Indium was used to mount the zinc selenide samples to the cold copper finger since it provided good electrical

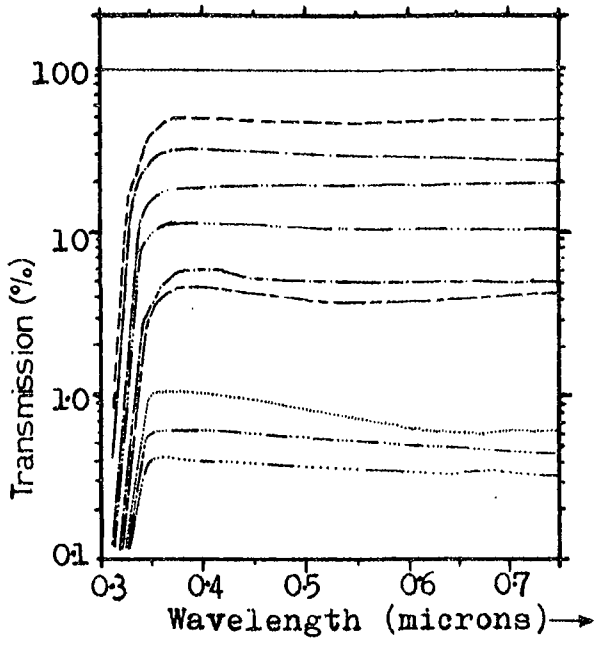

Figure 3.5 (a) The transmission characteristics of neutral density filters.

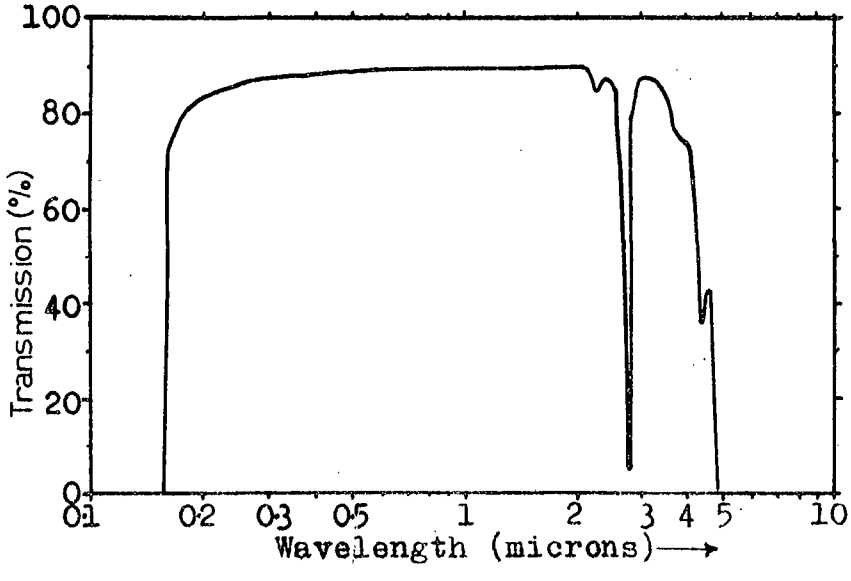

Figure 3.5 (b) The transmission characteristic of 1mm. thick silica windows.

and thermal contact. The cold finger was detached from the cryostat and heated until the indium, covering the sample area, was molten. The heating was then stopped and the crystal placed on the indium just before it solidified. It was assumed that the effects of any heat treatment upon the samples during the course of mounting upon the copper block were negligible.

A carbon radio resistor gave an indication of the depth of liquid in the helium pot, and greatly assisted the estimation of the stage reached during the transfer of liquid helium. A copper-constantan thermocouple was used to measure the temperature of the crystal. The thermocouple was embedded in indium on the copper sample holder at a position near to the crystal. No attempt was made to achieve equilibrium at temperatures intermediate between helium and nitrogen. A small temperature lag may well have existed between the indicated thermocouple temperature and actual crystal temperature. After liquid helium had been transferred to the helium pot the temperature recorded with , and without, incident ultraviolet radiation was between 6 K and 10 K, rising to 23 K to 25 K under QI (quartz iodine lamp radiation) excitation. When heat absorbent filters (HA 1) were used the temperature fell to between 10 K and 12 K. With liquid nitrogen in the helium pot, the temperature measured under the same conditions of excitation was 82, 85 and 82 K respectively. If the liquid nitrogen was pumped to a pressure of 1 mm Hg the temperature measured under the above conditions of illumination fell to 65, 68 and 65 K.

The cryostat could be cooled to temperatures intermediate between those or liquid nitrogen and liquid helium.

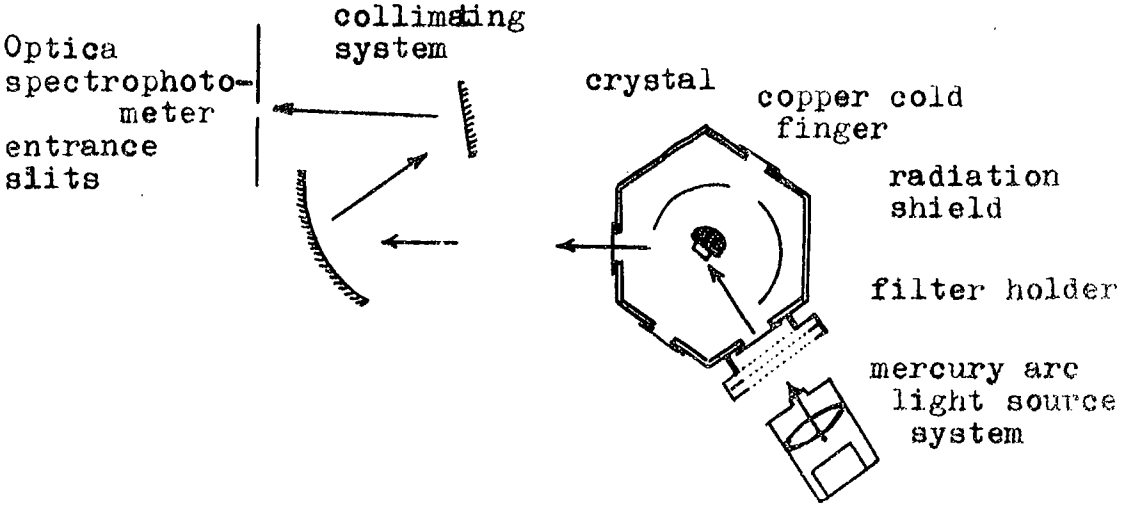

(a) For the luminescence measurements using the Optica.

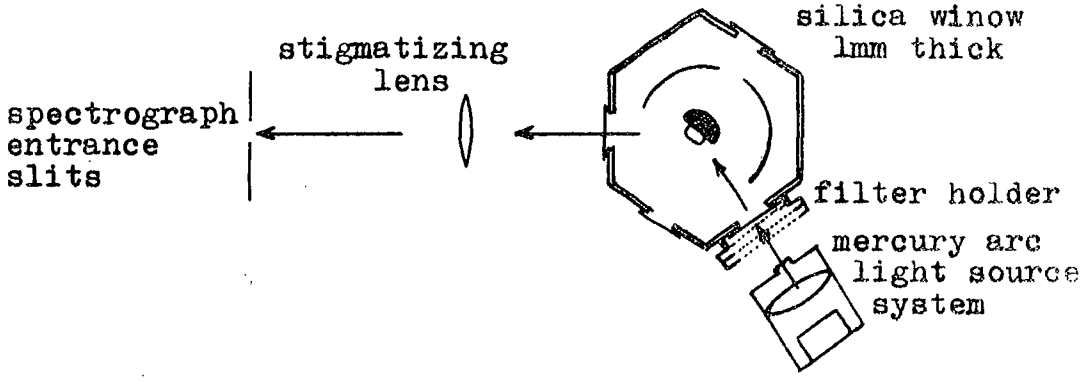

(b) For the luminescence measurements using the Bausch and Lomb Spectrograph.

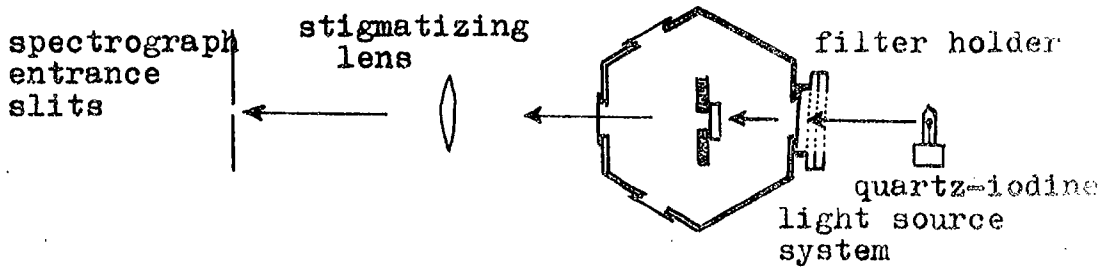

(c) For the absorption measurements using the Bausch and Lomb Spectrograph

Figure 3.6 Diagrammatical representation of the arrangement of the cryostat and optical collimation system.

A quick and easy method of transferring liquid helium is as follows: firstly the cryostat vacuum system is evacuated to a pressure of 10^{-3} torr after which the nitrogen jacket and helium pot are filled with liquid nitrogen. Then liquid nitrogen is evacuated from the helium exhaust pipe until a pressure of 1 mm Hg is obtained. The evacuation is stopped and nitrogen gas at 4 pound/mm pressure is supplied, this removes all liquid nitrogen from the helium pot via the vacuum syphon. Then the helium pot is re-evacuated to a pressure of 10^{-2} mm Hg to ensure that no liquid nitrogen remains. The vacuum is let down to atmospheric pressure with helium gas and approximately two litres of liquid helium is transferred. This quantity of helium can keep the specimen at 6 K for periods of up to four hours.

3.5 Photo-excitation

The photoluminescence of the zinc selenide crystals was excited by U.V. radiation from a 250 watt high pressure mercury lamp filtered by two Chance glass OX1A filters to pass 3650 Å radiation. The 250 watt mercury lamp with a 5Ω series resistance was run under 82 volts, 4 amps. stabilised d.c. and provided a total radiative flux of approximately 100 watts. The radiative energy emitted at 3650 Å is approximately 16.4% of the total radiated intensity. The transmission of each OX1A filter is 70%, so the total percentage of the radiation emitted at 3650 Å is 8.04%, which amounts to 8 watts to be focussed on the crystal. This radiant energy was reduced using the various neutral density filters, manufactured by Barr and Stroud Ltd. A

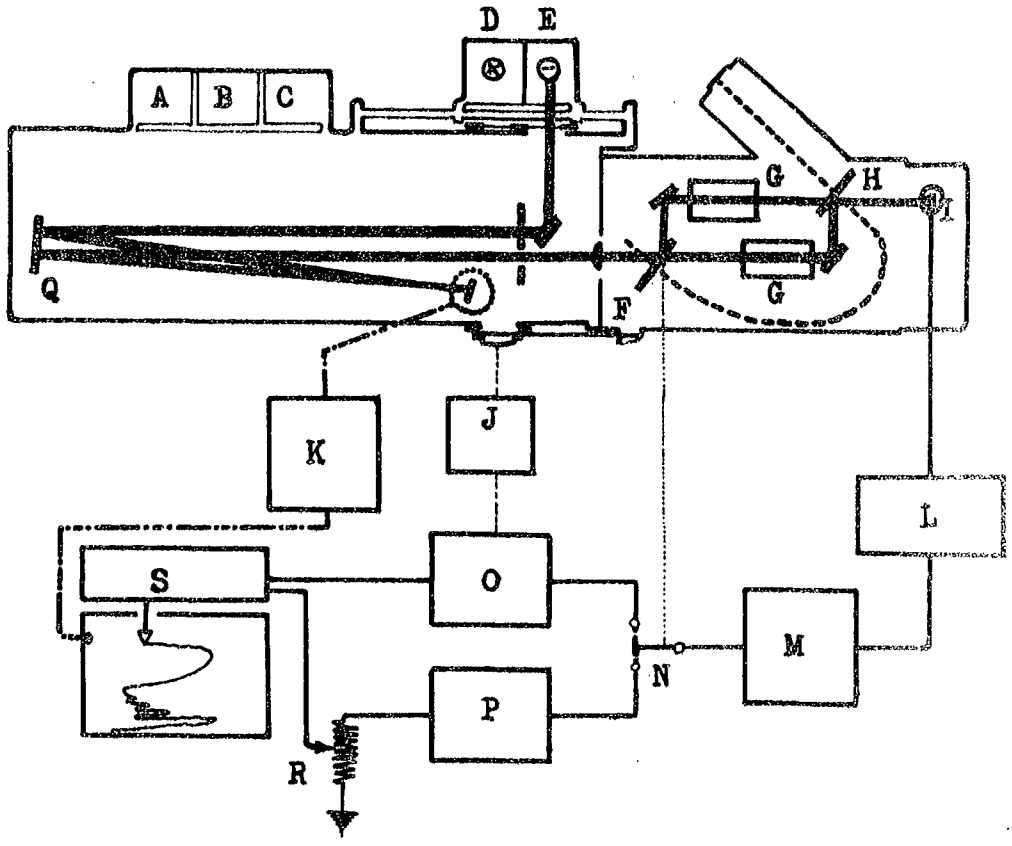

Figure 3.7 Block diagram of the Optica spectrophotometer.

A Hydrogen power supply
B Photomultiplier power supply
C Tungsten power supply
D Hydrogen lamp
E Tungsten lamp
F Rotating mirror
G Reference cell and sample cell
H Rotating mirror
I Detector
J Slit Servo
K Wavelength drive
L Pre-amplifier
M Amplifier
N Commutator
O Reference Demod.
P Sample Demod.
Q Grating
R 100% adjustment
S Pen recorder

set of 50%, 30%, 10% and 1% transmission filters were used and in combination 15%, 5%, 3%, 0.5%, 0.3% and 0.1% of the unfiltered energy could be obtained. Figure 3.4(a,b, and c) shows the transmission characteristics of the selective filters used, i.e., a 3 inch cell containing a saturated solution of copper sulphate, an OX1A and heat absorbent HA1 filter. Figure 3.5 (a and b) shows the transmission of the neutral density filters and silica windows.

The arrangement used to excite the specimen and collimate the luminescence via two mirrors is shown in Figure 3.6(a). The number "one" window allowed the sample to be irradiated with U.V. and the number "three" window was used for the collimation system. The same arrangement was used with the spectrograph but a stigmatizing lens was used to collimate the luminescence via the third window as shown in Figure 3.6(b).

A second arrangement which was used for the transmission and absorption measurements is shown in Figure 3.6(c). The sample was irradiated via the number "four" window with light from the quartz iodine lamp. Light left the cryostat via the number "two" window and entered the condensing system via the quartz stigmatizing lens.

3.6 Optica CF4N1 Spectrophotometer

The Optica CF4N1 is a double beam, recording spectrophotometer principally designed for absorption and transmission measurements. The spectral range is 0.185 μm to 3.1 μm. When used as an emission measuring instrument, the spectral range depends upon the response of the detectors. For absorption and transmission measurements

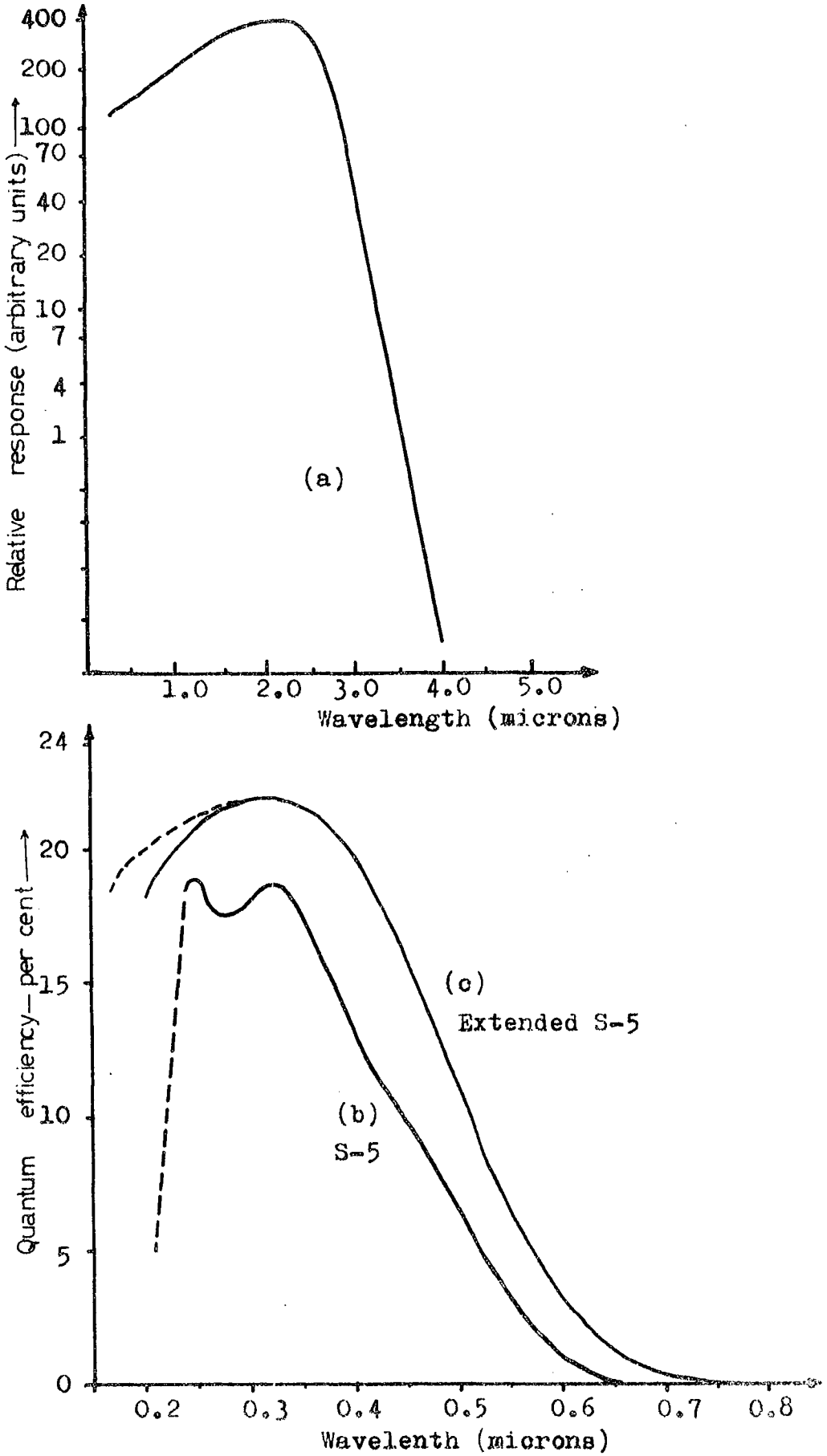

Figure 3.8 Spectral response characteristics

(a) Kodak Ektron PbS detector.

(b) Type 1P28 (S-5 Response) photomultiplier.

(c) Type 9781R (Extended S-5 response) Pm.

two sources were provided, namely a hydrogen discharge lamp and a low voltage tungsten lamp. The hydrogen lamp was used over the wavelength range 0.185 to 0.400 μm whereas the tungsten lamp was used over the range from 0.320 to 3.1 μm.

The monochromator was of the Littrow type, with two interchangeable plane gratings as the dispersive elements. The standard monochromator dispersion was approximately 16 Å/mm with a ruled grating with 600 lines/mm for the ultraviolet and visible regions (0.185 to 1.0 μm). The dispersion was 32 Å/mm for the near infra-red region (0.9 μm to 3.1 μm), when a 300 lines/mm ruled double grating arrangement was used. The monochromator slit width was 3.6 mm at its maximum and the smallest division on the slit drum was 0.02 mm, which was either automatically servo operated by the reference signal level or could be changed by turning the handle.

The light beam emerged from the monochromator through the only lens in the instrument which condensed the light on to a system of mirrors. A rotating mirror and fixed mirror in each beam passed the light through the reference and sample cells, alternately at 18 cycles per second. The two rotating mirrors were driven by an external motor and displaced one against the other by 180°, so that only one was in the beam at any one time. Both beams were exactly identical in length and were optically symmetrical. The detector always saw the light from the two cells along the same optical path. The differential electrical signal from the detector was amplified and displayed on a Honeywell chart recorder. Figure 3.7 illustrates the block diagram

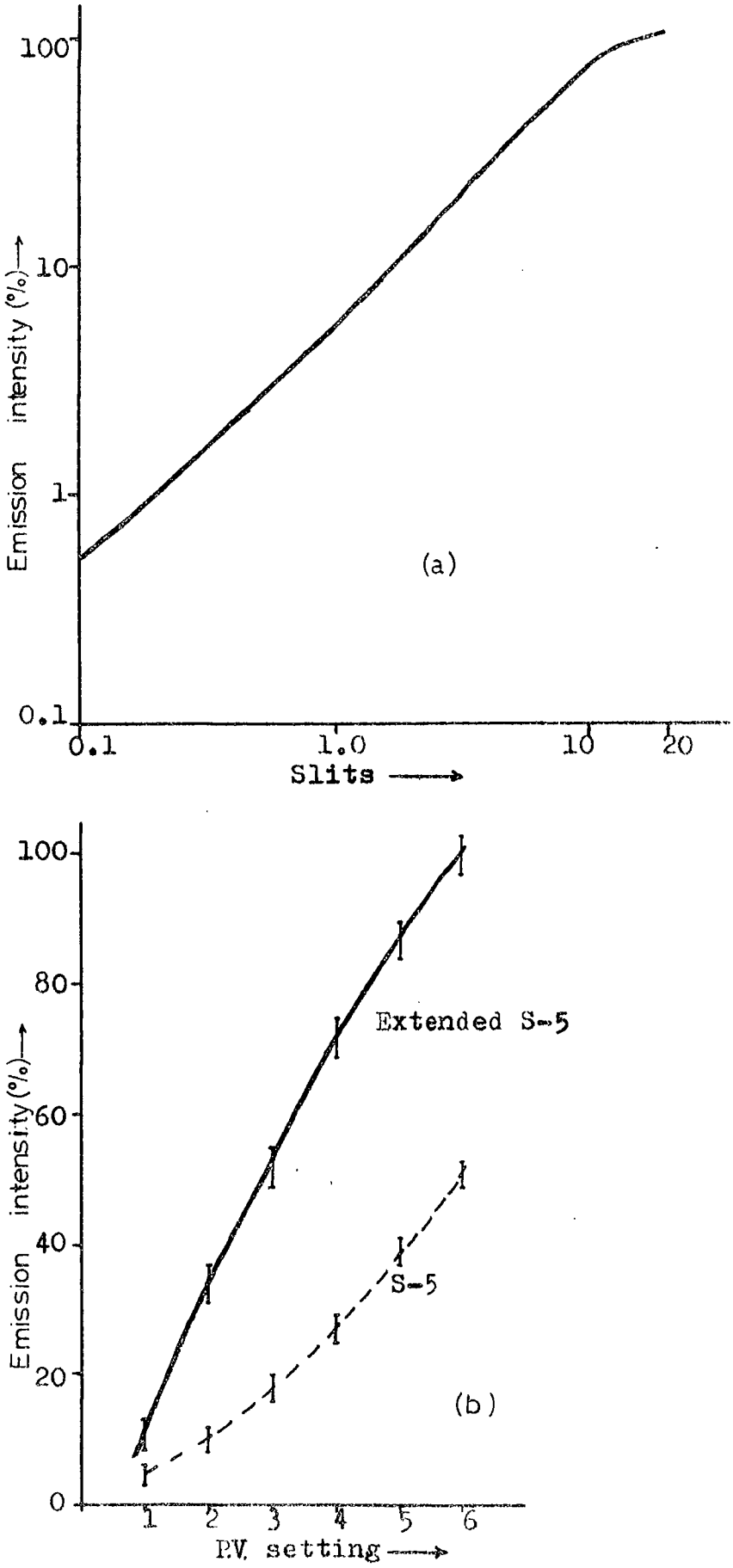

Figure 3.9 "Correction factors" used to convert the intensity of the emission to the standard of slits 1, wavelength 0.47 micron.

of the Optica spectrophotometer. For absorption measurements, the double beam system avoided any necessity to compensate for the spectral response of the photomultiplier and the spectral emission of the source.

To study an emission spectrum, light from the source was focussed on to the entrance slit of the monochromator. The double beam ratio amplifier was switched to the "Single beam mode" when an electrical reference signal replaced that provided by the reference beam. The slit width was set manually to the resolution required.

Two types of photomultiplier were used to span the ultraviolet and visible regions. Their spectral sensitivities are shown in Figure 3.8. An RCA type 1P28 photomultiplier with an S-5 photocathode covered the range 0.185 to 0.62 μm while a higher sensitivity EMI type, 9781R with extended S-5 response was used in the 0.2 to 0.75 μm range. A much less sensitive Kodak Ektron lead sulphide detector was provided for use in the near infrared. Figure 3.9(a) shows the effect of the applied voltage on the photomultiplier response for a constant monochromator slit width, Figure 3.9(b) shows the photomultiplier response as a function of slit width at constant photomultiplier voltage in the 0.53 μm region. These calibration curves were used to estimate the relative intensity of the emission components of different ZnSe crystals.

To calibrate the spectrophotometer the emission spectra of sodium, mercury, and neon discharge tubes were recorded. The wavelengths were on average ±2Å different from the accepted values. More accurate wavelength analysis was made using the Bausch and Lomb spectrograph.

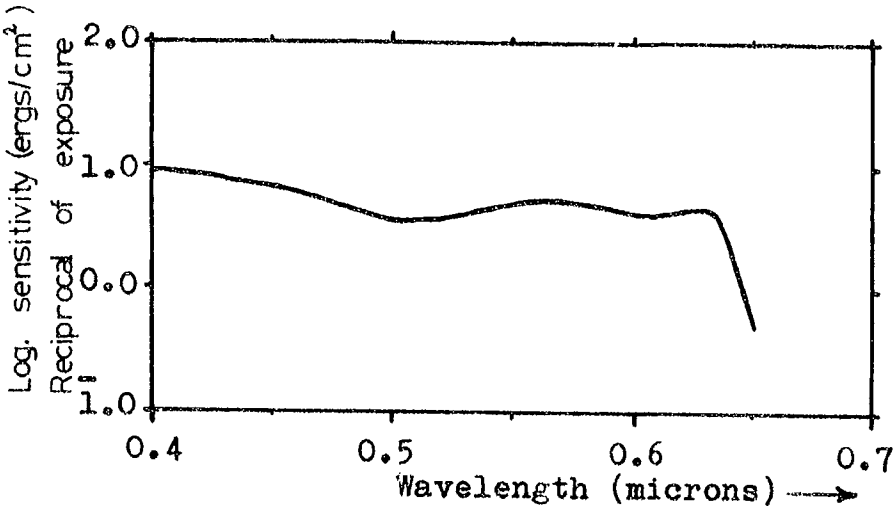

Figure 3.11(a) **Spectral response of Kodak "Tri-X" Pan film.**

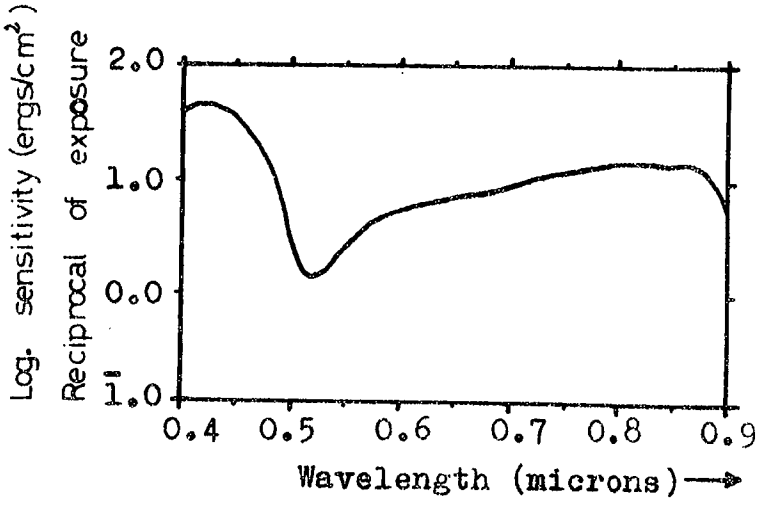

Figure 3.11(b) **Spectral response of Kodak High Speed Infrared 2481 film.**

3.7 Bausch and Lomb Spectrograph

A Bausch and Lomb (model 12) 1.5 metre grating spectrograph gave results in good agreement with those obtained from the Optica. The spectral ranges available were 0.45 to 0.700 μm in first order, and 0.225 to 0.350 μm in second order. The dispersion was 10 Å/mm in the first order and 5 Å/mm in the second. The instrument is shown diagrammatically in Figure 3.10. A fixed slit system was used on the grating spectrograph which incorporated the following components.

(a) The fixed slit assembly provided three fixed slit widths of 10, 32 and 60 μm which could be inserted as required.

(b) A Hartmann slide included a diagonal slit and sliding scale with a fish tail notch, which controlled the height of the spectrum recorded on the film. The diagonal slit was 1.5 mm wide and could be moved across the input aperture so that it was possible to arrange eleven spectra 1.5 mm high on the same film.

The light entered the spectrograph through the fixed slit and travelled through the stigmatizing lens to be diffracted by the grating. (635.3 lines per mm). The light was then reflected on to the film which was held in a specially curved 10 inch long cassette. The dispersion remained linear along the length of the film.

Two different 35 mm films were used to record the spectra. The colour sensitivity was evenly balanced throughout the spectrum, Kodak "Tri X" pan high speed film was used in the range 0.45 to 0.65 μm while Kodak 2491 high speed infra-red film was used in the range 0.45 to 0.7 μm.

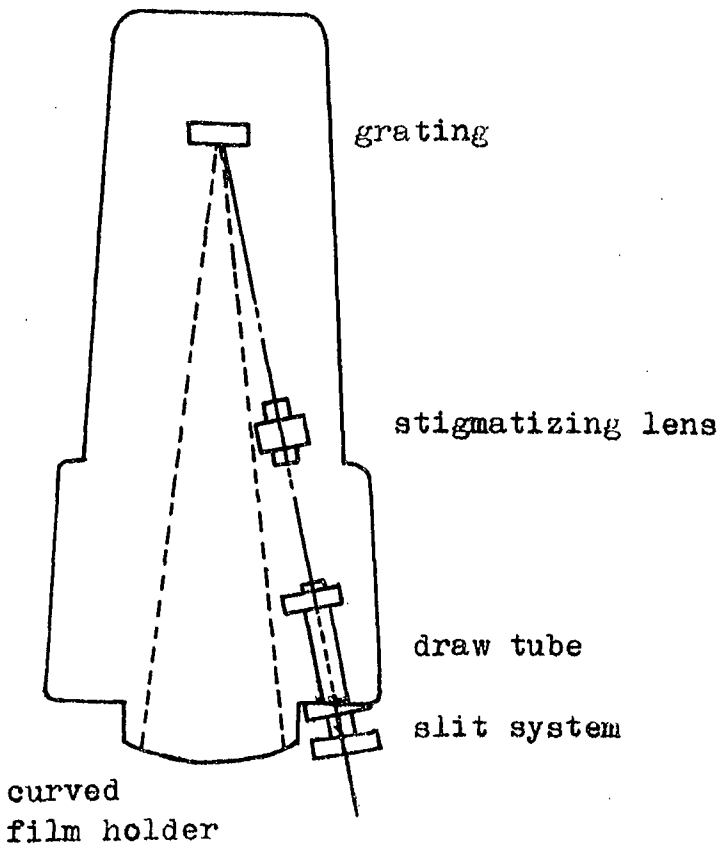

Figure 3.10 Diagram of the Bausch and Lomb 1.5 meter grating spectrograph.

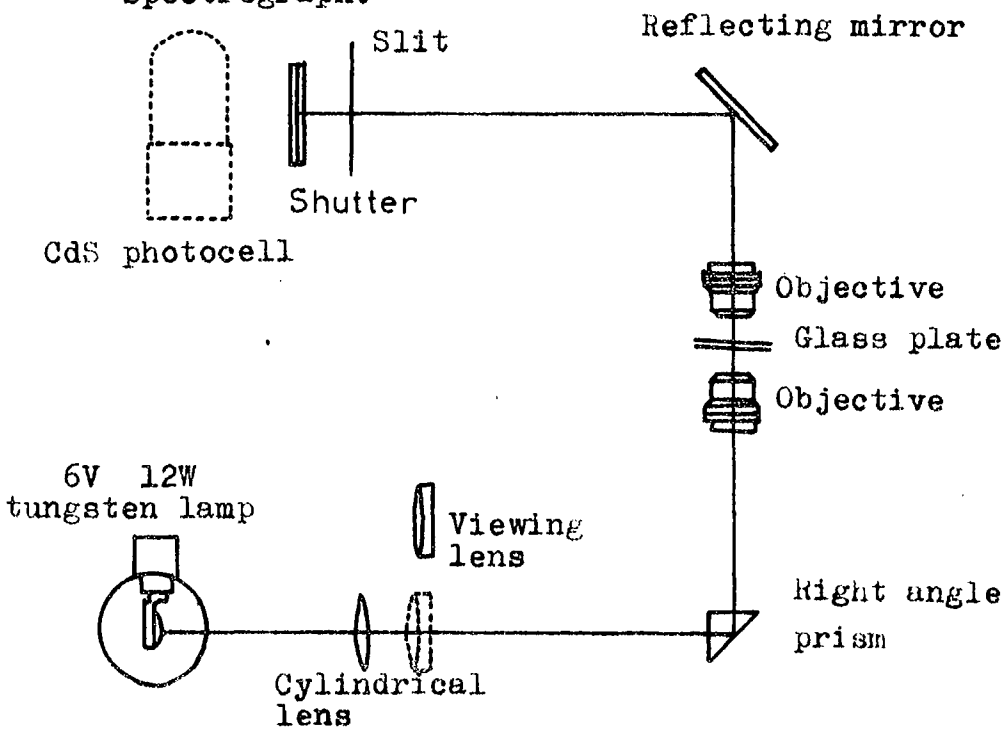

Figure 3.12 Diagram of the Hilger and Watts Microdensitometer

The spectral responses of both films are shown in Figures 3.11(a and b). It was necessary to make trial exposures (from 5 - 45 min) to determine the best exposure time for a given emission intensity. Both films were processed in Kodak D-76 developer.

3.8 Microdensitometer

A Hilger and Watts microdensitometer was used to measure the spectral lines on the recorded film to determine the optical density. The instrument is shown diagramatically in Figure 3.12. In addition to providing a spectrographic reference mark, a sodium discharge tube provided calibration lines, and allowed the dispersion to be determined.

The light was transmitted through the film by a microscope objective arrangement and was detected by a cadmium sulphide photocell via an adjustable slit system. The output from the cell was displayed on a Honeywell Electronic 194 pen recorder. The slit width was adjusted to be as narrow as possible while providing a measurable signal level. Best results were obtained with a width of 0.2 mm. A synchronous electric motor was used to drive the glass table on which the film was sandwiched between thick and thin glass plates.

CHAPTER 3

REFERENCES

1. L. Clark and J. Woods, Brit. J. Appl. Phys. 17 (1966) 319.
2. L. Clark and J. Woods, J. Crystal Growth 3,4 (1968) 127.
3. K.F. Burr and J. Woods, J. Mat. Sci. 6 (1971) 1007.
4. Y.S. Park and F.L. Chan, J. Appl. Phys. 36, 3 (1963) 800.
5. S. Gezci and J. Woods, J. Mat. Sci. 7 (1972) 603.

CHAPTER 4

EDGE EMISSION OF UNDOPED ZINC SELENIDE

4.1 Introduction

The edge emission of undoped crystals of zinc selenide excited by continuous ultra-violet radiation has been studied at liquid nitrogen and helium temperatures. The crystals were grown in the ways described in chapter three. With most samples a relatively broad band with longitudinal optical phonon replicas was observed at 87 K. As the temperature was reduced to pumped liquid nitrogen temperature at 65 K the intensity of the emission usually increased and in general a high energy series (free to bound recombination) became dominant. At liquid helium temperatures bound exciton lines and pair bands could be detected in the majority of crystals.

Three types of undoped crystals were examined over a range of temperatures from 10 to 87 K. These were flow crystals, and boule type crystals grown in a slight excess of selenium or zinc. It was found that the relative intensities of the major components of the U.V. excited emission at 10 K could be correlated with the conditions under which the crystals were grown, provided that the starting charge was of a consistent, good quality. The Optica spectrophotometer was used to determine the basic trends, while the Bausch and Lomb grating spectrograph was used to make a more detailed study of the components of interesting spectra.

In this chapter, the first section is concerned with a brief description of the edge emission at liquid nitrogen temperature of the three different types of undoped crystal.

This is followed by a description of the emission spectra of the same crystals at liquid helium temperatures. With some samples the recombination kinetics of the edge emission was studied by varying the excitation intensity and the temperature. The origin of the edge emission is discussed and the conclusions compared with those of other workers. Unless otherwise stated, the measurements referred to were recorded using the Optica, and are uncorrected for photomultiplier response. When two different recordings have been superimposed on the same figure, the emission intensities are not directly comparable when the term "emission intensity (arbitrary units)" is used. "Relative intensity" means that the curves may be compared directly.

4.2 Edge emission characteristics at liquid nitrogen temperatures

At liquid nitrogen temperatures edge emission is due to the recombination of a free electron with a hole bound at an acceptor, the energy of the emitted photon is given by,

$$E_p = E_G - (E_A - E_K) \qquad (1)$$

E_G is the band gap energy, E_A is the acceptor binding energy and E_K the kinetic energy of the free electron. The acceptor binding energy E_A can be determined from this equation by using the observed peak energy of the emission band and known values of $E_K \simeq kT$. The edge emission spectra at liquid nitrogen temperatures of the various undoped crystals can be summarized as follows:

4.2.1 Flow run crystals

Only a few zinc selenide crystals grown from the

vapour phase in a continuous flow of argon were luminescent under U.V. excitation at liquid nitrogen temperatures. A typical emission spectrum of a luminescent crystal consists of a series of equally spaced bands decreasing in intensity at longer wavelengths. The emission spectrum of such a crystal (for example No.87) exhibits five peaks with maxima at 4610, 4662, 4715, 4773 and 4830Å at 87 K. At 65 K this series shifts by about 2Å to shorter wavelengths while a small shoulder appears at 4560Å. At this temperature the five major bands were located at 4608, 4660, 4714, 4770 and 4828Å. The maxima of these bands have an equal-energy separation of approximately 0.0308 ± 0.0006 eV. The band at the shortest wavelength with a maximum at 4608Å is the zero order phonon component, while with the remainder, recombination occurs with the co-operation of one, two, three and four longitudinal optical (LO) phonons. The energy separation of adjacent bands is in good agreement with the LO phonon energy of 0.0314 eV for cubic ZnSe determined by Halsted et al (1).

The origin of the shoulder at 4560Å has not hitherto been well understood. Results to be described later show that it is almost certainly a different no-phonon band with replicas too weak to be detectable and obscured by the major series. This band was also observed by Reynolds et al (2) at 4.2 K. They offered no explanation as to its origin. No spectral change in any of the emission was observed at 65 K when the excitation intensity was varied. This suggests that the free to bound assignment of the 4608Å series is correct. In addition to this blue edge emission, a broad green band with a half-width of about 380Å was located at about 5360Å.

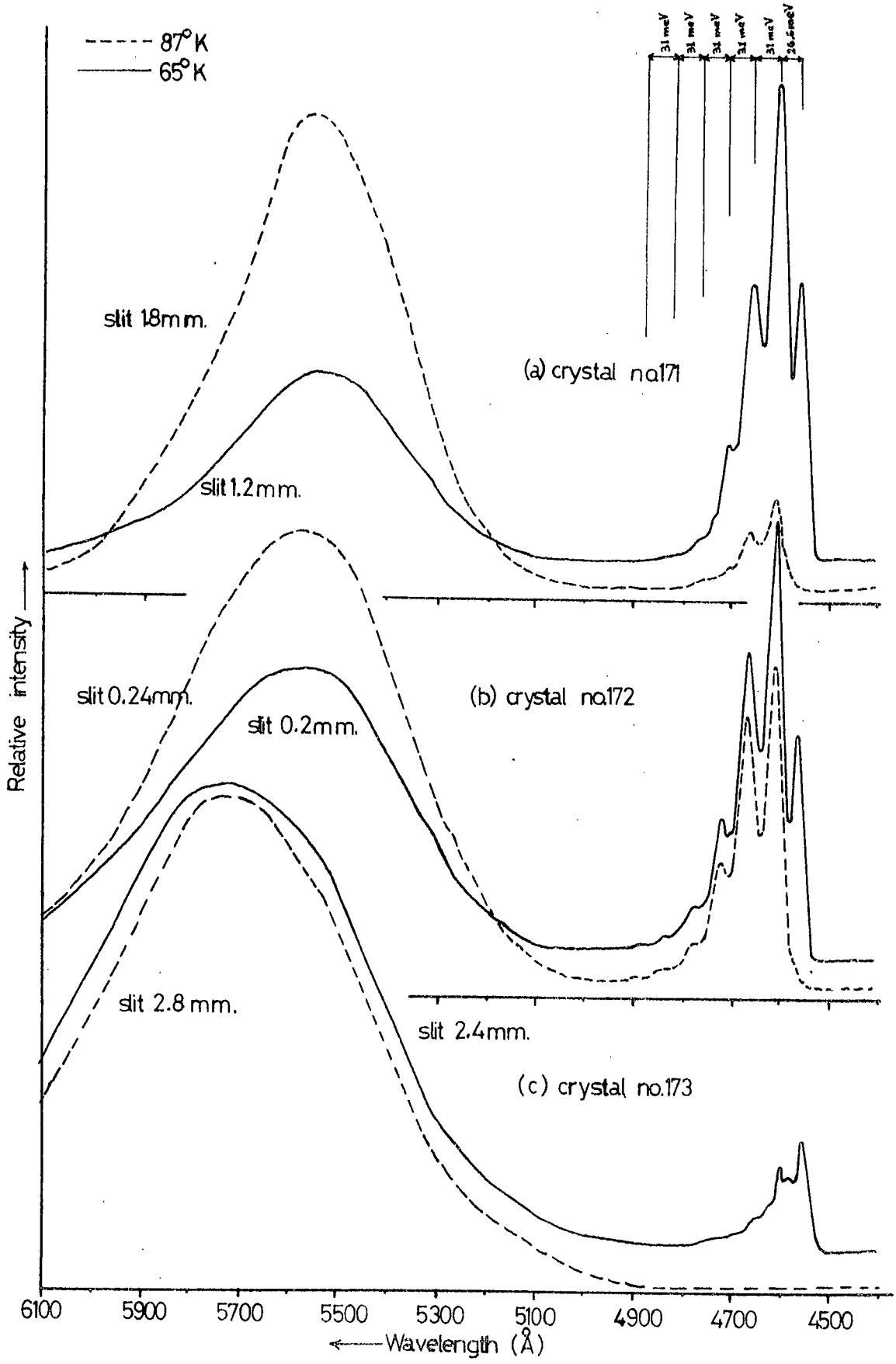

Figure 4.1 Comparison of the emission spectra of crystals grown with different reservoir temperatures.

4.2.2 Crystals grown in selenium vapour

These were crystals grown in the sealed tube system with selenium added to the reservoir. The crystals were grown from charges at temperatures of 1115°C. The P_{min} condition was obtained when the selenium in the reservoir was held at 360°C. Crystals were grown with a variety of selenium reservoir temperatures ranging from 335 to 385°C. Figure 4.1 shows the edge emission spectra of three crystals grown with different selenium reservoir temperatures.

Examination of the emission spectrum of a crystal (No.171) grown under a selenium pressure less than that at P_{min} conditions (i.e. with a reservoir temperature at about 335°C), shows a zero-phonon band at 4605Å at 87 K and three LO phonon replicas at about 4668, 4712 and 4766Å. At 65 K this series shifted by about 5Å to higher energies and the bands increased in intensity. The bands had a half-width of about 46Å and were equally spaced in energy of 4600, 4653, 4708, 4764 and 4822Å. The energy separation of adjacent members was 0.031 ± 0.0004 eV. In addition to this series a higher energy band with a half-width of about 25Å appeared near 4555Å. This is close to the shoulder observed in the emission of flow run crystals.

Emission spectra were recorded with various intensities of the exciting light at 65 K and are shown in Figure 4.2. No shifts in the positions of the maxima of the LO phonon assisted emission were observed. The band at 4555Å however disappeared when the excitation intensity was reduced. In addition to the edge emission a broad band with a half-width of 430Å was also observed at longer wavelengths. This

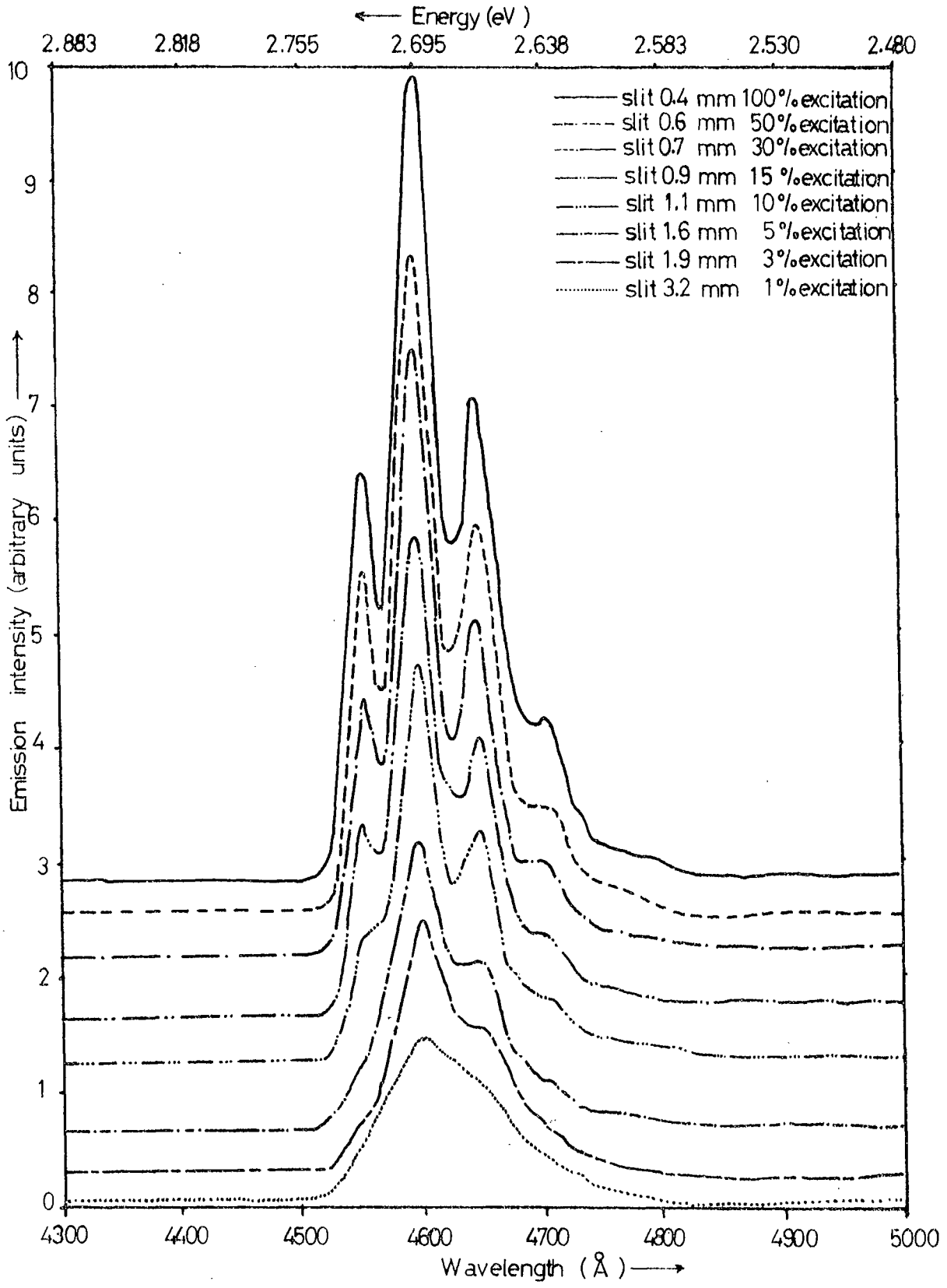

Figure 4.2 Edge emission spectra of the ZnSe crystal No.172 were recorded with various intensities of the exciting U.V. radiation at 65° K.

had at its maximum about 5560Å in the green. This broad band had a small shoulder at about 5350Å.

The second crystal (No.172) was grown under exact P_{min} conditions with a reservoir temperature of 360°C. This sample showed edge emission similar to that of crystal No.171 at 88 and 65 K. However the intensity of the emission was higher and a fifth LO phonon replica was easily resolved at about 4880Å at 65 K. The spectrum is shown in Figure 4.1b. This crystal was subsequently annealed at 850°C for five days in molten zinc, after which the intensity of the phonon assisted series had increased by nearly four times. The band maxima also shifted to shorter wavelengths by about 5Å while the band at 4555Å disappeared.

The third crystal examined was grown with a selenium reservoir temperature of 385°C, which means the selenium pressure exceeded that obtained under P_{min} conditions. No edge emission peaks were observed at 87 K. A weak broad band was detected at about 5750Å with a half-width of approximately 600Å. At 65 K (Figure 4.1c) this broad band had decreased in intensity and small peaks appeared at 4553, 4584, 4605, 4630, 4658, 4685, 4712 and 4766Å. The peaks at 4605, 4658, 4712 and 4766Å are attributed to the dominant high energy series. It is probable that the bands at 4553 and 4584Å constitute the zero order components of associated high and low energy series, while the emission bands at 4630 and 4685Å are probably the zero and first order components of the LES associated with the dominant HES (see later).

This crystal was also annealed in molten zinc for 10 days at 850°C after which a drastic change was revealed in the edge emission spectrum. For example the short wavelength lines at 4553 and 4584Å had disappeared but the intensity of the zero order line at 4605Å and its series had increased nearly fifteen fold.

For crystal No.172, an acceptor binding energy of 0.122 eV was calculated from equation (1) using the observed photon energy of the zero phonon line, 4600Å at 65 K. The magnitude of the band gap was taken to be 2.812 eV as estimated from the observed value of 2.813 eV at 60 K (3). The acceptor ionization energy of 0.122 eV is in good agreement with that reported by Reynolds et al (2), namely 0.12 eV. For crystal No.173, acceptor binding energies were found to be 0.095 and 0.125 eV from the observed photon energies of the two different zero phonon lines at 4553 and 4605Å respectively.

4.2.3 Crystals grown in zinc vapour

Numerous crystals have been grown with an excess of zinc in the reservoir. With this arrangement a reservoir temperature of 555°C was necessary to obtain the P_{min} condition. A large number of crystals have been examined at liquid nitrogen temperature and their emission properties are rather variable. Figure 4.3 illustrates the emission spectra of seven different crystals at 65 K. Some of them show a single broad band emission (deep centre luminescence) in the green and most of them exhibit two narrower bands,

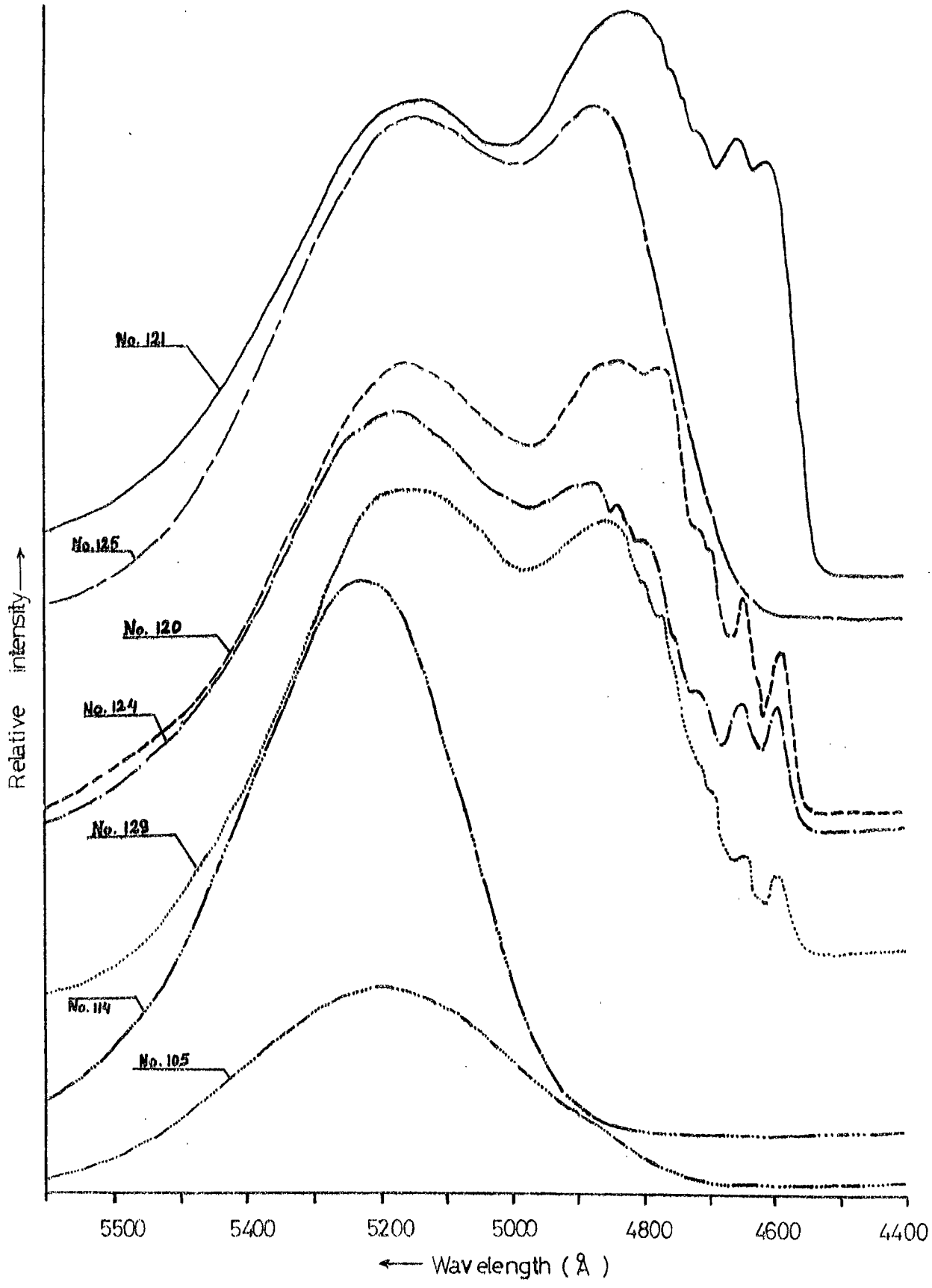

Figure 4.3 The emission spectra of various Zn Se crystals at 65°K.

with associated phonon structure at shorter wavelengths. In general the emission spectra of crystals grown with zinc reservoirs are rather broad at liquid nitrogen temperatures with poorly resolved structure, and precise measurements of the maxima become difficult. As a result no attempt has been made to fit any mathematical distribution to the more intense of the phonon components. However, for completeness the details of the observed emission are summarized below.

For example one crystal (No.114) grown with a zinc reservoir at 600°C had a single Gaussian shaped band at about 5230Å with a half-width of approximately 380Å. Two crystals grown under P_{min} conditions exhibited different emission bands, one of them (No.105) had a single broad band at 5220Å with a half-width of approximately 520Å, while the other (No.125) had two broad bands at about 4860 and 5150Å with half widths of about 250 and 450Å respectively. These latter two bands were a common feature of most of the crystals grown with zinc reservoirs (for example crystals No.120, 121, 124 and 129), which are shown in Figure 4.3. Less intense phonon assisted emission bands were also observed in these crystals on the high energy side of the 4860Å band. At 88 K three components of an LO phonon assisted series were resolved at about 4600, 4654, and 4710Å in some samples. When the crystals were cooled to 65 K the intensity of this series increased, and the emission bands shifted by about 15Å towards shorter wavelengths. At this temperature four phonon components of the emission could be resolved at about 4585, 4645, 4700 and 4757Å.

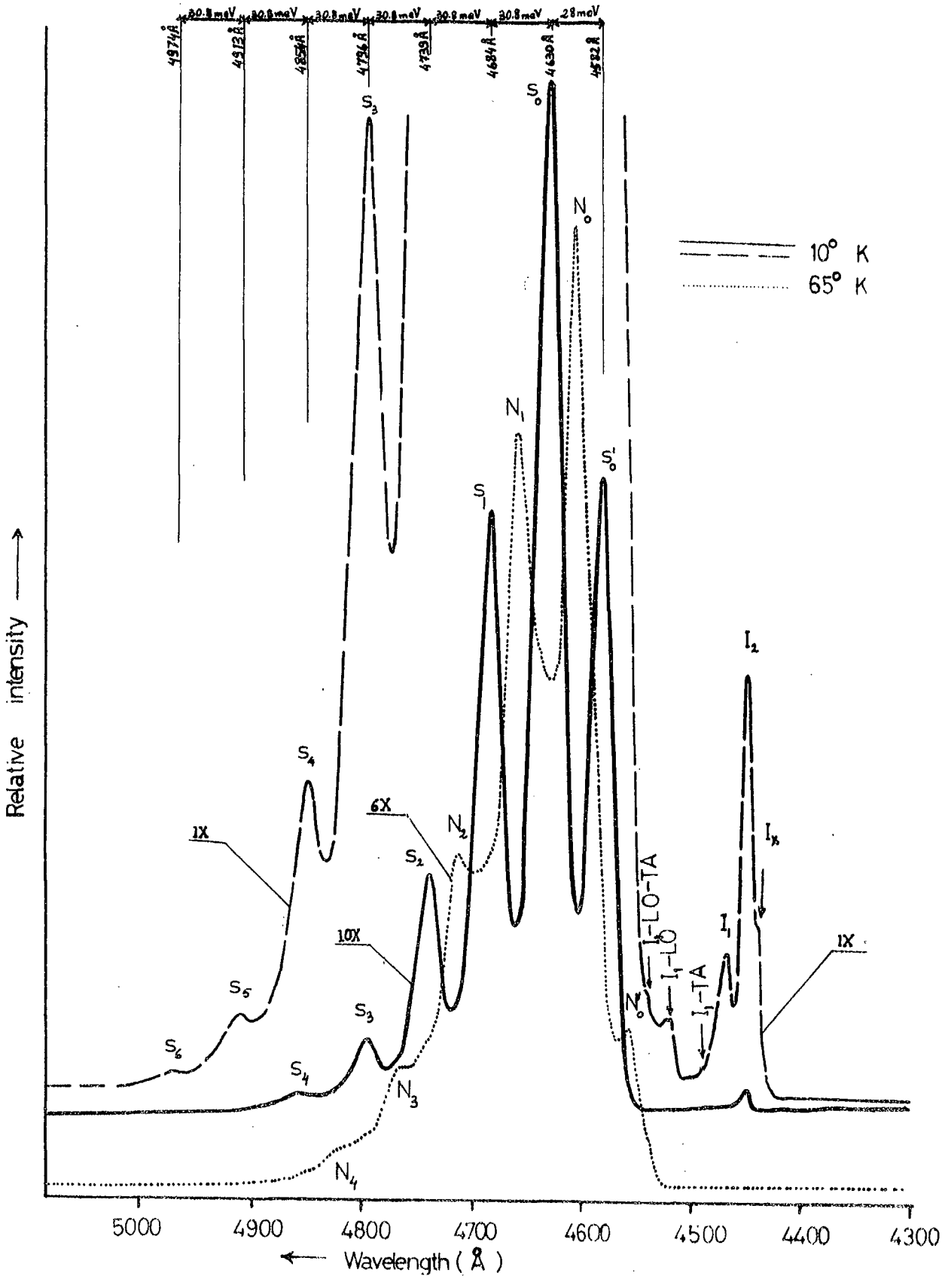

Figure 4.4 The edge emission spectra of a flow-run crystal (No.87) at 10 and 65° K.

The energy separation of the components of this series is 0.0313 ± 0.0003 eV. When comparing all the crystals examined at 65 K the positions of the peaks of the components of this series vary by up to 5Å, which might be due to the broad nature of the emission, or to errors in the wavelength marker. The intensity of the 5150Å emission was not appreciably dependent on the temperature, but the intensity of the 4860Å band increased and became a dominant feature together with the phonon assisted series at 65 K. No wavelength shifts were observed when the excitation intensity was decreased by two orders of magnitude. However, at low excitation intensities the phonon replicas disappeared and the tail of the 4860Å band and the zero order band of the phonon assisted series merged into two broad bands.

The acceptor binding energy calculated from equation (1) using the observed wavelength value of 4585Å for the first zero phonon line is 0.112 ± 0.002 eV. This is in close agreement with the value reported by Iida (4), for zinc annealed ZnSe crystals.

4.3 Edge Emission Characteristics at Liquid Helium Temperatures

The edge emission of zinc selenide excited by 3650Å radiation at liquid helium temperature consists of several series of sharp lines and broad bands. Such emission spectra, which exhibit well developed structure and systems of lines or bands with regularly spaced energies, have been identified by various workers (2, 4, 5, 6) see Chapter 2. The sharp lines, which are mostly at the high energy limit,

TABLE 4.1

Position of bound excitons and phonon assisted emission maxima of flow run crystals (No.87) at 10 and 65 K

Observed Spectrum at 10 K					Observed Spectrum at 65 K			
Lines	Wave-Length (Å)	Energy (eV)	Strength	Possible Assignment	Lines	Wave-Length (Å)	Energy (eV)	Possible Assignment
I_x	4438	2.79385	Shoulder (weak)	(?)	N'_o	4560	2.71910	Zero-phonon
I_2	4447	2.78819	Medium	Exciton bound to neutral donor	N_o	4608	2.69078	Zero-phonon
I_1	4468	2.77509	Medium	Exciton bound to neutral acceptor	N_1	4660	2.66018	One-phonon
I_{1c}	4490	2.76113	Weak	I_1-Acoustic phonon	N_2	4714	2.63027	Two-phonon
I_{1a}	4518	2.74438	Medium	I_1-LO	N_3	4770	2.59939	Three-phonon
I'_{1c}	4538	2.73218	Shoulder (weak)	I_1-LO-Acoustic phonon	N_4	4828	2.56816	Four-phonon
S'_o	4582	2.70604	Strong	Zero-phonon				
S_o	4630	2.67790	Strong	Zero-phonon				
S_1	4684	2.64712	Strong	One-phonon				
S_2	4739	2.61639	Strong	Two-phonon				
S_3	4796	2.58530	Medium	Three-phonon				
S_4	4854	2.55441	Medium	Four-phonon				
S_5	4913	2.52373	Weak	Five-phonon				
S_5	4974	2.49278	Weak	Six-phonon				

are attributed to the annihilation of the free and bound excitons, and their phonon replicas. Under argon ion laser excitation sharp lines have been identified as I_1 (at about 4456Å) and I_2 (at about 4432 and 4435Å) which are associated with the annihilation of excitons bound to neutral acceptors and donors, respectively (7). The bands to slightly longer wavelengths with unfformly spaced replicas are attributed to the LO phonon assisted high energy series (HES) which results from the recombination between free electrons and holes bound to acceptor levels some 0.12 and 0.10 eV above the valence band (2, 4). The low energy series (LES) is due to the distant pair recombination of electrons bound to shallow donors and holes bound to the same acceptors (6,7).

The edge emission components have been identified by comparing their wavelengths with the reported values. The behaviour of these components under various excitation conditions and the variations of the spectra from crystal to crystal suggest that these assignments are correct.

4.3.1 Flow run crystals

The edge emission of a cubic, flow run crystal (No.87) of ZnSe excited by U.V. radiation was studied at 10 K. The observed emission spectrum consisted of a number of sharp lines with a half-height width of about 10Å, followed by an LO phonon assisted series of bands with widths of 25Å. The emission spectrum is shown in Figure 4.4. The positions of the emission peaks are summarized in Table 4.1. With this crystal the maxima of the sharp lines which lay within the

range 4438Å to 4530Å were assigned to exciton recombination, while the broader bands within the range of 4582 to 4974Å were assigned to LES recombination processes. In Figure 4.4 the intensity of the LES was nearly 10 times greater than that of the exciton lines. The zero phonon component (labelled S_o) at about 4630Å, was replicated at lower energies with a spacing of 30.88 ± 0.3 meV. This repetition is associated with the simultaneous emission of longitudinal optical phonons. A zero phonon component of what is presumably a second series (labelled S_o') has been observed on the high energy side of the zero order LES band, at about 4582Å with a half-width of approximately 20Å, which suggests that it is not an exciton. This band has a 28 meV energy separation from the zero order LES band (S_o) and its replicas are presumably too weak to be detectable being mixed in the S_o, S_1, S_2 ..... S_6 bands. Our results are very similar to those of Dean and Merz (7), who found two comparable series which they labelled Q and R. The wavelengths of the Q_o and R_o components were 4610 and 4575Å which are close at least to those called S_o and S_o' here. It seems reasonable to assume that the lines labelled S_o' and N_o' (Table 4.1) are associated with the same donors as are those labelled S_o and N_o.

The strongest line in the exciton region is the I_2 line at 4447Å, resulting from the recombination of an exciton bound to a neutral donor. On the short wavelength side of the I_2 line a small shoulder appeared at 4437Å and has been labelled I_x. This shoulder is close to a similar unidentified line observed by Dean and Merz (7), which they reported to increase with increasing zinc concentration,

under which conditions they observed the discrete pair spectra. A second strong emission line at 4468Å has been labelled I_1, and is believed to result from the recombination of an exciton bound to a neutral acceptor. The two weak shoulders I_{1c} and I'_{1c} at about 4490 and 4538Å, may be due to the emission of the acoustic phonons associated with I_1. This gives an acoustic phonon energy of 13.2 ± 0.6 meV which is similar to the value of 13.0 ± 0.3 meV observed by Dean and Merz (7). The medium intensity I_{1a} line at about 31.6 meV energy separation from the I_1 line, is attributed to I_1 recombination with the emission of one LO phonon. This supports the suggestion that I_1 excitons couple much more strongly with both the optical and acoustical phonons than excitons bound at neutral donors (which leads to the I_2 line). This means that excitons are more tightly bound to the acceptor centres than the donor centres in ZnSe. In fact the intensity of the I_2 line was three times higher than that of the I_1 line. Unfortunately it was not possible to make Zeeman measurements to confirm the identity of the I_1 and I_2 lines.

When the excitation intensity was varied over three orders of magnitude using neutral density filters a shift of about 12Å was observed in the position of the LES emission. With decreasing excitation, the spectral peak shifted to longer wavelengths as is to be expected with a bound to bound recombination mechanism. The shift ΔE in the position of the maximum of the zero order component of the LES between two excitation intensities (I' and I") was found to be $\Delta E = 1.73 \ln(I'/I")$ meV, at 10 K.

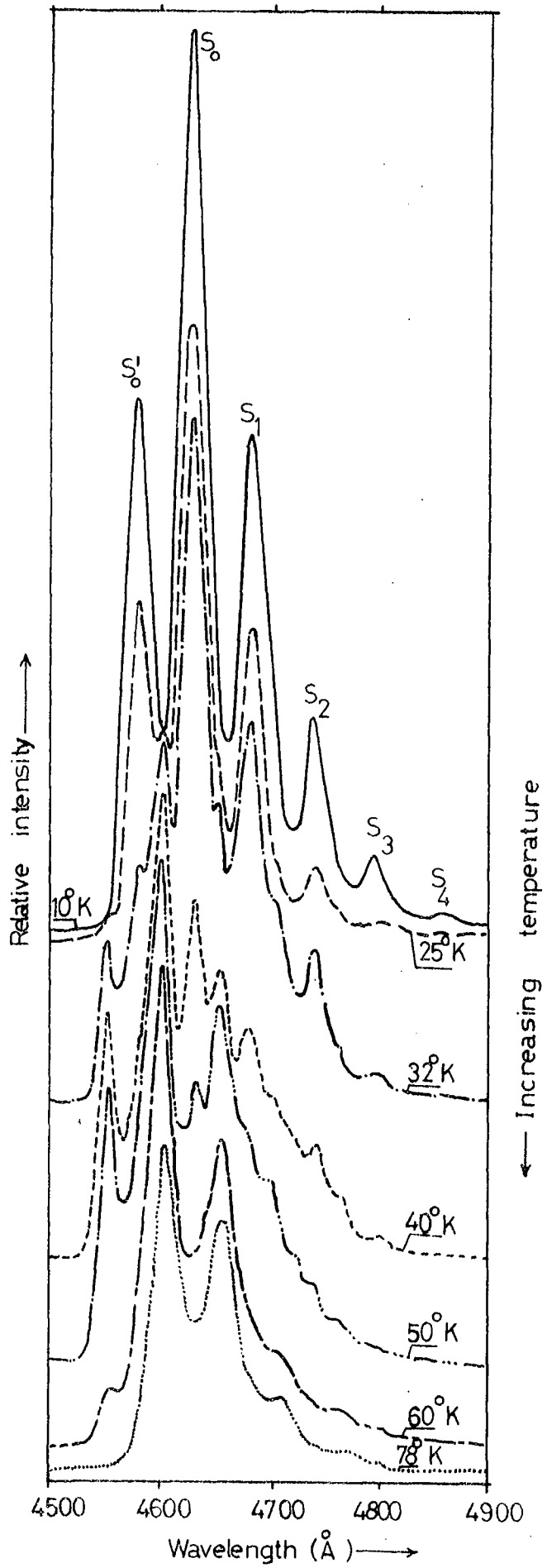

Figure 4.5 Edge emission of the ZnSe crystal No.87, recorded with increasing temperature from 10 to 78° K.

Figure 4.4 shows that the observed phonon assisted S emission series at 10 K was at lower energies than the corresponding N series observed at 65 K. An experiment was carried out to investigate whether or not these two series were of the same origin. Following the studies at liquid helium temperature, the spectral distribution of the emission near the zero phonon line was scanned over a range of wavelengths at short time intervals as the temperature rose slowly to 78 K. The temperature was sufficiently constant over one scan period for satisfactory spectra to be obtained. The spectra observed are shown in Figure 4.5. It is clear from the figure that as the temperature increased new emission lines appeared and at 32 K both the HES and LES emission are apparent in the same spectra. Eventually the HES dominated the spectrum at 78 K, while the emission band at 10 K gradually decreased in intensity and disappeared as the temperature was increased. This will be discussed further in Section 4.4. The difference in energy between the S_o and N_o and S'_o and N'_o band was found to be 0.013 eV in both cases. This behaviour is consistent with the mechanism suggested by Pedrotti and Reynolds (8). At 4 K there are two series both due to donor acceptor recombination. At higher temperatures, the donors are ionized and two HES result. In this sample there is one active donor and two active acceptors.

4.3.2 Crystals grown in Selenium Vapour

The edge emission spectra of undoped crystals grown with selenium reservoirs at a variety of different temperatures show the LES and HES bands only. Even at the

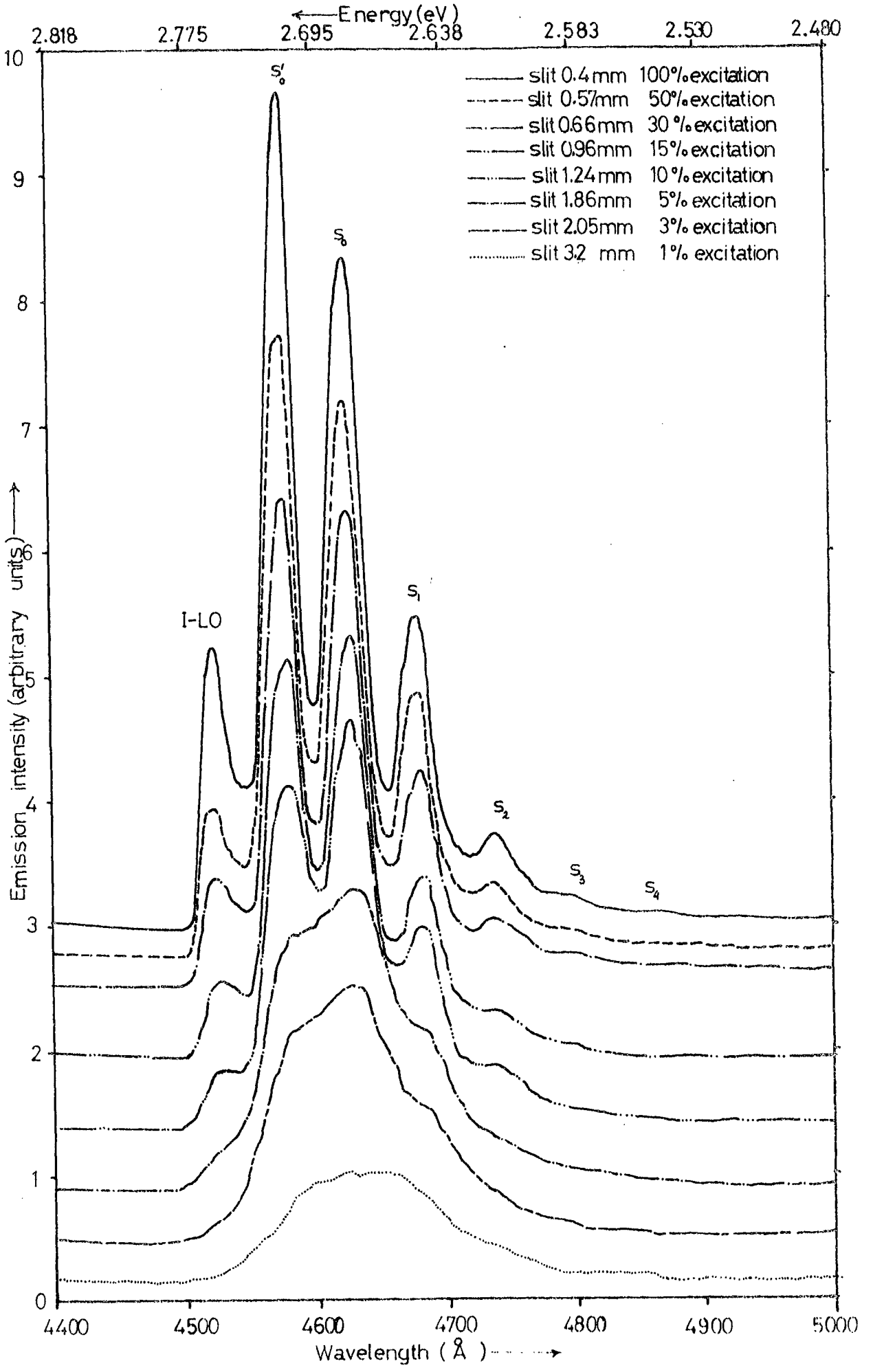

Figure 4.6 Edge emission spectra of the ZnSe crystal No.171 recorded at 10° K for various levels of U.V. excitation.

lowest temperature, 4 K, and with the highest excitation intensity available, no bound exciton or discrete pair lines were observed. The existence of strong LO phonon replicas of the edge emission provides adequate evidence of a high acceptor concentration.

The emission spectrum of crystal (No.171) grown under a selenium pressure less than that at P_{min} shows two different zero phonon bands at 4579 and 4628Å with half-height widths of about 24 and 35Å respectively. Although the relative intensities of these two bands might suggest they are members of the same series they are not, as their variations with excitation intensity and temperature clearly indicate. The wavelengths and energies of these bands, their LO phonon replicas and assignments are displayed in Table 4.2a. The bands observed are very similar to those found in the flow run crystals. In addition to these series a high energy band with a half-height width of about 19Å appeared at 4525Å. The origin of the band at 4525Å is not well understood. It could be that this peak corresponds to the I_1-LO bound exciton line but this is unlikely since the I_1 line was not detectable. It might also correspond to the zero order band reported by Liang and Yoffe (5) in hexagonal ZnSe at 4527Å. However, they reported the HES of hexagonal ZnSe at about 4515Å at 77 K whereas we never observed such a series in any undoped sample at 77 K.

The maximum of the zero phonon component of the LES shown in Figure 4.6 shifted by about 6.2 meV per order of magnitude decrease in excitation intensity towards longer wavelengths. The shift is more apparent in the diagram for the phonon replicas. Since there was no shift in the positions of the emission maxima with excitation intensity

TABLE 4.2a.

Position of phonon assisted emission bands of crystals grown with a variety of selenium reservoir temperatures

Crystal (No.171) was grown under less P_{min} condition

Observed Spectrum at 10 K					Observed Spectrum at 65 K			
Lines	Wave-length (Å)	Energy (eV)	Strength	Possible Assignment	Lines	Wave-length (Å)	Energy (eV)	Possible Assignment
I_{1a}	4525	2.74013	Medium	I_1-LO(?)	N'_o	4555	2.72208	Zero-phonon
S'_o	4579	2.70782	Strong	Zero-phonon	N_o	4600	2.69546	Zero-phonon
S_o	4628	2.67915	Strong	Zero-phonon	N_1	4653	2.66475	One-phonon
S_1	4683	2.64768	Strong	One-phonon	N_2	4708	2.63362	Two-phonon
S_2	4735	2.61861	Medium	Two-phonon	N_3	4764	2.60266	Three-phonon
S_3	4790	2.58854	Weak	Three-phonon	N_4	4822	2.57136	Four-phonon
S_4	4848	2.55757	Weak	Four-phonon				

at 65 K, the phenomena can again be interpreted in terms of the Pedrotti and Reynolds (8) model. The LES is dominant at 4 K and the HES at 77 K. In this respect the behaviour is identical with that of the flow run crystals, and once again one donor and two acceptors are involved.

The second (No.172) and third (No.173) crystals grown under higher partial pressures of selenium show essentially the same phonon assisted series as crystal No.171. However, the emission of sample 172 grown under P_{min} conditions was more intense than that of the sample 173 grown with an even higher selenium pressure and five longitudinal phonon replicas were easily resolved. The wavelengths and energies of the components of the edge emission series are recorded in Tables 4.2b and 4.2c. The S_o' zero phonon band was separated by 28.8 meV from the corresponding S_o band and was often much more intense (for example in crystals 171 and 173). The phonon replicas of the S_o' series were mixed in with and overlapped the S_o series. The two zero phonon bands also had different half widths, i.e. 14.6 (S_o') and 22.1 meV (S_o), as did their high energy partners at 65 K, i.e. 14.8 (N_o^s) and 32 meV (N_o). These differences, and the fact that the ratios of the intensities of the S_o' and S_o bands changed with variations in the intensity of excitation show that the proposed assignment is correct.

The emission spectra of these two crystals were examined under different intensities of excitation and both showed a shift of the S_o and S_o' series by about 12Å to longer wavelengths as the excitation intensity decreased by an order of magnitude. The shift is illustrated more clearly in Figure 4.7 which shows the emission spectra of

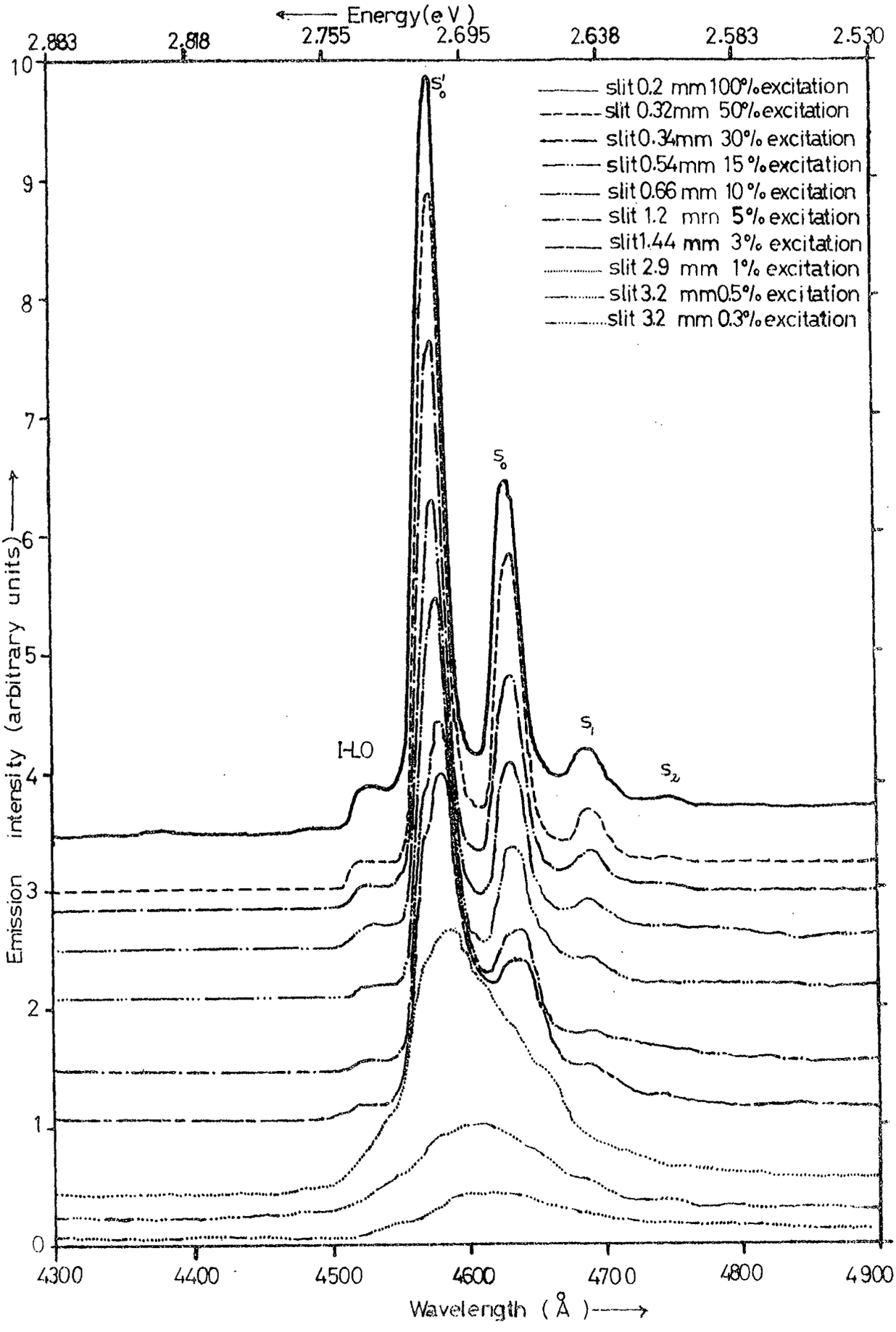

Figure 4.7 Edge emission spectra of the ZnSe crystal No.173 recorded at 10°K for various levels of U.V. excitation.

TABLE 4.2b

Position of phonon assisted emission bands of crystals grown with a variety of selenium reservoir temperatures

Crystal (No.172) was grown under exact P_{min} condition

Observed Spectrum at 10 K					Observed Spectrum at 65 K			
Lines	Wave-length (Å)	Energy (eV)	Strength	Possible Assignment	Lines	Wave-length (Å)	Energy (eV)	Possible Assignment
I_{1a}	4526	2.73953	Medium	I_1-LO(?)	N'_o	4555	2.72208	Zero-phonon
S'_o	4580	2.70723	Strong	Zero-phonon	N_o	4600	2.69546	Zero-phonon
S_o	4630	2.67790	Strong	Zero-phonon	N_1	4653	2.66475	One-phonon
S_1	4684	2.64712	Strong	One-phonon	N_2	4708	2.63362	Two-phonon
S_2	4739	2.61639	Medium	Two-phonon	N_3	4764	2.60266	Three-phonon
S_3	4796	2.58530	Medium	Three-phonon	N_4	4822	2.54080	Four-phonon
S_4	4854	2.55441	Weak	Four-phonon	N_5	4880	2.54080	Five-phonon
S_5	4915	2.52322	Weak	Five-phonon				

crystal No.173 for various excitation intensities. Once again such a shift indicates a pair band mechanism in the recombination.

The heights of the maxima of the phonon components of the spectra obtained from the Optica with different intensities of excitation were corrected for photomultiplier response and then compared. The ratios of the heights for the emission of zero, one, two, three, four and five phonons were found for crystal No.172 to be

$$S_o=1.00 : S_1=0.71 : S_2=0.26 : S_3=0.06 : S_4 = 0.018 : S_5=0.010$$

The large number of replicas emitted suggests that there is strong coupling between the carrier and the lattice. Hopfield (9) showed that the intensity of the (n+1) th band I(n) is given by,

$$I(n) = \frac{\bar{N}^n}{n!} I_o \qquad (2)$$

where n is the number of phonons, I_o is the intensity of the zero phonon band and $\bar{N}$ is the parameter measuring the average number of phonons. This relation shows that the value of $\bar{N}$ is simply I_1/I_o which for this crystal was 0.71. Using this value of $\bar{N}$, equation (2) yields the following ratios

1.00 : 0.71 : 0.252 : 0.058 : 0.0106 : 0.0015

The agreement between measured and theoretically calculated intensities is excellent and indicates that the probability of a multiphonon emission process is well described by equation (2).

Tables 4.2 shows that the two sets of luminescence peaks observed at 10 K were to the lower energy side of the

TABLE 4.2c

Position of phonon assisted emission bands of crystals grown with a variety of selenium reservoir temperatures

Crystal (No.173) was grown under high P_{min} condition

Observed spectrum at 10 K					Observed spectrum at 65 K			
Lines	Wave-length (Å)	Energy (eV)	Strength	Possible Assignment	Lines	Wave-length (Å)	Energy (eV)	Possible Assignment
I_{1c}	4525	2.74013	Medium	I_1-LO(?)	N'_o	4553	2.72328	Zero-phonon
S'_o	4578	2.70841	Strong	Zero-phonon	S'_o	4584	2.70486	LES of zero-phonon
S_o	4630	2.67790	Strong	Zero-phonon	N_o	4605	2.69253	Zero-phonon
S_1	4685	2.64655	Medium	One-phonon				
S_2	4736	2.61805	Weak	Two-phonon	S_o	4630	2.67790	LES of one-phonon
S_3	4792	2.58746	Weak	Three-phonon	N_1	4658	2.66189	One-phonon
					S_1	4685	2.64655	LES of two-phonon
					N_2	4712	2.63139	Two-phonon
					N_3	4766	2.60157	Three-Phonon

sets at 65 K. The sets of luminescence peaks were studied as the temperature was increased slowly from 10 K. The resultant spectra are shown in Figure 4.8 for crystal 172 (similar spectra were also observed from the crystal Nos.171 and 173). It is clear from the figure that the intensity of the I_{1a} line (at 4525Å) decreased with increasing temperature and at about 38 K this line disappeared completely. No shift in the spectral location of the line was observed with decreasing intensity. At 30 K the HES band N_o' (4552Å) appeared as a shoulder on the high energy side of S_o' (at 4580Å). This shoulder became an intense emission at 65 K, when it had shifted slightly to longer wavelengths. Thereafter the intensity decreased with further increase in temperature. In the meantime the S_o' zero phonon line decreased in intensity with increasing temperature and disappeared at about 55 K. The S_o zero phonon line also disappeared at 55 K. At about 30 K the HES band N_o (4600Å) began to appear as a shoulder on the high energy side of the S_o (4630Å) band. This shoulder became a strong peak with increasing temperature. The same behaviour was observed for the S_1, S_2, S_3, S_4 and S_5 and the N_1, N_2, N_3 and N_4 phonon replicas. This can be seen from Figure 4.8. In this diagram both the LES and HES emissions can be observed most readily in the 50 K curve. The temperature dependences of the S_o and N_o emissions will be discussed in Section 4.4. The observation of the N_o and N_o' lines at liquid nitrogen temperature suggests that at 77 K the Schön-Klasens (10,11) model is valid, i.e. the emissions are associated with transitions between electrons in the conduction band and trapped holes, while at 10 K the

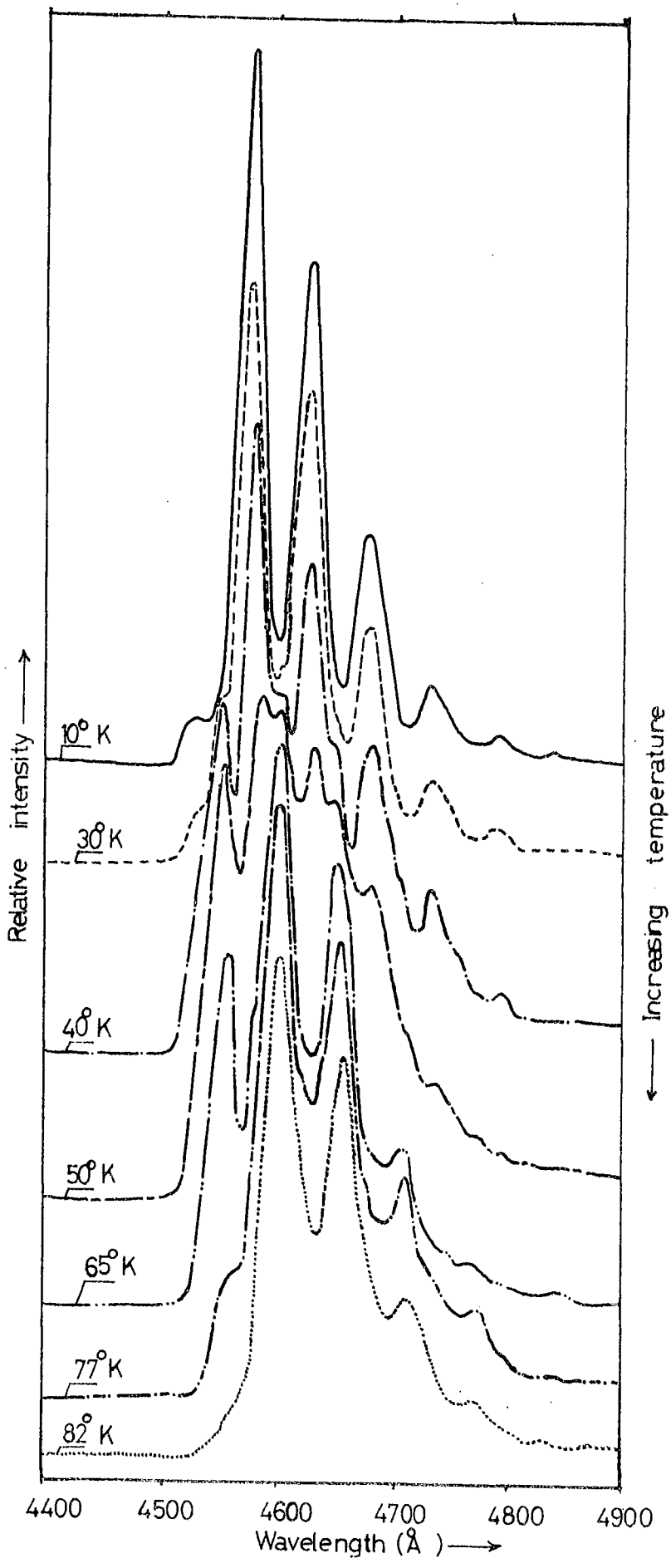

Figure 4.8 Zero phonon component of the ZnSe crystal No.172 recorded with increasing temperature from 10° K to 82° K.

Prener-Williams model (12) is more appropriate to explain the S_o and S_o' lines. The energy differences between the N_o' and S_o', and N_o and S_o zero phonon components were found to be 14.5 ± 0.3 meV and 17.5 ± 0.5 meV respectively, which may be attributed to the binding energy of the donor or donors involved.

After annealing crystal No.172 in molten zinc for four days of 850°C only one main zero phonon band at 4615Å and four LO phonon replicas at 4674, 4730, 4789 and 4874Å were observed. No discrete pair lines or second series of LO phonon components were detected. This 4615Å series is very similar to the low energy series of crystals grown in zinc vapour pressure (see S_o'' in Tables 4.3 and 4.4 and discussed in the following section). Further annealing of crystal No.173 in molten zinc (for 15 days at 850°C) led to a further shift of the zero phonon band to shorter wavelengths so that it now occurred at 4605Å. The intensity ratio of the zero order line of the phonon assisted series to that of the first replica increased by a factor of five which suggests that an entirely new emission process is involved.

4.3.3 Crystals grown in zinc vapour

The luminescence of crystals grown with excess zinc in the reservoir was dominated by a series of sharp lines as shown in Figure 4.9, 4.10 and 4.11. The wavelengths and energies of the features of the three spectra and their suggested assignments are given in Tables 4.3 and 4.4. In the bound exciton region three sharp lines each with a shoulder were observed between 2.691 and 2.690 eV, which

TABLE 4.3

The details of observed emission characteristics illustrated in the figures 4.9 and 4.10 at 10 K.

Crystal No.114					Crystal No.105				
Lines	(Å)	Energy	Strength	Possible Assignment	Lines	(Å)	Energy	Strength	Possible Assignment
I_1	4464	2.77758	Strong	Exciton bound to neutral acceptor	I_2	4442	2.79133	Strong	Exciton bound to neutral donor
I'_1	4474	2.77137	Weak						
I_{1a}	4515	2.74620	Strong	I_1-LO	I_1	4466	2.77633	Strong	Exciton bound to neutral acceptor
I'_{1a}	4525	2.74013	Weak	I_1-LO					
I_{1b}	4568	2.71438	Medium	I_1-2LO	I_{1a}	4517	2.74498	Strong	I_1-LO
I'_{1b}	4576	2.70959	Weak	I_1-2LO	I_{1b}	4570	2.71315	Medium	I_1-2LO
S''_o	4618	2.68495	Strong	Zero-phonon	S''_o	4620	2.68379	Strong	Zero-phonon
S_o	4632	2.67683	Weak	Zero-phonon	S_o	4640	2.67722	Shoulder Weak	Zero-phonon
S''_1	4674	2.65278	Strong	One-phonon	S''_1	4675	2.65212	Strong	One-phonon
S_1	4687	2.64542	Weak	One-phonon	S_1	4695	2.64091	Shoulder Weak	One-phonon
S''_2	4730	2.62137	Strong	Two-phonon	S''_2	4732	2.62027	Strong	Two-phonon
S_2	4743	2.61419	Weak	Two-phonon	S_2	4752	2.60924	Shoulder Weak	Two-phonon
S''_3	4789	2.58908	Strong	Three-phonon	S''_3	4790	2.58854	Medium	Three-phonon
S_3	4800	2.58315	Weak	Three-phonon		4820	2.57243	Weak	(?)
S''_4	4847	2.55812	Strong	Four-phonon	S''_4	4850	2.55651	Weak	Four-phonon
S_4	4860	2.55125	Weak	Four-phonon		4870	2.54602	Weak	(?)
S''_5	4906	2.52733	Strong	Five-phonon	S''_5	4910	2.52527	Weak	Five-phonon
S_5	4918	2.52117	Weak	Five-phonon		4942	2.50892	Weak	(?)
					S''_6	4972	2.49378	Weak	Six-phonon
						5050	2.45527	Medium	(?)

are labelled I_1, I_{1a}, I_{1b}. With the exception of crystal 105, the I_1 lines can be seen to be doublets with splittings of approximately 6 meV. The two components appear at 4464 and 4474Å with a half-height width of about 10Å. The I_1 lines are attributed to the recombination of excitons bound to neutral acceptors. The I_{1a} and I_{1b} lines are due to the (I_1-LO and I_1-2LO) LO phonon-assisted recombination of the bound excitons. This gives the LO phonon energy at about 31.46 ± 0.08 eV, which is similar to the reported value of 31.4 meV (1).

In addition to the above lines the crystals No.120 and 121 show small peaks with maxima at about 4585 and 4531Å, which are shown in Figure 4.11 and Table 4.4. These are labelled I_{1c} and I'_{1c} and attributed to the emission of acoustic phonons associated with I_1-LO-TA, I_1-2LO-TA replicas, respectively. This gives the acoustic phonon energy as 13 meV, which is very similar to the reported value (7).

The spectrum of the crystal 105 was dominated by the I_1 exciton emission with its maximum at about 4466Å. The first and second LO phonon replicas lay at about 4517 and 4570Å respectively. With this sample some of these lines were split and also exhibited another sharp line at the shorter wavelength of 4442Å, as shown in Figure 4.10. This line is labelled I_2 and is attributed to the recombination of excitons bound to neutral donors. The I_1 exciton coupled much more strongly to phonons than the I_2 excitons. This is in accord with the fact that excitons are more tightly bound to the acceptor centres than to the

TABLE 4.4

The position of the emission maxima of crystal No.120 and 121.

Line	Wavelength (Å)	Energy (eV)	Strength	Possible Assignment
I_1	4460	2.78007	Strong	Exciton bound to neutral
I_1'	4468	2.77509	Shoulder (Weak)	Acceptor
I_{1a}	4511	2.74864	Strong	I_1 - LO
I_{1a}'	4521	2.74256	Soulder (Weak)	
I_{1c}	4531	2.73650	Weak	I_1 - LO - TA
I_{1b}	4563	2.71731	Strong	I_1 - 2LO
I_{1b}'	4572	2.71196	Weak	
I_{1c}'	4585	2.70427	Weak	I_1 - 2LO - TA
S_o''	4615	2.68669	Strong	Zero-phonon
S_o	4630	2.67799	Weak	Zero-phonon
S_1''	4670	2.65505	Strong	One-phonon
S_1	4686	2.64599	Weak	One-phonon
S_2''	4726	2.62359	Strong	Two-phonon
S_2	4743	2.61419	Weak	Two-phonon
S_3''	4784	2.59178	Strong	Three-phonon
S_3	4800	2.58315	Weak	Three-phonon
S_4''	4844	2.55968	Medium	Four-phonon
S_4	4860	2.55125	Weak	Four-phonon
S_5''	4905	2.52785	Medium	Five-phonon
S_5	4922	2.51912	Weak	Five-phonon
S_6''	4968	2.49579	Weak	Six-phonon
S_6	4985	2.49728	Weak	Six-phonon

donor centres. The Bausch and Lomb spectrograph was used to confirm that the wavelengths of the I_2 and I_1 lines were 4442 and 4466Å. No facilities for the measurements of the Zeeman splitting of these lines were available to confirm the assignments. The wavelengths of the I_1 and I_2 lines reported here are approximately 10Å (5 meV) larger than those previously reported (7,13,14,15). It is unlikely that these differences are due to the different intensities of excitation, but some displacement will be associated with the different temperatures employed (10 K as against 4.2 K). The band gap increases with decreasing temperature by about $4.5\ 10^{-4}$ meV per°K so that at 10 K the band gap is about 1.8 meV less than that at 4.2 K. It may be that the Dean and Merz crystals contained a trace of sulphur which would increase the band gap, which according to their results they would appear to have taken to be 2.83 eV. Elastic strain is another possible cause of the displacement.

The crystals grown with excess zinc in the reservoir also emitted in two relatively broad bands at 10 K, which were centred at about 5200 and 4830 Å. The blue band at 4830Å has not been reported previously. In between the bound exciton line and the band at 4830Å there are at least two phonon assisted series (see Figures 4.9, 4.10, 4.11). The series with higher energy was quite prominent with the zero phonon component S_o'' located at about 4618Å whereas the lower energy series S_o was noticeably weaker. Its zero order component S_o lay at 4632Å, i.e. in much the same position as the series observed in samples grown with selenium reservoirs. The shapes of the spectral components suggest

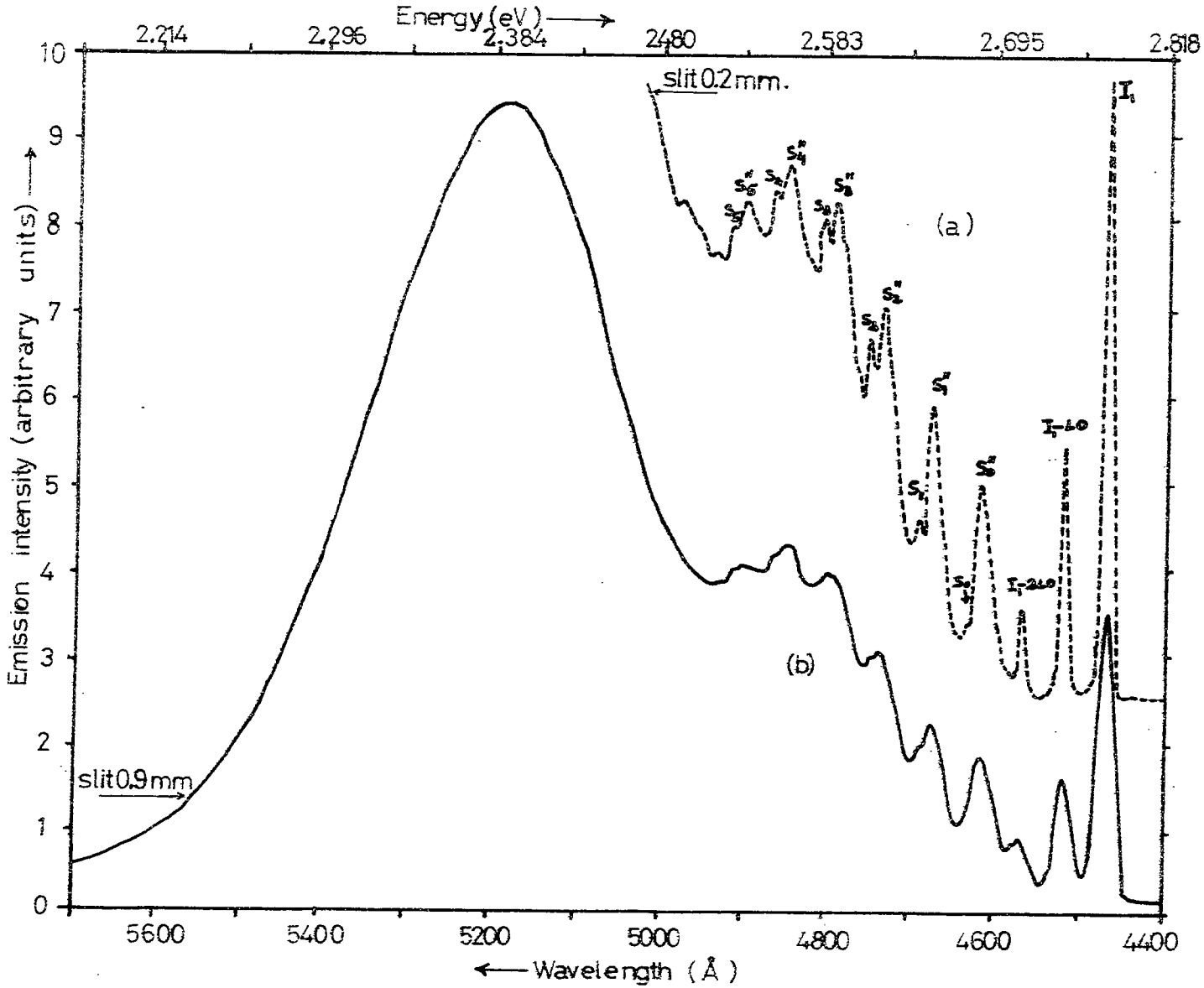

Figure 4.9 The emission spectra of the ZnSe crystal No. 114 at 10°K. (a) 100 % scale, (b) 10 % scale.

that both these series are associated with donor-acceptor distant pair recombination.

Two I_1 lines were observed in the emission spectra of most of the crystals grown with zinc reservoirs, for example in crystals Nos. 114, 120 and 121. The energy difference between the longest and shortest wavelength I_1 lines was about 6 meV, which corresponds to a difference of acceptor depth of $\sim$60 meV according to the Halsted and Aven (16) relation between the exciton dissociation energy and ionization energy of the acceptor. This will be discussed in Section 4.6. Crystals with two I_1 lines would be expected to show two series of phonon-assisted edge emission bands. In fact, all crystals grown with zinc reservoirs had two such series with zero phonon components which are labelled S_o and S''_o. This indicates the existence of two acceptors with ionization energies of 0.122 and 0.112 eV. These values have been calculated from the measured positions of N_o(4600Å) and N''_o(4585Å).

The emission spectra of sample 105 were measured at different excitation intensities and the results are shown in Figure 4.10. Generally both the bound exciton and the edge emission series shifted to higher energies with increasing intensity of excitation. The shift was by about 3Å per order of magnitude for the bound excitons, whereas a much larger shift of about 10Å was observed with the zero order components of both edge emission series. The shift was more apparent at the lowest excitation intensities and the bands eventually overlapped, leaving a broad peak.

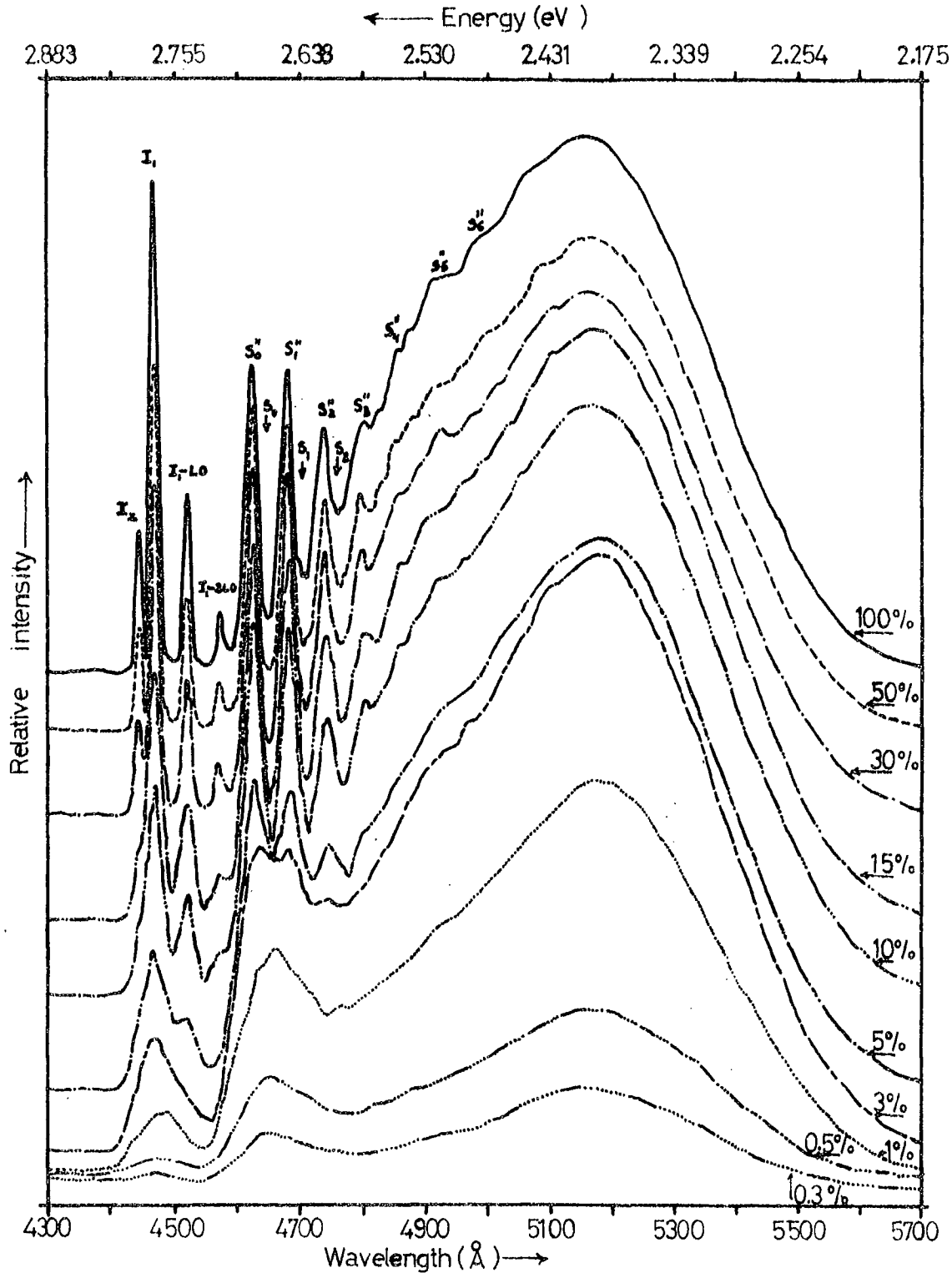

Figure 4.10 The emission spectra of the ZnSe crystal No. 105 recorded at 10° K for various levels of U.V. excitation.

Consider the zero phonon component of a distant pair series. The recombination then takes place at distant pairs and the energy $E_{S''}$ of the zero phonon component of the LES is given by,

$$E_{S''} = E_G - (E_A + E_D) + E_C \qquad (4)$$

where E_G, E_A and E_D are the band gap, acceptor and donor energies respectively. E_C is the Coulombic term appropriate to a donor acceptor separation r, so that $E_C = \frac{e^2}{\epsilon r}$. If the dielectric constant is taken as 8.66 (17), $r = 1.65/E_C$, where r is in Å and E_C in eV. The problem is to determine r. It was observed that the LES shifted by about 5.8 meV to lower energy per order of magnitude decrease in the excitation intensity. Any change in $E_{S''}$, $dE_{S''}$, must be due to a change dE_C in E_C because E_G, E_A and E_D remain constant under different intensities of excitation. Thus $dE_{S''}=dE_C=1.65\ dr/r^2$. Inserting the observed value of $dE_{S''}$ we find $dr=3.4\ r^2\ 10^{-3}$ Å, where dr represents the change in the mean separation of the donor acceptor pairs through which the recombination is proceeding, when the excitation intensity is changed by one order of magnitude. If $r \sim 20$Å, $dr \sim 1.3$Å. Such a small change in r could not encompass a sufficient number of donor and acceptors to account for the shift in the emission band. If $r \sim 1000$Å, $dr \sim 3400$Å, which would imply that the luminescence intensity should saturate with increasing excitation intensity. This is not observed. It follows therefore that r will be of the order of 115Å when $dr \sim 54$Å, an estimate which is in agreement with Iida's (4) conclusion. With this value for r, a value of E_C of 0.014 eV was used in equation (4) as a correction for the Coulombic

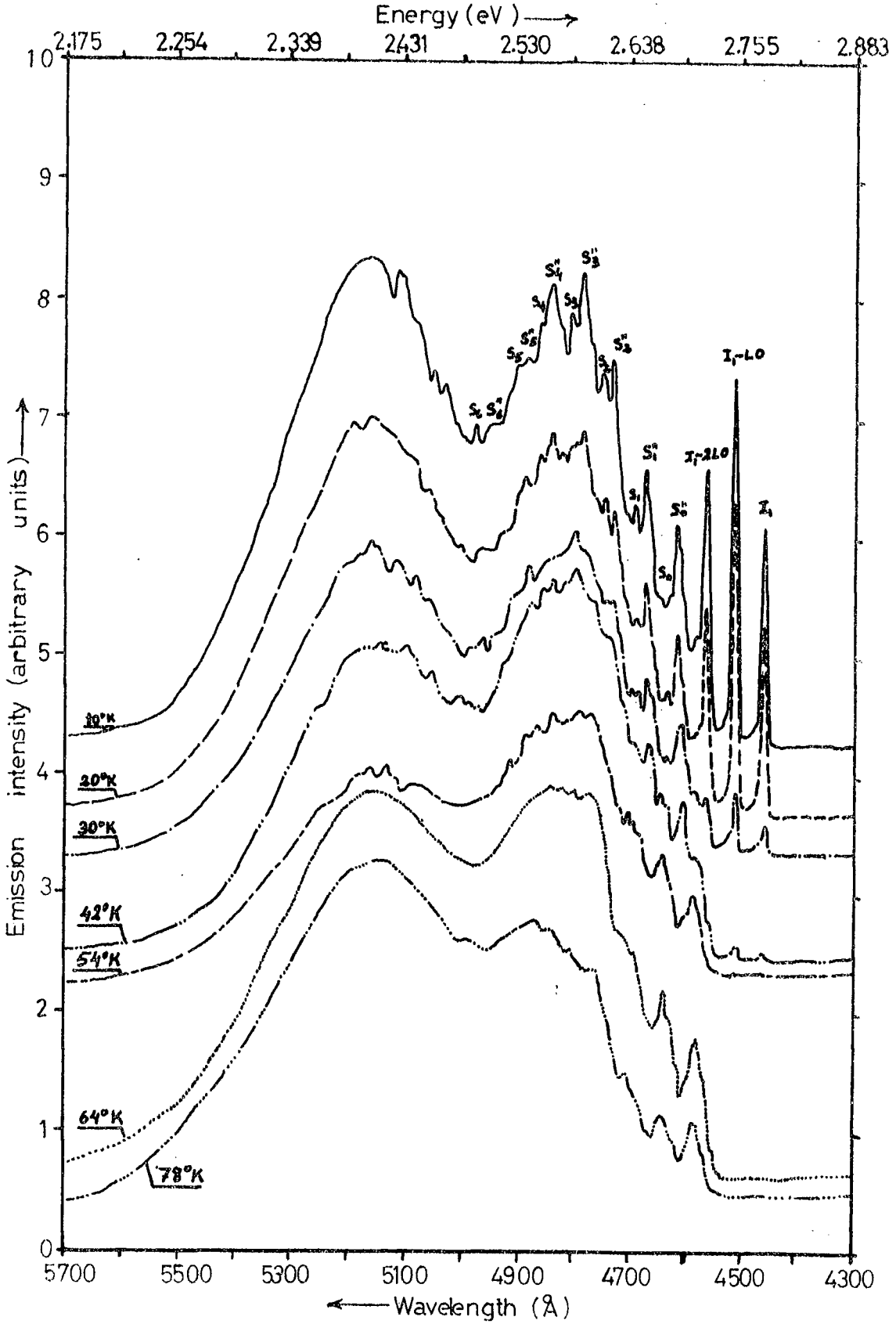

Figure 4.11 The emission spectra of the ZnSe crystal No.120 recorded with increasing temperature from 10° K to 78° K.

interaction. Combining the observations on four different crystals grown with zinc reservoirs leads to a corrected value of the donor binding energy of E_D = 0.034 eV. This is to be compared with Iida's value of E_D = 0.026 eV. Similar calculations have been made on the second (S_o) zero phonon component, which was observed as a small shoulder at 4602Å at 54 K. If it is assumed that there is no spectral shift and S_o also occurs at 4602Å at 77 K, then by using the above Coulombic correction with an acceptor ionization energy of 0.123 eV in equation (4), the donor binding energy is found to be 0.031 eV.

The conventional spectra obtained under continuous excitation could all be analysed in a similar way to provide a measure of the binding energies of the donors and acceptors involved in the LES. However, the uncertainty in the magnitude of the Coulombic interaction term leads to substantial error in the donor ionization energies. Time revolved spectroscopy is undoubtedly the best method of determining accurately any differences in the donor level or levels responsible for the edge emission in ZnSe.

Finally the emission spectra of sample 120 were recorded between 10 and 77 K, see Figure 4.11, in an attempt to investigate whether or not the I_1, I_{1a} and I_{1b} bound exciton lines were of the same origin and also to produce the free-to-bound HES bands which should result from the LES bands on ionising the donors. It is clear from the figure that the bound exciton lines gradually decreased in intensity as the temperature was increased and above ∿40 K all bound exciton lines had disappeared. The intensity of the S_o series falls exponentially with decreasing temperature

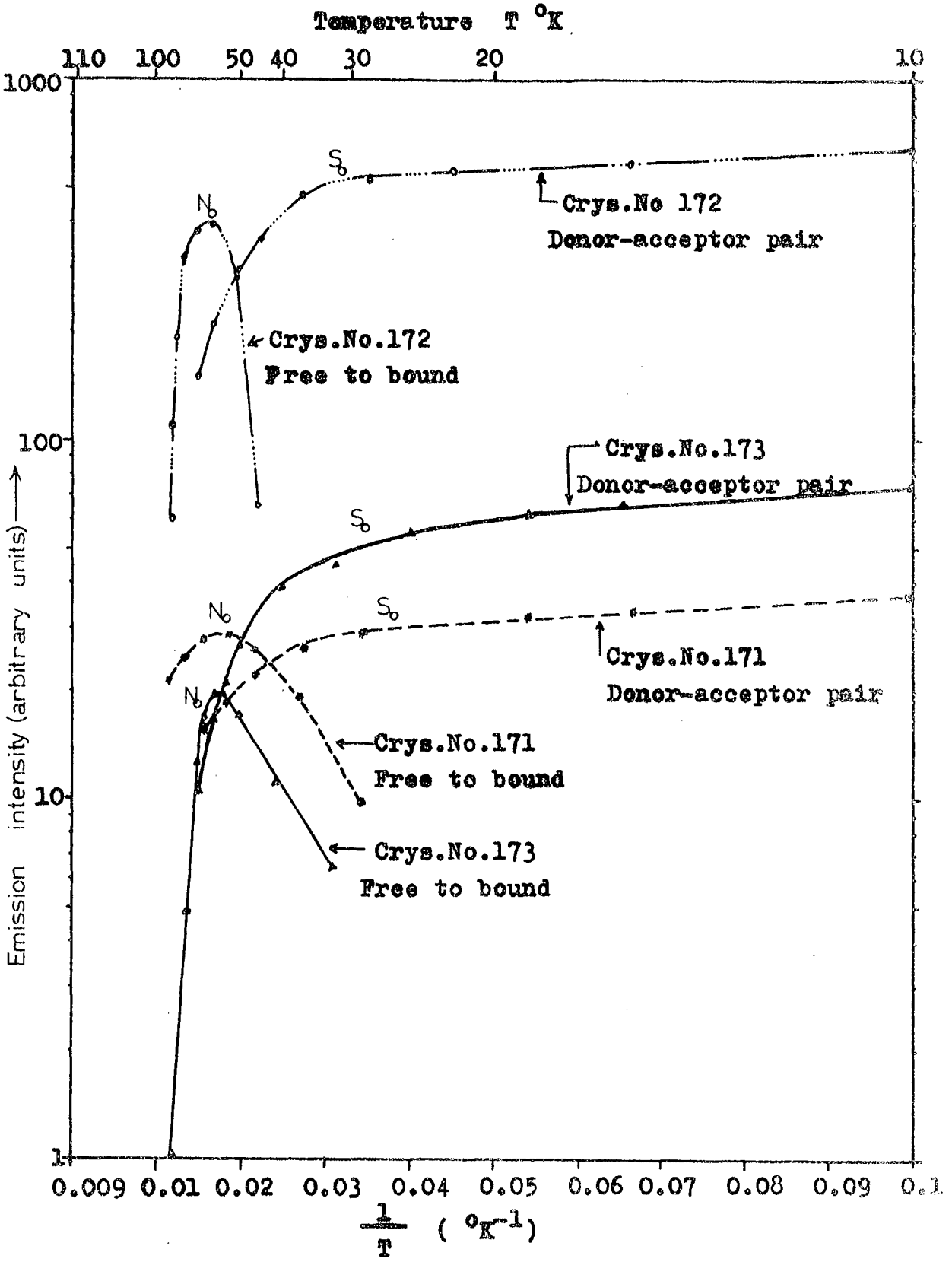

Figure 4.12 The temperature dependence of the intensities of the S_0 and N_0 zero phonon components from the crystals grown with selenium reservoirs.

which will be discussed in Section 4.4. Above about 50 K, S''_o and S_o disappear, new emission bands appear at about 4585 and 4602Å, and with increasing temperature the N''_o zero phonon band (4585Å) and its three replicas (4645,4700 and 4757Å) dominate the spectrum. The second series disappears into the broad band at 65 K. These new lines are the HES corresponding to free electron-bound hole recombination, with acceptor levels at approximately 112 and 122 meV above the valence band.

4.4 Variation with Temperature

4.4.1 Crystals grown with Se reservoirs

The variations of the HES and LES with temperature as illustrated by the variations in the intensities of their zero phonon components N_o and S_o are shown in Figure 4.12. It can be seen that the intensity of the zero phonon component (S_o) of the LES emission decreased slowly with increasing temperature until at about 45 K it began to quench rapidly. This behaviour is taken to indicate that the donors associated with the LES bound to bound recombination begin to be ionized at about 45 K, so that the LES decreases while the HES increases as the temperature is raised above 45 K. This is also implied by the results shown in Figure 4.13 for crystals grown with zinc reservoirs. With increasing temperature between 45 and 88 K the free to bound recombination of the HES dominates. The intensity of HES reaches a maximum at about 58 K, then decreases. The temperature at which the emission begins to be quenched

is approximately the same for all the undoped crystals. The process is presumably associated with the increasing ionization of the acceptors. However, the LES emission could still be observed at these temperatures which suggests that the life time of the emission must be comparable to the escape time of an electron in a donor level.

Similar quenching of the N_o' and S_o' zero phonon components was also observed. However the quenching curves for the N_o' zero phonon components were slightly displaced to lower temperatures compared with N_o and yielded an activation energy of $\sim$0.089 eV. The activation energy for the quenching of the N_o band was $\sim$0.106 eV. The two different activation energies for the quenching of the N_o' and N_o zero phonon components agree reasonably with the different acceptor ionization energies of 0.094 and 0.122 eV, previously deduced. The intensities of both the S_o and S_o' bands fell rapidly from about 45 K with an activation energy of $\sim$0.018 eV. This is of the same order as the ionization energy for the donor, which is approximately the same for all undoped crystals.

Consider the relative intensities of the S_o and N_o bands in a spectrum which displays both series (at a temperature of 58 K for example). If thermal equilibrium is assumed to determine the population of the donor states the ratio of the intensities of the two series is given by, (18),

$$I_{HES}/I_{LES} = A \exp(-\Delta E/kT) \qquad (5)$$

where ΔE is the ionization energy of the donors, and A involves the ratio of transition probabilities which is

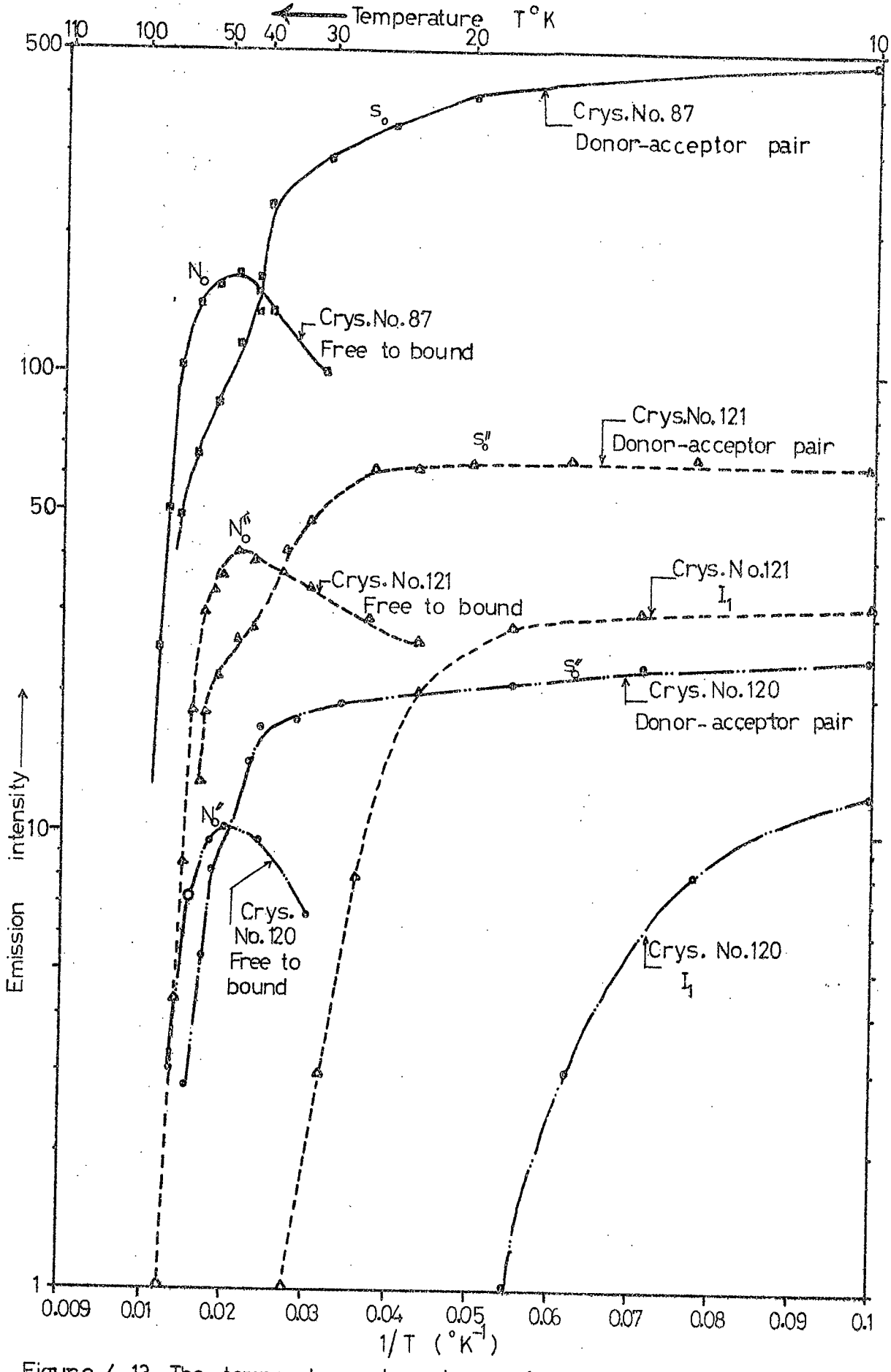

Figure 4.13 The temperature dependence of the intensities of the S_o pair and HES emission, from the flow run and with zinc vapour grown ZnSe crystals

estimated theoretically to be about 10^3. Using equation (5) the binding energy ΔE was found to be 0.018 eV, which compares very favourably with the spacing of 0.0175 eV between the S_o and N_o zero phonon components in crystal 172.

4.4.2 Flow crystals and crystals grown with Zn reservoirs

The intensities of the components of the emission of the flow run crystals and of those grown with zinc reservoirs are plotted against temperature in Figure 4.13. The variations of the intensities of the zero phonon components of the HES and LES emissions are similar to those observed with crystals grown with selenium reservoirs. The variation in intensity of the I_1 exciton emission is also shown in Figure 4.13.

Examination of the curves in Figure 4.13 for crystal No.121 reveals that the LES emission shows that two quenching processes are operative and these begin at about 25 and 60 K. The first quenching point occurs in the range where the associated HES begins to be observed, whereas the second quenching point coincides with the onset of quenching in the HES emission. The latter process is certainly associated with acceptor ionization.

Thermal quenching can be described by the relation

$$I_{RE} = 1/\left[1 + A \exp\left(-E_{AC}/kT\right)\right]$$

where E_{AC} is the activation energy for quenching. Values of E_{AC} of 0.0083 eV for the quenching of the I_1 line and 0.018 eV for the LES emission have been obtained. Once again a value of the donor binding energy of 0.018 eV is found and 0.0083 eV is the binding energy of I_1. This latter is

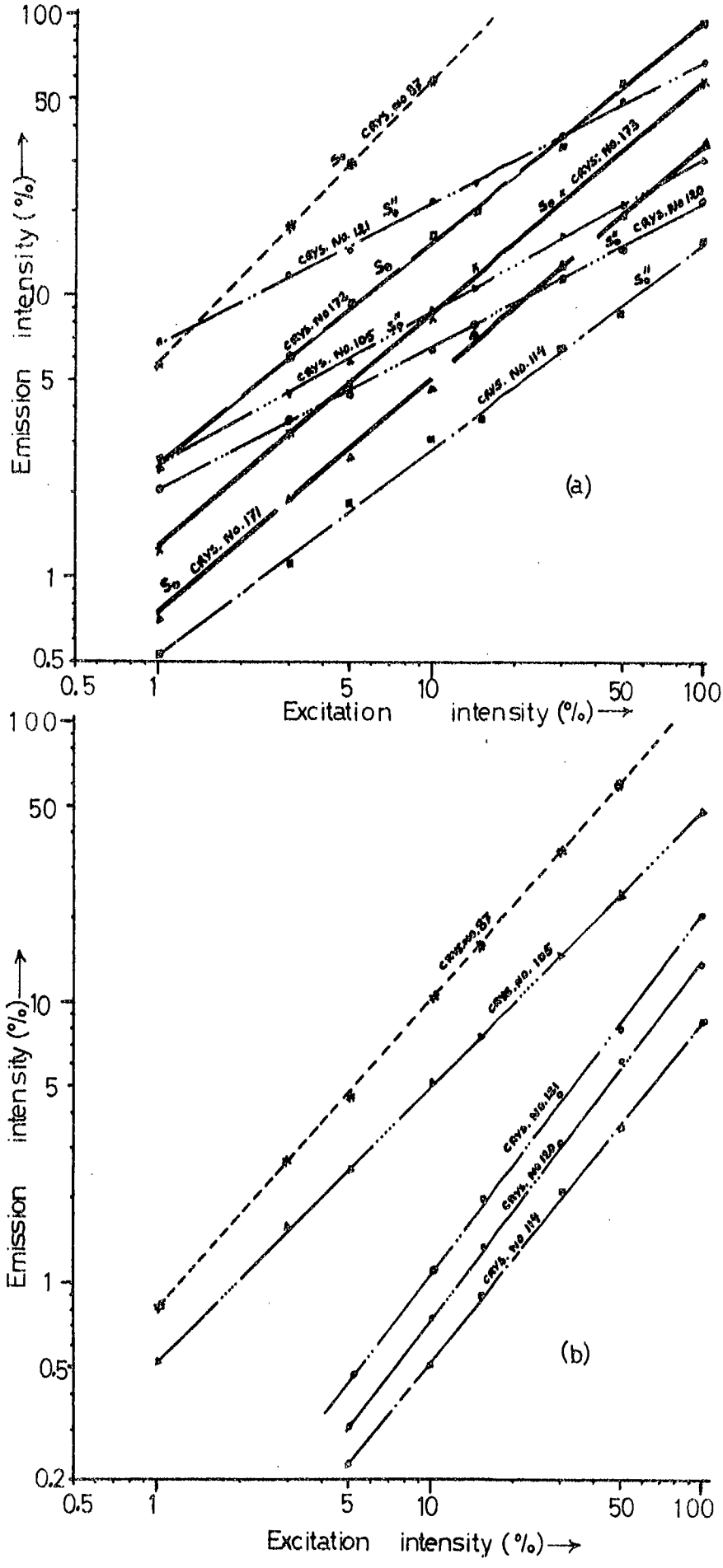

Figure 4.14 The comparison of the excitation intensity dependence of the a) zero phonon maxima b) I_1 excitation emission, at 10°K.

a much lower value than that calculated previously from the displacement of the I_1 line from the band gap. The intensity of the S_o'' zero phonon line decreases rapidly with temperature above ∿78 K at the same rate as N_o''. The activation energy involved was approximately 0.094 eV. This agrees reasonably well with the ionization energy of the acceptor associated with the S_o'' series (i.e. 0.112 eV).

When the quenching curves of flow-run crystals (S_oN_o) are compared with those of crystals grown with zinc reservoirs ($S_o''N_o''$) see Figure 4.13, the S_o and S_o'' bands are seen to be quenched at approximately the same temperature, but the N_o band is quenched at a slightly higher temperature than the N_o'' band, and has an activation energy of ∿0.106 eV at temperatures above ∿88 K. This is once again in reasonable agreement with the acceptor ionization energy of 0.122 eV determined from the spectral position of the N_o zero phonon component.

4.5 Variation with intensity of excitation

The variations of the intensities of the various emission components at 10 K with excitation intensity (λ = 3650Å) are shown in Figures 4.14a and 4.14b. The straight lines obtained from the double logarithmic plots show that there is a power law relationship between the emission and excitation intensities. The slopes of the lines give values of n, the intensity dependence index. The value of n, for the S_o zero phonon components of the flow run crystal was 1.05 ± 0.01, and typically 0.80 ± 0.01 for the crystals grown in an excess selenium pressure (crystals No. 171, 172 and 173).

TABLE 4.5

Average of all undoped crystals zero phonon components and values of donor and acceptor binding energies

Lines	Wavelength (Å)	Energy (eV)	Energy of assignments
S_o	4630	2.67799	E_D = 0.032 eV
N_o	4600	2.69546	E_A = 0.122 eV
S'_o	4580	2.70723	E_D = 0.031 eV
N'_o	4555	2.72208	E_A = 0.095 eV
S''_o	4618	2.68496	E_D = 0.034 eV
N''_o	4585	2.70427	E_A = 0.112 eV

With the exception of crystal 114, the mean value n, for the S_o'' zero phonon components of the crystals grown under zinc vapour pressure was 0.48 ± 0.02.

The dependence of the intensity of the I_1 line on excitation was approximately the same for all undoped crystals with an intensity dependence index of 1.11 ± 0.02.

4.6 Summary and discussion

The results described so far in this chapter appear to indicate that there are at least three distinct pairs of edge emission series. The low energy components of these pairs are revealed at 10 K and have been labelled S_o, S_o' and S_o''. At 65 K the donors are thermally ionised and the high energy partners N_o, N_o' and N_o'' are then observed. Averaged over all undoped samples studied the wavelengths of various zero phonon lines are as shown in table 4.5.

The crystals grown with selenium in the reservoirs were all very similar and displayed the S_oN_o and $S_o'N_o'$ series. The $S_o'N_o'$ pair of series was dominant in the samples grown in the higher pressures of selenium so that it seems to be reasonable to conclude that this pair is enhanced with increasing selenium pressure. This is also supported by the observation that these two coupled series disappeared when the crystals grown in selenium vapour were annealed in zinc. The acceptor involved which has an ionization energy of 0.095 eV is therefore introduced in the presence of excess selenium and removed by heating in zinc.

From the evidence obtained from the crystals grown in selenium, first impressions would suggest that the longer wavelength coupled pair S_oN_o was enhanced considerably by

heating in zinc. However it was noted that the series also appeared to shift to shorter wavelengths with prolonged annealing in zinc.

The studies on the crystals grown in zinc vapour show that such samples contained the S_oN_o and $S''_oN''_o$ pairs of series, but now the S''_o and N''_o paired components were dominant. The S''_o zero phonon line appeared at 4618Å while the weaker S_o band was observed at 4630Å. The conclusion would appear to be that the $S''_oN''_o$ pair is dominant in crystals grown in zinc vapour and it could well be that the apparent shift in the position of the S_o band observed in the crystals grown in selenium after annealing in zinc was due to the appearance of the $S''_oN''_o$ pair of series following such treatment.

A useful working hypothesis therefore is that there are three possible acceptors in undoped zinc selenide with ionization energies of 0.095, 0.112 and 0.122 eV. The acceptors with activation energies of 0.112 eV are enhanced by heating crystals in zinc or by growing crystals in excess zinc. They do not appear in crystals grown in selenium. In contrast the acceptor with an ionization energy of 0.095 eV does not appear in the presence of excess zinc but is enhanced by excess selenium. The deepest acceptor appears in both types of crystals but tends to disappear with excesses of either zinc or selenium.

The donor binding energies were determined by adding the Coulombic energy correction to the measured values obtained from the zero phonon components of the three low energy series. The results show a variation from 0.031 to 0.034 eV. The lowest donor energies were found in

crystals grown with excess selenium and flow run crystals, while the highest were observed in crystals grown with excess zinc. However the very small difference (3 meV) in the donor binding energies suggests that one donor level only is involved in all these crystals and that it is situated about 0.032 eV below the conduction band.

Before leaving the topic of donor and acceptor ionization energies it should be remarked that the thermal quenching of both the S and N series at temperatures exceeding 65 K is consistent with acceptors with an ionization energy of about 0.1 eV being involved. Thermal quenching of the S series also takes place at temperatures above 25 K when the activation energy is 0.018 eV. This is of the order of the effective donor depth as modified by the Coulombic interaction.

The bound exciton lines were only observed in the samples grown in excess zinc. Split I_1 lines were detected with the stronger I_1 component at 4464Å and the weaker I_1' at 4474Å. This suggests that the acceptor associated with I_1 is that with an ionization energy of 0.112 eV, while I_1' is perhaps associated with the acceptor with E_A = 0.122 eV. However according to Halsted and Aven (16) a rule for excitons bound to neutral acceptors in II-VI compounds is that $E_{\Theta^+_-}/E_A \simeq 0.1$ where $E_{\Theta^+_-}$ is the dissociation energy of the exciton. The two bound excitons observed have disocciation energies of 0.0239 eV (I_1) and 0.0302 eV (I_1') (which were calculated from the energy differences between the observed bound exciton emissions and the previously reported value of 2.8015 eV for the free exciton emission (7,14)), so that the appropriate ratios are 0.213 and 0.248

which are substantially larger than 0.1. If the Halsted and Aven rule is valid the two I_1 lines should be associated with acceptors with ionization energies of 0.239 and 0.302 eV respectively. Free electron transitions to such acceptors would produce emission bands at 4806 and 4927Å. It is interesting to note that a band at 4830Å containing phonon structure, i.e. at 4800 (S_3), 4860 (S_4) and 4920 (S_5) was found in crystals grown in zinc vapour whereas this was absent in samples grown in excess selenium.

It seems probable however that the dissociation energies of the exciton complexes given above are excessively large. Thermal quenching of the I_1 line takes place with an activation energy of 0.0083 eV, so that Halsted and Aven's rule would then indicate an acceptor ionization energy of 0.083 eV, which agrees quite well with experiment. If this interpretation is correct then the value of the free exciton energy would have to be 2.785 eV and not 2.8015 eV.

A priori it is difficult to decide whether the flow crystals should resemble samples grown in excess zinc or selenium. The general shapes of the spectra suggest that the flow crystals grow in an atmosphere similar to that of crystals grown with selenium reservoirs. The absence of the $S_O''N_O''$ pair of series also supports this view, but it is then difficult to account for the appearance of the I_1 line in the emission of the flow crystal. It is perhaps significant however that the flow crystals exhibit a broad band emission at 5360Å.

One feature is quite clear, namely that crystals grown under the P_{min} condition with selenium in the reservoir are quite different from crystals grown under P_{min} conditions with zinc in the reservoir. Since these latter are most similar to crystals annealed in liquid zinc it seems reasonable to assume that zinc reservoirs lead to the incorporation of excess zinc whereas the selenium reservoirs lead to the incorporation of excess selenium. Since crystal growth is a dynamic process and since the reservoir communicates with the growth capsule via a narrow orifice it is perhaps not surprising that the ambient atmosphere over the growing crystals is not related in any simple manner to the pressure in the reservoir.

Returning briefly to the topic of the I_1 lines it is perhaps worth recording the following facts. If it can be assumed that a hydrogenic model can be used to describe the energy levels of the acceptor responsible for the I_1 exciton, the energy of the photon which would be emitted when the I_1 exciton recombines but at the same time raises the trapped hole to its first excited state with n = 2, would be $I_1 - 0.75\ E_A$. Substituting the values for I_1 and E_A of 2.77758 and 0.112 eV, respectively such a process is found to have an energy of 2.69358 eV or 4603Å. The n = 3 excited state would lead to a photon energy $(I_1 - 0.88\ E_A)$ = 2.67458 eV or 4632Å. These two values are of course very similar to the observed wavelengths of the N_o and S_o bands. Similar processes with an acceptor with E_A = 0.098 eV would lead to bands at 4585 and 4606 which are close to the observed values of N_o'' and S_o''.

CHAPTER 4

REFERENCES

1. R.E. Halsted, M.R. Lorentz and B. Segall, J. Phys. Chem. Solids 22 (1961) 109
2. D.C. Reynolds, L.S. Redrotti and O.W. Larson, J. Appl. Phys. Suppl. 32 (1961) 2261
3. G.H. Hite, D.T.F. Marple, M. Aven and B. Segall Phys. Rev. 156 (1967) 850
4. S. Iida, J. Phys. Soc. of Japan 25 (1968) 177
5. W.Y. Liang and A.D. Yoffe, Phil. Mag. 16 (1967) 1153
6. R.E. Halsted and M. Aven, Phys. Rev. Letters 14 (1965) 64
7. P.J. Dean and J.L. Merz, Phys. Rev. 178 (1969) 1310
8. L.S. Pedrotti and D.C. Reynolds, Phys. Rev. 119 (1960) 1897.
9. J.J. Hopfield, J. Phys. Chem. Solids 10 (1959) 110
10. M. Schön, Z. Phys. 119 (1942) 463
11. H.A. Klasens, Nature 158 (1940) 306
12. J.S. Prener and F.E. Williams, J. Electrochem. Soc. 103 (1956) 342
13. K. Era and D.W. Langer, J. Luminescence 1, 2 (1970) 514
14. J.L. Merz, H. Kukimoto, K. Nassau and J.W. Shiever, Phys. REv. B 6 (1972) 545
15. S. Iida,& M. Toyama, J. Phys. Soc. of Japan 31 (1971) 190
16. R.E. Halsted and M. Aven, Phys. Rev. Letters 14 (1965) 64
17. S. Roberts and D.T.F. Marple, in "Phys. and Chem. of II-VI Compounds" ed. M. Aven and J.S. Prener (N.Holland) 1967 Ch.7
18. E. Gutsche and O. Goede, J. Luminescence 1,2 (1970) 200

CHAPTER 5

EDGE EMISSION OF SUBSTITUTIONAL DONORS IN ZINC SELENIDE CRYSTALS

5.1 Introduction

The edge emission and self-activated emission of zinc selenide crystals doped with aluminium, gallium, indium and chlorine are described in this chapter. The dopant, in suitable form, was added to the charge of zinc selenide, and crystals were grown from the vapour phase in a continuous flow of argon. The doped flow run crystals were then either studied or used as the starting material for the production of large boules by sublimation under excess zinc pressure. Unless otherwise specified, the doped flow run crystals were grown at 1050^{o}C while the boule crystals were all grown with the upper furnace control set at 1155^{o}C.

The edge emission characteristics of deliberately doped zinc selenide crystals were essentially similar in broad outline to those of undoped crystals. There were changes in individual components in certain cases. For example, aluminium doped flow run and gallium doped samples showed no edge emission at all, however some doped crystals showed well resolved exciton emission and phonon assisted bands, so that the absence of edge emission in particular crystals probably indicated poor crystal quality. On the other hand the observed emission spectra of the doped crystals were different in detail from those of undoped crystals grown under the same conditions. This indicates that the dopant was successfully incorporated in the crystals.

The emission characteristics are described and discussed below in separate sections dealing with the individual dopants. In order to facilitate the presentation of results, the crystals will be referred to as (X, Y) and (X, flow-run), where X indicates the dopant element, Y the element providing the excess pressure during the growth, while (X, Flow-run) refers to the crystal or crystals grown in a continuous flow of argon with dopant X added.

5.2 Aluminium doped crystals

Two aluminium doped crystals were studied, one (Al, flow-run) sample, and a (Al, Zn) one grown under P_{min} conditions. It was hoped that these growth conditions would allow the aluminium to substitute for zinc and form a donor. The emission spectra of these two types of crystal were different from one another. The (Al, flow-run) crystals emitted two broad bands only at about 5400 and 6100Å at 65 K. These broad bands which were of weak and medium intensity increased by about two orders of magnitude as the temperature was reduced to 10 K. At the same time the 5400Å band shifted by about 30Å to longer wavelengths. No discrete pair lines or phonon assisted emission was detected at either temperatures.

The emission spectra of the (Al, Zn) doped crystal No.149 consists of two broad bands and edge emission components at 65 K, which are shown in Figure 5.1 with dotted lines. The two broad bands at about 5430 and 6180Å are the self-activated green and red emissions of these crystals. The peaks at about 4585, 4610, 4639, 4665 and 4694Å belong

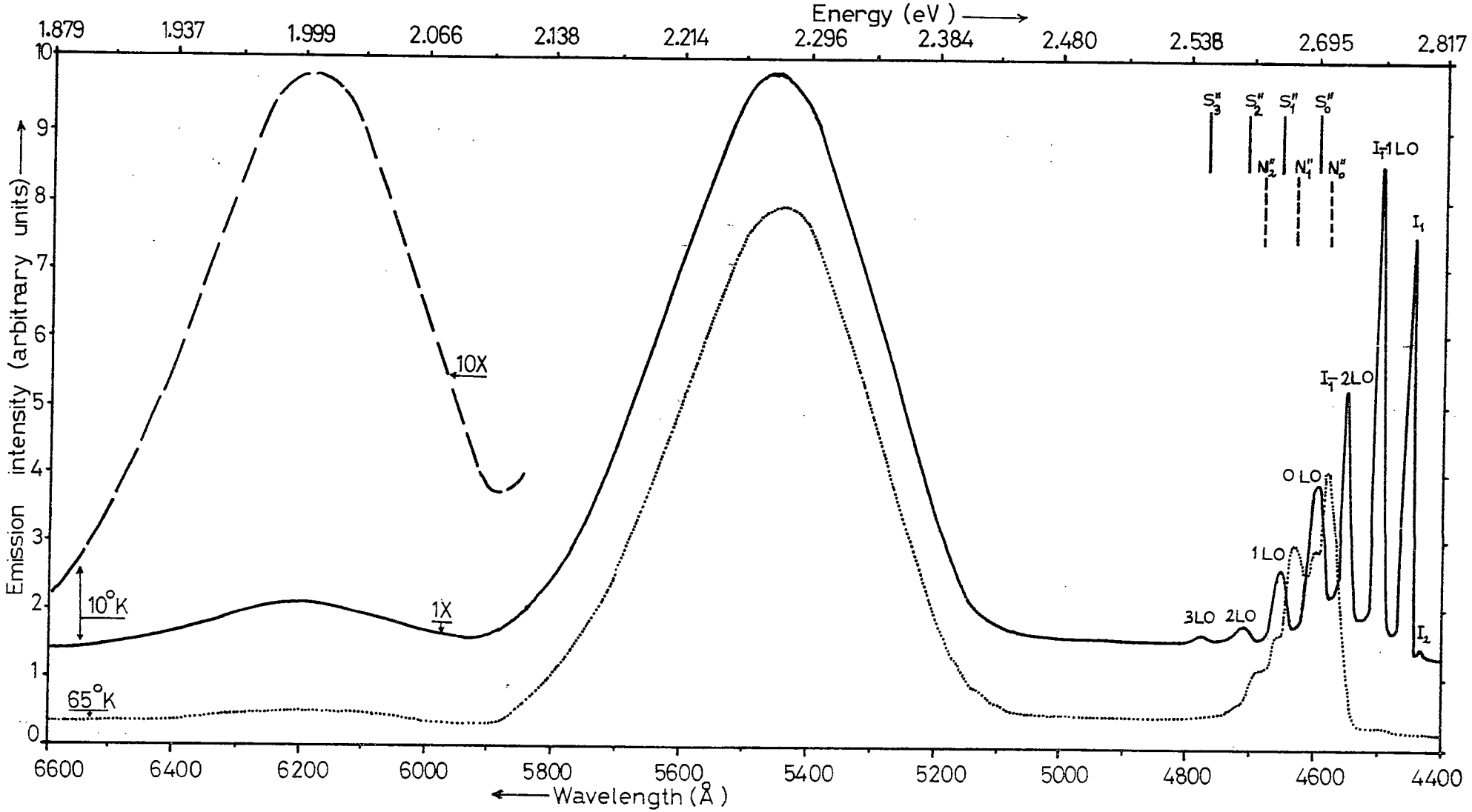

Figure 5.1 Luminescence emission spectra of (Al, Zn) doped cubic ZnSe at 10°K (solid curve) and 65°K (dotted curve).

to two LO phonon assisted series. The bands at 4585, 4639 and 4694Å are attributed to the HES while those at 4610, 4665Å are the corresponding LES components. The value of 4585Å for the wavelength of the zero phonon component of the HES leads to a value of 0.112 eV for the separation of the acceptor level from the valence band. This acceptor is identical with that observed in the undoped crystals No.120 and 121 grown with zinc reservoirs.

A bound exciton was also observed at 10 K in the (Al, Zn) samples. The wavelengths, energies and the possible assignments of the various spectral features are listed in Table 5.1 and the emission spectrum is shown in Figure 5.1 (solid curve). In the bound exciton region the small shoulder appearing in the high energy region at about 4440Å is attributed to the exciton bound to a neutral donor (I_2 line) while the three sharp lines at 4460, 4510 and 4561Å with half widths of about 22Å are attributed to the exciton bound to a neutral acceptor with two LO phonon replicas, i.e. I_1, I_1-1LO and I_1-2LO. These bound exciton lines have identical wavelengths to those observed in the undoped crystals No.120 and 121 (see Chapter 4, Section 3). However the intensities and half widths of the exciton emission were higher than those of the exciton lines in the undoped crystals, and with the (Al, Zn) samples no splitting of the exciton emission occurs.

The I_1 emission formed the largest component of the luminescence at 10 K, although the LES appeared with medium intensity with the zero phonon band and three weak replicas at 4608, 4663, 4719 and 4777Å. These bands shifted by about

TABLE 5.1

The position of the emission maxima of the (Al, Zn) doped crystal No.149.

Observed spectrum at 10 K					Observed spectrum at 65 K			
Lines	Wave-length (Å)	Energy (eV)	Strength	Possible assignment	Lines	Wave-length (Å)	Energy (eV)	Possible assignment
I_2	4440	2.79259	Shoulder	(I_2) exciton bound to neutral donor				
I_1	4460	2.78007	Strong	Exciton bound to neutral acceptor (I_1)				
I_1'	4510	2.74924	Strong	I_1-1LO				
I_1''	4561	2.71850	Strong	I_1-2LO	N_o''	4585	2.70427	HES of zero phonon
S_o''	4608	2.69078	Strong	Zero-phonon	S_o''	4610	2.68961	LES of zero phonon
S_1''	4663	2.65904	Medium	One phonon	N_1''	4639	2.67280	HES of one phonon
S_2''	4719	2.62748	Medium	Two phonon	S_1''	4665	2.65790	LES of one phonon
S_3''	4777	2.59558	Weak	Three phonon	N_2''	4694	2.64148	HES of two phonon
	5460	2.27090	Strong	Self-activated		5430	2.28344	Self-activated emission
	6230	1.99025	Weak	Emission				

10Å towards longer wavelengths when the excitation intensity was reduced by one order of magnitude. This effect is clearly shown in Figure 5.2. The process is once again attributable to the recombination of donor acceptor pairs. In comparison with the undoped crystals No.120 and 121, the zero phonon component occurred at an energy some 4 meV larger than S_o'' in the undoped crystals, so that if the 4608Å zero phonon band is associated with a transition of electrons from aluminium donors to acceptors the ionization energy of the aluminium donor will be 27 meV. This is in good agreement with the donor binding energy of 26.3±0.6 meV for aluminium doped ZnSe reported by Merz et al. (1).

The relative intensities of I_1, and its phonon replicas, change as the excitation intensity is varied. Thus at the highest intensities of excitation the I_1 emission line is most intense, but at 15% excitation the first phonon replica is the most intense, and at the weakest level of excitation this is the only feature which can be observed. This clearly indicates that careful consideration must be given to the intensity of excitation used when interpreting spectra. With many of the undoped samples described in the previous chapter a single exciton-like line was observed at about 4515Å. This information obtained from the present crystal strongly suggests that this line is I_1-1LO.

The variation of the relative intensities of the I_1 line and its replicas with decreasing excitation intensity is caused by increasing phonon coupling. This may be associated with the fact that the weaker excitation will be absorbed in the surface region only.

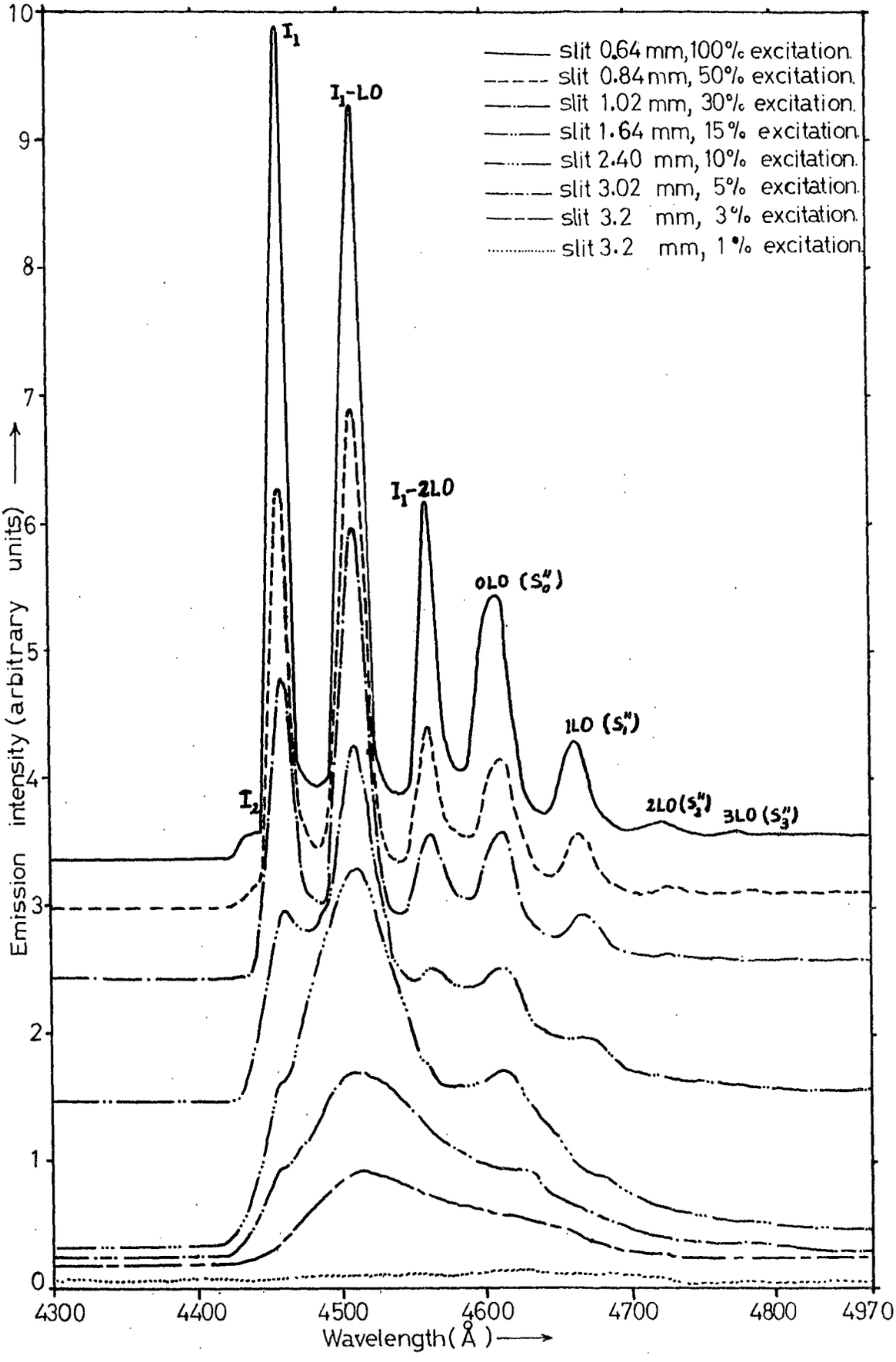

Figure 5.2 Bound exciton and LO phonon assisted emission spectra of (Al, Zn) doped ZnSe crystal No 149, were recorded with various intensities of the exciting U.V. radiation at 10°K.

The self-activated emission bands were located at approximately 5460 and 6230Å with half widths of about 320 and 390Å at 10 K. The intensity of the green emission was higher than that of the red and shifted by about 30Å towards longer wavelengths with decreasing temperature. At the same time the half widths decreased by about 30Å. Unfortunately, the shift of the maximum and the variation of the half width of the red band could not be measured particularly well because of the low intensity. The band is shown by the dotted curve in Figure 5.1 which was obtained using a large slit (3,2 mm). The observed variations of the half widths with temperature suggest that several sub-bands may be involved in both the green and red bands. The shift to higher energies with increasing temperature may be evidence of a donor acceptor pair model with redistribution of trapped electrons. The luminescence centre responsible for the red emission may consist of an association at nearest neighbour sites of an ionized zinc vacancy (acceptor) and an ionized Al_{Zn} impurity donor. A similar explanation for the red (at 6400Å) emission in ZnSe:Al crystals at 80 K has been offered by Holton et al. (2). The difference between the position of the red band reported here and the previously reported value of 6400Å emission may be a consequence of the very low concentration of Al in our crystals. This is supported by Aven and Halsted (3) who found that Al diffuses very slowly in ZnSe, probably because of association between the charged Al donors and the negatively charged intrinsic acceptors. Alternatively the crystals used by Holton et al. (2) may have been contaminated with copper (see Chapter 6).

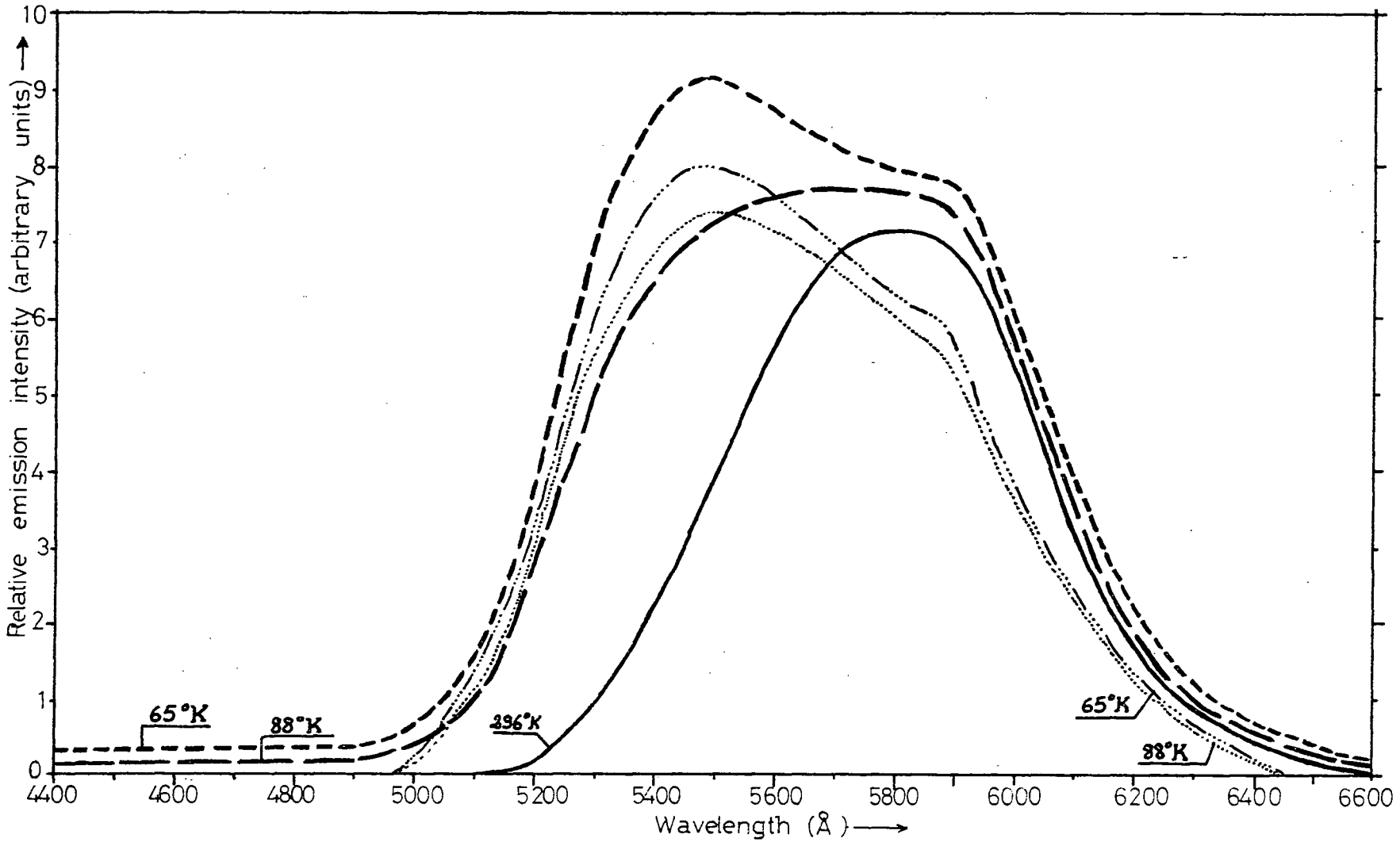

Figure 5.3 Luminescence emission spectra of (Ga, Zn) doped ZnSe crystal No. 176 at room temperature (thick solid curve), 88°K (thick large dash curve) and 65°K (thick small dash curve) and crystal No. 140 at 88°K (dot lines) and 65°K (small dash and dot lines).

5.3 Gallium doped crystals

Two different crystals doped with 1000 ppm gallium were studied. Both were grown under an excess pressure of zinc (Ga, Zn). If gallium substitutes for zinc it should act as a donor, but even under the highest excitation intensity, no bound exciton or phonon assisted pair emission was detected. This may have been the result of poor crystal quality or more probably the doping level in these samples may have been too high. A similar effect has been reported recently with the bound exciton emission of Ga doped crystals by Merz et al. (1). They found that as the Ga concentration increased the edge emission became broad and weak.

Figure 5.3 shows the self-activated emission of both (Ga, Zn) doped crystals at various temperatures. At room temperature (296 K) the emission consists of a single broad band at 5830Å with a half width of about 600Å. As the sample was cooled to 88 K, the half width increased, and a shoulder appeared at approximately 5470Å. This shoulder dominated the spectrum with decreasing temperature and peaked at 5490Å at 65 K. Unfortunately no measurements were made at liquid helium temperature. It is believed that the yellow band at 5830Å is characteristic of gallium and once again may consist of a complex between a gallium donor and a cation vacancy.

5.4 Indium doped crystals

Four indium doped crystals were studied, two were flow-run samples which had been grown with different concentrations of indium and the two others (In, Zn) were grown under P_{min} conditions from flow run crystals

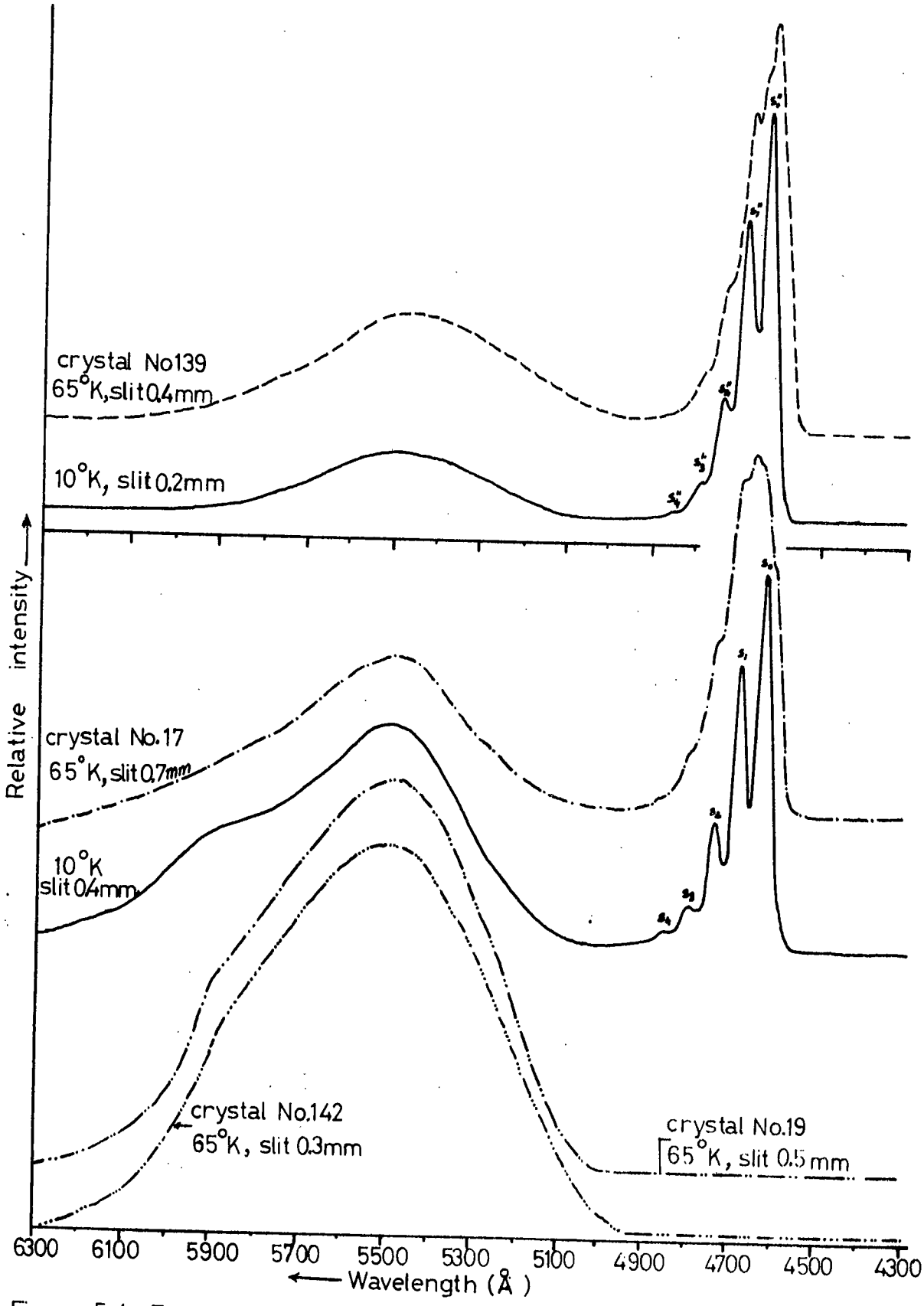

Figure 5.4 Emission spectra of crystals containing two different concentrations of In at 65 and 10°K.

containing different concentrations of indium. The crystals with the lower concentration of In were yellow in colour, with a resistivity of the order of 10^9 ohm cm. The crystals with a higher concentration of In were yellow or yellowish orange in colour, with a resistivity of the order of 10^4 ohm cm. The different concentration of In was reflected in the emission spectra of the various crystals. The crystals containing the higher concentration of In (In, flow-run) and (In, Zn) crystals 19 and 142 showed no edge emission at 88 and 65 K. Only a single broad band was observed at about 5480 Å with a half width of about 630 Å (see Figure 5.4). This broad band had an extended tail on the longer wavelength side and a shoulder was observed at approximately 5900 Å. Unfortunately no measurements were made at liquid helium temperature.

The edge emission spectra of the crystals containing small quantities of indium were very similar to those of undoped crystals, with the exception that the bound exciton emission was not observed. At 65 K, the spectrum of the (In, flow-run) crystal No.17 consisted of the 4600 Å zero phonon component while the (In, Zn) crystal No.139 spectrum contained a different zero phonon component at about 4585 Å. These two different HES zero phonon components and their accompanying series were also observed in undoped crystals and have been labelled N_o and N''_o (see Chapter 4). In addition to the HES, two small peaks were observed in both crystals which were obviously the corresponding low energy S associates. The emission spectra are shown in Figure 5.4 and their wavelengths and possible assignments are listed in Table 5.2. The edge emission spectra of these crystals

TABLE 5.2

The position of the emission maxima of the (In, flow-run) and (In, Zn) doped crystals at 10 and 65 K.

Observed spectrum at 10 K				Observed spectrum at 65 K			
Lines	Wave-length (Å)	Energy (eV)	Possible assignment	Lines	Wave-length (Å)	Energy (eV)	Possible assignment
(In, flow-run) doped crystal No.17							
S_o	4625	2.68089	Zero phonon	N_o	4600	2.68379	Zero phonon
S_1	4680	2.64938	One phonon	S_o	4627	2.67973	LES of zero phonon
S_2	4737	2.61750	Two phonon	N_1	4674	2.65278	One phonon
S_3	4794	2.58638	Three phonon	N_2	4730	2.62137	Two phonon
S_4	4852	2.55546	Four phonon	N_3	4788	2.58962	Three phonon
	5490	2.25849	Self-activated emission band		5480	2.26261	Self-activated emission
	5960	2.08039					
(In, Zn) doped crystal No.139							
S''_o	4610	2.68961	Zero phonon	N''_o	4585	2.70427	Zero phonon
S''_1	4664	2.65847	One phonon	S''_o	4614	2.68728	LES of zero phonon
S''_2	4719	2.62747	Two phonon	N''_1	4638	2.67337	One phonon
S''_3	4776	2.53613	Three phonon	S''_1	4664	2.65847	LES of one phonon
S''_4	4834	2.56498	Four phonon	N''_2	4693	2.64204	Two phonon
	5500	2.25438	Self-activated emission	N''_3	4750	2.61034	Three phonon
					5480	2.26261	Self-activated emission

exhibited well resolved phonon components and four replicas at 10 K. The zero phonon components lay at about 4625 Å for (In, flow-run) crystal and at 4610 Å for the (In, Zn) sample. These two zero phonon bands are close to those observed in corresponding undoped crystals which were labelled S_o and S_o''.

Acceptor binding energies of 0.122 and 0.112 eV were calculated for these two indium-doped crystals using the observed wavelengths of N_o (4600) and N_o'' (4585 Å) respectively. These acceptors are of course identical with those observed in the undoped crystals grown in the corresponding ways, i.e. crystals Nos.120 and 121. The spectra of samples Nos. 17 and 139 were measured at various excitation intensities at 65 and 10 K. No spectral shift was observed at 65 K, but a shift of about 12 Å was observed in both the S_o and S_o'' components at 10 K. The results are shown in Figure 5.5. for the (In, Zn) crystal No.139. The shifts once again indicate the presence of distant pair transitions between indium donors and the same acceptors as in the undoped samples. Using the estimated value of the Coulombic interaction and the measured displacements between the S_o and N_o and the S_o'' and N_o'' bands, the ionization energy of the indium donor is found to be 0.029 eV. This compares very well with the value of 28.9 ± 0.6meV determined by Merz et al (1).

At 65 K a broad emission band was located at 5480 Å in the lightly doped samples. At 10 K this broad band had shifted slightly to 5500 Å and a small shoulder appeared at approximately 5960 Å. This shoulder is

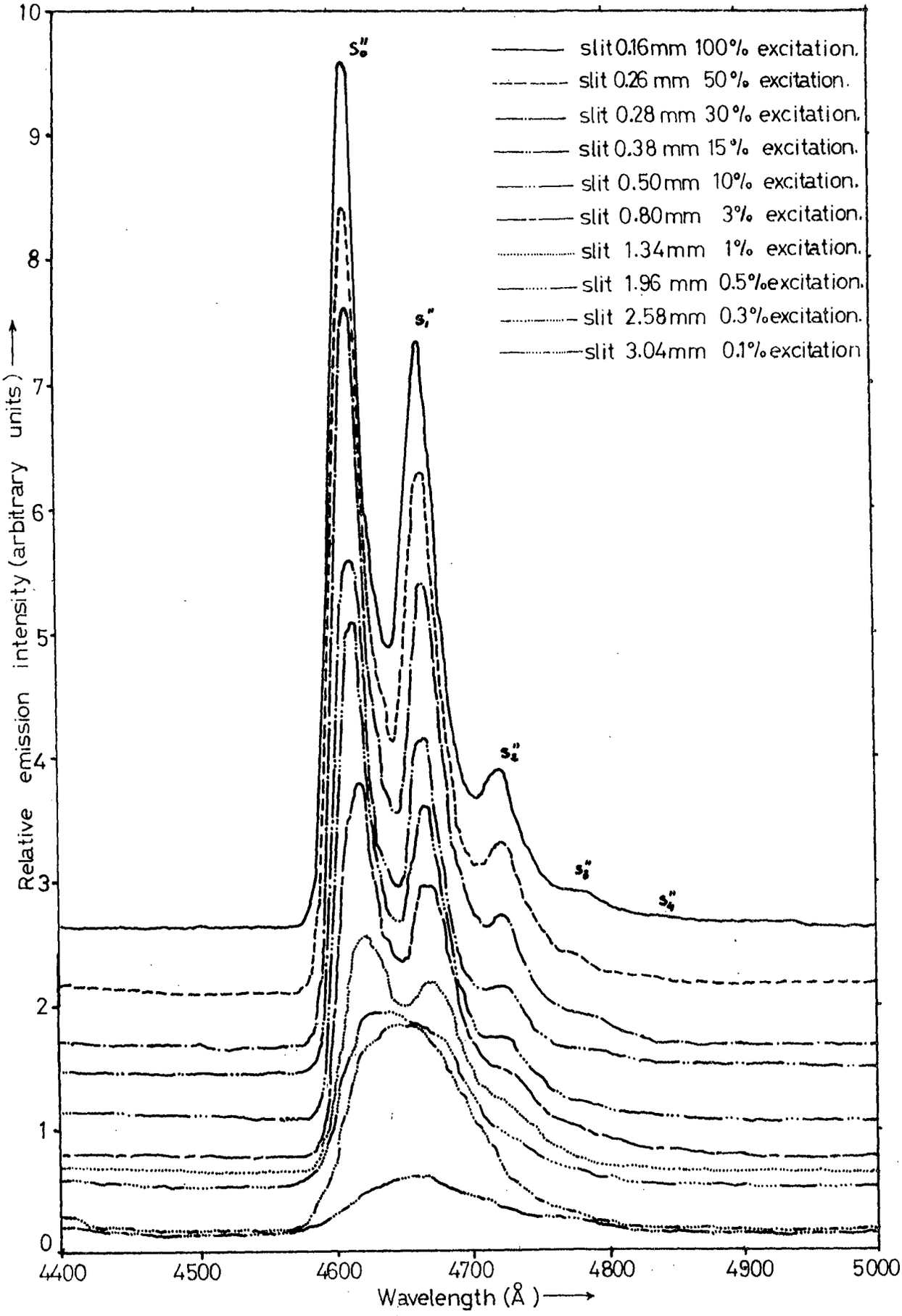

Figure 5.5 The emission spectra of the (In, Zn) crystal No.139, with various intensties of excitation at 10°K.

presumably the characteristic band for In since it is more apparent in the heavily doped samples. The corresponding luminescent centre may consist of a complex of an indium donor and a cation vacancy.

5.5 Chlorine doped crystals

The emission properties of chlorine doped crystals (Cl, flow-run) and (Cl, Zn) were studied under U.V. excitation at 65 and 10 K. The wavelengths and energies of the various spectral features are recorded in Table 5.3. The edge emission of the (Cl, flow-run) crystal No.13 is composed of two phonon assisted series of bands at 65 K with zero phonon components at 4557 and 4600 Å. The emission spectra over a range of temperatures from 78 to 10 K are shown in Figure 5.6. The series beginning at 4600 Å was dominant with three well resolved replicas separated by 0.031 eV. The series starting at 4557 Å is much weaker and appears as shoulders on the high energy side of the components of the main series. As the sample was cooled to 10 K, the bound exciton line I_2 and the main LES emission S_o' dominated the spectra. The single bound exciton line at 4440 Å was very strong with a half width of 15 Å. This is close to the medium intensity I_2 lines observed at 4447 and 4442 Å in the undoped flow-run crystals and sample No.105 grown in excess zinc. Comparison of the previously observed I_2 emission, with this line shows that the present line is stronger and broader which is attributable to the presence of a high concentration of chlorine. Such a strong and broad I_2 line was observed by Merz et al. (1) in their Cl doped ZnSe crystals.

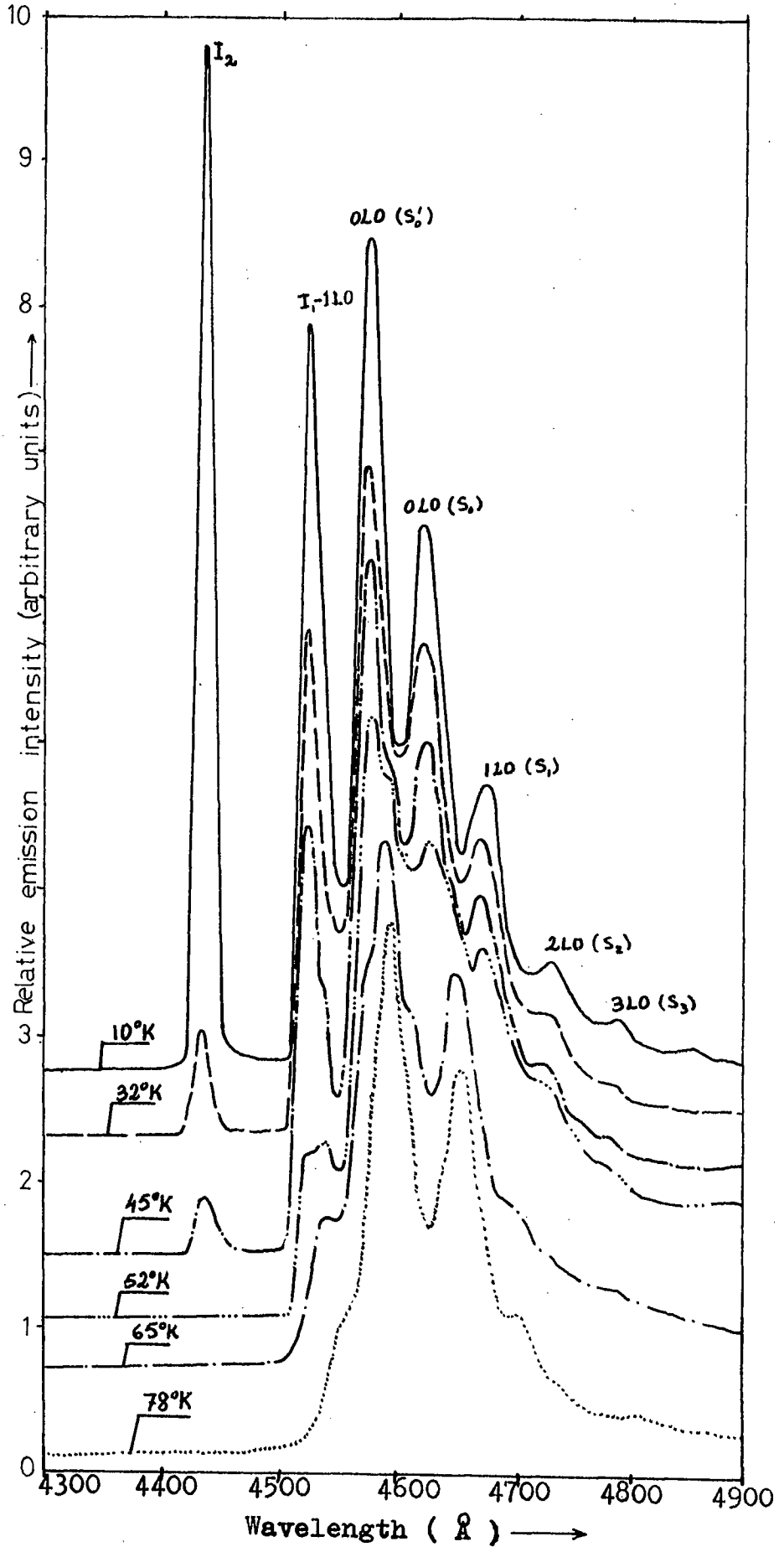

Figure 5.6 Bound exciton and LO phonon assisted emission spectra of (Cl, flow-run) crystal No. 13 at various temperatures.

A second strong and sharp exciton-like band was also observed at 4526 Å with a half width of about 18 Å. The origin of this band has been discussed earlier and the correct assignment is I_1-1LO. The two strong zero phonon components of the edge emission were observed on the long wavelength side of this line at 4578 and 4628 Å with half widths of 25 and 35 Å respectively. These two zero phonon components are very similar to those observed in undoped flow-run crystals and labelled S'_o and S_o. Examination of the emission spectra as a function of temperature (Figure 5.6) and of excitation intensity (Figure 5.7) once again indicates that this identification is correct.

In contrast with the flow-run crystals, the (Cl, Zn) samples showed only the high and low energy N''_o and S''_o series, no bound exciton lines were observed even at 4 K. The observed emission spectra are illustrated in Figure 5.8 and the wavelengths and energies of the various features are listed in Table 5.3. The zero phonon component of the HES was located at 4585 Å and no shift was observed with variation of excitation intensity. The zero phonon component of the LES was located at 4605 Å and an 8 Å shift to longer wavelength was observed with decreasing intensity at 10 K. Once again such a shift indicates a pair band mechanism in the recombination. The acceptor ionization energy was found to be 0.112 eV, so that the band at 4605 Å which is associated with transitions of electrons from chlorine donors to these acceptors implies that the ionization energy of the

TABLE 5.3

The position of the emission maxima of the (Cl, flow-run) and (Cl, Zn) doped crystals at 10 and 65 K.

Observed spectrum at 10 K				Observed spectrum at 65 K			
Lines	Wave-length (Å)	Energy (eV)	Possible assignment	Lines	Wave-length (Å)	Energy (eV)	Possible assignment
(Cl, flow-run) doped crystal No.13							
I_2	4440	2.79259	Exciton bound to a neutral donor (I_2)	N'_o	4557	2.72089	Zero phonon
				N_o	4600	2.69546	Zero phonon
I'_1	4526	2.73953	I_1-1LO	N_1	4654	2.66418	One phonon
S'_o	4578	2.70841	Zero phonon	N_2	4709	2.63306	Two phonon
S_o	4628	2.67915	Zero phonon	N_3	4765	2.60212	Three phonon
S_1	4682	2.64825	One phonon		5480	2.26261	Self-activated emission
S_2	4738	2.61695	Two phonon				
S_3	4795	2.58584	Three phonon				
	5490	2.25849	Self-activated emission				
	5880	2.10869					
(Cl, Zn) doped crystal No.123							
S''_o	4605	2.69253	Zero phonon	N''_o	4585	2.70427	Zero phonon
S''_1	4659	2.66132	One phonon	S''_o	4607	2.69136	LES of zero phonon
S''_2	4715	2.62971	Two phonon	N''_1	4637	2.67395	One phonon
S''_3	4772	2.59830	Three phonon	N''_2	4692	2.64260	Two phonon
	5490	2.25849	Self-activated emission		5480	2.26261	Self-activated emission
	5890	2.10511			5870	2.11228	

chlorine donor is 0.027 eV. This donor binding energy is also very close to the previously reported value of 26.9 ± 0.6 meV for the chlorine doped ZnSe crystals observed by Merz et al. (1).

The (Cl, flow-run) crystals also emitted a single broad band at 5480 Å with a half width of about 520 Å at 65 K. A small shoulder was observed to the longer wavelength side of this band at approximately 5880 Å at 10 K. The (Cl, Zn) doped crystals exhibited two self-activated emission bands which were located 5480 and 5870 Å at 65 K. The yellow emission at 5870 Å was rather more intense than the green. It is believed that the yellow emission band is characteristic of chlorine and once again may consist of a complex between a chlorine donor and anion vacancy. The yellow self-activated emission of ZnSe:Cl is equivalent to the self-activated blue luminescence of ZnS:Cl (4).

5.6 Lithium doped crystals

The emission properties of a (Li, flow-run) crystal have also been studied under U.V. excitation at 65 and 10 K. The effects of alkali metal dopants in ZnSe have not been examined extensively in the past even though compounds such as NaCl have frequently been used as fluxes in the preparation of powder phosphors. If the lithium enters the lattice substitutionally at a zinc site it will act as an acceptor. If it enters interstitially it will act as a donor.

Lithium doped crystals were prepared by passing the stream of argon in the flow-run process over a heated boat of lithium carbonate before the argon passed over

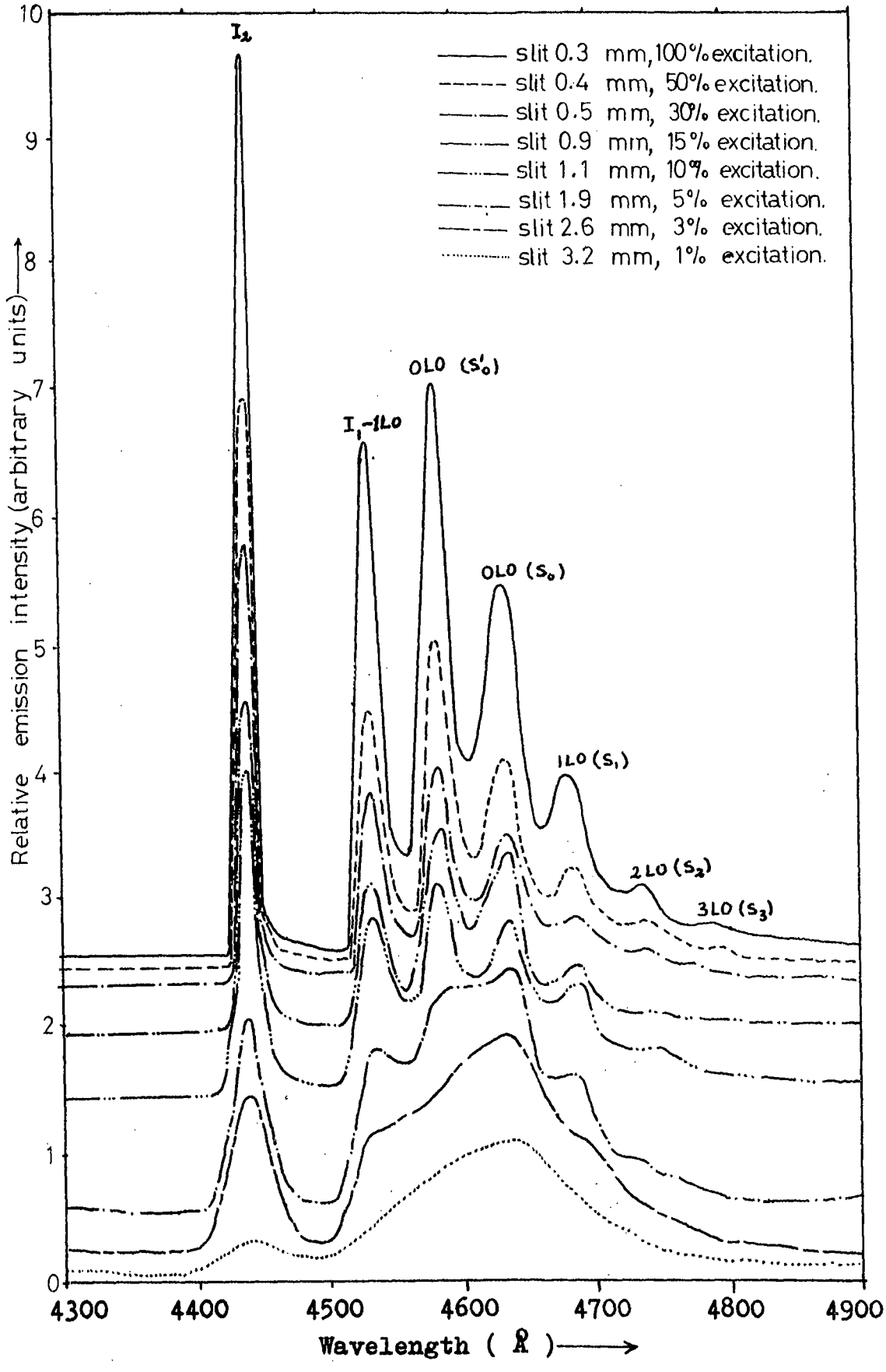

Figure 5.7 Bound exciton and LO phonon assisted emission spectra of (Cl, flow-run) crystal No 13, with various intensities of excitation at 10°K.

the heated charge of ZnSe. The emission spectrum of the resultant (Li, flow-run) crystals is composed of two different phonon assisted series the zero phonon components of which are located at 4562 and 4605 Å at 65 K. Only the 4562 Å zero phonon component of the first series is observed while the 4605 Å zero phonon component of the second series appears with three replicas. No self-activated emission bands were observed at either 65 or 10 K. The measured emission spectra are shown in Figure 5.9 and the wavelengths and energies of the various features and their possible assignments are listed in Table 5.4. At 10 K, the emission spectrum consists of bound exciton emission and the phonon assisted HES and LES emissions. In contrast to the undoped crystals, the intensity of the bound exciton emission was much higher than that of the LES. This probably results from the presence of a high concentration of lithium in the crystal. Such a behaviour has been observed by Merz et al. (5) in ZnSe heavily doped with Li_2Co_3.

The first sharp line in the high energy region is I_2 at 4442 Å, and the second sharp line is I_1 at 4472. The intensity of the I_2 line is higher than that of the I_1 line. Much stronger LO and acoustical phonon coupling was observed with the I_1 line. Such a strong I_2 line was also observed by Merz et al. (5) in their heavily doped ZnSe:Li crystals at 1.6 K. They also found that the intensity of the I_2 line decreased when the Li concentration was reduced.

On the longer wavelength side of the bound exciton emission the two zero phonon components of the low energy

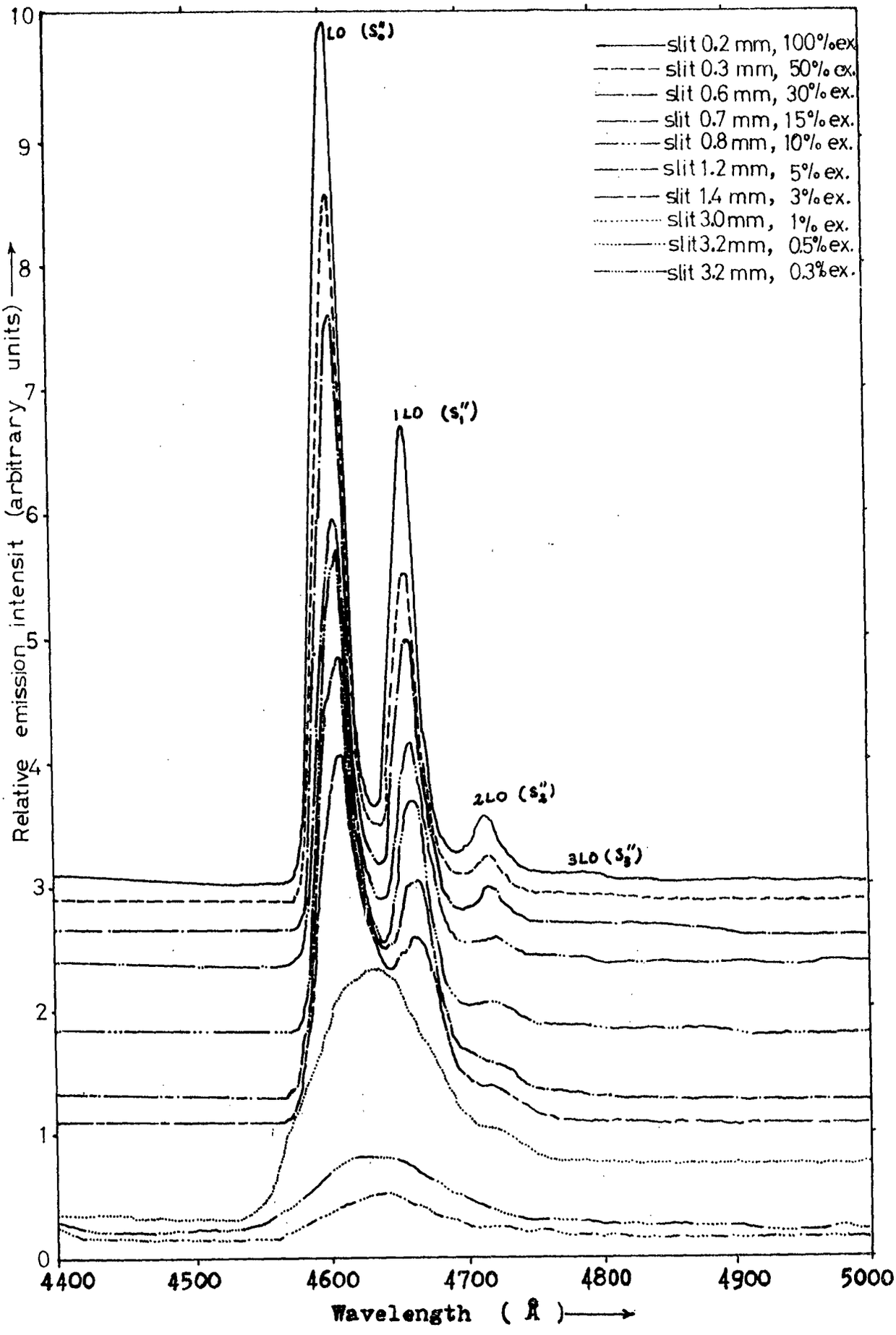

Figure 5.8 Phonon assisted edge emission of the (Cl, Zn) doped crystal No. 123 at various intensities of the exciting U.V. radiation at 10°K.

series were observed at about 4575 and 4630 Å. The second series beginning at 4630 Å is identical with that observed in undoped crystals and labelled S_o. In addition to the LES, the HES also appears in the same spectrum at 10 K which is clearly shown in Figure 5.9. This is unusual for zinc selenide and differs from the behaviour found in the undoped crystals.

No shift in the spectral position of the HES and bound exciton emission was observed when the excitation intensity was changed. The LES shifted by approximately 10 Å to longer wavelengths when the excitation intensity was decreased by two orders of magnitude. Once again such a shift indicates that a pair band mechanism is operative. Using the wavelengths of the zero phonon bands at 65 K, i.e. 4562 and 4605 Å, two acceptor binding energies of 0.099 and 0.122 eV were calculated. Donor binding energies of 0.023 and 0.032 eV were calculated from the displacements between the two S and N components. It should be noted that an acceptor binding energy of 0.114 eV for Li doped crystals was reported by Merz et al. (5) from the direct observation of the individual distant pair lines.

5.7 Discussion

When this work was started it was hoped that deliberate doping of zinc selenide with different impurities would lead to changes in the edge emission spectra, which would be readily identifiable, and thus provide information about the various defects associated with those impurities. The experimental work reported here shows that this hope was not justified and that the changes observed are subtle

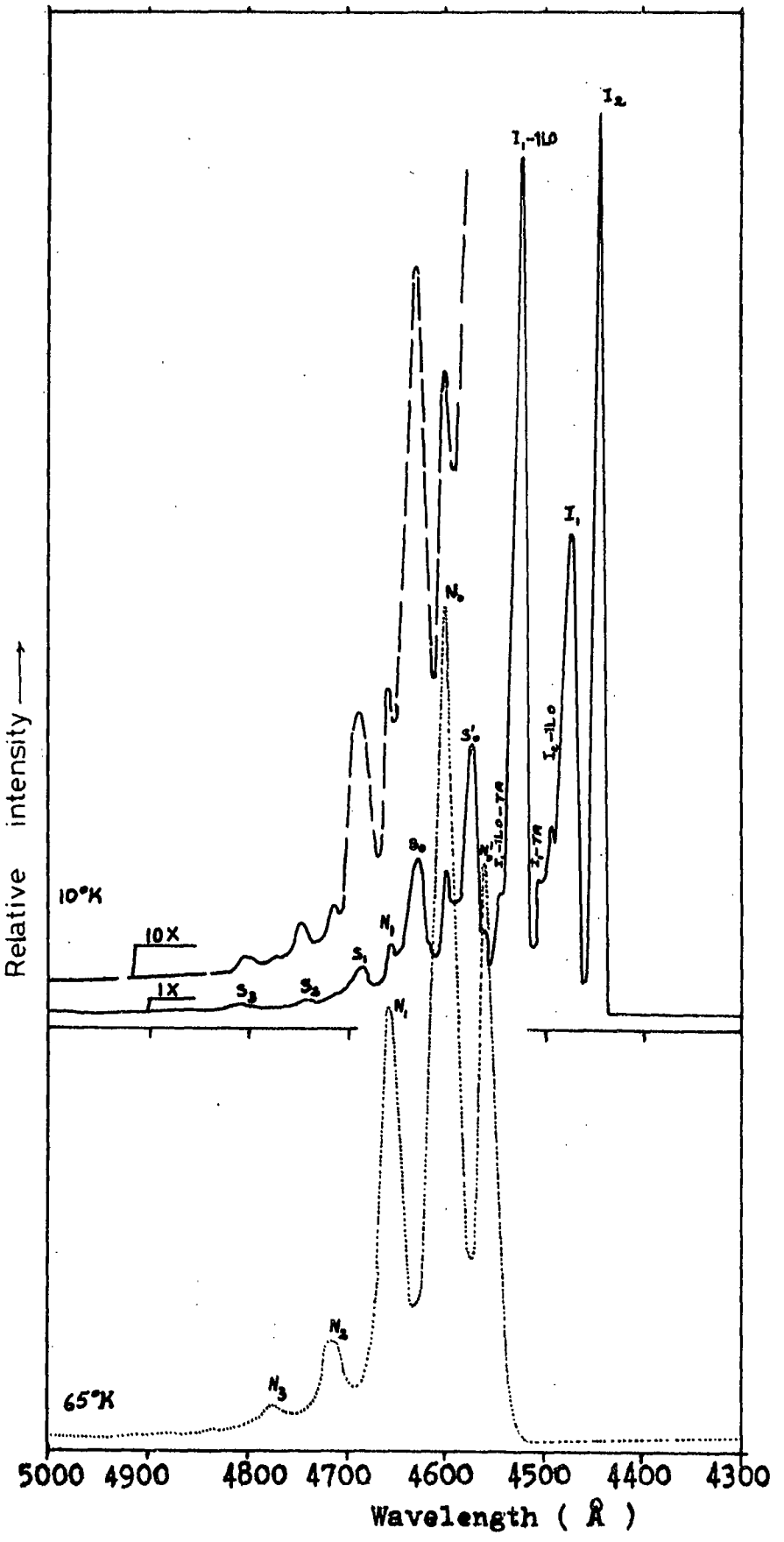

Figure 5.9 Emission spectra of the (Li, flow-run) crystal at 65 and 10 °K.

and difficult to interpret. It is clear that additional experimental information is required. In particular high intensity excitation, which should reveal the individual pair lines, would be invaluable. Such excitation, for example with an argon ion laser should greatly enhance the bound exciton spectra and reveal the two electron transitions.

The work reported in this chapter has been concerned with crystals to which five different dopants have been added. The crystals were either grown using the flow technique or in sealed tubes in an excess of zinc. The most striking result is that three different pairs of HES and LES emission bands were observed and that they occurred at much the same wavelengths as the three pairs of series in the undoped samples, so much so that the same symbols N_OS_O,$N'_OS'_O$ and $N''_OS''_O$ have been used to described them. The occurrence of a particular pair of series in any crystal was not affected by the dopant used but was determined solely by the manner in which the crystal had been grown. Thus the $N''_OS''_O$ series were observed in crystals grown in excess zinc, whereas the other two series were found in the flow run crystals. In this respect the crystals behaved in exactly the same was as the undoped samples. It can be concluded therefore that the ambient atmosphere during growth is the dominant parameter determining which pairs of emission series will be observed.

With the majority of the doped crystals the high energy N series bands lay at exactly the same wavelengths as the corresponding bands in the undoped samples grown

TABLE 5.4

The position of the emission maxima of the (Li, flow-run) doped crystals at 10 K and 65 K.

Observed spectrum at 10 K				Observed spectrum at 65 K			
Lines	Wave-length (Å)	Energy (eV)	Possible assignment	Lines	Wave-length (Å)	Energy (eV)	Possible assignment
I_2	4442	2.79133	Exciton bound to a neutral donor (I_2)	N'_o	4562	2.71791	Zero phonon
				N_o	4605	2.69253	Zero phonon
I_1	4472	2.77261	Exciton bound to a neutral acceptor (I_1)	N_1	4660	2.66075	One phonon
				N_2	4717	2.62860	Two phonon
I'_1	4492	2.76026	I_2-1LO	N_3	4772	2.59830	Three phonon
I'_{1a}	4500	2.75535	I_1-TA				
I''_1	4522	2.74195	I_1-1LO				
I''_{1a}	4545	2.72807	I_1-1LO-TA				
N'_o	4562	2.71791	HES of zero phonon				
S'_o	4575	2.71019	Zero phonon				
N_o	4600	2.69546	HES of zero phonon				
S_o	4630	2.67799	Zero phonon				
N_1	4658	2.66189	HES of one phonon				
S_1	4686	2.64599	One phonon				
N_2	4715	2.62971	HES of two phonon				
S_2	4742	2.61474	Two phonon				
S_3	4795	2.58584	Three phonon				

in the same way. This once again leads to the conclusion that three acceptors, unaffected by the impurities introduced, are involved, with ionization energies of 0.122, 0.095 and 0.112 eV corresponding to the N_o, N_o' and N_o'' series respectively. When lithium was introduced into the flow run crystals the N_o' and N_o series appeared but the N_o' series was displaced to slightly longer wavelengths compared with all the other crystals. This suggests an acceptor ionization energy of 0.099 instead of 0.095 eV.

In contrast with the situation with the N bands, the positions of the S bands were slightly different from those of their counterparts in the undoped samples. This suggests that all four dopants Al, In, Cl and Li introduced shallow donors with slightly different depths. The first three of these impurities would enter the lattice substitutionally whereas the lithium would enter interstitially. Rough estimates of the donor ionization energies have been obtained from the separation of the corresponding N and S bands and are shown in Table 5.5. The estimates are necessarily rough because of the crude approximation used to find the magnitude of the Coulombic interaction term. Two sets of donors were observed in the lithium doped samples. The shallower set may be characteristic of interstitial lithium whereas the deeper set may be associated with native donors. The lower ionization energy was calculated from the positions of the N_o' and S_o' bands whereas the higher energy was derived from the N_o and S_o components.

On the evidence available from the positions of the S and N bands in the undoped and doped crystals it

TABLE 5.5

Values of donor binding energy and wavelengths of the bound exciton lines.

Impurity	E_D (eV)	E_D (eV) after Merz et al.	I_1 (Å)	I_1-1LO (Å)	I_2 (Å)
Aluminium	0.027	0.0263	4460	4510	4440
Indium	0.029	0.0289			
Chlorine	0.027	0.0269		4526	4440
Lithium	0.023 0.032		4472	4522	4442
undoped flow	0.031 0.032		4468	4518	4447
undoped, excess Zn	0.032 0.034		4464	4517	4442

seems reasonable to conclude that the same three acceptors can occur in all the crystals, with the possible exception of ZnSe:Li, where an acceptor with an ionization energy of 0.099 eV may be present. The various dopants all produce shallow donors with slightly different depths. In the undoped crystals a donor depth of 0.032 eV was found, which suggests that a native defect such as a selenium vacancy was responsible. The three acceptors would also seem to be associated with native defects.

It is interesting to compare our results with those of Dean and Merz (6) and of Merz, Nassau and Shiever (5). Dean and Merz were the first to observe the discrete line spectra in the edge emission of zinc selenide. They also observed two series of bands at 1.6 K, the zero-phonon components of which they labelled Q_o and R_o. The wavelength of Q_o was 4600 and of R_o 4575 Å, corresponding more or less to our bands S''_o and S'_o. Dean and Merz were of the opinion that the R_o band was the distant pair band associated with the discrete lines. In a reappraisal of this work, Merz, Nassau and Shiever questioned this conclusion. They observed two different sets of discrete pair lines, one of which they associated with Q_o, but the assignment of the second set (the original Dean and Merz lines) was unresolved. By studying lithium doped samples they were able to attribute the lines associated with Q_o with the acceptor Li. They then concluded that the ionization energy of the lithium acceptor was 0.114 eV. Our results suggest a value of 0.099 eV but it is interesting to note that the $S''_oN''_o$ pair of series is associated with an acceptor

with an ionization energy of 0.112 eV.

In attempting to draw some conclusions, one feature which should not be overlooked, is that whereas many samples showed two sets of S and N bands, these two sets were always composed of S_o and N_o with either S_o' and N_o' or S_o'' and N_o''. The two latter pairs of bands were never found together in the same sample. Now Bryant, Hagston and Radford (7) who studied the effects of radiation damage on the edge emission of cadmium sulphide found evidence for preferential pairing in crystals heated in sulphur vapour, whereas the pairing was random in samples heated in cadmium. The effect of this was that with samples heated in sulphur many close pairs were involved so that the Coulombic interaction term was large and the S bands were therefore displaced to shorter wavelengths compared with the corresponding bands in samples heated in cadmium. Thus although two pairs of series were involved they argued that only one acceptor was present. They also proposed that the N series was subject to a modified Coulombic interaction so that the N bands would also be displaced to shorter wavelengths in sulphur rich crystals. Our results are somewhat similar to those of Bryant et al. (7) if we consider the $S_o'N_o'$ and $S_o''N_o''$ pairs of bands. For example they never occur together. The shorter wavelength pair $S_o'N_o'$ was dominant in crystals grown in excess selenium, whereas on heating in liquid zinc, or in crystals grown in excess zinc, the $S_o''N_o''$ series appeared. It may be therefore that these two particular sets of series are in fact associated with one donor and one acceptor only, and

that preparation in excess selenium leads to preferential pairing of the donors and acceptors at near neighbour sites, whereas preparation in excess zinc leads to random pairing. Some evidence to support this suggestion can be seen in the curves of Figures 5.2 and 5.7. In Figure 5.2 the S_o'' band shifts appreciably to longer wavelengths as the excitation intensity is reduced. In contrast in Figure 5.7 the shift of the S_o' band is relatively small. If this latter band is associated with preferential pairs only a small shift would be expected since the recombination probability of the various different pairs would be very similar. This is not true for random pairs.

If this interpretation is correct then the three observed pairs of series are not associated with three acceptors but only with two, namely those with ionization energies of 0.112 and 0.122 eV. Furthermore the value of 0.099 eV for the ionization energy of the lithium acceptor would be in error because it was deduced from the N_o' series which is subject to a large Coulombic interaction from the neighbouring, preferentially paired donors.

Another question which is difficult to resolve is whether the bound exciton lines observed are associated with the same donors and acceptors involved in the pair emission process. The wavelengths of the I_1, I_1-1LO and I_2 lines found in the various crystals are also recorded in Table 5.5. In general the bound exciton lines are found in crystals grown by the flow-run technique and in those grown in excess zinc. No exciton lines were found in any crystal grown in excess selenium. There is no evidence therefore to associate any excitons at all with

the $S'_oN'_o$ series. This may be very reasonable if this particular pair of series only appears when preferential pairing occurs, since the proximity of a neighbouring defect may inhibit the formation of a localised exciton. It is interesting to note that Bryant et al. (7) also found the exciton emission to be very weak or non-existent in their samples which had been heated in excess sulphur.

The data recorded in Table 5.5 show that the I_2 line lay in the range 4440 to 4447 Å. It was very intense in the chlorine and lithium doped samples, which indicates the presence of many neutral donors, but there does not appear to be any correlation between the intensities of any of the pair bands and the strength of the I_2 line. In lithium doped material the intensity of the exciton emission was much stronger than that of the pair band emission but in most other crystals the reverse was true. Aluminium certainly diffuses into ZnSe with difficulty and the weak I_2 line may indicate that few neutral donors were present. The indium and gallium samples were heavily doped and no exciton emission was observed. This again supports the view that excitons cannot be formed at defects when other defects lie in the close vicinity.

One possibility which must be admitted is that all the samples may have been contaminated with the same residual impurity. It is well known that it is extremely difficult to remove the last traces of chlorine from II-VI compounds and it could be that most of the observed I_2 emission indicates the presence of chlorine. One reason for this suggestion derives from a consideration of the I_1

lines. Crystals doped with Al and Li had clearly defined I_1 lines with several phonon replicas. When the excitation intensity was reduced the relative intensity of the I_1-1LO replica increased, particularly in the aluminium doped samples, until it became the main feature of the I_1 spectrum. The I_1-1LO line lay in the wavelength range 4510-4522 Å. In the chlorine doped sample no I_1 line was detected but a strong exciton-like line was observed at 4526 Å. A similar feature was observed in many of the undoped samples which could well be evidence of contamination with chlorine. It is concluded that more evidence is needed before any firm conclusions can be drawn concerning the association of the bound exciton lines with the pair band emission.

Finally various broad bands were observed at lower energies which were found to be quite consistent with a complex centre as the origin of the characteristic emission of particular dopants in the crystals, so that the observed broad bands at about 6230, 5960 and 5890 Å are tentatively assigned to the characteristic emission of Al, In and Cl impurities at 10 K. In addition to these emissions, most of the doped crystals show a green self-activated emission band at 10 K with a maximum between 5470 and 5490 Å. It is believed that this emission is characteristic of samples doped with group III impurity elements. The self-activated emission at about 5460 Å in Al doped crystals may be associated with a free electron transition to an empty acceptor level.

CHAPTER 5

REFERENCES

1. J.L. Merz, H. Kukimoto, K. Nassau and J.W. Shiever Phys. Rev. B 6 (1972) 545
2. W.C. Holton, M. deWit and T.L. Estle, in "Phys. and Chem. of II-VI compounds" ed. M. Aven and J.S. Prener (N. Holland) 1967 Ch.9
3. M. Aven and R.F. Halsted, Phys. Rev. 137 (1965) A228
4. J.S. Prener and D.J. Weil, J. Electrochem. Soc. 106 (1959) 409
5. J.L. Merz, K. Nassau and J.W. Shiever to be published
6. P.J. Dean and J.L. Merz, Phys. Rev. 178 (1969) 1310
7. F.J. Bryant, W.E. Hagston and C.J. Radford, Proc. Roy. Soc. A323 (1971) 127

CHAPTER 6

COPPER AND MANGANESE DOPED CRYSTALS

6.1 Introduction

The emission properties of copper and manganese impurity in II-VI compounds have been investigated by several workers (1-9) and many different models have been proposed for the physical mechanisms of the luminescence transitions. However, the identification of the impurity states involved is still a matter of considerable debate and uncertainty.

The primary aim of this chapter is to describe some experimental information about the emission spectra of zinc selenide crystals deliberately doped with Cu^{++} or Mn^{++} halides or selenides, i.e. copper chloride, copper selenide, manganese chloride and manganese selenide. The emission of Cu doped crystals was blue, green or red, while the manganese doped crystals emitted in the green and orange-red. In this chapter the spectra of the copper doped crystals are described first. Then follows a description of the results obtained with the manganese doped samples and the results are compared with previously reported work. At the end of this chapter manganese doped crystals containing additional Al impurity are discussed. The reason for this is that crystals containing manganese and aluminium are used in the preparation of electro-luminescent Schottky diodes. The other optical properties of these crystals, i.e. their transmission, absorption and reflection will be discussed in the following chapter.

6.2 Copper selenide doped crystals

The emission spectra of two crystals doped with copper (CuSe, Zn) were studied under U.V. excitation at liquid nitrogen and helium temperatures. The results are very similar for both. The emission spectra of one (No.158) is shown at various temperatures in Figure 6.1. At 87 K, the spectrum consists of broad blue, green and red bands centred at 4535, 5290, 6250 Å with half widths of about 160, 385, and 430 Å respectively. At this temperature the intensity of the green emission band was at least an order of magnitude greater than the corresponding band in the undoped crystals, while the blue and red bands were rather weak. When the crystals were cooled to 65 K, the blue band was resolved into four sharp emission bands with maxima at 4462, 4512, 4565 and 4615 Å, which are attributed to I_1, I_1-1LO, I_1-2LO and S''_o respectively.

The blue emission spectra at 10 K are shown for several levels of excitation intensity in Figure 6.2. The first emission peak at the higher energy is at 4462 Å, with a shoulder at 4468 Å. These are I_1 lines. Below the I_1 line, two strong LO phonon replicas appear at 4515 and 4564 Å. The half width of the bound exciton lines is about 19 Å which is slightly broader than that observed in undoped crystals. The I_1 line did not shift on varying the excitation intensity and once again the I_1-1LO component became the dominant feature at low intensities. At lower energies than the bound exciton emission, a rather weak zero phonon component appeared at 4618 Å with a replica at 4670 Å. This zero phonon component is similar to the S''_o band, and

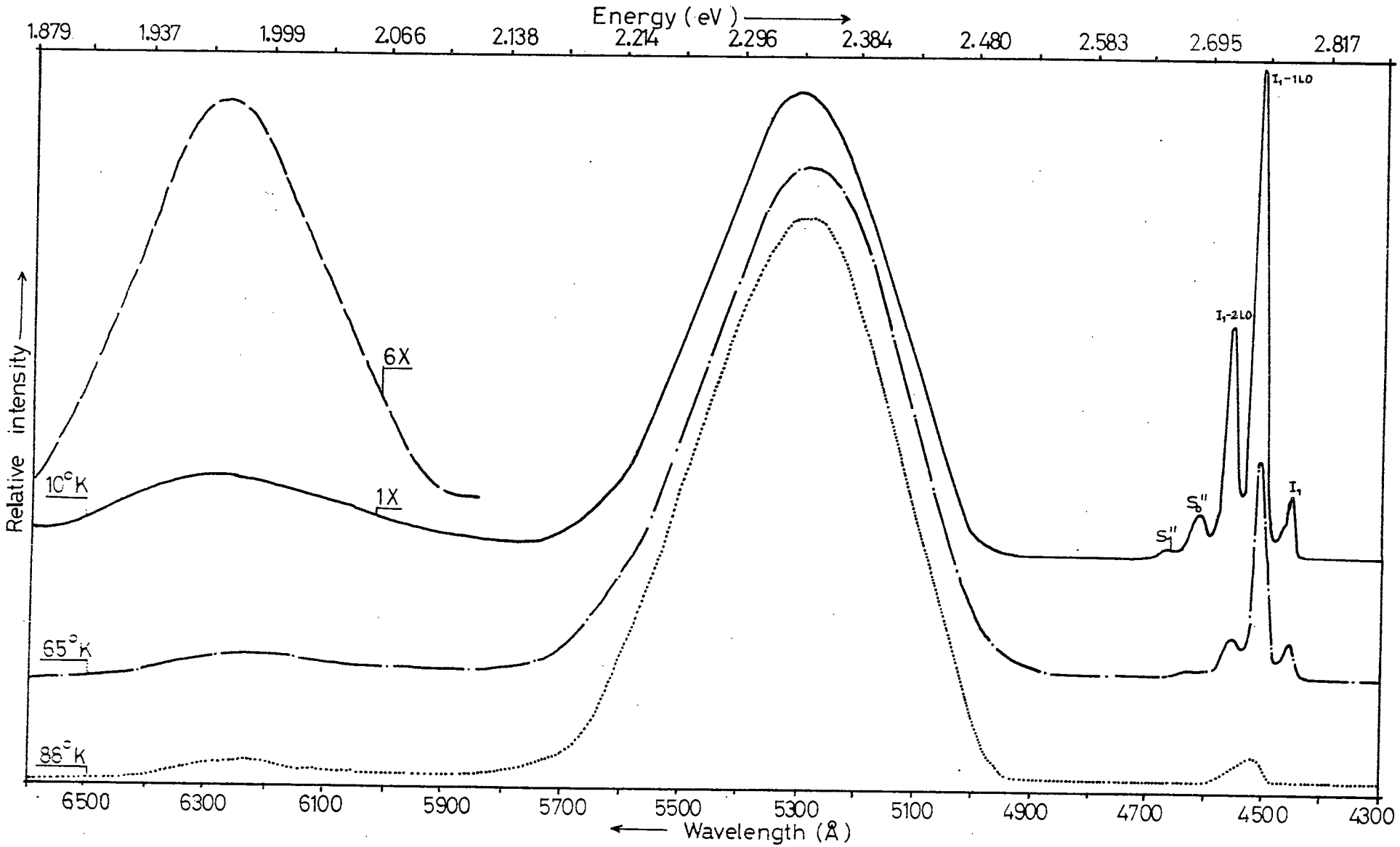

Figure 6.1 Emission spectra of (CuSe, Zn) doped ZnSe crystal No. 158 at three different temperatures.

once again it was observed in a crystal grown in excess zinc. Note however that the corresponding N''_O component was not observed at 65 K. At that temperature the zero phonon band also lay at 4618 Å. The low intensity of the S''_O series may be explained in terms of substitutional copper reducing the incidence of native acceptors. However the intensity of the blue emission indicates that the copper concentration was not too high.

At 10 K, the strong broad green band has a maximum at 5300 Å and the weak broad red band is centred at 6290 Å. These emission bands are very similar to bands previously reported in the green at 5300 Å and the red 6300 Å in ZnSe:Cu crystals (1, 2, 3, 4). The green emission band did not shift with variation of excitation intensity while the red emission band shifted to longer wavelengths with reduction in intensity of excitation. The absence of a shift in the position of the green band with excitation intensity, and the rather small shift of about 10 Å (which is due to the temperature dependence of the band gap) with increasing temperature, can be explained in terms of recombination between free electrons and holes bound at copper acceptors. This mechanism is consistent with the model proposed by Stringfellow and Bube (2, 3) of free-to-bound recombination at a multivalent copper impurity model. Using a value of the energy gap of 2.818 eV the corresponding level of the acceptor centre is found to be 0.474 eV above the valence band.

The shift of the red emission band with decreasing excitation intensity is characteristic of donor-acceptor

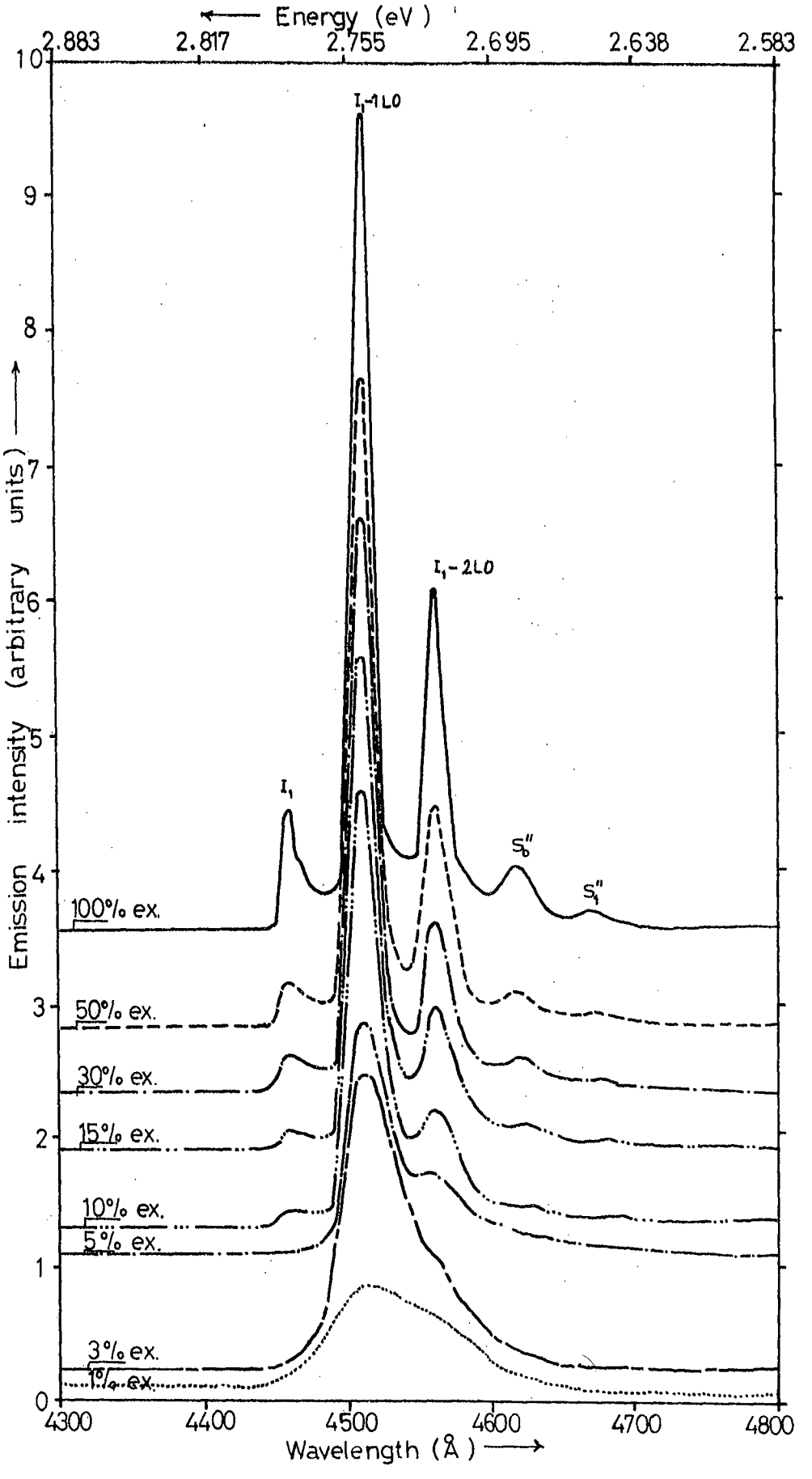

Figure 6.2 The blue emission spectra of (CuSe, Zn) doped ZnSe crystal No. 158 recorded at 10°K for several levels of excitation intensity.

pair emission. A similar shift of the red emission band to shorter wavelengths with increasing excitation intensity has been reported by Stringfellow and Bube (3, 4), and explained in terms of a donor acceptor pair model. Taking the value of 1.971 eV as the observed photon energy from the red band (at 6250 Å) at 88 K, the second acceptor ionisation energy was found to be 0.829 eV. This is close to the value of 0.72 eV reported by Stringfellow and Bube (3, 4) from their photoconductivity measurements. The energy difference between the observed red emission at 88 and 10 K, indicates the presence of a shallow donor level with an apparent depthof 0.013 eV below the conduction band. Using this energy with a correction factor of 0.014 eV for the Coulomb interaction, the donor binding energy becomes 0.032 eV. This is remarkably similar to the donor binding energy of 0.032 eV determined from the differences between the HES and LES emission bands in undoped crystals grown with zinc reservoir. The suggestion is therefore that a native donor is involved in the red emission band and also with the appearance of the LES at 4618 Å (S''_o undoped crystals).

6.3 Copper Chloride doped crystals

Only one ($CuCl_2$, Zn) doped crystal was studied. Unfortunately no measurements were made at liquid helium temperature and as is shown in Figure 6.3 the emission spectrum at 88 K consisted of broad green, yellow and red emission bands with maxima at 5260, 5830 and 6250 Å. No edge emission or other emission bands were detected at 65 K.

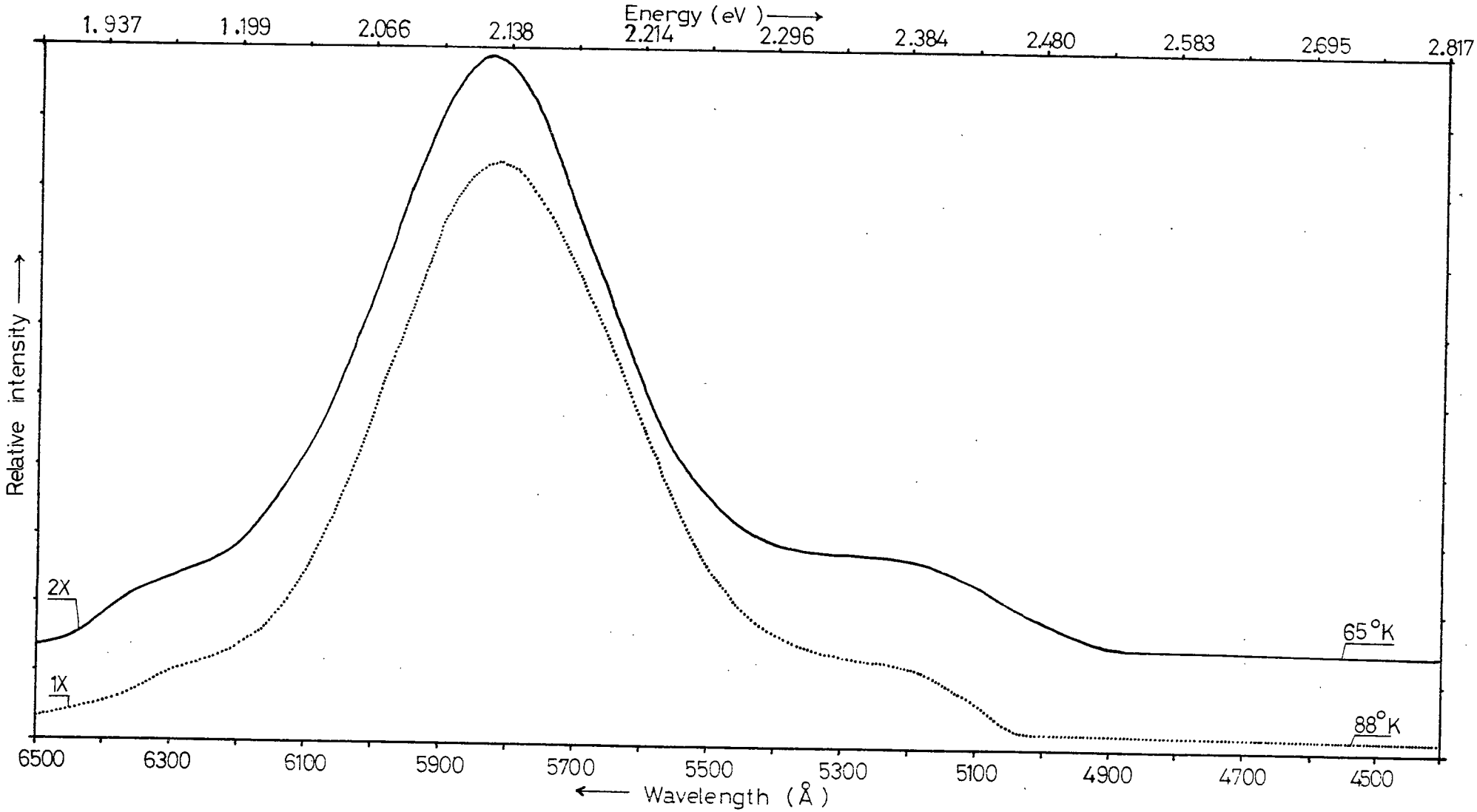

Figure 6.3 Emission spectra of ($CuCl_2$, Zn) doped ZnSe crystal No.136 at two different temperatures.

At 65 K the observed green emission band at 5260 Å is rather flat. It is suggested that two different emission bands are in fact involved namely a green copper emission at 5290 Å and a self-activated emission at 5480 Å. The last self-activated emission band is rather similar to the green emission band observed in (Cl, Zn) doped crystals. The broad yellow emission band at 5840 Å dominated the spectrum with the red emission band as a small shoulder. The yellow emission band is presumably the characteristic band for chlorine as observed in chlorine doped crystals grown with zinc reservoirs. However Iida (4) found a yellow emission band at 5700 Å in copper doped crystals which he attributed to a donor-copper acceptor pair mechanism. Nevertheless the differences in the spectral emission and absence of the yellow emission in our (CuSe, Zn) doped crystals is strong evidence that the observed yellow emission is not associated with copper. We attribute the yellow band to chlorine and the red and green bands to the two different levels of substitutional copper.

6.4 Manganese doped crystals

Numerous manganese, $MnCl_2$ and MnSe doped crystals were studied to identify the photo-luminescence emission band associated with substitutional manganese. The first study was made on flow-run crystals doped with manganese metal and the emission spectrum of a (Mn, flow-run) sample is shown in Figure 6.4. This emission spectrum consisted of phonon assisted edge emission in the blue and two broad emission bands in the green and red. At 65 K the edge

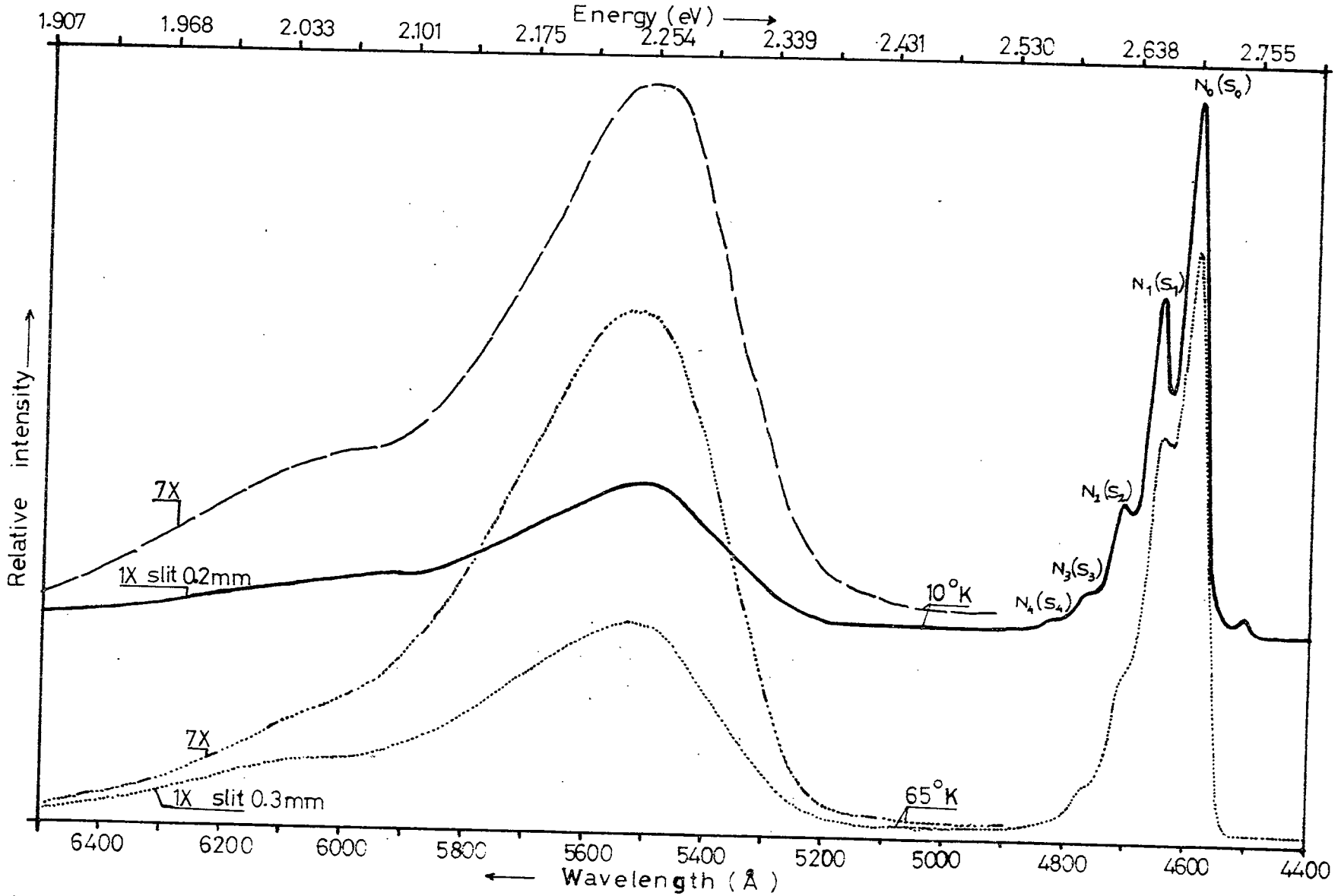

Figure 6.4 Emission spectra of manganese metal doped flow-run crystal at two different temperatures.

emission exhibited five poorly resolved peaks with maxima at 4604, 4656, 4710, 4770 and 4828 Å which were similar to the N_o series in undoped flow-run crystals. The green emission band at 5560 Å was rather strong and dominated the spectrum while a red emission band at approximately 6100 Å appeared as a shoulder on the longer wavelength side of the green band.

The intensity of the various emissions increased with decreasing temperature and the edge emission spectrum exhibited well developed structure at 10 K. However the increase in intensity was at least an order of magnitude less than that in the undoped crystals. It is also surprising that this well developed phonon assisted emission did not show much displacement in wavelength from the corresponding position at 85 K. The five major bands were located at 4608, 4660, 4714, 4772 and 4830 Å and may have been members of the N_o or S''_o series. However the zero phonon component (at 4608 Å) shifted with variation of excitation intensity by about 15 Å when the excitation intensity was decreased by two orders of magnitude which suggests that we are observing an S series at both temperatures. A similar situation was observed with the copper doped samples.

The strongest broad peak at 10 K is the green band located at 5548 Å which is believed to be a self-activated emission. This band is similar to that observed in undoped crystals and attributed to a free-to-bound recombination mechanism because no shift was observed with variation in excitation intensity. On the lower energy

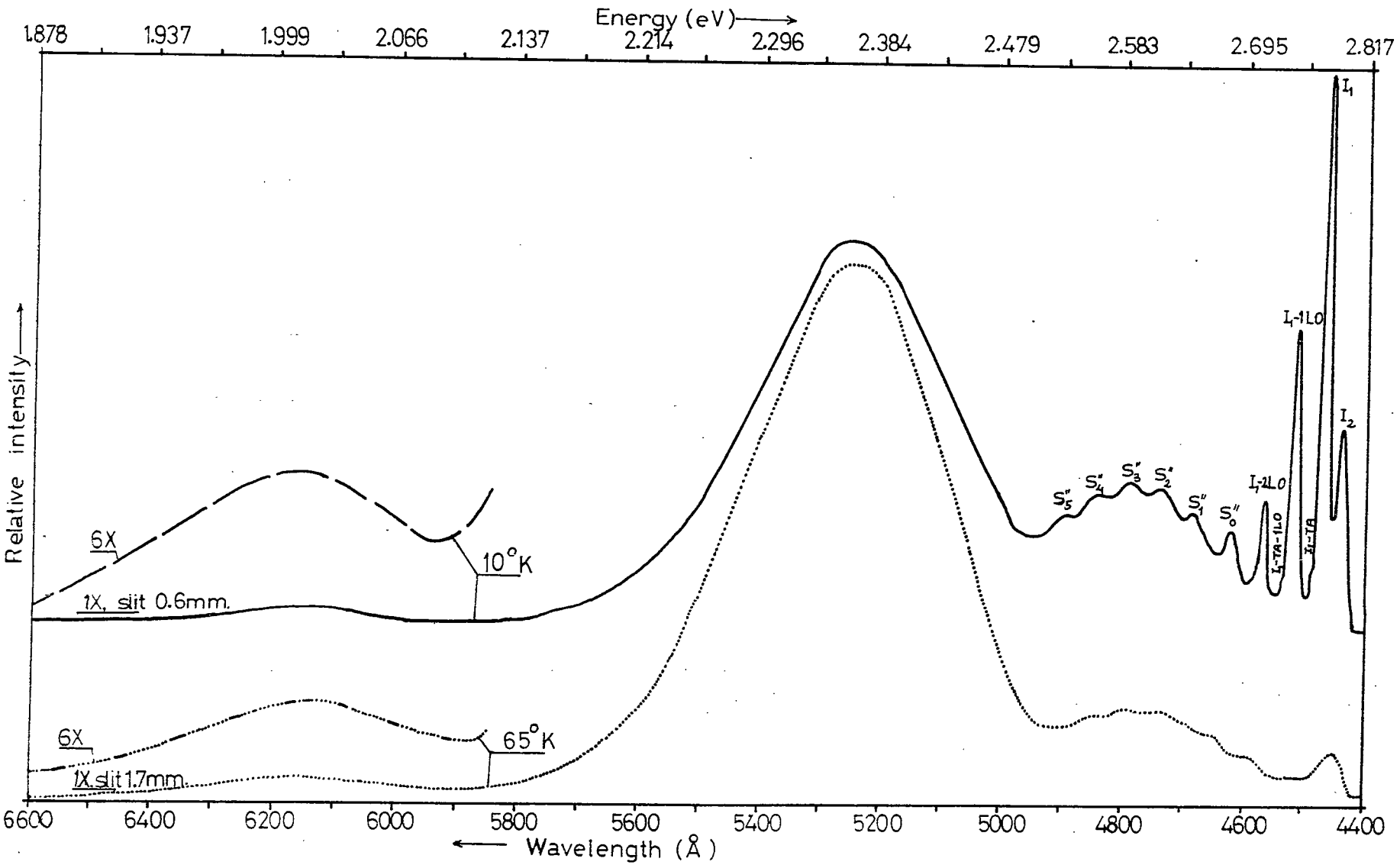

Figure 6.5 Emission spectra of (MnSe, Zn) doped ZnSe crystal No.141 at two different temperatures.

side of the green emission band there was a broad red emission band at 6060 Å with a half width of approximately 630 Å. It is important to note that this broad red emission band was not found in the undoped or any other doped ZnSe crystals, so that, this band is tentatively attributed to the characteristic emission of 3d shell transitions in the Mn^{++} ion. However, it is very difficult to make any unambiguous statements about the identification of this emission because the broad nature of the emission makes precise measurements very difficult, and confusion with other impurity bands, for example the self-activated, red-copper, silver, aluminium, chlorine emission bands is quite possible.

It should be noted that according to reports in the literature the self-activated emission band lies in the vicinity of the manganese band. Previously reported values for the self-activated emission in zinc selenide range from 6020 to 6450 Å (5,6). Very recently a value of 6150 Å was reported by Jones and Woods (7) which is very close to the red manganese band observed in the present work. In comparison with Mn^{++} in ZnS there are relatively few published reports of the luminescent properties of ZnSe:Mn. According to Asano et al. (8) ZnSe:Mn has a band centred at about 6450 Å at 300 K, which shifts to 6200 Å or thereabouts at 80 K. The results of Apperson et al. (9) appear to indicate a band with its maximum at 6350 Å at both 291 and 90 K. Under U.V. excitation an emission band was found by Jones and Woods (7) at 6550 Å at 293 K and 6250 Å at 85 K. The half widths of the

various bands were about 900 Å at 80 K (8), 700 Å at 90 K (9) and 1000 Å at 85 K (7) which are much broader than that of the red band reported here.

6.5 Manganese Selenide doped crystals

Manganese Selenide was incorporated into ZnSe by two different methods and (MnSe, flow-run) and (MnSe, Zn) crystals were studied under U.V. excitation at various temperatures. The emission spectrum of (MnSe, flow-run) crystals consists of a strong blue and two weak green bands. At 65 K, the weak green emission bands were located at 5230 and 5460 Å in the (MnSe, flow-run) crystals and the strong blue emission contained three poorly resolved edge emission bands at about 4608, 4660 and 4714 Å which are similar to the N_o series of the undoped crystals. No red and bound exciton emission was observed at 65 K and unfortunately measurements were not made at 10 K for this crystal.

As is shown in Figure 6.5 the green and red emission bands in the (MnSe, Zn) crystal were centred at about 5230 and 6140 Å and two blue emission bands appeared at 4790 and 4450 Å at 65 K. At 10 K the green and red emission bands were at 5235 and 6180 Å, and the blue bands were resolved into a number of narrow bands and sharp lines. The assignment of the narrow bands is indicated in Figure 6.5 as S''_o, S''_1....S''_6 and the sharp lines are I_2, I_1, I_1-TA, I_1-1LO, I_1-1LO-TA and I_1-2LO. The emission maxima of S''_o, I_1 and I_2 occurred at about 4618, 4463 and 4442 Å respectively. This spectrum is essentially similar

to that observed in the edge emission of undoped crystals grown with zinc reservoirs. The broad green emission is also centred at the same wavelengths as in undoped crystals grown with zinc reservoirs so that it is attributed to the self-activated emission.

As seen from Figure 6.5 the red band shifts to longer wavelengths with decreasing temperatures. A shift in this direction has been reported for the self-activated band in ZnS (10) and ZnSe (11). It is reasonable to conclude that no manganese entered the crystals from the MnSe and the red emission band at 6180 Å is therefore attributed to the self-activated red emission in ZnSe. This is close to the recently reported (7) value of 6150 Å for self-activated emission in ZnSe.

6.6 Manganese chloride doped crystals

Three different manganese chloride doped crystals were studied. Of these two Nos.163 and 222 ($MnCl_2$, Zn) were grown by the usual method with a zinc reservoir while the third No.213 ($MnCl_2$+Mn) was grown by placing $MnCl_2$ in the zinc reservoir and manganese metal in the charge. These two different crystal growth methods led to two very different concentrations of manganese in the crystals. A low concentration of 20-50 p.p.m. was achieved with the ($MnCl_2$, Zn) samples, while a high concentration of 2000 p.p.m. was obtained in the ($MnCl_2$+Mn) sample.

Figure 6.6 shows the emission spectra of three samples at 65 and 10 K. The spectra of samples No.163 and 222 containing a low concentration of manganese consisted of broad blue, green, yellow and red emission bands

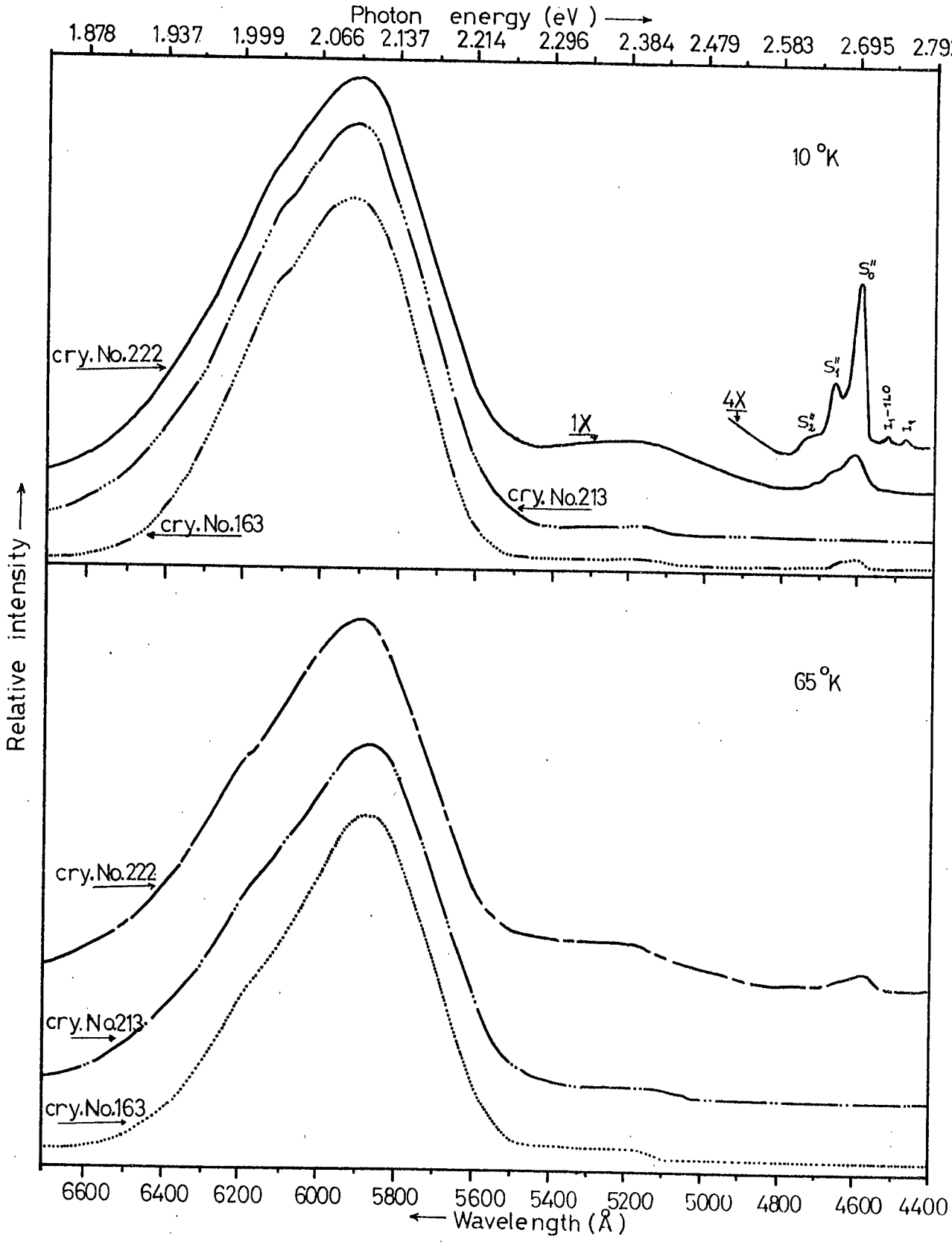

Figure 6.6 Emission spectra of ($MnCl_2$,Zn) and ($MnCl_2$:Mn) doped crystals at two different temperatures.

located at 4590, 5220, 5860 and 6160 Å at 65 K. With the exception of the blue and red emissions, the bands shifted to longer wavelengths with decreasing temperature and the green and yellow emission bands were centred at about 5230 and 5890 Å at 10 K. These weak green and strong yellow emission bands were very similar to the self-activated and characteristic yellow chlorine bands observed in chlorine doped crystals, so that these bands may well be attributable to the self-activated and characteristic chlorine emission. The red emission band appeared as a shoulder on the longer wavelength side of the yellow emission and shifted to shorter wavelengths with decreasing temperature and was located at 6090 Å at 10 K. This red emission band is similar to that of the (Mn, flow-run) crystals and is attributed to the characteristic manganese emission in ZnSe. At 10 K the blue emission was resolved into five rather weak emission bands at about 4465, 4514, 4610, 4664 and 4720 Å in crystal No.222. These bands are attributed to I_1, I_1-1LO, S_o'', S_1'' and S_2''. However the blue band was not observed at 65 K in crystal No.163 and only a broad blue emission centred at 4612 Å was observed at 10 K. This may be due to a higher manganese concentration in the second crystal.

The spectrum of the sample containing a high concentration of manganese was approximately the same as those of the ($MnCl_2$, Zn) samples but no blue edge emission was observed even at the highest excitation and the lowest temperatures. Once again the donor-acceptor pair emission was quenched in a heavily doped sample.

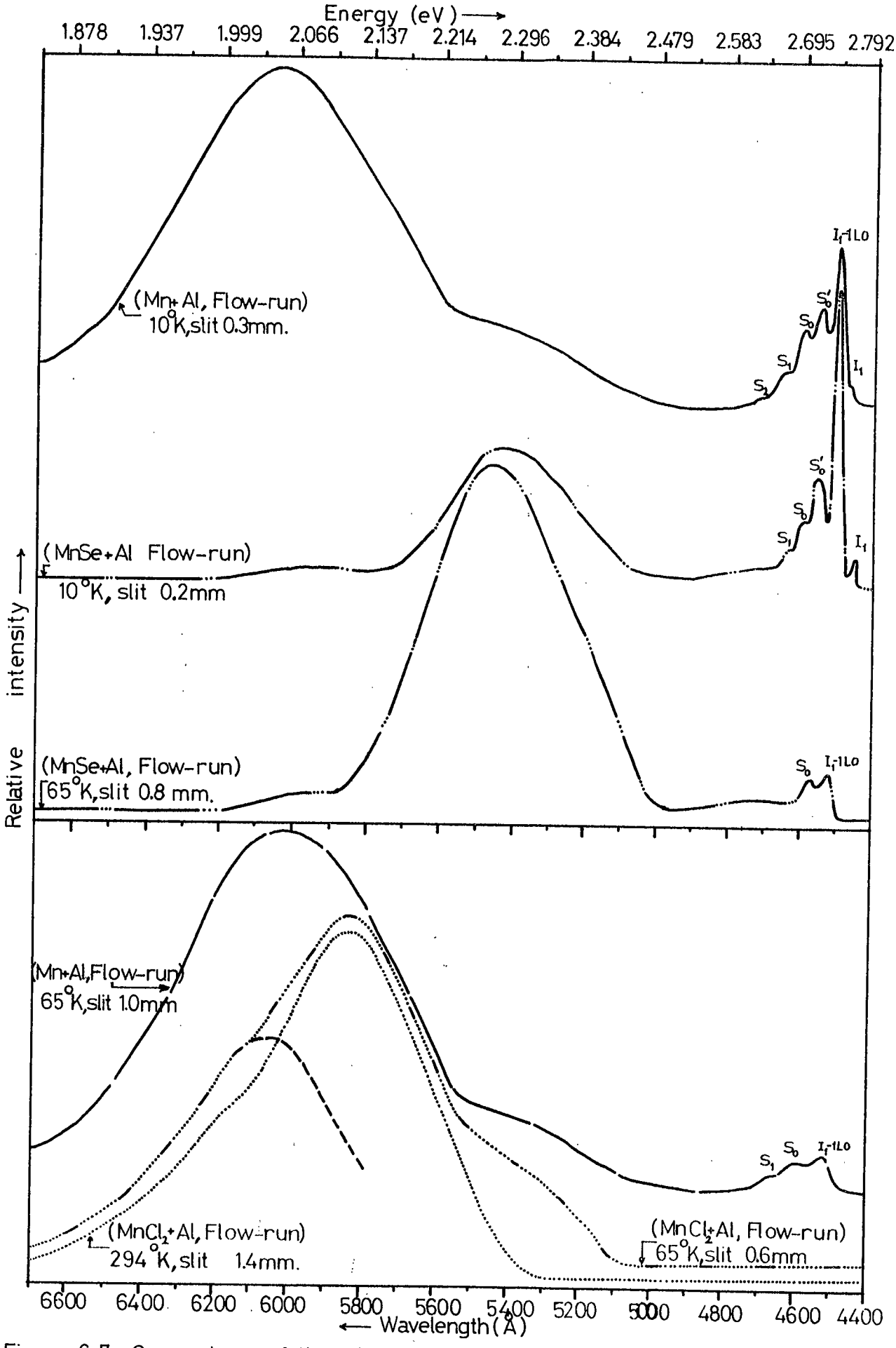

Figure 6.7 Comparison of the observed emission spectra of the manganese and aluminium doped flow-run crystals at two different temperatures.

Examination of Figure 6.6 shows that the emission of sample No.213 consists of the characteristic manganese band in the red and that due to self-activated chlorine in the yellow. The red band at about 6060 Å appears at shorter wavelengths than the corresponding feature in the ($MnCl_2$, Zn) crystals, so that there is a difference of about 30 Å between the positions of the bands which is probably due to the high concentration of manganese in crystal No.213. Such a shift was reported by Asano et al. (8) with increasing manganese concentration in their Zn(S:Se):Mn crystals. Therefore, once again it is reasonable to assume that the band at 6060 Å is associated with manganese.

Sample No.213 was also examined after it had been heated in liquid zinc at 850°C for 15 days. Following this treatment the emission was almost identical to that of chlorine doped samples, but no bound exciton and edge emission bands were observed. These results could be interpreted as indicating that the heating in zinc removed the manganese from the crystal. On the other hand optical absorption measurements have been made for this crystal (see Chapter 7) and the same three absorption bands associated with manganese were found before and after the heating in liquid zinc. This shows that the manganese impurity content was not reduced by heating in liquid zinc, which is known to remove copper and other impurities from ZnSe (12). The failure to observe the characteristic Mn^{++} emission in samples heated in liquid zinc is associated with the onset of competing Auger processes in the highly conducting ZnSe (7).

TABLE 6.1

The position of the emission maxima of Figure 6.7 and their assignment

Observed spectrum at 10 K				Observed spectrum at 65 K			
Lines	Wave-Length (Å)	Energy (eV)	Possible Assignment	Lines	Wave-Length (Å)	Energy (eV)	Possible Assignment
(Mn+Al, flow-run) crystal							
I_1	4462	2.77882	Exciton bound to a neutral acceptor				
I_1'	4510	2.74924	I_1-1LO	I_1'	4511	2.74864	I_1-1LO
S_o'	4578	2.70841	Zero-phonon	S_o'	4576	2.70959	Zero phonon LES
S_o	4628	2.67915	Zero-phonon	S_o	4624	2.68147	Zero phonon LES
S_1	4680	2.64938	One phonon	S_1	4678	2.65051	Zero phonon LES
S_2	4734	2.61916	Two phonon	S_2	4732	2.62027	Zero phonon LES
Broad	5466	2.26840	Self-activated emission	Broad	5460	2.27090	Self-activated emission
Broad	6080	2.03932	Mn+Al emission (?)	Broad	6060	2.04605	Mn+Al emission (?)
(MnSe+Al, flow-run) crystal							
I_1	4460	2.78007	Exciton bound to neutral acceptor				
I_1'	4510	2.74924	I_1-1LO	I_1'	4510	2.74924	I_1-1LO
S_o'	4576	2.70959	Zero phonon	N_o'	4560	2.71910	Zero phonon
S_o	4625	2.68089	Zero phonon	N_o	4608	2.69078	Zero phonon
S_1	4680	2.64938	One phonon				
Broad	5460	2.27090	Self-activated green emission	Broad	4720	2.62693	Edge emission
Broad	6040	2.05283	Mn+Al emission (?)	Broad	5450	2.27506	Self-activated green emission
				Broad	6040	2.05283	Mn+Al emission (?)
($MnCl_2$+Al, flow-run) crystal							
				Broad	5440	2.27925	Self-activated emission
				Broad	5860	2.08039	Cl emission
				Broad	6120	2.02600	Mn+Al emission (?)

6.7 Crystals doped with manganese and aluminium

Three different types of crystal were examined, in which Mn+Al, MnSe+Al and $MnCl_2$+Al had been added during growth by the flow-run method. Figure 6.7 shows the observed emission spectra of typical crystals at two different temperatures. The wavelengths and energies of the various features are recorded in Table 6.1. In general the emission of all these crystals consisted of green and red bands, and except for the ($MnCl_2$+Al, flow-run) sample, the blue edge emission was easily detectable.

The emission of the (Mn+Al, flow-run) crystal shown in Figure 6.7, contains an intense red and a weak green band at about 6080 and 5466 Å. The bound exciton and edge emission bands were well developed and appeared at shorter wavelengths at 10 K. The bound exciton and edge emission peaks were essentially similar to those of undoped flow-run crystals, with I_1, I_1-1LO, S_o' and S_o prominant. See Figure 6.7 and Table 6.1. However the I_1 line was not observed at 65 K, but once again a strong I_1-1LO phonon assisted line was detected. The zero phonon pair band components observed at 65 K were S_o' and S_o rather than N_o' and N_o.

The curves in Figure 6.7 reveal that the (MnSe+Al, flow-run) crystal shows similar emission bands at much the same wavelengths except that the relative intensities of the broad green and red emissions are opposite to those of the same bands in the (Mn+Al, flow-run) sample. This suggests that the manganese concentration is higher in the (Mn+Al, flow-run) crystal, and

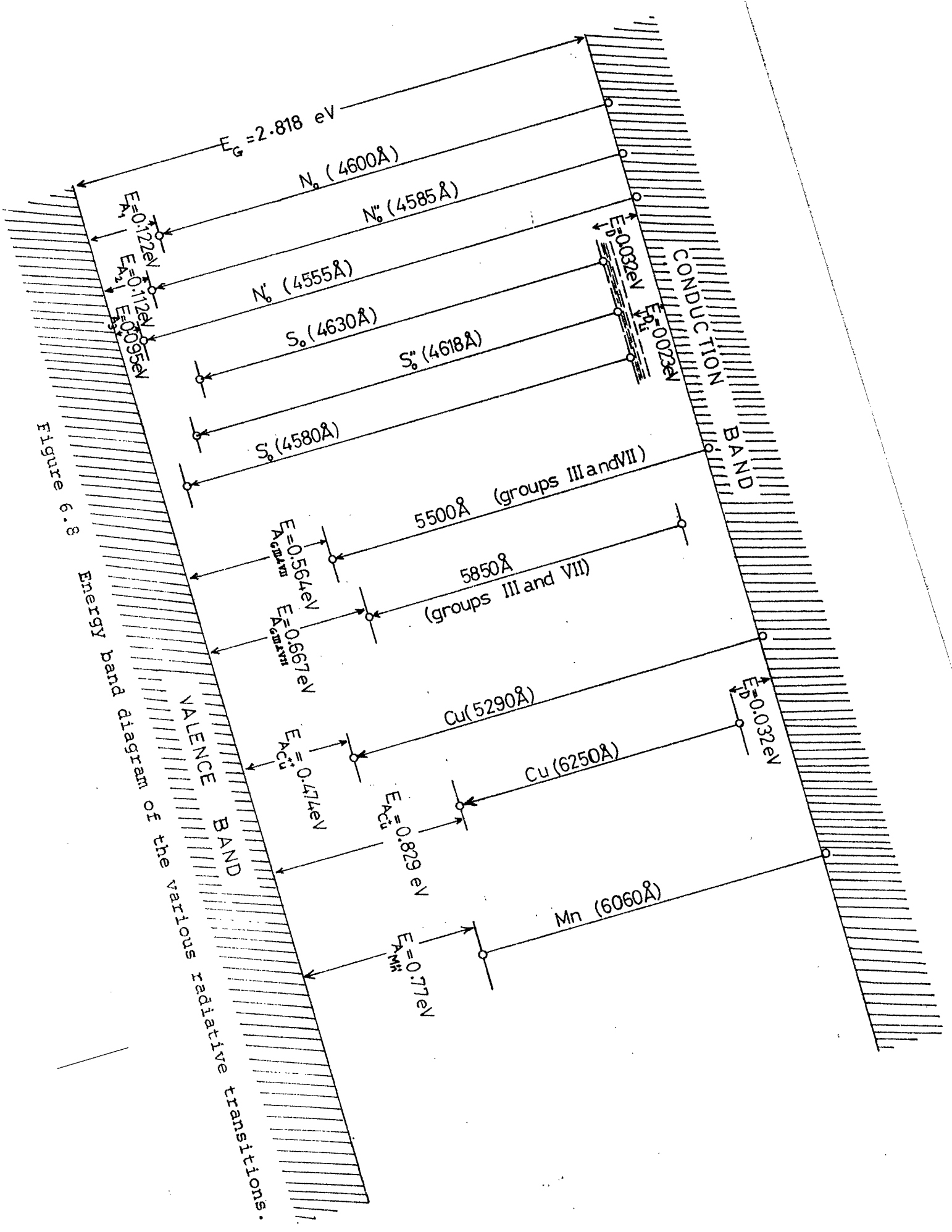

Figure 6.8 Energy band diagram of the various radiative transitions.

rather low in (MnSe+Al, flow-run) sample.

With the ($MnCl_2$+Al, flow-run) crystal, no edge emission bands were observed at 65 K and unfortunately no liquid helium measurements were made. Once again the addition of chlorine led to a characteristic broad yellow chlorine emission at 5860 Å while the manganese and aluminium impurities gave rise to a long tail extending into the red. A small shoulder appeared at about 6200 Å in the tail of the yellow emission at 296 K. This shoulder shifted to shorter wavelengths with decreasing temperature and was located at 6120 Å at 10 K. This result suggests that the band giving rise to this shoulder may not be the self-activated red emission. In fact when the red band was drawn by extrapolation (see Figure 6.7) it was found to be very similar to the red band emitted by the (Mn+Al, flow-run) sample. It is therefore reasonable to assume that the shoulder at 6120 Å is due to complex centre of manganese and aluminium ions in very close association.

6.8 Discussion

The deliberate introduction of copper or manganese impurity in any appreciable concentration quenches the bound exciton and edge emissions so that only deep centre luminescence remains. Several closely neighbouring bands have been observed in both the green and the red and although it is possible to assign some of the bands to particular luminescent centres it is by no means possible to explain all the broad bands observed. The wavelengths of the various bands are recorded in Table 6.2, and an energy band diagram depicting all the radiative transitions discussed in this thesis is shown in Figure 6.8.

TABLE 6.2

The features of the emission characteristics illustrated in the figures of Chapters 5 and 6

Sample	Temperature ^{o}K	Deep centre emission			Bound exciton emission	Zero phonon assisted emission
		Green	Yellow	Red		
CuSe,Zn	87	5290		6250		
	65	5290		6265		
	10	5300 (E_A=0.474eV)		6290 (E_D=0.032eV) (E_A=0.829eV)	4462 (I_1) 4468 (I_1)	4618 (S''_o)
$CuCl_2$,Zn	88	5260	5820	6240		
	65	5260 5290 (Cu) 5480	5840 (Cl)	6250 (Cu)	None	None
Mn,flow-run	65	5560 (SA)		6100 (Mn)		4604 (S''_o)
	10	5548 (SA)		6060 (Mn)	None	4608 (S''_o)
MnSe,flow-run	65	5230 (SA) 5460		None	None	None
MnSe,Zn	65	5230 (SA) [No Mn enters the crys. & spectrum similar to undoped.]		6140 (SA)		
	10	5235 (SA)		6180 (SA)	4463 (I_1), 4442 (I_2)	4618 (S''_o)
$MnCl_2$,Zn	65	5220 (SA)	5860 (Cl)	6160 (Mn)		4590 (N''_o)
	10	5230 (SA)	5890 (Cl)	6090 (Mn)	4463 (I_1)	4610 (S''_o)
$MnCl_2$,Mn	65	5230 (SA)	5860 (Cl)	6160 (Mn)		
	10	5235 (SA)	5890 (Cl)	6060 (Mn)	None	None

Continued on next page

Table 6.2 (continued)

Sample	Temperature °K	Deep centre emission			Bound exciton emission	Zero phonon assisted emission
		Green	Yellow	Red		
$MnCl_2$+Mn (after heated zinc)	10	5230(SA)	5890(Cl)	None	None	None
Mn+Al flow-run	10	5466(G3)		6080	4462(I_1)	4578(S_o') 4628(S_o)
MnSe+Al flow-run	10	5460(G3)		6040	4460(I_1)	4576(S_o') 4625(S_o)
$MnCl_2$+Al flow-run	65	5440(G3)	5860(Cl)	6120	None	None
Al,flow-run	10	5430(G3)		6100	None	None
Al,Zn	10	5460(G3)		6230(Al)	4460(I_1),4440(I_2)	4608(S_o'')
Ga,Zn	65	5490(G3)	5830(Ga)		None	None
In,flow-run	10	5490(G3)	5960(In)		None	4625(S_o)
In,Zn	10	5500(G3)	None			4610(S_o'')
Cl,flow-run	65	5480	Long tail			4557(N_o') 4600(N_o)
	10	5490	5880(Cl)		4440(I_2)	4578(S_o') 4628(S_o)
Cl,Zn	65	5480	5870(Cl)			4585(N_o'')
	10	5490	5890(Cl)			4605(S_o'')

The work on the photoluminescence of the copper doped crystals indicates that the green (5290 Å) and red (6250 Å) bands are due to substitutional copper. From the experimental observation of the effects of varying the excitation intensity the green emission is attributed to a transition between an electron at the bottom of the conduction band and the Cu^{++} level, while the red emission is considered to be a transition from a donor level to the different Cu^{+} level. The donor level has been calculated to lie at about 0.013 eV below the conduction band and after using the correction factor for the coulombic interaction the binding energy becomes 0.032 eV, which is identical with that reported earlier in this thesis for native donors which are presumably selenium vacancies. The copper acceptor levels calculated from the photon energies of the green and red emission are some 0.47 and 0.83 eV above the valence band respectively. Stringfellow and Bube (2,3) also proposed a model involving multivalent copper to account for these two emissions and their results are in excellent agreement with those reported here. However they used a different value of the energy gap and consequently found values of 0.35 and 0.72 eV for the copper acceptor levels and 0.012 eV for the donor level.

With copper doped crystals edge emission was only observed in the samples grown in the presence of copper selenide. When copper chloride was used no edge emission was found. Fairly clearly the use of copper selenide with its low vapour pressure leads to a lightly

doped sample whereas copper chloride has a higher vapour pressure so that more copper would be incorporated. At the same time copper would be incorporated more readily in the presence of chlorine when charge compensation would occur. The bound exciton emission, i.e. the I_1, I_1-1LO and I_1-2LO, lines in the (CuSe, Zn) crystal was very intense and similar to that in the undoped samples grown in excess zinc. On the other hand the zero phonon pair band S_o'' was weak and only just detectable. Once again there appears to be no correlation between the intensity of the I_1 lines and the distant pair emission. A reasonable hypothesis would be that the I_1 line at 4462 Å is associated with substitutional copper whereas the distant pair bands are associated with native acceptors. All the I_1 lines observed in all the samples examined lay within 3 Å of 4462 Å except in the sample doped with lithium where the I_1 line was detected at 4472 Å. Since copper and lithium were the only acceptors to be used during this work it seems reasonably to suggest that in fact only two different I_1 lines have been observed. It is well known that copper is a residual contaminant which it is difficult to remove from II-VI compounds. It could well be that the observation of an emission line at 4462 Å indicates the presence of this contaminant in many of our samples.

The weak LES of distant pair bands in the copper doped sample was again identical to the S_o'' series which is typical of samples grown in excess zinc. The corresponding high energy N_o'' series was not detected at 65 K. This may be the result of the presence of other

free-to-bound recombination routes in a crystal deliberately doped with an acceptor impurity such as copper. To resolve such an issue it would be necessary to measure the response times of the various emissions.

One obvious difference in the observed emission spectra of the (CuSe, Zn) and ($CuCl_2$, Zn) crystals (see Figures 6.1 and 6.3), was that an intense yellow band was observed in the ($CuCl_2$, Zn) samples. This emission is attributed to the characteristic chlorine self-activated emission. An identical emission band was observed in the ($MnCl_2$, Zn) and ($MnCl_2$+Al, flow-run) crystals (see Figures 6.6 and 6.7) which did not appear in other manganese-doped samples when chlorine was not used. The work on samples doped with chlorine only, which was described in the preceding chapter, showed that the band characteristic of chlorine was centred at 5890 Å. There can be little doubt therefore that a yellow band at 5840 Å is characteristic of chlorine.

One of the major subsidiary interests in this work was to try and determine the spectral position of the characteristic manganese emission and at the same time to find a satisfactory way of introducing substitutional Mn^{++} in the ZnSe. The results recorded in Table 6.2 allow us to conclude that Mn^{++} leads to a characteristic emission band centred at 6040-6060 Å. Little manganese was incorporated when attempts were made to introduce the dopant via manganese selenide. Thus when manganese selenide was used in the flow process or in the sealed capsule with an excess of zinc, no band at 6060 Å was observed. A band

in the red at 6180 Å was observed, particularly in the samples grown in excess zinc with MnSe added, but the spectral shift of this band with temperature indicates that it is a self-activated emission.

The most satisfactory way of introducing manganese was to use manganese chloride. Atomic absorption spectroscopy showed that up to 2000 p.p.m. were incorporated in a crystal grown in a sealed capsule from a charge of ZnSe plus metallic Mn while the reservoir contained $MnCl_2$. This is the sample designated ($MnCl_2$+Mn). These crystals showed the characteristic manganese emission but the yellow emission at 5890 Å associated with chlorine was much more intense.

When aluminium was used in conjunction with manganese or manganese compounds in the flow process the resultant crystals emitted in the characteristic manganese band. No yellow band was detected except in the sample where manganese chloride had been used during growth. However in each of the three types of sample containing manganese and aluminium a green band was observed at about 5450 Å. This is very probably a band characteristic of aluminium. Many different green bands have been observed in the course of this work but one quite notable feature is that a band near 5490 Å has been observed in all crystals doped with group III impurities, i.e. Al, In and Ga. It is difficult to be certain of how many green bands there are but undoubtedly a band near 5300 Å is characteristic of copper and one at 5490 Å indicates a group III impurity.

It is questionable whether there is any great benefit to be derived from speculating on the atomic nature of the centres responsible for the various luminescent transitions reported in this thesis. However, for completeness some remarks are necessary, see also Figure 6.8.

A study of the wavelengths of the various broad bands listed in Table 6.2 shows that the bands can be divided roughly into four groups. Thus there are two groups of green bands; in one group the wavelengths lie between 5200 and 5300 Å and in the other the wavelengths range from 5450 to 5500 Å. There is also a yellow group with wavelengths from 5820 to 5900 Å and a red group with wavelengths between 6040 and 6230 Å.

From the results reported here it seems reasonable to assert that copper is associated with a green band at 5290 Å and a red one at 6250 Å. It might be reasonable to assume that most of our samples were contaminated with copper and that this could account for the band at 5230 Å observed in many samples not deliberately doped with copper. However this seems unlikely for two reasons:-

(1) The spectral position of the copper green band did not shift when the intensity of the excitation was varied, whereas a definite shift was detected with the band at 5230 Å.

(2) All the samples doped with Al, In, Ga or Cl failed to show the 5230 Å green band. We conclude that this band is different from the copper one and in fact that there are at least three green bands since every sample deliberately doped with a group III impurity or

chlorine had a green emission at about 5480 Å.

Referring back to Chapter 4 it will be recalled that undoped crystals grown in excess zinc exhibited a green band at 5230 Å whereas those grown in excess selenium had a green band at 5560 Å. Assuming no contaminating impurities are involved there are either two quite different native acceptors present or alternatively some different complexes of the basic point defects are formed depending on the atmosphere during growth.

Since a green band at about 5500 Å is found both in undoped samples grown in excess selenium and in samples doped with the elements of groups III and VII it is tempting to assume that this band indicates the presence of zinc vacancies. Simple arguments based on the principle of charge compensation require that zinc vacancies are produced when ZnSe is heated in excess Se or when In^{+++} or Cl^{-} ions are substituted. The band at 5500 Å would then be explained in terms of a transition in which a free electron in the conduction band recombines with a hole at the zinc vacancy acceptor.

The yellow band at about 5850 Å was observed in samples deliberately doped with In, Ga or Cl. It could well be that this band is associated with a complex centre consisting of a zinc vacancy and a foreign donor at nearest neighbour sites. In ZnS such an associate is referred to as an A-centre and has been shown to be responsible for the self-activated blue emission of that material. Work in this department on the Hall coefficient and electrical conductivity of ZnSe doped with donor

impurities (13) has shown that both deep and shallow donor levels are produced by In, Ga or Cl but that aluminium seems to lead to shallow donors only. It could be therefore that the yellow band in In, Ga or Cl doped material corresponds to the red (6230 Å) band in aluminium doped samples and that all these bands are attributable to complexes of the A-centre type. The remaining self-activated band at 6150 Å or thereabouts could then be evidence of the existence of an A-centre formed from native donors and acceptors, i.e. zinc and selenium vacancies.

This explanation is self consistent as far as it goes but leaves two difficulties, (1) no account is given of the nature of the centre responsible for the short-wave green band at 5230 Å and (2) if either one or both of the S_o and S''_o series of edge emission bands are attributable to transitions involving native acceptors, the native acceptors must have at least two levels of ionization in order to be involved with both green and edge emission. The latter difficulty could be overcome by suggesting that a zinc vacancy can capture one or two holes, the second of which would lie in a relatively shallow level and hence be responsible for the edge emission. An alternative explanation invoked by Brown et al. (14) for CdS might be that the recombination leading to edge emission involves an excited hole state of the acceptor.

CHAPTER 6

REFERENCES

1. W. Lehmann, J. Electrochem. Soc. 113 (1966) 449
2. G.B. Stringfellow and R.H. Bube, J. Appl. Phys. 39 (1968) 3657
3. G.B. Stringfellow and R.H. Bube, Phys. Rev. 171 (1968) 903
4. S. Iida, J. Phys. Soc. of Japan 26 (1969) 1140
5. R.E. Halsted, M. Aven and H.D. Coghill, J. Electrochem. Soc. 112 (1965) 177
6. W. Lehmann, J. Electrochem. Soc. 114 (1967) 83
7. G. Jones and J. Woods, J. Phys. D, Appl. Phys. 6 (1973) 1640
8. S. Asano, N. Yamashita, M. Oishi and K. Amori, J. Phys. Soc. of Japan 24 (1968) 1302
9. J. Apperson, Y. Vorobiov and G.F.J. Garlick, J. Appl. Phys. 18 (1967) 389
10. D. Curie and J.S. Prener in "Phys. and Chem. of II-VI Compounds" ed. M. Aven and J.S. Prener (N. Holland) 1967 Ch.9
11. S. Iida, J. Phys. Soc. of Japan 25 (1968) 177
12. M. Aven and H.H. Woodbury, Appl. Phys. Lett. 1 (1962) 53
13. G. Jones, Ph.D. Thesis, Durham 1973
14. M.R. Brown, A.F.J. Cox, D.A. Orr, J.M. Williams and J. Woods, J. Phys. C:Solid St. Phys. 3 (1970) 1767

CHAPTER 7

OPTICAL TRANSMISSION AND ABSORPTION IN UNDOPED AND DOPED CRYSTALS

7.1 Introduction

Measurements of the spectral dependence of transmission, absorption and reflection coefficients are useful independent methods for studying the energy gap and band structure of II-VI compounds. Thus, in an attempt to learn more about the various electronic transitions in ZnSe, the transmission and absorption spectra of undoped and doped crystals were measured in the wavelength region from 4000 to 7200 Å. The spectra were obtained from mechanically and chemically polished parallel-sided plates of widely differing thickness (see Chapter 3).

In general the absorption coefficient increases rapidly as the photon energy approaches the value of the energy gap. The magnitude of the absorption coefficient then lies in the range 10^2 - 10^6 cm^{-1}. The marked increase in the absorption coefficient with decreasing wavelength is characteristic of all semiconductors and is responsible for what is called the absorption edge. With decreasing photon energies below the absorption edge, the absorption coefficient gradually drops and the crystal becomes increasingly transparent.

The large increment in the absorption coefficient is due to the onset of absorption in which electrons are excited from the valence band across the forbidden energy gap to the conduction band. The work described in this chapter has been devoted to a study of the absorption edge

and defect structure to try and obtain some information about the energy gap and the states close to the band edges.

In the investigation of the absorption edge, most of the transmission measurements were made on very thin samples using the Optica spectrophotometer. The values of the absorption coefficients, reflection coefficients and refractive indexes were calculated using Fortran-4 computer programs. Some absorption spectra were also measured directly on thick samples using the Bausch and Lomb spectrograph. In this chapter the observed transmission spectra and calculated absorption and reflection coefficients are discussed for both undoped and doped samples. Then follows a description of the results obtained from the directly observed absorption spectra of $MnCl_2$ doped crystals.

7.2 Transmission and absorption spectra of undoped crystals

Transmission spectra of two undoped crystals (grown with zinc reservoirs) No.113 and 155 were measured using slices of two different thicknesses. The observed transmission spectra are shown in Figure 7.1. In both samples the transmission rose sharply at about 4690 Å at room temperature and thereafter increased slowly as the wavelength was increased. The curves at 85 K are similar but the transmission minimum shifts towards shorter wavelengths with decreasing temperature. The rapid increase occurred at about 4470 Å at 85 K. If interference effects are ignored, the transmission of a parallel plate of

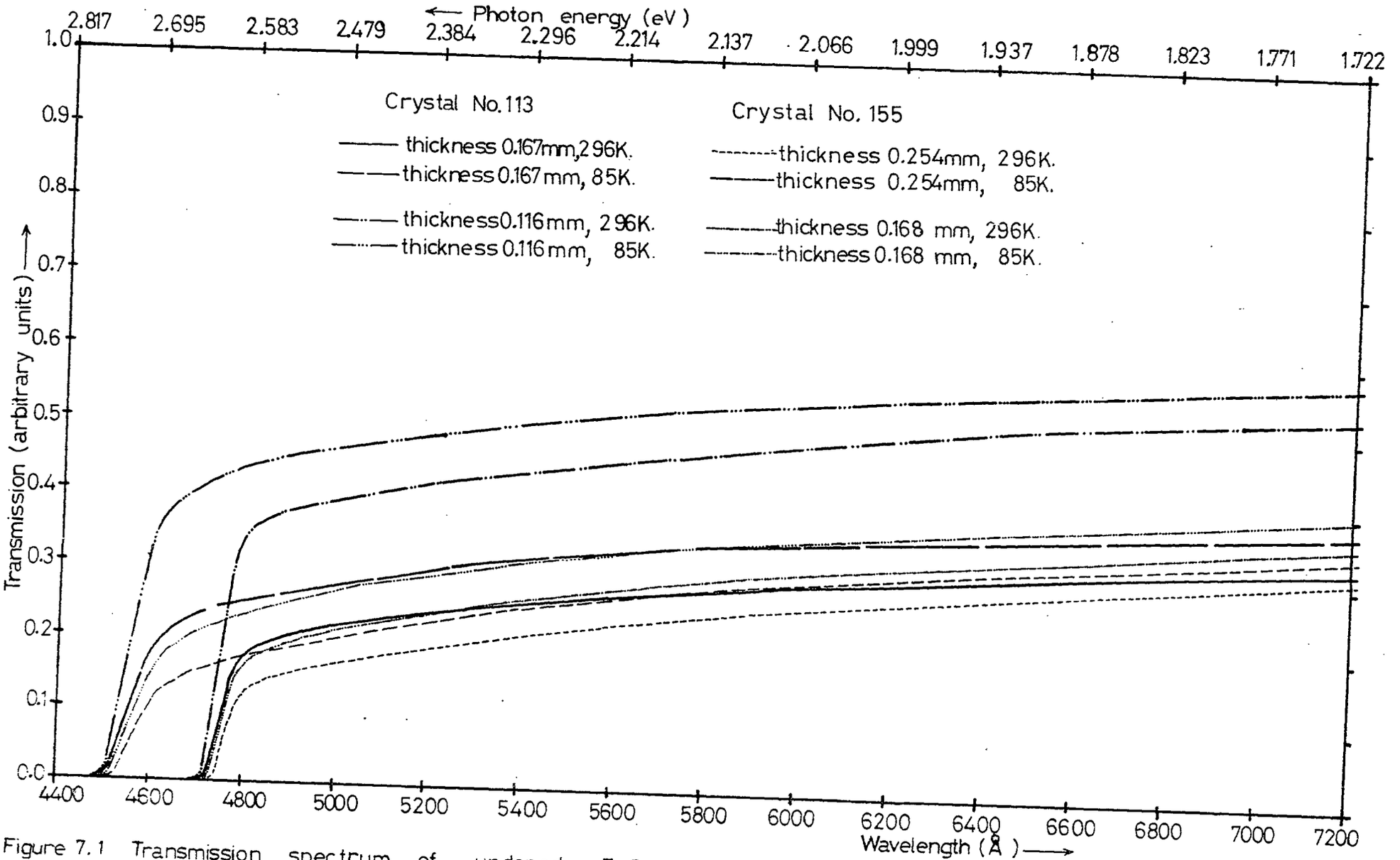

Figure 7.1 Transmission spectrum of undoped ZnSe crystals at room and liquid nitrogen temperatures.

thickness d is (1),

$$T = \frac{(1-R)^2 \, e^{-\alpha d}(1+\frac{k^2}{n^2})}{(1-R^2 \, e^{-2\alpha d})} \qquad (1)$$

where α is the absorption coefficient, R is the coefficient of reflection, n is the refractive index and k is the extinction coefficient ($k = \alpha\lambda/4\pi$). For most transmission experiments $k^2 << n^2$. If d is then chosen to ensure that $R^2 \, e^{-2\alpha d} << 1$, equation (1) takes the very simple form of,

$$T = (1-R)^2 \exp(-\alpha d) \qquad (2)$$

Hence, the absorption coefficient α can be obtained by measuring the transmission of two samples of different thickness without knowing the reflection coefficient provided it is the same for both samples.

Using equation (2) with the transmission data described above for crystals Nos.155 and 113 the absorption coefficient was calculated using a Fortran-4 computer program. The output of the computer plotter giving the absorption coefficient at 296 and 85 K is shown in Figure 7.2. With both crystals the absorption coefficient increased steeply at about 4700 Å at 296 K and 4480 Å at 85 K. There is no evidence of structure at the longer wavelengths, although small peaks and shoulders may be seen at noise level in the tail of the absorption edge. Examination of the spectrum in this region with higher resolution indicated the presence of four very small peaks at about 4560, 4585, 4820 and 4880 Å in crystal No.155 at 85 K. No evidence of exciton absorption was found.

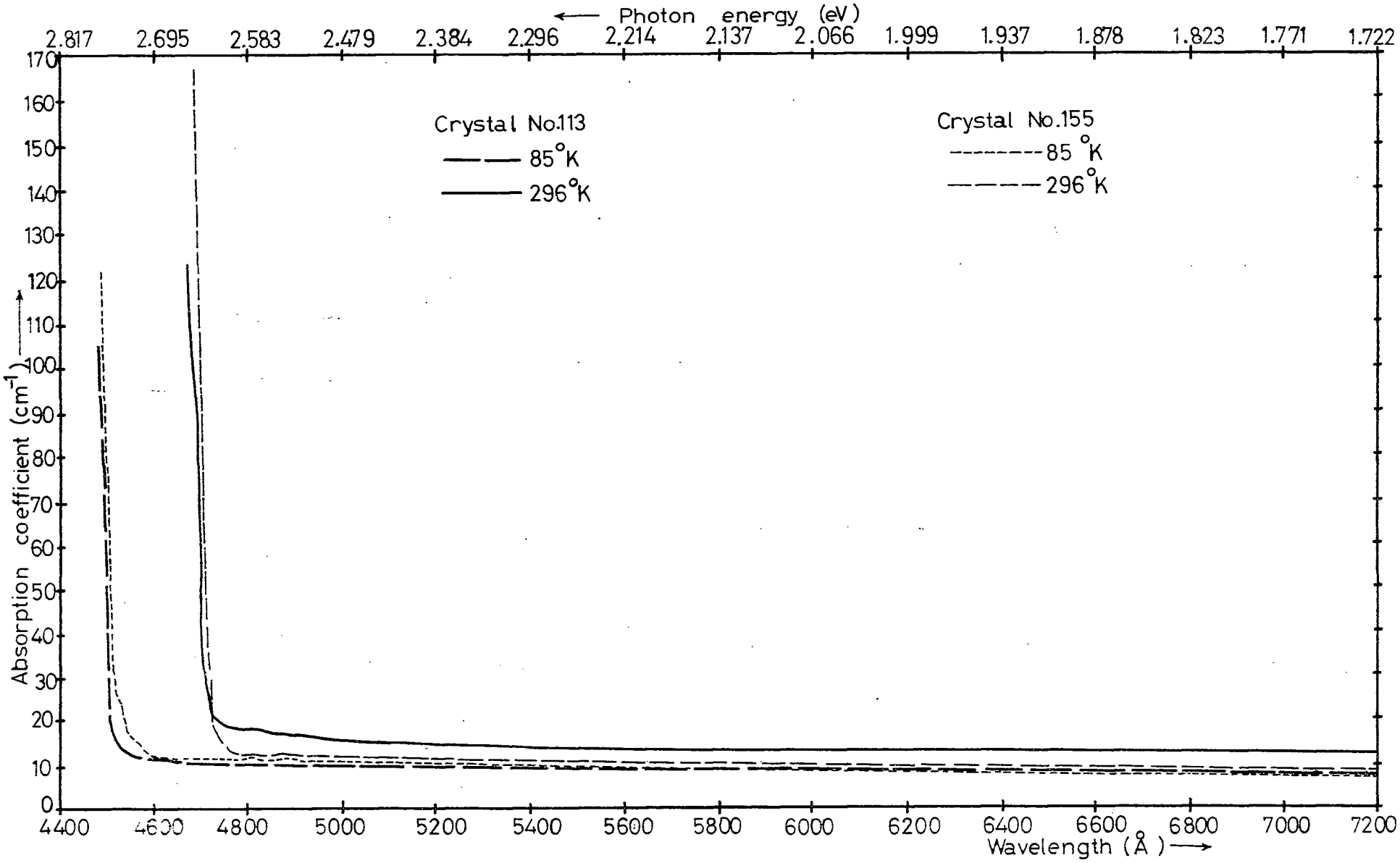

Figure 7.2 Absorption spectrum of undoped ZnSe crystals at room and liquid nitrogen temperatures.

In order to determine the forbidden gap of the two crystals, direct absorption processes were assumed and the square of the absorption coefficient was plotted as a function of photon energy. The resultant curves are shown in Figure 7.3. Extrapolation of the straight line portions to $\alpha^2 = 0$, gives a value of the forbidden gap of 2.634 eV at room temperature and 2.765 eV at 85 K for both crystals. These values would appear to be about 0.03 eV lower than previously published results i.e. 2.67 eV at 300 K (2) and 2.809 eV at 79 K (3).

The reflection coefficients were computed using the calculated absorption coefficients in equation (2), the resultant reflection spectra are shown in Figure 7.4. In this preliminary calculation of reflection coefficient, two different curves were found for two different samples. A value of the refractive index of 3.18 was found for $\lambda = 5890$ Å. This should be compared with previously published values of 2.89 (4) and 2.61 (5).

7.3 Transmission and absorption spectra of doped crystals

Transmission spectra of Al, Ga, In, Cl, CuSe and $MnCl_2$ doped boules (grown with zinc reservoirs) were also measured in the same wavelength region of 4000 to 7200 Å and the results are shown in Figure 7.5.

As seen from the curves of Figure 7.5 all doped crystals, except that grown with CuSe, show similar and structureless transmission spectra. However, the transmission was quite sharp in samples doped with group III impurities and noticeably less sharp in samples doped with

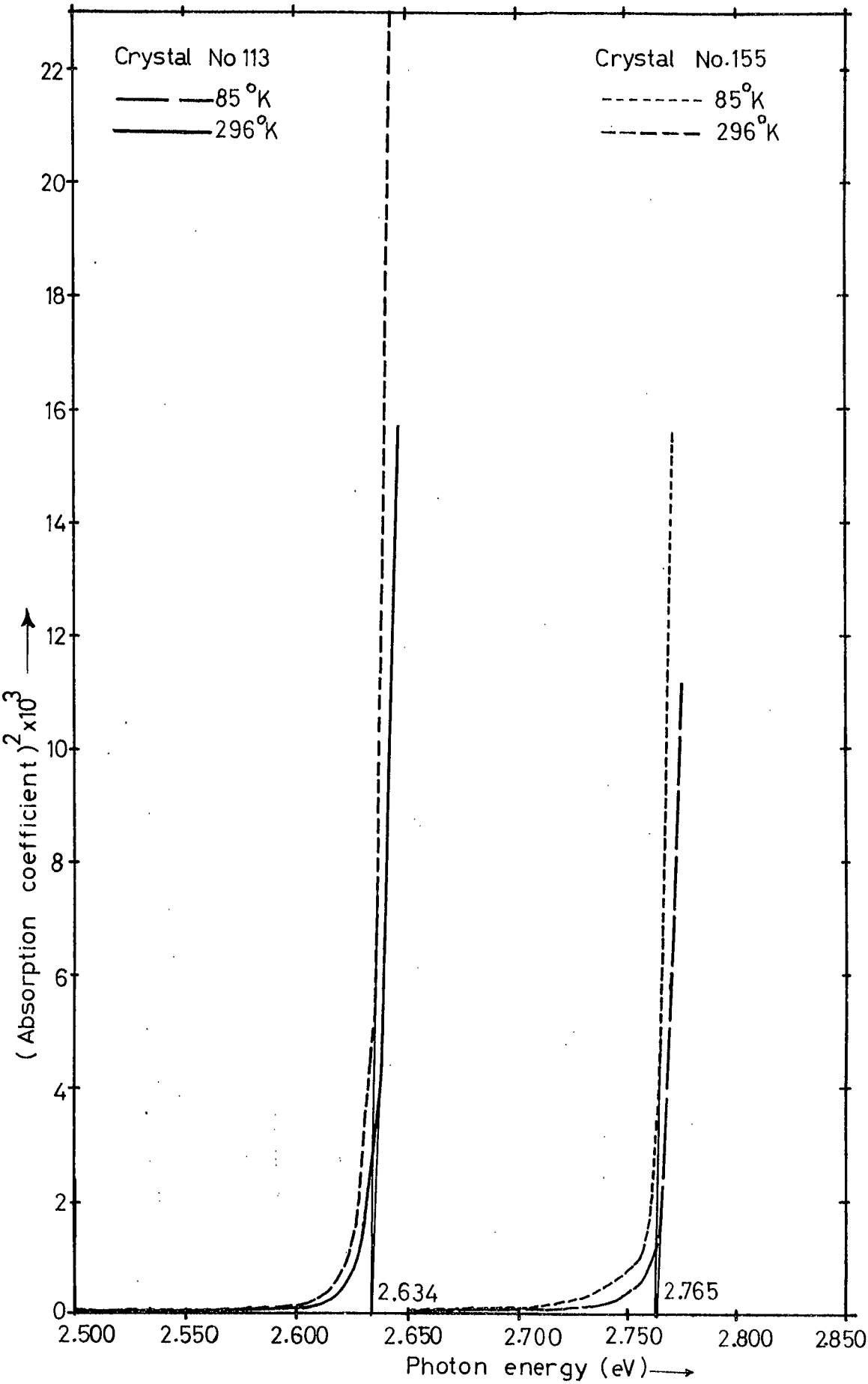

Figure 7.3 The square of the absorption coefficient versus photon energy in ZnSe crystals at two different temperatures.

Cl and $MnCl_2$. With the CuSe doped crystal the transmission curve suggests that two broad absorption bands are present.

The absorption coefficients of the various doped samples have been computed and are plotted in Figure 7.6. Once again, except for the CuSe doped crystal, no structure was observed near the absorption edge at 85 K. It is clear however that near band-gap absorption is quite strong in chlorine-doped samples.

The most interesting results were obtained with the CuSe doped crystal which shows three broad bands below the absorption continuum at about 4600, 5050 and 6750 Å. The bands at 5050 and 6750 Å may be due to internal transitions within the $3d^{10}$ shell of Cu^{+} and $3d^{9}$ shell of Cu^{++} ions on the substitutional zinc sites. Similar bands have also been reported by Pappalardo and Dietz in CdS:Cu crystal (6).

7.4 Optical absorption of $MnCl_2$ doped crystals

In an attempt to determine the position of the manganese energy levels in the ZnSe crystal field, the absorption spectra of crystals grown in the presence of $MnCl_2$ (see Chapter 6, Section 6) were examined using polished slices 5 mm. thick. In these experiments the Bausch and Lomb grating spectrograph was used to record the transmission photographically.

Densitometer traces of the absorption spectra at 10 K for one ($MnCl_2$ + Mn) and two ($MnCl_2$, Zn) crystals are shown in Figure 7.7. The absorption spectra of the two ($MnCl_2$, Zn) samples (crystal No.163 dotted curve and crystal No.222 dotted and dashed cruve) both of which

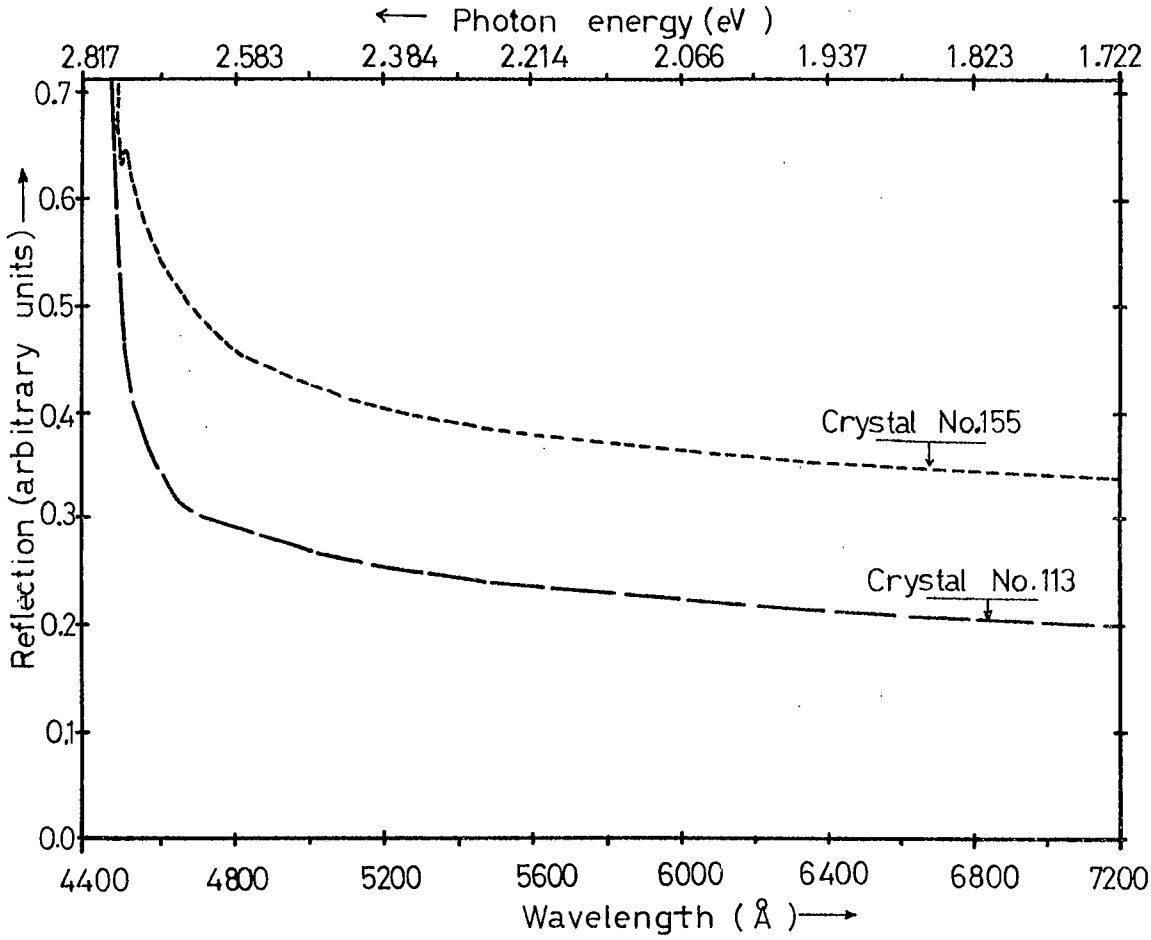

Figure 7. 4 Reflection spectrum of undoped ZnSe crystals at 85 °K.

contained a low concentration of manganese (20-50 p.p.m.), show no structure below the absorption continuum. However the absorption spectrum of the ($MnCl_2$ + Mn) doped crystal No.213 containing a high concentration of manganese (2000 p.p.m.) did exhibit broad bands and sharp lines in the region of the absorption tail at 10 K. The continuous curves of Figure 7.7. show that a broad band at 5050 Å was superimposed on to the tail of the absorption edge. On the low energy side of this band a doublet appeared with components at 5134.8 and 5137.4 Å. The half-widths of the components were about 1 Å. The line at 5137.4 Å was approximately twice as intense as that at 5134.8 Å. Rather broader and weaker lines were also apparent at about 5086, 5097 and 5119 Å. The broad band centred at 5050 Å and its associated structure corresponds to the $^6A_1 \rightarrow {}^4T_2$ transition within the $3d^5$ shell of the Mn^{++} ion. Phonon coupling occurs and this accounts for the fine structure. The line at 5137.4 Å is probably the zero phonon line. Similar optical absorption spectra in ZnSe:Mn have been reported previously by Langer and Richter (7) and the spectrum reported here has recently been discussed by Jones and Woods (8).

In their work on melt grown ZnSe:Mn crystals, Langer and Richter (7) were able to observe three absorption bands at 4.2 K which correspond to the following transitions in the tetrahedrally co-ordinated Mn^{++} ion in zinc selenide: $^6A_1 \rightarrow {}^4T_1$, $^6A_1 \rightarrow {}^4T_2$ and $^6A_1 \rightarrow {}^4A_1$, ^4E. They were studying phonon coupling and reported one zero phonon line for the $^6A_1 \rightarrow {}^4A_1$, ^4E absorption band and a zero phonon doublet for the $^6A_1 \rightarrow {}^4T_2$ absorption band, together with

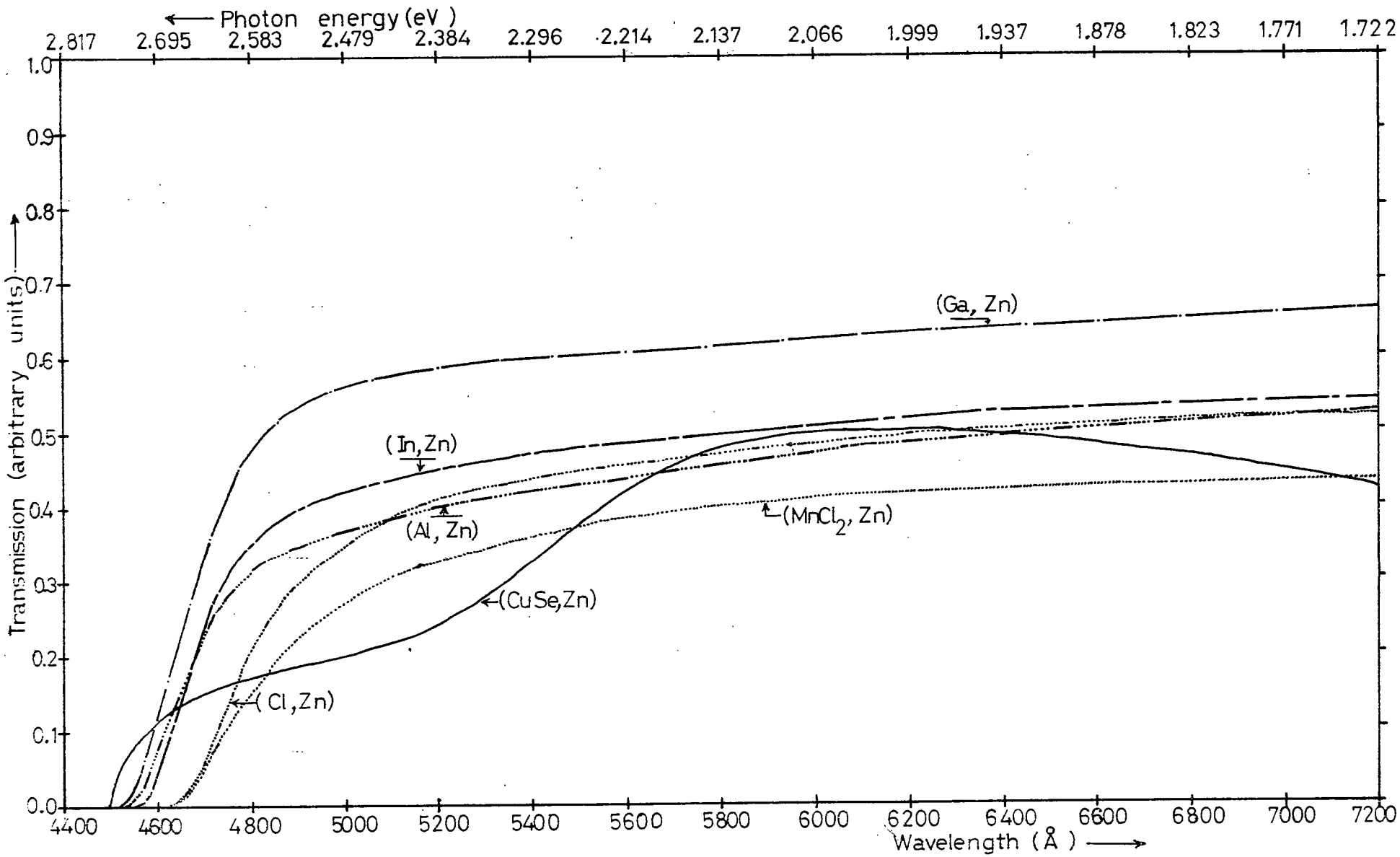

Figure 7.5 Transmission spectrum of Al, Ga, In, Cl, CuSe and $MnCl_2$ doped ZnSe crystals at 85 °K.

other phonon lines. No phonon structure was observed with the $^6A_1 \rightarrow {}^4T_1$ absorption band. Using this interpretation to explain the spectrum of the ($MnCl_2$+Mn) doped crystal No.213 the most clearly resolved broad band corresponds to the $^6A_1 \rightarrow {}^4T_2$ transition. The $^6A_1 \rightarrow {}^4A_1$, E_1 transition at higher energies was not observed, neither was that at the lowest energy, although it does appear after heat treatment (see later). With our sample the maximum of the broad band associated with the $^6A_1 \rightarrow {}^4T_2$ transition lies at 5050 Å compared with the value of 4995 Å reported by Langer and Richter (7). Phonon structure similar to that reported by Langer and Richter for this band is quite evident. The zero phonon line is split by 2.6 Å (10 cm^{-1}) and the more intense longer wavelength component lies at 5137.4 Å. Langer and Richter found the same splitting with the longer wavelength component at 5102.6 Å. As for the structure at higher energies in Figure 7.7, the displacements from the zero phonon line of the three features marked are 18.4 (71 cm^{-1}), 40.4 (154 cm^{-1}), and 48.4 (197 cm^{-1}) Å. It is interesting to note that Carnall et al. (9) have reported multiple-phonon absorption spectra in ZnSe and have found the following lattice phonons at the X and L points on the zone boundary: TA_X = 17.4 Å (69 cm^{-1}), LA_X = 41.2 Å (160 cm^{-1}) and TO_X = 48.8 Å (200 cm^{-1}).

In an attempt to remove any contaminating copper and other impurities, and also because ZnSe:Mn used for electroluminescent lamps is subjected to the same treatment, the ($MnCl_2$+Mn) doped crystal No.213 was annealed

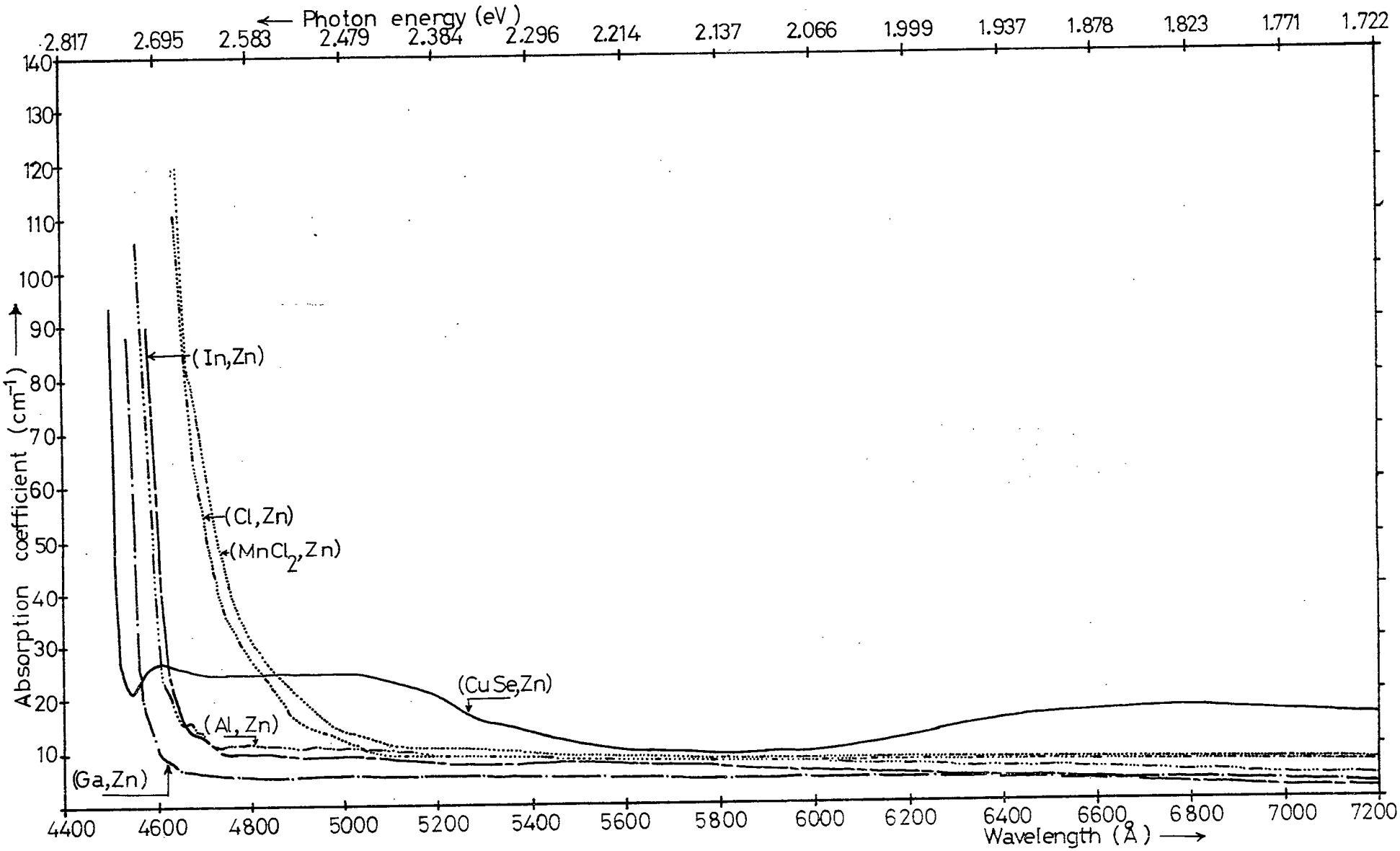

Figure 7.6 Absorption spectrum of Al, Ga, In, Cl, CuSe and $MnCl_2$ doped ZnSe crystals at 85 °K.

in molten zinc for 15 days at 850°C. The absorption spectrum measured after this treatment is shown by the dashed cruve in Figure 7.7. The resulting densitometer trace was almost identical to the original curve, but two new phonon bands could now be resolved at 5074 and 5112 Å. The zero phonon lines had shifted slightly towards shorter wavelengths with maxima at 5134.3 and 5136.9 Å. At the same time the longer wavelength absorption band with a maximum at 5340 Å was now detectable. The phonon structure associated with the 5050 Å band was much more clearly resolved and new separations from the zero phonon line were found at about 24.9 Å (97 cm^{-1}) and 62.9 Å (242 cm^{-1}). These separations are similar to the reported phonon wavelengths of TA_L = 24.2 Å (95 cm^{-1}) and LO_X or LO_Γ, 59.6 Å (237 cm^{-1}) or 62.9 Å (242 cm^{-1}). These modes were determined by Cornall et al. (9) and Reynolds et al. (10).

The appearance of the rather weak longer wavelength band and extra phonon lines following heat treatment in zinc may well be associated with the removal of a small trace of copper impurity from the crystal. Copper leads to an absorption band at around 5050 Å (see Section 7.3). Therefore it is reasonable to suggest that heating in liquid zinc removes the copper impurity from the crystal but has no effect on the state of substitution of the manganese in the zinc selenide lattice. Consequently the manganese transition can be observed more clearly after heat treatment in zinc.

7.5 Discussion

All the absorption measurements reported here were

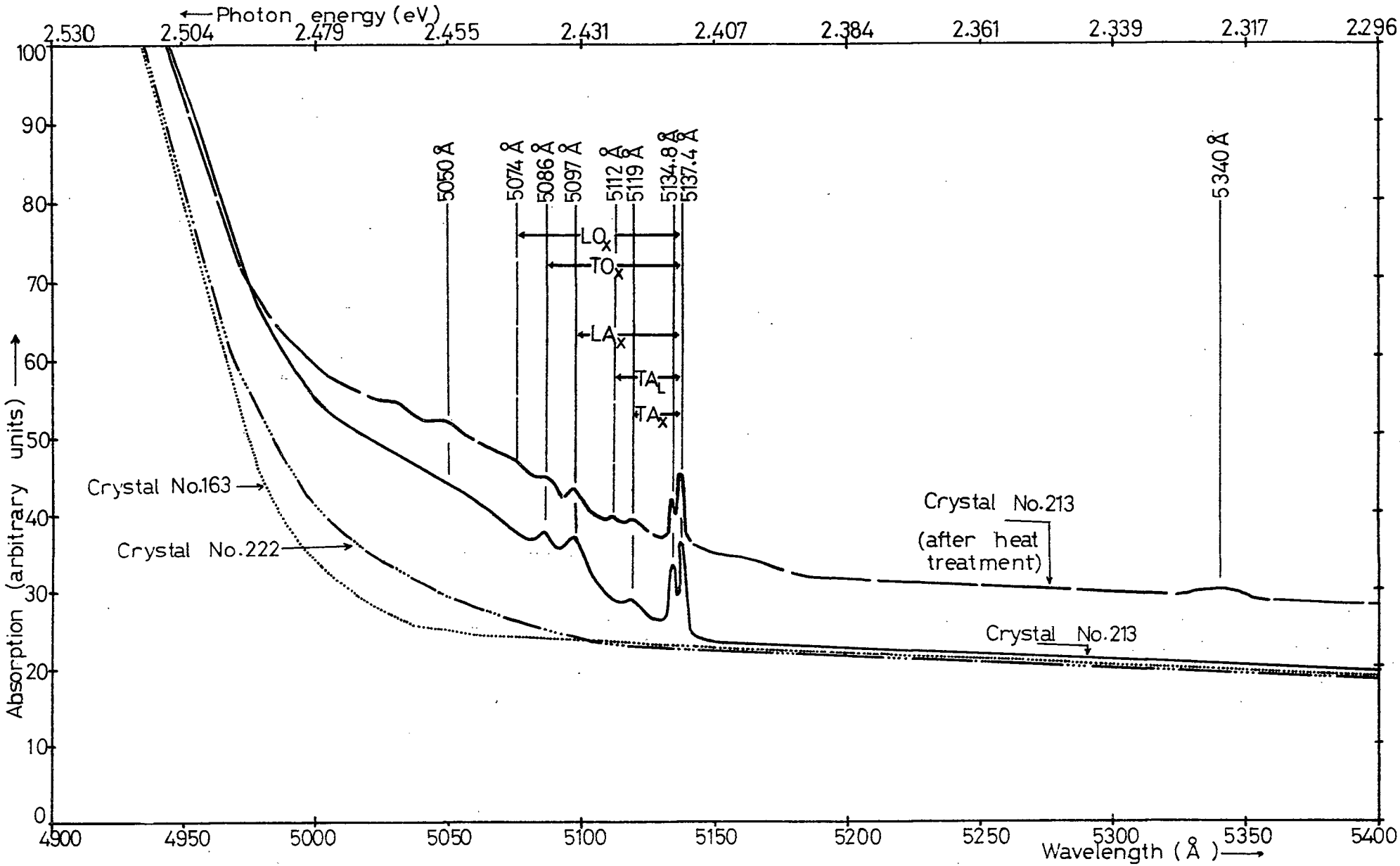

Figure 7.7 Microdensitometer trace of the optical absorption of two ($MnCl_2$,Zn), and before and after heat treatment of ($MnCl_2$+Mn) doped ZnSe crystals at 10 °K.

made on relatively thick samples such as are normally used to obtain information about impurity or defect absorption processes with small oscillator strengths. To study excitons in absorption it is necessary to use thin specimens so that the excitons can be observed in a wavelength region where the continuous absorption coefficient is high. Since no measurements were made on such samples it is not surprising that no exciton absorption was observed.

The measured absorption spectra of undoped samples, and of those doped with Al, Ga, In and Cl, yield relatively little information. Reasonable values have however been obtained for the forbidden gap in ZnSe and the variation of the square of the absorption coefficient with photon energy confirms the accepted view that absorption processes in ZnSe are direct. The samples doped with elements of group III show no evidence of deep-centre absorption at all, but crystals containing chlorine do have an appreciable impurity absorption region close to the absorption edge. However no structure was resolved at 85 K. It might be profitable to repeat the experiment at helium temperatures.

Evidence of deep-centre absorption was observed in the crystal grown in the presence of CuSe. Jones (11) has shown that the red copper emission is excited in a band at 5100 Å but he was unable to measure the excitation spectrum of the copper green emission. It may well be that the absorption bands observed at 4600 and 5050 Å correspond to the excitation bands for the green and red

copper emissions respectively. By analogy with ZnS and CdS it might be expected that the absorption at 6750 Å is associated with infra-red luminescence. The resolution of these problems calls for further work.

The absorption spectrum of the sample most heavily doped with manganese was by far the most interesting. Two broad bands were observed at 5340 and 5050 Å which correspond to the $^6A_1 \rightarrow {}^4T_1$ and $^6A_1 \rightarrow {}^4T_2$ transitions between the levels of the isolated Mn^{++} ions. The band at 5050 Å was much the stronger and displayed considerable phonon structure. The zero phonon line was split into an easily identifiable doublet. The reason for the splitting is not known. The other structural features are all separated from the zero phonon line by energies which can be closely correlated with those of lattice phonons in ZnSe. Thus we observe five phonon lines with separations of 71, 97, 154, 197 and 242 cm^{-1} from the zero phonon line, which are identified as TA_X, LO_X, LA_X, TO_X and LO_Γ. X and Γ refer to the usual points within the Brillouin zone. It is clear that the electronic transitions in the Mn^{++} ion couple with the lattice phonon spectrum.

Jones and Woods (8) have studied the excitation spectrum of the characteristic manganese emission. They found three excitation bands at 4650, 5025 and 5370 Å at 85 K. The two longer wavelength bands are clearly identical with the two absorption bands reported here. The excitation process $^6A_1 \rightarrow {}^4T_1$ which leads to the absorption band at 5340 Å is clearly the reverse of the

luminescence emission process which leads to the band at 6060 Å.

In an isolated Mn^{++} ion the ground state is ^6S and the first excited state is ^4G. In the tetrahedral crystal field of the ZnSe the ground state is unaffected and becomes $^6A_1$ whereas ^4G splits into $^4T_1$, $^4T_2$ and ^4E, $^4A_1$ and other higher levels. Transitions to these latter higher bands are obscured by the onset of optical absorption in the host lattice.

Finally it should be emphasised that heating a manganese doped sample in liquid zinc does not remove the manganese from the crystal even though the luminescence emission is changed by this treatment. Copper and other impurities are removed so that the manganese absorption is more clearly observed.

CHAPTER 7

REFERENCES

1. B. Segall and D.R.F. Marple, in "Phys. and Chem. of II-VI Compounds," ed. M. Aven and J.S. Prener (N. Holland) 1967 Ch.7
2. M. Cardona, in "Phys. and Chem. of II-VI Compounds," ed. M. Aven and J.S. Prener (N.Holland) 1967 Ch.7
3. G.E. Hite, D.T.F. Marple, M. Aven and B. Segall, Phys. Rev. 156 (1967) 850
4. International Critical Tables (McGraw-Hill Book Company, New York) 1 (1926) 165
5. D.T.F. Marple, J. Appl. Phys. 35 (1964) 539
6. R. Pappalardo and R.E. Dietz, Phys. Rev. 123 (1961) 1183
7. D.W. Langer and H.J. Richter, Phys. Rev. 146 (1966) 554
8. G. Jones and J. Woods, J. Phys. D. Appl. Phys. 6 (1973) 1640
9. E. Carnall, S.S. Mitra and R. Marshall, Bull. Am. Phys. Soc. 10 (1965) 1086
10. D.C. Reynolds, L.S. Pedrotti and O.W. Larson, J. Appl. Phys. 32 (1961) 2250
11. G. Jones, Ph.D. Thesis Durham 1973

CHAPTER 8

CONCLUSIONS

8.1 Introduction

The edge emission of a large number of crystals of zinc selenide has been studied extensively and it is clear that acceptor states lying about 1/10 eV above the valence band and shallow donors are responsible for the edge emission in both the undoped and doped samples. The spectra of most ZnSe crystals exhibiting edge emission under U.V. excitation, usually contain sharp lines and broad bands which are attributed respectively to bound exciton recombination and recombination of free or trapped electrons with holes trapped at the acceptor centres. In the bound exciton spectra a weak I_2 line and a more intense I_1 line were usually observed (in some cases the I_1 line appeared as a close doublet separated by about 10 Å). LO phonon coupling was more pronounced with the I_1 than with the I_2 lines (1). The broad bands occurred as a series of LO phonon replicas. At 77 K the so-called high energy series (HES) was observed, this arises from the recombination of free electrons with holes bound to acceptors. At liquid helium temperatures the HES is quenched and is replaced by the low energy series (LES) which results from the recombination of electrons bound to shallow donors with holes bound at the same acceptors (2). It is believed that the observation of the same I_2 line in all the crystals indicates the presence of the same donors in all the samples. This is probably a native defect, possibly a selenium vacancy. It has not been possible to find a

connection between the acceptors responsible for the I_1 lines and those associated with the broader edge emission. However, the purpose of this chapter is to summarize briefly the implication of the results and as a consequence to give some suggestions for further work.

8.2 Acceptor Centres

The crystals studied during the course of this research were generally grown under excess partial pressures of the constituent elements and it was found that the optical properties of samples grown in excess zinc were significantly different from those of samples grown in excess selenium. For this reason undoped crystals grown in three different ways were examined and at least three distinct pairs of edge emission series (S and N bands) were observed. In any one crystal two of these S and N pairs of series were observed. The N series were attributed to free-to-bound transitions at 65 K and the S to bound-to-bound transitions at 10 K. The edge emission spectra of the flow run crystals were identical to those of crystals grown in excess selenium. All crystals have one pair of edge emission bands in common, i.e. those labelled S_o, N_o. Crystals grown in excess selenium also exhibit the S_o', N_o' pairs whereas with those grown in excess zinc the S_o'', N_o'' pair is dominant. Thus, it is concluded that three distinct acceptor states must be involved in our undoped samples with ionization energies of 0.095, 0.112 and 0.122 eV. The deepest acceptor was the one common to all three types of crystal and may well be associated with a common acceptor-type impurity.

With the majority of the doped crystals the same three S and N pairs of bands were found with the N components at exactly the same wavelengths as the corresponding bands in undoped samples grown in the same way. Once again three identical acceptor states were responsible for the observed emission. Since doping with donor type impurities such as Cl and In would introduce native acceptors such as zinc vacancies for charge compensation purposes, the results tend to suggest that the N'_o and N''_o bands are associated with these native acceptors. Only two foreign acceptors were examined. No edge emission which could be identified as characteristic of copper could be found. This is consistent with the idea that copper forms deep acceptor levels which are responsible for the broad band emission at longer wavelengths. With lithium a different edge emission spectrum was observed and an acceptor ionization energy of 0.099 eV was obtained. This does not agree with the value of 0.114 eV reported by Merz et al (3) for lithium doped ZnSe. It would be valuable to examine crystals doped with other alkali metal impurities.

Most of the crystals grown in excess zinc show two I_1 lines. The energy difference between the lines was 6 meV which should correspond to a difference in acceptor depth of $\sim$60 meV. This is very large and implies that the acceptors responsible for I_1, are not the same as those responsible for the N bands. As for previously published data on ZnSe, Dean and Merz (4) and Merz et al (3) found discrete pair line spectra. They also observed

two I_1 lines at 4456 and 4462 Å and two series of S bands. They did not report the observation of the N bands. Iida and Toyama (5) also reported two I_1 lines at 4455 and 4471 Å and two distant pair bands at 4560 and 4590 Å indicating two acceptor levels differing by 18 meV. Thus a wide variety of acceptors must be responsible for the I_1 lines and band edge emission in ZnSe. This clearly suggests that different investigators have different impurities in their samples.

In contrast with crystals grown using the flow run technique or in excess zinc, no bound exciton emission was found in crystals grown in excess selenium. Therefore there is no evidence to associate any excitons at all with the acceptor with an ionization energy of 0.095 eV. The absence of exciton lines in crystals grown in excess selenium may well be consistent with the idea that preferential pairing of donors and acceptors occurs in crystals grown in excess selenium. Bryant et al (6) have shown that such preferential pairing does occur in CdS crystals heated in excess sulphur. If preferential pairing did occur it would be reasonable to assume that bound excitons could not form on an acceptor surrounded by closely neighbouring donors. In any event Bryant et al found very little or no I_1 emission in samples heated in excess sulphur.

If preferential pairing does occur our results should be interpreted to indicate the presence of two acceptors with ionization energies of 0.112 and 0.122 eV. The value of 0.095 eV determined from the N'_o band would in fact, on this interpretation, be associated with a large

correction factor of 0.027 eV to allow for the Coulombic interaction of the surrounding donors. The conclusion would then be that 0.112 eV is the ionization energy of an unknown foreign impurity while 0.122 eV is the ionization energy of a native acceptor.

8.3 Donor Centres

In cadmium sulphide the I_2 line has been assigned to the recombination of an exciton bound to a complex consisting of a singly ionizable donor composed of a sulphur vacancy and a neighbouring singly ionizable acceptor (7). Similarly the I_2 line in the emission spectra of ZnSe crystals can be explained in the same manner. However two different I_2 lines were observed in undoped crystals grown in different ways, for example the 4447 Å line appeared in crystals grown in excess zinc, while the line appeared at 4442 Å in flow run crystals. This is similar to that observed at 4440 Å in the chlorine doped crystals. These differences are difficult to explain but it may be that the line at 4447 Å is associated with a native donor, either a zinc interstitial or a selenium vacancy, while the lines at 4440 and 4442 Å are evidence of chlorine donors either as chlorine in isolation or in the same donor complex.

A study of the temperature dependence of the intensities of the observed three S series of bands of all the crystals, has permitted a careful and unambiguous identification of the donor centres. The donor binding energies were determined by adding a Coulombic energy correction and only small differences (of the order of

3 meV) were found in the resultant binding energies. The conclusion is that one donor level is common to all undoped ZnSe crystals and that it is situated about 32 meV below the conduction band. In contrast slightly different donor levels are found in Al, In, Cl and Li doped crystals. The donor binding energies for the first three vary from the 27 to 29 meV. The lithium doped samples contain two sets of donors with binding energies of 23 and 32 meV. Native donors only were found in the copper doped samples.

The observation of the very intense I_2 line in many of the undoped and some doped crystals indicates the presence of many neutral donors but it is difficult to determine whether the same donor is associated with the pair band emission. However, it is reasonable to suggest that native defects such as a selenium vacancy are responsible for the donor with an ionization energy of 32 meV in the undoped crystals.

8.4 Deep Centre Luminescence

The deliberate introduction of particular impurities in the crystals gave rise to several closely neighbouring red, yellow and green bands with energies well below that of the band gap. The origin of these bands was investigated and as a result the red and yellow broad bands at 6230, 5960, 5890 and 5830 Å are identified as the emission characteristic of Al, In, Cl and Ga impurities. Green bands with maxima between 5470 to 5490 Å were also observed in samples doped with group III and VII impurity elements. However these green bands together with that observed

about 5560 Å in undoped crystals grown in excess selenium probably indicate the presence of zinc vacancies, so that the self-activated emission at about 5500 Å may be explained in terms of a transition in which a free electron in the conduction band recombines with a hole at a zinc vacancy acceptor. Copper doped crystals exhibited a green band at 5290, together with a red one at 6250 Å. These have been attributed to substitutional Cu^{++} and Cu^{+}. Furthermore manganese impurity emission was observed with a maximum between 6040 and 6060 Å under the U.V. excitation.

8.5 Suggestions for further work

The studies described in this thesis go some way in helping to understand the luminescent transitions which occur in ZnSe. However, further experimental work is necessary before all the processes can be clarified. For example the important discrete pair lines and two electron transitions which have been observed at the Bell Telephone Laboratories (3,4,8) have not been observed in our crystals, probably because these lines need much more intense excitation, i.e. with an argon ion laser, for their observation. In addition accurate values of the ionization energies of the donors involved in the distant pair emission can only be obtained by using time resolved spectroscopy. In the present work the calculated magnitude of the Coulombic correction term is subject to substantial error. For this reason it would be interesting to repeat the measurements described here using laser excitation and the techniques of time resolved spectroscopy. Furthermore

the effect of irradiation with high energy electrons on the pair bands could be studied with advantage. This should allow one to determine unambiguously whether preferential pairing occurs in crystals grown in excess selenium.

It might also be helpful to look for Anti-Stokes processes which would provide additional information about the location of levels within the band gap. With better resolution the I_1 and I_2 lines may be resolved into more components and then Zeeman studies would be essential if the various exciton lines were to be positively identified. It may also be possible to observe differences in the Zeeman splitting of an exciton line according to which dopant element is associated with the complex to which the exciton is bound.

CHAPTER 8

REFERENCES

1. D.G. Thomas and J.J. Hopfield, Phys. Rev. 128 (1962) 2135.
2. L.S. Pedrotti and D.C. Reynolds, Phys. Rev. 120 (1960) 1664
3. J.L. Merz, K. Nassau and J.W. Shiever, to be published.
4. P.J. Dean and J.L. Merz, Phys. Rev. 178 (1969) 1310
5. S. Iida and M. Toyama, J. Phys. Soc. Japan 31 (1971) 190
6. F.J. Bryant, W.E. Hagston and C.J. Radford, Proc. Roy. Soc. Lond. A 325 (1971) 127
7. D.G. Thomas, R. Dingle and J.D. Cuthbert in "II-VI Semiconducting Compounds" ed. D.G. Thomas (New York: Benjamin) 1967 P.863
8. J.L. Merz, H. Kukimoto, K. Nassau and J.W. Shiever, Phys. Rev. B 6 (1972) 545